JUSTUS-LIEBIG-
UNIVERSITÄT
GIESSEN

# Early response to subinhibitory antibiotic exposure in *Sinorhizobium meliloti*

**Dissertation**
To obtain the academic degree of
"doctor rerum naturalium" (Dr. rer. nat.)

Submitted by
**Jennifer Anja Franziska Kothe**

This thesis was drawn up at the Institute of Microbiology and Molecular Biology at the Faculty of Biology and Chemistry

Justus-Liebig-University Giessen
December 2024

# Table of contents

# I. Abstract

The Gram-negative Alphaproteobacterium *Sinorhizobium meliloti* is frequently exposed to antibiotics in its natural soil habitat. In this study, transcriptome changes after 10 min of subinhibitory tetracycline (Tc) exposure were analyzed. RNA sequencing revealed 373 mRNAs with significant changes in mRNA level, with genes with the highest increase in mRNA level being rather short, and genes encoding for proteins with a domain of unknown function 1127 (*duf1127*$_1$ to *duf1127*$_6$) were overrepresented. RNA stability analysis revealed that the mRNA half-lives of several up- and down-regulated genes was increased upon Tc exposure. After initial validation, selected up-regulated genes were tested for their response to different stressors and analyzed using reporter fusions. The gene with highest mRNA increase, *duf1127*$_1$, responded specifically to translation inhibitors and for its regulation, the mRNA leader was crucial.

In the *duf1127*$_1$ mRNA leader, three short upstream open reading frames were found, uORF1, uORF2, and uORF3, the latter overlapping *duf1127*$_1$. RNA and protein analyses revealed that uORF1 translation is necessary for transcriptional attenuation of *duf1127*$_1$. This operon was not regulated by intrinsic termination. A deletion analysis suggested an attenuation element, a potential, C-rich Rho utilization (*rut*) site downstream of uORF1. 3' RACE revealed multiple 3' ends downstream of this *rut* site, further supporting Rho-dependent transcription termination. These 3'-ends were around the start codon of uORF2, which was co-regulated with *duf1127*$_1$ at the level of RNA, but not at the protein level, suggesting regulation of the *duf1127*$_1$ translation in response to Tc. However, start to stop mutation destroying uORF2 did not influence *duf1127*$_1$ regulation. Translation of uORF3 could not be validated, but its Shine-Dalgarno sequence was necessary for *duf1127*$_1$ translation. While the translational regulation of *duf1127*$_1$ and the function of this gene were not deciphered, detailed mutational analysis of reporter fusions revealed an unexpected mechanism for transcription attenuation.

The presented data show that the first half of uORF1 (29 aa) must be translated for *duf1127*$_1$ regulation. In codons 3-10 of uORF1, another attenuation element was found, which is also C-rich and C to G mutations led to de-repression of the *duf1127*$_1$ fusion. This supports the existence of a *rut* site in this region. The unexpected localization of this *rut* site near the beginning of uORF1 could be explained by its regulation in the absence of translation, when it is masked by base-pairing with the ribosome binding site (RBS) of uORF1. This explanation was supported by mutational and deletion analyses.

Taken together, this work shows a complex regulation of *duf1127*$_1$ in response to Tc exposure, which includes mRNA stabilization, Rho-dependent transcription attenuation, and, possibly, translational control. The following mechanism is proposed for the *duf1127*$_1$ regulation by transcription attenuation: A rut site is present near the beginning of uORF1, which is only accessible upon translation. In between one ribosome translating and moving downstream, and before a new ribosome occupies the RBS of uORF1, a time window allows Rho to access the rut

site and terminate transcription further downstream. Upon Tc exposure, translation initiation is impaired, and the ribosome blocks the *rut* site, leading to *duf1127*$_1$ induction. In the absence of translation, the RBS and the *rut* site base-pair, abolishing premature transcription termination. This new mechanism is well-suited to monitor the availability of ribosomes and translation efficiency under stress conditions and control the expression of the *duf1127*$_1$ gene.

# II. Zusammenfassung

*Sinorhizobium meliloti* ist ein Gram-negatives Alphaproteobakterium, welches im Boden vorkommt. Dort kann es antibakteriellen Substanzen wie dem Antibiotikum Tetrazyklin ausgesetzt sein, welches auch in subinhibitorischen Konzentrationen eine spezifische Antwort auslösen kann. Nach 10-minütiger Exposition wurden durch RNA-Sequenzierung 373 mRNAs mit signifikanten Änderungen der Expression identifiziert. Besonders stark reguliert waren kurze Transkripte und solche, die für Proteine mit unbekannter Funktion 1127 (DUF1127; *duf1127*$_1$ bis *duf1127*$_6$) kodieren. Analysen der RNA-Stabilität zeigten, dass Tetrazyklin die mRNA-Halbwertszeit erhöht. Verschiedene Gene mit erhöhter Expression wurden auf verschiedene Stressoren untersucht und mittels Reporterfusionen analysiert. Das am Stärksten veränderte Gen, ein *duf1127*-Gen (*duf1127*$_1$), reagierte spezifisch auf Translationsinhibitoren, wobei seine mRNA-Leadersequenz eine große Rolle spielte.

In der Leadersequenz von *duf1127*$_1$ wurden drei kurze *upstream* offene Leserahmen (uORFs) identifiziert: uORF1, uORF2 und uORF3. Letzterer überlappt zum Teil mit *duf1127*$_1$. RNA- und Proteinanalysen zeigten, dass die Translation von uORF1 notwendig für die transkriptionelle Attenuation von *duf1127*$_1$ ist. Dieses Operon wird nicht durch intrinsische Termination reguliert, denn Deletionsanalysen legten nahe, dass ein Attenuationselement in Form einer C-reichen Rho *utilization* (*rut*) site stromabwärts von uORF1 existiert. 3'-RACE-Analysen zeigten mehrere 3'-Enden stromabwärts dieser *rut site*, was die Hypothese der Rho-abhängigen Transkriptionstermination weiter unterstützt. Diese 3'-Enden lagen im Bereich des Startcodons von uORF2. Dieser war auf RNA-Ebene mit *duf1127*$_1$ co-reguliert, nicht jedoch auf Proteinebene. Wurde uORF2 durch Mutationen zerstört, konnte kein Einfluss auf die Regulation von *duf1127*$_1$ nachgewiesen werden. Die Translation von uORF3 konnte nicht validiert werden, allerdings war die Shine-Dalgarno-Sequenz von uORF3 für die Translation von *duf1127*$_1$ notwendig. Trotz fehlender Erkenntnisse zur translationalen Regulation und Funktion des *duf1127*$_1$-Gens zeigten die Mutationsanalysen einen unerwarteten Mechanismus für die Transkriptionsattenuation.

Die Daten dieser Arbeit zeigen, dass die Translation der ersten Hälfte von uORF1 (29 Aminosäuren) notwendig für die Regulation von *duf1127*$_1$ ist. In den Codons 3–10 von uORF1 wurde ein weiteres, C-reiches Attenuationselement gefunden. Mutationen, die C durch G ersetzten, führten zur Derepression der *duf1127*$_1$-Fusion. Diese Ergebnisse unterstützen die Existenz einer *rut site* in diesem Bereich. Die unerwartete Lokalisation dieser Stelle am Anfang von uORF1 könnte dadurch erklärt werden, dass sie in Abwesenheit von Translation maskiert ist, wenn sie Basenpaarungen mit der Ribosomen-Bindungsstelle (RBS) von uORF1 eingeht. Diese Erklärung wurde durch Mutations- und Deletionsanalysen weiter gestützt.

Zusammenfassend zeigt diese Arbeit eine komplexe Regulation von *duf1127*$_1$ in Reaktion auf Tc-Exposition. Diese Regulation umfasst die RNA-Stabilisierung, Rho-abhängige Transkriptionsattenuation und möglicherweise translationale Kontrolle. In dieser Arbeit wird ein Modell für die Regulation von *duf1127*$_1$ durch

Transkriptionsattenuation wie folgt vorgeschlagen: Eine *rut site* befindet sich nahe dem Anfang von uORF1 und ist nur zugänglich, wenn Translation stattfindet.

Während ein Ribosom uORF1 translatiert und stromabwärts wandert, entsteht ein Zeitfenster, in dem Rho die *rut* site erreichen und die Transkription weiter stromabwärts terminieren kann. Bei Tc-Exposition wird die Initiation der Translation beeinträchtigt, wodurch das Ribosom am Anfang von uORF1 die *rut site* blockiert. Dies ermöglicht Induktion von *duf1127*$_1$. In Abwesenheit von Translation basenpaaren sich die RBS und die *rut site*, wodurch vorzeitige Transkriptionstermination verhindert wird. Durch diesen neuartigen Mechanismus könnten Zellen die Verfügbarkeit von Ribosomen und die Translationseffizienz unter Stressbedingungen überwachen. Dies erlaubt die Steuerung der Expression des *duf1127*$_1$-Gens.

# III. List of abbreviations

| | |
|---|---|
| % | per cent |
| °C | degrees Celsius |
| µ | micro |
| APS | Ammonium persulfate |
| ATP | Adenosine triphosphate |
| bp | Base pairs |
| cDNA | complementary DNA |
| Ci | Curie |
| C-terminus | Carboxyl-terminus |
| DNA | deoxyribonucleic acid |
| DNase | Deoxyribonuclease |
| dNTP | Deoxynucleotide triphosphates |
| DTT | Dithiothreitol |
| e. g. | *exempli gratia* (for example) |
| EDTA | Ethylenediaminetetraacetic acid |
| eGFP | enhancend green fluorescent protein |
| et al. | *et altera* (and others) |
| Fig. | Figure |
| g | Gram |
| IP | Immunoprecipitation |
| kb | Kilobase pairs |
| kDa | Kilodalton |
| l | Liter |
| LB | Lysogeny broth |
| LSD | Salmon sperm DNA |
| M | Molar |
| mg | Milligram |
| ml | Milliliter |
| mol | Base unit for amount of a substance |
| mRNA | Messenger RNA |
| ng | Nanogram |
| nm | Nanometer |
| nt | Nucleotide |
| N-terminus | Amino-terminus |
| OD | Optical density |
| ORF | Open reading frame |
| P | Promoter |
| PAGE | Polyacrylamide gel electrophoresis |
| PBS | Phosphate-buffered saline |
| PCR | Polymerase chain reaction |
| PNK | Polynucleotide kinase |
| qRT | Quantitative real time |
| RBS | Ribosome binding site |
| RNA | Ribonucleic acid |
| RNase | Ribonuclease |

| | |
|---|---|
| rpm | revolutions per minute |
| rRNA | Ribosomal RNA |
| SD | Shine-Dalgarno sequence |
| SDS | Sodium dodecyl sulfate |
| Seq | Sequencing |
| sRNA | Small RNA |
| t | Time point |
| Tab. | Table |
| TBE | Tris/Borate/EDTA buffer |
| TEMED | Tetramethyl ethylenediamine |
| Tris | Tris(hydroxymethyl)aminomethane |
| tRNA | Transfer RNA |
| TSS | Transcription start site |
| TY | Tryptone-yeast |
| UTR | Untranslated region |
| UV | Ultraviolet |
| V | Volume |
| v/v | Volume per volume |
| W | Watt |
| w/v | Weight per volume |
| WT | Wild type |
| Δ | Deletion |

# 1. Introduction

## 1.1 Gene regulation in bacterial cells

In bacteria, the expression of genes is required to change upon internal or external stimuli to adapt to a changing environment. That may involve physiological adaptation, developmental processes, or response to external signals leading to quorum sensing or influencing chemotaxis. Furthermore, it may involve the response to co-occurring microbes producing antibiotics, or interaction with a host (Madigan et al., 2021). Thus, the regulation of gene expression is crucial for cellular stress responses, development or homeostatic control of biosynthetic processes (Dever et al., 2021).

Changing environmental conditions are usually sensed and responses are mediated by signal transduction mechanisms in bacteria, which provide a selective advantage (Alvarez & Georgellis, 2023; Goudreau & Stock, 1998). Generally, changes in the environment are sensed by transmembrane receptors, many of which feature a periplasmic sensing domain and a cytoplasmic signaling domain (Goudreau & Stock, 1998). Mostly, these are two-component signal transduction systems featuring a signal receptor kinase, usually a histidine kinase, and a response regulator. Upon activation through phosphate transfer from the associated histidine kinase, the response regulator turns into an active transcription factor (Goudreau & Stock, 1998). The regulation via two-component system activation and transcription factor-dependent gene induction or repression is well understood. However, additional cellular pathways regulate gene expression, many of which may act in concert to determine expression of a specific gene.

Regulation of expression can occur on all levels from DNA to protein in bacteria (Ponath et al., 2022). At DNA level, gene copy number already may lead to different levels of mRNA as well as protein. In that case, multiple genes have the same function - and each of those genes may undergo differential regulation subsequently. In rhizobia, it has been shown that quorum sensing controls plasmid copy number (Acosta-Jurado et al., 2020). In addition, multiple members of a larger protein family may feature complementary proteins expressed under different conditions. This is especially true for genes encoding transcription factors, with the example of LysR-type transcriptional regulators being the largest protein family known for many bacteria (Reen et al., 2013). Their members, in turn, control different environmental responses including antibiotic resistance or initiation of nodulation in plant interactions, as well as nitrogen fixation (Demeester et al., 2024).

For transcriptional regulation, promotor sequence and induction or repression by transcription factors influence transcription by the RNA polymerase (RNAP). The binding of specific sigma factors will lead to differential gene expression through recognition of different promotor sequences (Kormanec, 2022). And finally, termination of transcription through intrinsic or Rho-dependent termination may occur at different sites. A general polar effect allows for higher expression of first genes encoded in an operon versus the genes encoded located more towards the 3' end of a transcript (Li & Altman, 2004; Mateus et al., 2021; Margolin, 1967). Thus, initiation and termination of transcription are important for mRNA level changes upon external stimuli.

Regulation of mRNA stability is involved in differential stability under changing conditions. For that, degradation can lead to low mRNA levels albeit high initiation rates of transcription. Among the regulation mechanisms acting at RNA level, small regulatory RNAs have gained attention. These came into focus upon the discovery that many transcriptomes contain a high proportion of small regulatory RNAs (Ponath et al., 2022; Wassarman et al., 1999, and citations therein). Among them, both coding and non-coding sRNAs can be involved in regulation.

The ribosome binding and finally codon usage can also influence gene expression. The resulting proteins then, of course, may also be regulated by differential stability, activation or inactivation, and differential folding (Chen et al., 2024).

Since different mechanisms often are involved in expression of a given gene and the production of its protein product. To address the different aspects of regulation on RNA level, the processes involved in initiation and termination of transcription, including transcription attenuation, and factors determining RNA stability are introduced.

### 1.1.1 Initiating mRNA transcription: Transcriptional gene regulation

Transcriptional gene regulation usually occurs by controlling promoter recognition or transcription initiation, with its central element being the multi-subunit RNA polymerase (RNAP; Browning & Busby, 2004). The core enzyme consists of subunits ββ'α2ω and, while it is competent for transcription, cannot function for promoter-directed transcript initiation (Browning & Busby, 2004). The transcription initiation with recognition and opening of promoters occurs via sigma (σ) factors (Paget, 2015). There are multiple groups of sigma factors, with $\sigma^{70}$, the major class of vegetative sigma factors, and structurally related alternative sigma factors that can direct the RNA polymerase to different promotors (Paget, 2015). The $\sigma^{70}$ family are the class of so-called housekeeping sigma factors and responsible for most of the transcription during growth (Paget, 2015). Some members of the $\sigma^{70}$ family also function as activator proteins (Paget & Hellmann, 2003).

Sigma factors direct the RNAP to the promotor, which for $\sigma^{70}$ consists of the -35 and -10 regions (Paget & Hellmann, 2003). The distance between the -35 and -10 boxes reflects the distance between the different binding domains within the respective sigma factor (Lee et al., 2012). The sequence similarity to the consensus promotor determines the promotor strength. In addition to the general $\sigma^{70}$, alternative sigma factors are known to bind to different promotors and regulate, for example, iron uptake, nitrate metabolism, chemotaxis, or general and heat stress (Lee et al., 2021; Paget & Hellmann, 2003).

In addition, the region upstream of the transcription start site can contain elements that allow binding of a transcription factor (TF; Balleza et al., 2009). Transcription factors can be classified into several families based on their domains, most of which feature a helix-turn-helix domain (Balleza et al., 2009; Madan Babu & Teichmann, 2003). Multiple transcription factors can be involved in the regulation of a gene and can either be positive or negative regulators (Balleza et al., 2009; Madan Babu & Teichmann, 2003). A specific role for a transcription factor in transcription initiation is found with *merR*-type transcription factors that can induce a conformational shift in DNA structure that alters the physical distance between the -35 and -10 region (Brown et al., 2003).

Bacterial transcription can be inhibited with rifampicin. This antibiotic specifically binds to the ß subunit of the bacterial RNA polymerase (Campbell et al., 2001). This leads to a bactericidal effect, which makes it useful in medical applications. However, the immediate stopping of transcription can also be used for half-life determination of bacterial transcripts.

### 1.1.2 Transcription termination in Rho-dependent and independent ways

In Bacteria, there are two ways to terminate transcription: Rho-dependent and Rho-independent (Mitra et al., 2017). Rho-dependent transcription termination relies on the Rho protein, while Rho-independent termination relies on the formation of RNA secondary structures. In case of attenuation, a kind of premature transcription termination, mutually exclusive structures can regulate transcription (Yanofsky, 1981; Yanofsky et al., 1981).

Rho-independent termination, or intrinsic termination, relies on structural features of the nascent RNA (Mandell et al., 2022). Formation of an RNA hairpin leads to release of the transcript due to melting of the RNA-DNA hybrid, or invades the main channel of the RNAP Mandell et al., 2022). Intrinsic terminators are characterized by a GC-rich dyad forming a hairpin structure, followed by a U-rich sequence (Ray-Soni et al., 2016). The RNAP pauses at the U-rich sequence which allows the hairpin to form, a process beginning when the RNAP transcribes downstream of that sequence (Ray-Soni et al., 2016). This step destabilizes the elongation complex (EC). Completion of the hairpin involves breaking bonds between the RNA and DNA hybrid, further destabilizing the EC. After hairpin formation is completed, the upstream RNA-DNA hybrid melts, which causes RNAP to release the RNA and terminate transcription (Ray-Soni et al., 2016).

Recent studies suggest that Rho-independent and Rho-dependent mechanisms are not mutually exclusive, in fact, many intrinsic terminators in *B. subtilis* require a combination of proteins NusA and NusG (both bacterial transcription elongation factors) and Rho (Mandell et al., 2022).

Rho-dependent termination relies on the binding of a factor called Rho. Rho is a hexameric protein, shaped like a ring, and its movement along RNA is driven by ATPase activity. It functions as an RNA translocase/helicase in a 5'→3' directionality (Mitra et al., Murayama et al., 2023; 2017; Said et al., 2024). Generally, Rho binds to pyrimidine-rich regions (RNA regions with more C than G bases) and terminates further downstream (Alifano et al., 1991). These stretches contain a so-called Rho utilization (*rut*) site (Richardson & Richardson, 1996). Each monomer of Rho contains an N-terminal domain with a primary binding site and a C-terminal domain with a secondary binding site (Mitra et al., 2017; Murayama et al., 2023; Said et al., 2024). The primary binding site binds two pyrimidine bases. Rho can exist in an open or closed form (Mitra et al., 2017; Murayama et al., 2023; Said et al., 2024). Upon binding of the RNA and ATP, Rho assumes a closed-ring conformation and becomes active. In particular, Rho binds the *rut* sites using its primary binding site, then captures neighboring regions using its secondary binding site (Mitra et al., 2017; Murayama et al., 2023; Said et al., 2024). RNA translocation occurs in 5'→3' direction and is powered by hydrolysis of ATP. There are two models to Rho-dependent transcription termination. The most commonly accepted model suggests that Rho trails along the RNA polymerase, and when reaching its termination site, it either extracts the RNA or it pushes the RNA polymerase forward. This leads to dissociation of the RNA polymerase from the DNA and effectively terminates transcription and releases the nascent RNA (Mitra et al., 2017; Murayama et al., 2023; Said et al., 2024). The protein NusG, a transcription elongation factor, can enhance the efficiency of termination, and is essential to recruit Rho to a subset of terminators (Mitra et al., 2017; Valabhoju et al., 2016).

Usually, RNA is protected from Rho invasion by a translating ribosome (Sevostyanova & Groisman, 2015). In *Salmonella enterica*, a leader region of the *mgtCBR* transcript features a Rho-dependent terminator, along with an RNA element antagonizing Rho, called "Rho-antagonizing RNA element" (RARE; Sevostyanova & Groisman, 2015). The latter traps Rho in a state where it is non-functional by forming a single stranded region. This hinders Rho activity but does not affect Rho binding to the RNA. The mechanism depends on the structural state of RARE. If it is sequestered in a double-stranded conformation, Rho can terminate transcription (Sevostyanova & Groisman, 2015). In *Escherichia coli*, it has been shown that a

compromised Rho-dependent transcription termination enhanced susceptibility to antibiotics (Hafeezunnisa & Sen, 2020). This was attributed to the inefficient efflux of the TolC efflux pump, showing that Rho regulates the antibiotic susceptibility through multiple pathways (Hafeezunnisa & Sen, 2020).

Rho can be specifically inhibited. Very recently, it was shown that, in *E. coli*, Rof, an Sm-like protein, blocks an extended primary binding site and interferes with the binding of Rho to the transcription elongation complex (Said et al., 2024). Bicyclomycin (BCM) is a drug that specifically inhibits the Rho protein and has been used in various Gram-negative bacteria to validate Rho-dependent transcription (Kohn & Widger, 2005; Wang et al., 2023). It was isolated first in 1972 from *Streptomyces sapporonesis* and *Streptomyces aizumenses* (Miyamura et al., 1972; Miyoshi et al., 1972). Tests in *E. coli* showed a minimal inhibitory concentration of 50 % inhibition ($MIC_{50}$) at 25 µg/ml (Wang et al., 2023). It was revealed that BCM binds closely to the ATPase domain of Rho as well as the secondary binding site. This leads to inhibition of the hexamer-ring closing step, thus affecting ATPase activity (Mitra et al., 2017).

Transcription termination can also occur prematurely, with the most common mechanism being attenuation.

### 1.1.3 Premature transcription termination

#### 1.1.3.1 Attenuation

Premature transcription termination (PTT) in bacteria can occur by attenuation, where the attenuators are often located in the 5' UTR of the gene (Naville & Gautheret, 2009). First discovered in the tryptophan operon in *E. coli* (Yanofski et al., 1981), where attenuation occurs based on tryptophan availability, 5' terminators have been discovered to be associated with many biological functions and sensing mechanisms (Naville & Gautheret, 2009). There are 5 major classes of attenuation elements in bacteria (Fig. 1; Naville & Gautheret, 2009).

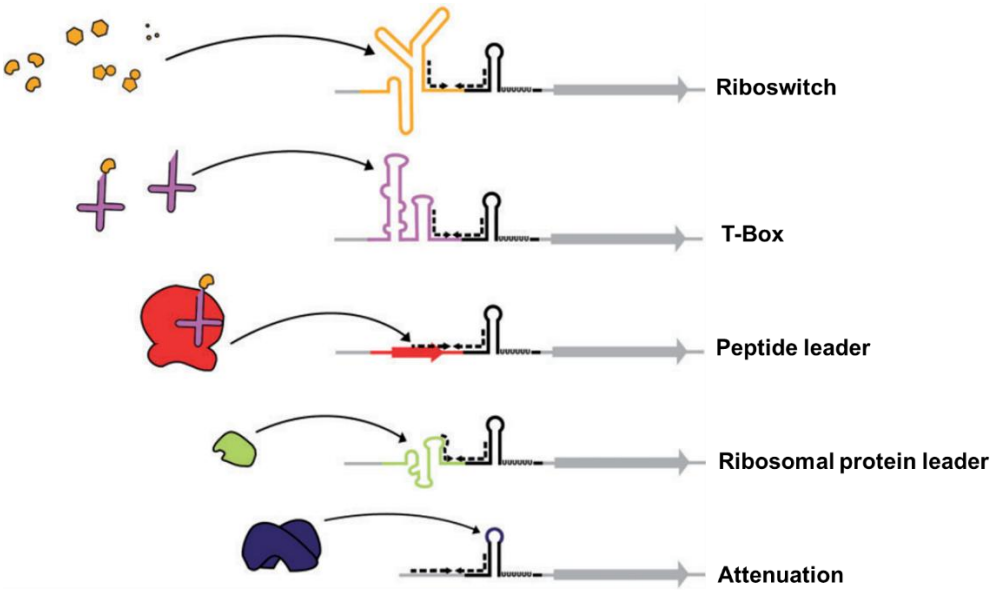


**Fig. 1:** The 5 major classes of attenuators in bacteria (modified after Naville & Gautheret, 2009). Attenuation can be achieved by riboswitches, T-Box attenuators, peptide encoding leaders, ribosomal protein leaders and by binding of a terminator or anti-terminator protein.

Riboswitches can sense the concentration of a metabolite in the cell by a direct interaction. The RNA aptamer binds small ligands, such as ions, whose concentration decides the folding of either the terminator structure (Fig. 1, straight lines) or the anti-terminator structure (Fig. 1, dotted arrows). When the small metabolite (the ligand) binds to the aptamer domain, a conformational change produces a signal via an expression platform, such as a terminator (Naville & Gautheret, 2009).

T-Box attenuators are often considered a family of riboswitches. Their signal element is an uncharged tRNA (Gutiérrez-Preciado et al., 2009; Naville & Gautheret, 2009). Segments of the upstream leader RNAs can form alternative hairpin structures, a terminator and anti-terminator (Gutiérrez-Preciado et al., 2009; Naville & Gautheret, 2009). The RNA element in T-Box attenuators, following interaction with a specific uncharged tRNA, forms an anti-terminator structure (Fig. 1, dotted arrows). This prevents transcription termination, while charged tRNAs are not able to interact with the T-Box, leading to formation of the terminator (Fig. 1, straight lines; Naville & Gautheret, 2009).

The alternative folding of the structure into a terminator or anti-terminator (Fig. 1, dotted arrows) that depends on the translation rate of particular codons in a short upstream ORF characterizes attenuation by peptide leaders (Naville & Gautheret, 2009). A short peptide showing an enrichment of a specific amino acid serves as the sensor element and is encoded by a small open reading frame in the nascent leader transcript (Naville & Gautheret, 2009; Vitreschak et al., 2004). A secondary structure causes a pause of the RNA polymerase which in turn allows the ribosome to start translation of the leader peptide. Subsequent enrichment of codons for a certain amino acid then leads to one of two outcomes. If there is an excess of the specific amino acid in the cell, there is also an excess of charged tRNAs. The ribosome can then synthesize the leader peptide until the stop codon (Naville & Gautheret, 2009; Vitreschak et al., 2004). This prevents the formation of an anti-terminator and promotes the formation of a terminator structure. This causes premature transcription termination. If the cell is starved of the specific amino acid, the deficiency of charged tRNAs leads to ribosome stalling in the leader peptide at the specific codons. An anti-terminator structure is allowed to form as transcription continues. This causes a readthrough into the downstream genes, allowing for their transcription (Naville & Gautheret, 2009; Vitreschak et al., 2004).

The mRNA leader can also change its structure upon binding of a ribosomal protein. The transcription of ribosomal proteins is regulated by an interaction between ribosomal proteins and the RNA leader sequences of their own genes, where the leaders mimic the ribosomal RNA structurally (Naville & Gautheret, 2009). If the level of ribosomal proteins is high, they bind the 5’ leader of their own transcripts. This prevents further transcription and reduces protein production (Naville & Gautheret, 2009).

Finally, attenuation can be achieved by binding of a terminator or anti-terminator protein, where the folding into alternative structures is controlled by this specific interaction (Naville & Gautheret, 2009). This protein-RNA interaction affects the folding of the terminator structure.

RNA attenuators act in cis, as they are part of the same mRNA they regulate and form alternative secondary structures that allow or prevent downstream gene expression (Dersch et al., 2017). Since the publication of the Term-seq method, the ribo-regulation of many antibiotic resistance genes has been discovered (Dar et al., 2016; Dersch et al., 2017). Usually, translation of a short leader peptide by the ribosome is monitored (Fig. 2).

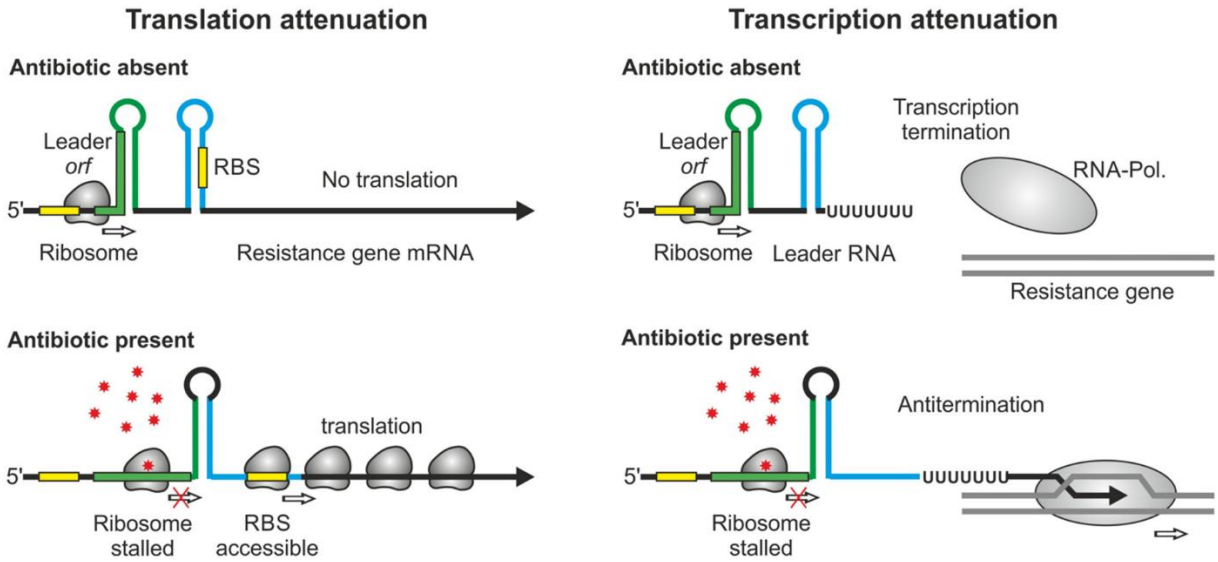


**Fig. 2:** Regulation by RNA attenuation of antibiotic resistance genes (modified from Dersch et al., 2017). Regulation can occur by translational attenuation (left) or transcriptional attenuation (right). Attenuation depends on the translation of a leader open reading frame (ORF), leading to formation of mutually exclusive structures.

For translational attenuation, translation of a leader ORF by the ribosome leads to formation of an RNA secondary structure. This represses translation of the mRNA, as its ribosome binding site (RBS) is sequestered (Fig. 2, upper left). Antibiotic exposure leads to stalling of the ribosome in the leader ORF and allows an alternative RNA structure to form, making the RBS accessible, therefore allowing translation of the mRNA (Fig. 2, bottom left; Dersch et al., 2017). For transcriptional attenuation, transcription by the RNA polymerase is affected, as translation of the leader ORF causes formation of an intrinsic terminator (Fig. 2, upper right). Ribosome stalling due to antibiotic exposure leads to formation of an alternative structure, an anti-terminator. This allows the RNAP to continue transcription beyond the terminator (Fig. 2, bottom right; Dersch et al., 2017).

#### 1.1.3.2 Disruption of transcription and translation

To maintain the integrity of gene expression, it is crucial for bacteria to have a tight coordination between the processes of transcription and translation. Losing this coordination, for example by a pausing ribosome, can lead to premature transcription termination in Gram-negative bacteria (Zhu et al., 2019). One such example is the polarity observed in operons, where the expression of downstream genes is affected (Adhya & Gottesman, 1978; Newton et al., 1965; Zhu et al., 2019). Treatment with antibiotics inhibiting translation can cause PTT, dissociating translation and transcription, and mediating a polarity effect for long operons. This was shown for the long *lacZ* gene and for two large operons containing ribosomal genes in *E. coli* (Zhu et al., 2019).

## 1.2 Post-transcriptional gene regulation

Post-transcriptional regulation allows rapid adjustment to changing environments as well as fine-tuning of gene expression (Dever et al., 2021; Martínez & Vadyvaloo, 2014; Vargas-Blanco & Shell, 2020). Formally, this regulation is classified as control of gene expression after transcription initiation but before translation (Martínez & Vadyvaloo, 2014), however, translational control will also be discussed in this chapter.

On the post-transcriptional level, fine-tuning occurs by mechanisms of RNA stabilization and degradation (Rochat et al., 2013). However, cells can also control the protein level, fine-tuning each step of the translation of mRNA into protein (Tollerson & Ibba, 2020).

Proteins are usually stable in the cell. Their degradation, proteolysis, is energy-consuming, yet it provides another essential mechanism of regulation (Gottesman, 2003). In contrast, RNAs are more labile molecules in the cell, and their half-life is much shorter (Bernstein et al., 2002; Gottesman, 2003). In *E. coli*, the vast majority of all mRNAs showed a half-life of 3 to 8 in (Bernstein et al., 2002).

### 1.2.1 RNA stability regulated by processing and degradation

Transcription and translation in bacteria are coupled in space and time, therefore RNA stability is regulated in various ways (Rochat et al., 2013). RNA degradation is a crucial mechanism in RNA metabolism (Deutscher, 2006).

Regulation of mRNA stability under changing conditions can lead to low mRNA levels albeit high initiation rates of transcription. The concentration of mRNA in the cells is not only affected by transcriptional regulation, but also mRNA degradation as well as dilution as the cells grow (Dressaire et al., 2013).

RNA degradation and maturation in the Gram-negative bacterium *E. coli* can be achieved by various endo- and exonucleolytic processing, where RNases are cleaving at internal points or attacking from either RNA end, respectively (Rochat et al., 2013; Vargas-Blanco & Shell, 2020). A degradation system named the degradosome had first been transcribed in *E. coli* as well (Carpousis et al., 1994; Py et al., 1994; Vargas-Blanco & Shell, 2020). The two main RNases involved are RNase E and PNPase, alongside the DEAD-box RNA helicase RhlB and the enzyme enolase (Deutscher, 2006; Rochat et al., 2013; Vargas-Blanco & Shell, 2020). RNase E cleaves at specific sites in the RNA that are A/U-rich and lack secondary structures (Deutscher, 2006; McDowall et al., 1994), and its C-terminal domain is used to form the degradosome complex with the other components (Förstner et al., 2018; Vargas-Blanco & Shell, 2020). The 3'-5' exoribonuclease PNPase is a phosphorolytic nuclease, which generates 5'-diphosphates (Deutscher, 2006). The helicase RhlB can unwind DNA while using ATP and, when bound to RNase E, it leads to degradation of an RNA fragment by PNPase (Liou et al., 2002). Enolase is a glycolytic enzyme, potentially functioning as a sensor (Carpousis, 2007; Vargas-Blanco & Shell, 2020). Many nucleases recognize monophosphates at the 5' end of the mRNA, which are generated from triphosphates by RppH, a pyrophosphohydrolase (Deana et al., 2008; Rochat et al., 2013). The resulting fragments of RNA are further degraded by other RNases, such as RNase III that cleaves double-stranded structures (Deutscher, 2006; Rochat et al., 2013).

In contrast to *E. coli*, the Gram-positive bacterium *Bacillus subtilis* lacks RNase E, however, the degradosome features similar components (Cho, 2017). The degradosome consists of RNase Y, RNases J1 and J2, PNPase, CshA, as well as the glycolytic enzymes enolase and a phosphofructokinase (Cho, 2017). RNases Y, J1 and J2 are endoribonucleases and RNase Y is the major scaffold in the degradosome. RNase J1 and J2 furthermore have a 5'-3' exonuclease activity, while CshA functions as an ATP-dependent RNA helicase (Cho, 2017). In *Sinorhizobium meliloti*, a Gram-negative alphaproteobacterium, RNase E was involved in post-transcriptional silencing of quorum sensing, mediated by small RNAs (Baumgardt et al., 2017; Saramago et al., 2018). *S. meliloti* encodes an RNase J-type enzyme, despite being Gram-negative, which is involved in final maturation of 23S rRNA and 16S rRNA (Madhugiri & Evguenieva-Hackenberg, 2009; Saramago et al., 2018).

The mRNA half-life can be affected by many factors, such as growth rate, RNA binding proteins or structural features as well as ribonucleases or 5' RNA modifications like cap structures or tri-phosphate groups (Dressaire et al., 2013; Evguenieva-Hackenberg & Klug, 2011; Rauhut & Klug, 1999; Vargas-Blanco & Shell, 2020). Many studies in various bacteria, albeit mostly *E. coli*, have shed light on how mRNA stability changes under various stress or growth conditions, with many studies showing stabilization under stress or at slower growth rates (Vargas-Blanco & Shell, 2020, and citations therein). 5' modifications such as triphosphates or m6A as well as non-canonical cap structures like NAD can function in stabilization of mRNAs (Vargas-Blanco & Shell, 2020). Cleavage sites can be blocked by secondary structures or RNA binding proteins, protecting mRNAs from cleavage and degradation (Vargas-Blanco & Shell, 2020). Another factor for mRNA stability are small RNAs (sRNAs), binding to mask cleavage sites or blocking access to the ribosome binding sequence for the ribosome (Vargas-Blanco et al., 2020).

## 1.3 Small RNAs and small open reading frames in Bacteria

Among the regulation mechanisms acting at RNA level, small regulatory RNAs have gained attention. These came into focus upon the discovery that many transcriptomes contain a high proportion of small RNAs (Ponath et al., 2022; Wassarman et al., 1999, and citations therein). Among them, both coding and non-coding sRNAs can be involved in regulation.

Small RNAs (sRNAs) and small proteins, in recent years, have sparked rising interest (Chen et al., 2002; Storz et al., 2014). Particularly small RNAs have been identified to be a major part of post-transcriptional regulators, as Bacteria can regulate gene expression at all levels (Ponath et al., 2022). Different sources state different length for sRNAs, from 100-200 nt, 50-250 nt or 50-400 nt in length, however, all agree that sRNAs are involved in many processes in the cell (Nitzan et al., 2017; Papenfort & Melamed, 2023; Ponath et al., 2022; Wassarman et al., 1999; Vogel & Wagner, 2007).

In bacteria, sRNAs often have a broad network, usually functioning at the post-transcriptional level, regulating their targets via imperfect base-pairing or with the help of RNA-binding proteins (Papenfort & Melamed, 2023). There are different families of sRNAs, and the major ones include: (i) true antisense RNAs (or *cis*-encoded RNAs) that regulate the strand complementary to the one they were synthesized from, (ii) sRNAs that base-pair with limited complementarity (or *trans*-encoded RNAs) and finally (iii) sRNAs that regulate proteins (Gottesman & Storz, 2011). While *cis*-encoded sRNAs show full complementarity to their target, *trans*-encoded RNAs only form partial duplexes due to being encoded elsewhere in the genome (Brantl, 2007; Gottesman & Storz, 2011). Partial base-pairing allows trans-encoded RNAs to bind multiple different transcripts, allowing not only gene regulation within a single network, but also connecting and synchronizing multiple outputs from various networks (Papenfort & Melamed, 2023).

### 1.3.1 *Cis*-encoded RNAs and their mechanism of action

Cis-encoded RNAs are transcribed from the same locus as their target, and therefore show full complementarity (Brantl, 2007). The transcription of a cis-encoded sRNA and its target comes from opposite strands (Waters & Storz, 2009). They are often expressed from plasmids or bacteriophages (Brantl, 2007; Waters & Storz, 2009). Their role is regulation of fundamental cellular processes, such as replication initiation, translation initiation or RNA degradation (Brantl, 2007). They can also act as antitoxins, thereby repressing translation of toxic proteins, as is the case for e. g. the *hok*/*sok* system in *E. coli* (Waters & Storz, 2009). Cis-encoded RNAs

can also modulate gene expression in an operon, binding in between ORFs. This was shown for the GadY sRNA and the *gadXW* mRNA, where binding of the sRNA between *gadX* and *gadW* leads to cleavage and the levels of the *gadX* transcript increased (Opdyke et al., 2004; Tramonti et al., 2008).

### 1.3.2 *Trans*-encoded RNAs and their mechanism of action

sRNAs encoded in *trans* usually show imperfect base-pairing to their target due to being located elsewhere in the genome yet are involved in a wide regulatory network in the cell (Gottesman, 2005; Hoyos et al., 2020; Papenfort & Melamed, 2023; Vogel & Wagner, 2007). This is often facilitated by RNA chaperone proteins, like Hfq, helping with efficient base-pairing to their target mRNAs (Chao et al., 2012; Gottesman, 2005). Around 20% of the expression of all genes in enteric model bacteria are impacted by Hfq and its associated sRNAs (Smirnov et al., 2016).

Regulation can be positive or negative, e. g. the McaS sRNA can activate genes for flagellar synthesis or suppress a gene for curli biosynthesis, both mediated by Hfq. In the former mechanism, it resolves a hairpin structure that blocked translation by binding in the 5' UTR. In the latter, it causes mRNA degradation by recruitment of RNase E (Jørgensen et al., 2020). Other sRNAs in bacteria interact with CsrA, a post-transcriptional regulator typically repressing translation (Jørgensen et al., 2020; Smirnov et al., 2016). Its activity is modulated by sRNAs CsrB and CsrC, which sequester CrsA and prevent binding to its target mRNA (Jørgensen et al., 2020). Despite this, it can also function as a positive regulator, e. g. by binding to the 5' UTR of the *moaA* mRNA, where it then induced translation (Jørgensen et al., 2020). Finally, ProQ is another RNA binding protein in Gram-negative bacteria capable of binding and forming stable complexes with many sRNAs and mRNAs (Jørgensen et al., 2020). ProQ is involved in transcript stabilization for both mRNAs and sRNAs, e. g. the sRNA RaiZ (Jørgensen et al., 2020).

sRNA binding can promote degradation or protect mRNAs from degradation (Gottesman & Storz, 2011). A study demonstrated that the phosphorylation state of a mRNA 5' end impacts sRNA-mediated regulation (Schilder & Görke, 2023). sRNAs have also been shown to be involved in control of Rho-dependent termination at the 5' UTR of *rpoS* in *E. coli* (Sedlyarova et al., 2017).

Most *trans*-encoded RNAs are negative regulators, where base-pairing between sRNA and target mRNA leads to translational inhibition, thereby repressing protein levels, or mRNA degradation (or both; Waters & Storz, 2009). The *ompC* sRNA, encoded upstream of *ompF*, inhibits the production of the latter, reducing the amount of *ompF* mRNA (Mizuno et al., 1984). Its sequence is complementary to the 5' region of *ompF*, and hybridizes with it, causing premature transcription termination (Mizuno et al., 1984).

### 1.3.3 Translational control by sRNAs

The process of translation is split into three processes: initiation, elongation and termination. During initiation, the small subunit of the ribosome (30S) binds to a sequence 5-9 nt upstream of the translation start codon, the so-called Shine-Dalgarno (SD) sequence (Osada et al., 1999; Tollerson & Ibba, 2020; Shine & Dalgarno, 1974). The 16S rRNA in the 30S subunit shows complementarity to the SD sequence, allowing recognition. The initiation step is supported by three initiation factors (IF1, IF2 and IF3; Tollerson & Ibba, 2020). The shift to elongation starts with assembling of the 70S ribosome (30S subunit and 50S subunit are forming the 70S ribosome). The fully assembled ribosome starts translation at a start codon, usually an AUG. However, alternative start codons GUG and UUG as well as non-canonical start codons like

CTG exist as well (Hecht et al., 2017). The first amino acid (aa) brought to start translation by tRNAs is N-formyl methionine (fMet). Afterwards, translation occurs by tRNAs bringing amino acids according to the RNA sequence that are then added to a growing peptide chain with the help of elongation factor EF-Tu, while the ribosome catalyzes the formation of a peptide bond between amino acids (Tollerson & Ibba, 2020). Translation is normally terminated at a stop codon with the help of release factors (RF1, RF2 and RF3). The peptide chain is released, and the ribosome is then recycled (Tollerson & Ibba, 2020).

Masking the ribosome binding site (RBS) is common for sRNAs, as was shown for several sRNAs in *E. coli* that interfered with binding of the 30S ribosomal subunit (Sharma et al., 2007). 5' UTRs can also sequester the RBS when being heavily structured, as was shown for the alpha-toxin gene *hla* in *Staphylococcus aureus*, where binding of the RNAIII into the 5' UTR makes the RBS accessible for translation (Morfeldt et al., 1995). This constitutes an example of an sRNA that stimulates translation instead of blocking (Morfeldt et al., 1995).

Another mechanism of control is by blocking ribosome standby sites. Ribosome standby allows initiation of translation at RBS that have stable structures. The 30S subunit binds to single stranded RNA regions, and upon opening of the inhibitory structure, relocates to the RBS (de Smit & van Duin, 2006; Romilly et al., 2019). This mechanism can occur even over long distances, as shown for the *tisB* mRNA in *E. coli*. The IstR-1 RNA base-pairs at the standby site more than a 100 nt upstream, reaching the RBS once the structure unfolds. This requires ribosomal protein S1 (Romilly et al., 2019).

### 1.3.4 sRNAs can mediate inter-kingdom control of gene expression

Inter-kingdom interactions are common in soil, where microorganisms and plants co-exist, both independently and in symbiosis. Such sRNAs have been shown to be central to these interactions, regulating gene expressions across organisms (Regmi et al., 2022).

In *Pseudomonas fluorescens*, three sRNAs protect cucumber plants from infection of a pathogen by de-repression of biocontrol factors. Rhizobacterial sRNAs have been shown to silence genes in soybean that are involved in root/hair development, thereby affecting rhizobial infection and nodulation (Regmi et al., 2022).

### 1.3.5 sRNAs in response to antibiotics

Antibiotic exposure can have severe effects on the transcriptome of bacteria (Bie et al., 2023). Cis-encoded RNAs often act as attenuators, coupling the expression of a resistance gene to the presence of a cognate antibiotic (Dersch et al., 2017). *Trans*-encoded sRNAs have been shown to influence or regulate antibiotic tolerance in bacteria as well. The sRNAs base-pair to certain mRNA targets that encode functions important for antibiotic tolerance, e. g. efflux pumps or transport proteins (Fig. 3; Dersch et al., 2017).

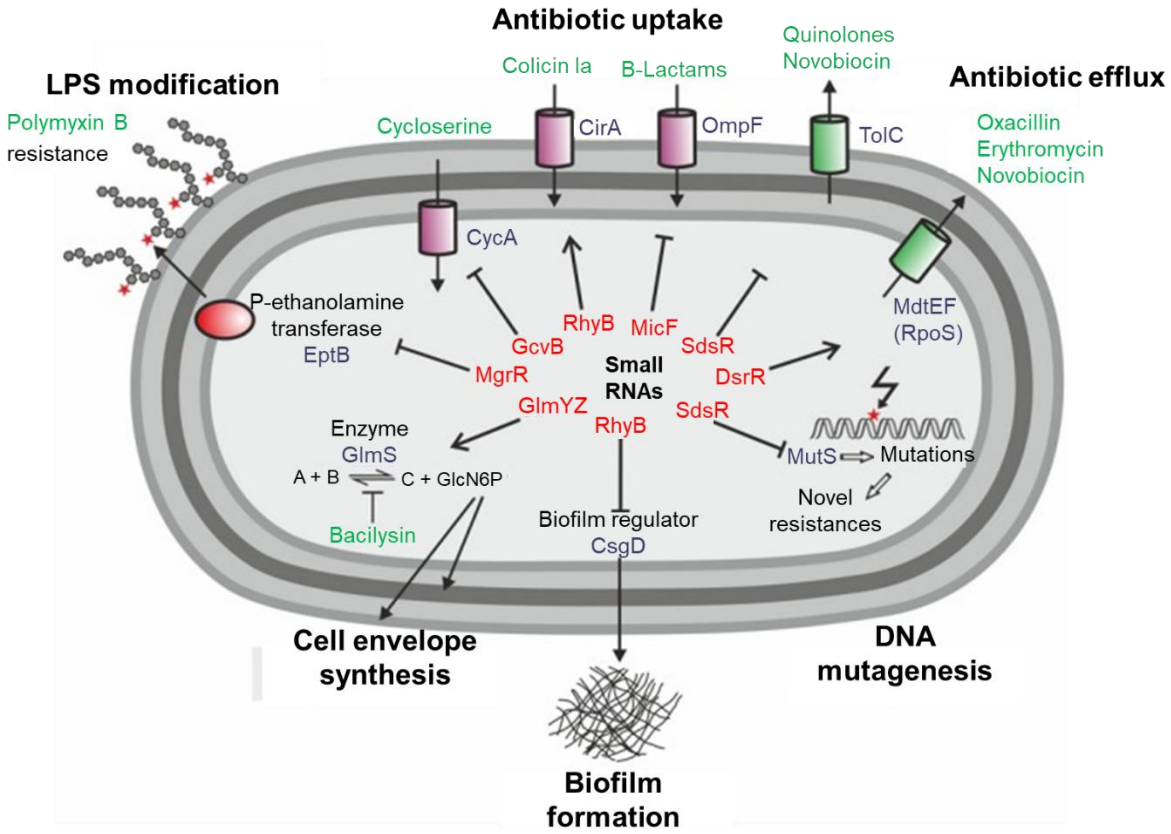


**Fig. 3:** RNAs encoded in trans which influence antibiotic susceptibility and resistance in *E. coli*. Red, small RNAs; blue, target proteins; green, antibiotics. Figure modified after Dersch et al., 2017.

A study in *Enterobacteriaceae* identified two small sRNAs GLmY and GlmZ that play a critical role in regulation of antibiotic resistance (Khan et al., 2016). They regulate the glucosamine-6-phosphate synthase (GlmS) which functions as a key component in bacterial cell wall synthesis. The small RNAs confer intrinsic resistance to antibiotics that target GlmS, as they modulate expression under antibiotic exposure (Khan et al., 2016). The small RNA RhyB from *E. coli* was shown to be involved in bacterial persistence, a way that allows bacteria to survive exposure to antibiotics (Zhang et al., 2018). sRNA MgrR was shown to be involved in changing the sensitivity of cells to antimicrobial peptides (Moon & Gottesman, 2009). The GcvB sRNA in *E. coli* was found to modulate expression of transport systems for dipeptides and oligopeptides (Urbanowski et al., 2000). A study in *Staphylococcus aureus* showed a small sRNA to influence not only cell wall synthesis but also contribute to antibiotic resistance (Borgmann et al., 2018). In the multi-resistant *S. aureus* (MRSA), alterations in sRNA profiles involved in regulating genes that are associated with stress responses were found upon subinhibitory antibiotic exposure (Howden et al., 2013). In *Salmonella enterica*, response to the antibiotic tigecycline was conducted, showing that exposition to the antibiotic induced the production of four sRNAs (sYJ5, sYJ20, sYJ75, and sYJ118). It furthermore contributed to the bacterial stress response, and sYJ20 was shown to have a role in antibiotic stress response (Yu & Schneiders, 2012). In *Bacillus licheniformis*, an attenuation mechanism for the *ermK* gene was found to provide resistance to a certain class of macrolide antibiotics (Kwak et al., 1991). The *ermK* regulation occurs through a leader peptide, where a transcription attenuation mechanism modulates the expression of the gene in response to antibiotic exposure (Kwak et al., 1991). These studies show that sRNAs and their regulatory mechanisms have diverse roles in the cell, such as the adaptation to antibiotics or stress response.

### 1.3.6 Small upstream open reading frames

sRNAs, aside from their regulatory function, can harbor open reading frames (ORFs). Their identification and annotation proved difficult, as it requires specialized tools, such as ribosome profiling (Vazquez-Laslop et al., 2022). Computational tools to identify small ORFs exist mainly for eukaryotes, but not prokaryotes (Egorov & Atkinson, 2023). Alternative open reading frames either in or out of frame have been discovered (Fig. 4; Orr et al., 2020). These ORFs either upstream or downstream of annotated ORFs can express functional small proteins (Orr et al., 2020).

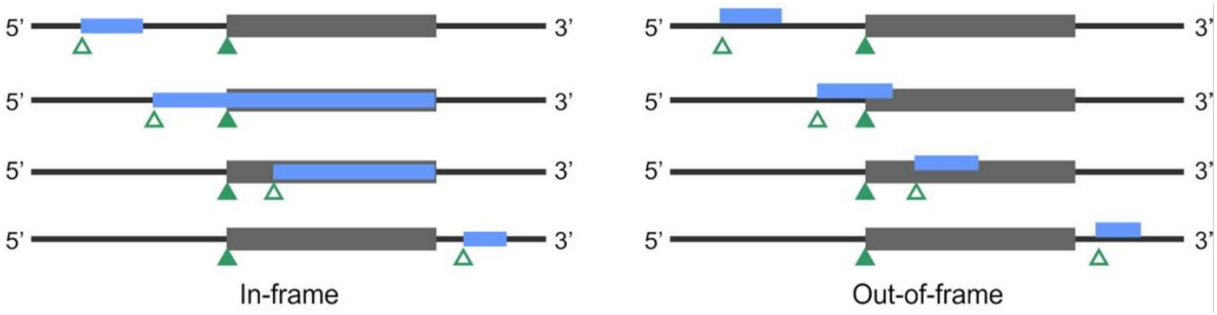


**Fig. 4:** Alternative ORFs on mRNAs (modified after Orr et al., 2020). sORFs (blue) can be found in or out of frame of annotated ORFs (dark grey). Solid green triangle, start codon, empty green triangle, alternative start codon.

uORF regulation occurs at the post-transcriptional or translational level, where they can regulate translation by various mechanisms that influence the ribosome, such as disrupting translation initiation, mediating mRNA decay or stalling or sequestering the ribosome (Ito & Chiba, 2013; Lovett & Rogers, 1996; Vind et al., 2024). Usually, upstream open reading frames (uORFs) are regulators of their downstream genes acting in *cis*, as was described above for attenuators. Attenuation dependent on the translation of an upstream ORF has been shown for many genes, including but not limited to the tryptophan attenuator where amino acid availability dictates translation efficiency (Lee et al., 2022; Yanofski et al., 1981). Antibiotics inhibiting translation can have a similar effect, where the downstream affected gene is usually a resistance gene (Dersch et al., 2017; Lee et al., 2022). This has been shown for the *wblC* gene in the actinomycete *Streptomyces coelicolor*, where a mechanism for riboregulation has been described in response to antibiotics targeting the ribosome (Lee et al., 2022). Recently, in *E. coli* the TopAI-YjhQ toxin-antitoxin system was shown to be regulated by an uORF (Baniulyte & Wade, 2024). The authors suggest that several ribosome-targeting antibiotics lead to stalling of ribosomes at different positions within the uORF. This alters the secondary structure of the RNA, making the RBS accessible (Baniulyte & Wade, 2024).

## 1.4 Small proteins and proteins containing a DUF1127 domain

Small proteins have only recently come into focus. Previously, they were often overlooked, such as a cutoff was introduced (e. g. 100 codons; Harrison et al., 2002), leaving smaller ORFs undetected, as there are proteins even smaller than 30 aa (Storz et al., 2014). Furthermore, sORFs were featured in intergenic regions or starting with non-canonical start codons, making annotation and detection challenging. Aside from difficulties in validating small proteins by SDS-PAGE since they run out of the gel, mutations often caused no clear phenotype (Storz et al., 2014). However, many small proteins have been identified in recent years, especially through small RNAs encoding small proteins (Storz et al., 2014).

Small proteins are involved in many cellular functions, e. g. stress response, morphology or regulatory networks. Small proteins have been shown to affect cell division (e. g. MciZ, 40 aa),

regulate transport (e. g. AcrZ, 49 aa) or endospore formation (SpoVM and CmpA, both 26 aa; Storz et al., 2014).

In many protein families, certain motifs are occurring that have not been yet associated with a function (Lv et al., 2023). Among the domains of unknown function (DUF), DUF1127 domains have been found to be widely spread, and being prominent especially in the Alpha- and Gammaproteobacteria. Especially within the Alphaproteobacteria, multiple members of this family have been reported in a single genome (Kraus et al., 2020). The Pfam database, in 2019, listed about 4 000 bacteria harboring 17 000 proteins with such a domain (El-Gebali et al., 2019, Kraus et al., 2020).

DUF1127 proteins are arginine rich. Identifying these proteins can be challenging, as they are relatively small (Kraus et al., 2020). In some Alphaproteobacteria, however, DUF1127 proteins have been characterized. In *Agrobacterium tumefaciens*, a plant-associated pathogen, seven proteins containing a DUF1127 domain were found: three short ones (less than 50 aa) and four longer ones. The genes are regulated by a LysR-type transcriptional regulator called LsrB (Kraus et al., 2020). The three smaller DUF1127 mRNAs in *A. tumefaciens* were shown to be produced in different phases of growth. Furthermore, different stressors resulted in changed expression patterns (Kraus et al., 2020). Deleting the three smaller DUF1127 genes led to significant changes in cell phenotype, such as increased cell aggregation or unusual growth defects in later stages of growth (Kraus et al., 2020). Transcriptome analysis of the same triple mutant showed that the genes were involved in phosphate uptake, nitrate respiration and homeostasis of serine and glycine (Kraus et al., 2020).

In *Rhodobacter sphaeroides*, a facultative phototrophic alphaproteobacterium, a member of the DUF1127 family was characterized to be an RNA binding protein (Grützner et al., 2021). RSP_6037 (renamed *ccaF1*) is followed by the genes of four sRNAs (named CcsR1-4). The CcaF1 protein was demonstrated to act on CcsR levels in *trans* and, together with RNase E, is involved in processing the transcript and maturation of the sRNAs (Grützner et al., 2021). In *R. sphaeroides*, the DUF1127 domain-containing protein CcaF1 affects the oxidative stress response (Grützner et al., 2021).

Three DUF1127 genes have been discovered in *Brucella abortus*, (Budnick et al., 2018). The study showed that the genes are regulated by the LysR-type transcriptional regulator VtlR. Furthermore, the three proteins are linked to fucose utilization as a carbon source (Budnick et al., 2018). *In Escherichia coli* and *Salmonella enterica*, typical Gammaproteobacteria, the gene *yjiS* contains a DUF1127 domain and seems to be involved in regulation of virulence (Kraus et al., 2020).

## 1.5 Antibiotics in the environment

Antibiotics have always been in the environment since many producers live in the soil habitat (Walsh & Duffy, 2013). However, antibiotics have also been introduced into the environment by humans, e. g. via agricultural practices or sewage slugs (Cycon et al., 2019). While antibiotics are degraded by biotic and abiotic processes, they impact the microbial communities in the soil, such as changing microbial diversity. Prolonged exposure of antibiotic treatment fosters resistance development which can be spread amongst microbes by horizontal gene transfer (Cycon et al., 2019).

Bacteria have developed several mechanisms to deal with antibiotic exposure, one being multidrug efflux pumps (Paulsen, 2003; Blair et al., 2015). These pumps, like AcrAB-TolC in *E. coli*, expel antibiotics, thus reducing the intracellular concentration of the antibiotic. Further mechanisms include the enzymatic inactivation of antibiotics, e. g. enzymes like β-Lactamases

that hydrolyze the β-lactam ring of penicillins. Target modification is another common mechanism, e. g. mutations or methylation of ribosomal RNA that protect against various antibiotics (Blair et al., 2015).

Bacterial producers of antibiotics originate from Actinobacteria, mainly members of the *Streptomyces* genus (Clardy et al., 2009). Their role can range from signaling molecules regulating microbial community interactions or gene expression to niche defense mechanisms to avoid competitors when resources are limited (Clardy et al., 2009).

For tetracycline (Tc), evidence for a signaling role has been found (Yuan et al., 2023; Vasilchenko & Rogozhin, 2019). This aligns well with the production of tetracycline by *Streptomyces aureofaciens*, a typical soil microbe. Indeed, the group of yellow antibiotics was first described with the chlorinated aureomycin derived from this actinobacterium in 1948 (Duggar, 1948). A naturally produced antibiotic in soil is prone to become diluted, depending on the amounts produced and the distance of the receiving cell to the producer, which makes it likely that a signaling role could evolve.

Thus, co-occurring organisms in soil might be expected to respond to diluted tetracycline. The natural occurrence of *Sinorhizobium* in soil is linked to its ability to infect nodule forming plants of the Fabaceae, where bacterial nitrogen fixation is established in mutual symbiosis. After plant death, the nodules in soil are disintegrating, the bacteroids are contributing to soil fertilization, while the non-bacteriodal, rod-shaped bacteria survive, grow and can infect another plant. At least during that part of their life cycle in soil, rhizobia will naturally be exposed to low concentrations of tetracycline. This is complementing the interactions with the host plant including attraction to the host root (Compton et al., 2020).

## 1.6 *Sinorhizobium meliloti*

Among the Alphaproteobacteria, the nitrogen fixing mutual symbionts of the *Rhizobium* group are prominent members with an interesting ecological function. *Sinorhizobium meliloti* is such a plant symbiont with alters in its life cycle between a soil-dwelling and a plant-associated phase (Wells & Long, 2002). The well-understood plant symbiosis requires signaling between host and symbiont, including the plant flavonoids attracting rhizobia, bacterial nod factors inducing root hair bending for invasion, and many more specific signals being exchanged to induce the leghemoglobin synthesis by the plant required to keep up anoxic conditions for the nitrogen fixation and at the same allowing for high ATP yields through aerobic respiration (Djordjevic, 2004; Madigan et al., 2021).

*Sinorhizobium meliloti* has many *trans*-encoded and antisense (3 % and 2 % of the encoded genes, respectively) sRNAs (Schlüter at al., 2010; Valverde, 2008). An example is given by the two sRNAs AbcR1 and AbcR2 (Torres-Quesada et al., 2013). They are stabilized by Hfq and show divergent unlinked regulation (Torres-Quesada et al., 2013). AbcR1 is expressed in dividing bacteria while Abcr2 is expressed when entering stationary phase or when subjected to abiotic stresses (Torres-Quesada et al., 2013). Further sRNAs as well as sORFs were also investigated, e. g. the dual-functioning tmRNA (SsrA) operates in *trans* to recycle stalled ribosomes and is expressed upon stress before being processed (Hadjeras et al., 2023; Robledo et al., 2020).

During the life phase in soil *ex planta*, signal exchange with co-occurring soil microbes will be required. While this is less understood, one of the factors influencing life in soil will be co-habitation with antibiotics-producing microorganisms (Hover et al., 2018; Panter et al., 2021). As streptomycetes are prominent members of the soil community, their ability to produce antibiotics will impact other community members. The production of an antibiotic leads to

gradients of different antibiotics, dependent on soil chemistry, producer and its metabolic abilities, and diffusion of the produced antibiotic in the soil water with increasing distance to the producer strain (Donald et al., 2022). Hence, a role different from being bacteriostatic or bacteriocidal will result at concentrations below the lethal dose in the natural environment, and hence roles for antibiotics as signals to other community members will result. One antibiotic first discovered from soil-derived streptomycetes, is tetracycline.

## 1.7 Aims

In this work, the early response of *Sinorhizobium meliloti* 2011 to tetracycline (Tc) was investigated. Focus was placed on transcripts with a distinct response to short-term, sublethal Tc application in logarithmically growing cultures of *S. meliloti* 2011. In addition to using tetracycline at sub-inhibitory concentrations, the antibiotic exposure time was chosen to identify the first line of response, with only 10 min of treatment. In a slow-growing organism like *S. meliloti* (Dai et al., 2018), this short-term treatment will predominantly identify direct transcriptional and post-transcriptional responses. Thus, an RNA sequencing was performed with the specific interest in short-term response of *S. meliloti* to a sub-inhibitory concentration of tetracycline.

The RNA sequencing revealed differentially expressed genes. The aim of this work was to analyze several up-regulated and down-regulated genes to get insight into the mechanisms leading to transcriptome remodeling upon tetracycline exposure. The gene with the highest increase in mRNA level, a *duf1127* gene, was found to be preceded by an uORF. A major aim of this study was to analyze the impact of the uORF on the regulation of the *duf1127* gene. Northern hybridization, RT-qPCR, 3'RACE and Western blot were used to verify working hypotheses and to propose a model for the post-transcriptional regulation mechanism.

# 2. Material and Methods

## 2.1 Materials

### 2.1.1 Strains and plasmids

For this study, *S. meliloti* 2011 was considered wildtype (WT). The knockout mutation Δ*duf1127₁*-part in this strain was generated via homologous recombination. The *Escherichia coli* DH5α was used for cloning, while *E. coli* S17-1 was used for biparental conjugation of plasmids into *S. meliloti* (Tab. 1).

**Tab. 1:** Strains used in this study.

| Strain | Description | Reference |
|---|---|---|
| *Sinorhizobium meliloti* 2011 | Insertion in *expR* gene; $Sm^R$ | Casse et al., 1979; Meade & Signer, 1977 |
| *S. meliloti* 2011 Δ*duf1127₁*-part | *S. meliloti* 2011 with a partial deletion of the *duf1127₁* gene between codon 10 and stop; $Sm^R$ | This study |
| *Escherichia coli* DH5α | Used for cloning and plasmid replication. F-Φ80*lacZ*ΔM15Δ(*lacZYA-argF*) U169 *recA1 endA1*, *hsdR17* (rK-, mK+), *phoA*, *supE44 thi-1* | NEB; Chan et al., 2013 |
| *Escherichia coli* S17-1 | Used for conjugation of plasmids into *S. meliloti* 2011. *recA*, *pro*, *hsdR*, *RP4⁻²* (Tc::Mu)(Km::Tn7); $TP^R$, $Str^R$, $Sp^R$ | Simon et al., 1983 |

Plasmids were constructed with different modifications in the genes of interest (Tab. 2) and introduced into the *S. meliloti* WT background by conjugation (see section 2.2.1.3).

**Tab. 2:** Plasmids used in this study. All nucleotide modifications are relative to the transcription start site (TSS; +1). Vector backbones were used according to Hadjeras et al., 2023.

| Name | Description | Vector backbone, resistance |
|---|---|---|
| pDUF'-SPA | Plasmid featuring *duf1127₁* promoter region (-237 to +1), uORF1 and the first 10 codons of *duf1127₁* fused to a *spa* tag; translational fusion | pSW1, $Gm^R$ |
| p*duf1172₁*-SPA | Plasmid featuring the entire *duf1127₁* operon and its promoter region (-237 to +1) with a *spa* tag; translational fusion | pSW1, $Gm^R$ |
| puORF1-SPA | *duf1127₁* promoter region + uORF1 fused to a spa tag; translational fusion | pSW1, $Gm^R$ |
| pM1/Stop | pDUF'-SPA derivate with a start to stop mutation in uORF1; translational fusion | pSW1, $Gm^R$ |
| pC11/Stop | pDUF'-SPA derivate with a stop mutation at codon 11 (Cys) in uORF1; translational fusion | pSW1, $Gm^R$ |
| pA15/Stop | pDUF'-SPA derivate with a stop mutation at codon 15 (Ala) in uORF1; translational fusion | pSW1, $Gm^R$ |
| pT17/Stop-SPA | pDUF'-SPA derivate with a stop mutation at codon 17 (Thr) in uORF1; translational fusion | pSW1, $Gm^R$ |
| pS19/Stop-SPA | pDUF'-SPA derivate with a stop mutation at codon 19 (Ser) in uORF1; translational fusion | pSW1, $Gm^R$ |
| pΔ1 | pDUF'-SPA derivate with nucleotide postions +121 to +168 of the IGR deleted; translational fusion | pSW1, $Gm^R$ |
| pΔ1-1 | Δ1 derivate with nucleotide positions +121 to 128 of the IGR deleted; translational fusion | pSW1, $Gm^R$ |

| | | |
|---|---|---|
| pΔ2 | pDUF'-SPA derivate with nucleotide positions +169 to +209 of the IGR deleted; translational fusion | pSW1, $Gm^R$ |
| pΔ3 | pDUF'-SPA derivate with nucleotide positions +212 to +265 of the IGR deleted; translational fusion | pSW1, GmR |
| pDUF'-ch121-128-SPA | pDUF'-SPA derivate with mutated residues at nucleotide positions +121 to +128; translational fusion | pSW1, $Gm^R$ |
| pM1-ch121-128-SPA | M1/Stop-SPA derivate with mutated residues at nucleotide positions +121 to +128; translational fusion | pSW1, $Gm^R$ |
| pS3-L10-ch | pDUF'-SPA derivate with codons 3 (Ser) to 10 (Leu) of uORF1 mutated to alter RNA but not protein sequence; translational fusion | pSW1, $Gm^R$ |
| pS3-L10-ch2 | pS3-L10 derivate now featuring no rare codons; translational fusion | pSW1, $Gm^R$ |
| pΔS3-L10 | pDUF'-SPA derivate with codons 3 (Ser) to 10 (Leu) of uORF1 deleted; translational fusion | pSW1, $Gm^R$ |
| pscramble | pDUF'-SPA derivate with codons 17 (Thr) to 23 (Ala) of uORF1 mixed up; translational fusion | pSW1, $Gm^R$ |
| pΔ18-33nt | pDUF'-SPA derivate with nucleotide positions +18 to +33 deleted; translational fusion | pSW1, $Gm^R$ |
| pCGC 192-194 ATC | pDUF'-SPA derivate with nucleotide positions +192 to +194 mutated to destroy a potential terminator; translational fusion | pSW1, $Gm^R$ |
| pGCC 135-137 CGG | pDUF'-SPA derivate with nucleotide positions +135 to +137 mutated to destroy a potential anti-terminator; translational fusion | pSW1, $Gm^R$ |
| puORF2-SPA | Plasmid featuring $duf1127_1$ promoter region (-237 to +1), uORF1 and uORF2 fused to a *spa* tag; translational fusion | pSW1, $Gm^R$ |
| pM2/Stop-SPA | uORF2-SPA derivate with a start to stop mutation in uORF2; translational fusion | pSW1, $Gm^R$ |
| pM2/Stop-DUF'-SPA | pDUF'-SPA derivate with a start to stop mutation in uORF2; translational fusion | pSW1, $Gm^R$ |
| pM1/Stop-M2/Stop-DUF'-SPA | pDUF'-SPA derivate with a start to stop mutation in uORF1 and uORF2; translational fusion | pSW1, $Gm^R$ |
| pPDUF-egfp | Plasmid featuring $duf1127_1$ promoter region (-237 to +1) fused to a sSD and *egfp*; promoter fusion | pRS1-sSD-egfp, $Gm^R$ |
| pDUF-egfp | Plasmid featuring $duf1127_1$ promoter region (-237 to +1), uORF1 and the first 10 codons of $duf1127_1$ fused to *egfp*; translational fusion | pRS1-egfp, $Gm^R$ |
| pPPha-egfp | Plasmid featuring *phaP1* promoter region (-217 to +1) fused to a sSD and *egfp*; promoter fusion | pRS1-sSD-egfp, $Gm^R$ |
| pPha-egfp | Plasmid featuring *phaP1* promoter region (-217 to +1) and the first 10 codons of *phaP1* fused to *egfp*; translational fusion | pRS1-egfp, $Gm^R$ |
| pP-RS24515 | duf11272 promoter region (-207 to +1) fused to a sSD and *egfp*; promoter fusion | pRS1-sSD-egfp, $Gm^R$ |
| p-RS24515 | $duf1127_2$ promoter region (-207 to +1) and full-length $duf1127_2$ fused to *egfp*; translational fusion | pRS1-egfp, $Gm^R$ |
| pRS24515-CDS-SPA | $duf1127_2$ promoter region (-207 to +1) and full-length $duf1127_2$ fused to a *spa* tag; translational fusion | pSW1, $Gm^R$ |
| pRS18160-SPA | RS18160 promoter region (-214 to +1) and RS18160 fused to a *spa* tag; translational fusion | pSW1, $Gm^R$ |
| pRS36240-SPA | RS36240 promoter region (-250 to +1) and RS36240 fused to a *spa* tag; translational fusion | pSW1, $Gm^R$ |
| pK18mob sacB | Suicide plasmid containing *sacB*, lethal in presence of sucrose | Schäfer et al., 1994; $Km^R$ |
| pK18mob sacB-duf11271-part | Suicide plasmid expressing a toxin upon sucrose exposure, used for generation of a partial chromosomal deletion of $duf1127_1$ | pK18, $Km^R$ |
| pJet | pJet 1.2/blunt cloning vector from CloneJET PCR cloning kit (Thermo Fisher Scientific) | $Amp^R$ |
| pRS1 | pSRKGm derivate where the *lac* module was replaced by a synthetic MCS | Hadjeras et al., 2023, $Gm^R$ |
| pSW1 | pRS1 derivative for cloning under the genes' own promotor and featuring a SPA tag preceded by a linker | Hadjeras et al., 2023, $Gm^R$ |

### 2.1.2 Oligonucleotides

Different primer sets (Microsynth, Tab. 3) were used for hybridization, cloning or PCR. Markers for gel electrophoresis used are given in Tab. 4.

**Tab. 3:** Oligonucleotides used in this study.

| Primer Name | Primer Sequence | Description (Primer efficiency) |
|---|---|---|
| NheI-P_SymBDUF1127-fwd | GCTAGCCGCAATAATGGCGGAGATCGATG | Primer used for construction of pDUF'-SPA and pDUF'-egfp and pPDUF-egfp and p*duf1172*$_1$-SPA using NheI and BamHI |
| BamHI-SymBDUF1127(10CD)-rev | CGGGATCCTTCGACAACTATAGCTTGTGGTTCAC | Primer used for construction of pDUF'-SPA and pDUF'-egfp using NheI and BamHI |
| BamHI-P_SymBDUF1127-rev | CGGGATCCATGAGGTGATCCTTGCACGAG | Primer used for construction of pPDUF'-egfp using NheI and BamHI |
| BamHI-DUF1127-rev | GGATCCATCCGGGCGCCCTGCCTT | Primer used for construction of p*duf1172*$_1$-SPA using NheI and BamHI |
| SEP26_ATG-TAG_fwd | GGCGTAAGTAGGATTCCAATCTCGTGTT | Primer used for construction of M1/Stop-SPA by mutagenesis of pDUF'-SPA |
| SEP26_ATG-TAG_rev | GAATCCTACTTACGCCTCCTCTGATTTGA | Primer used for construction of M1/Stop-SPA by mutagenesis of pDUF'-SPA |
| sORF26-C11Stop-Fw | GCCTCTGAGGCGGAACGGCTATCACGC | Primer used for construction of C11/Stop-SPA by mutagenesis of pDUF'-SPA |
| sORF26-C11Stop-Rv | TTCCGCCTCAGAGGCGCACAAACACGA | Primer used for construction of C11/Stop-SPA by mutagenesis of pDUF'-SPA |
| sORF26_A15-Stop_fwd | CGGAACGTGAATCACGCCTTCGATGCGTA | Primer used for construction of A15/Stop-SPA by mutagenesis of pDUF'-SPA |
| sORF26_A15-Stop_rev | GCGTGATTCACGTTCCGCCGCAGAGGCGC | Primer used for construction of A15/Stop-SPA by mutagenesis of pDUF'-SPA |
| sORF26_T17-Stop_fwd | GGCTATCTAGCCTTCGATGCGTAGCGCA | Primer used for construction of T17/Stop-SPA by mutagenesis of pDUF'-SPA |
| sORF26-T17-Stop_rev | CGAAGGCTAGATAGCCGTTCCGCCGCAG | Primer used for construction of T17/Stop-SPA by mutagenesis of pDUF'-SPA |
| PsORF26-S19Stop-Fw | ACGCCTTAGATGCGTAGCGCATCTCGT | Primer used for construction of S19/Stop-SPA by mutagenesis of pDUF'-SPA |
| sORF26-S19Stop-Rv | ACGCATCTAAGGCGTGATAGCCGTTCC | Primer used for construction of S19/Stop-SPA by mutagenesis of pDUF'-SPA |
| sORF-DUF1127_IGR_Mut1_up_rev | GTCATCCGGTCACGTCAGGTTCAGTAGCGGCTGAAACGAGATG | Primer used for construction of pΔ1 |
| sORF-DUF1127_IGR-Mut1_down_fwd | CATCTCGTTTCAGCCGCTACTGAACCTGACGTGACCGGATGAC | Primer used for construction of pΔ1 |
| duf1_IGR_d1-1Fw | CATCTCGTTTCAGCCGCTACTGATCACAAGCCCGCAATTCCGCCA | Primer used for construction of pΔ1-1 by mutagenesis of pDUF'-SPA |
| duf1_IGR_d1-1Rv | TGGCGGAATTGCGGGCTTGTGATCAGTAGCGGCTGAAACGAGATG | Primer used for construction of pΔ1-1 by mutagenesis of pDUF'-SPA |
| sORF-DUF1127_IGR-Mut2_down_fwd_new | CGCCATTTGGCGATCCCCTTTTTAGCGTTCCGCATCCGCACG | Primer used for construction of pΔ2 |

| | | |
|---|---|---|
| sORF-DUF1127_IGR-Mut2_up_rev_new | CGTGCGGATGCGGAACGCTAAAAAGGGGATCGCCAAATGGCG | Primer used for construction of pΔ2 |
| sORF-DUF1127_IGR_Mut3_up_rev | GTTCACGCATGACTGTCCGTCCCGCAAAAATGCGAACAATCGCCC | Primer used for construction of pΔ3 |
| sORF-DUF1127_IGR-Mut3_down_fwd | GGGCGATTGTTCGCATTTTTGCGGGACGGACAGTCATGCGTGAAC | Primer used for construction of pΔ3 |
| duf1_121-8_mutFw | GCTACTGAGTATTGGTTCACAAGCCCGCAATTCCG | Primer used for construction of pDUF'-ch121-128-SPA and pM1-ch121-128-SPA by mutagenesis of pDUF'-SPA |
| duf1_121-8_mutRv | GCTTGTGAACCAATACTCAGTAGCGGCTGAAACGA | Primer used for construction of pDUF'-ch121-128-SPA and pM1-ch121-128-SPA by mutagenesis of pDUF'-SPA |
| BamHI-SEP-26-rev | GGATCCGTAGCGGCTGAAACGAGATGC | Primer used for construction of puORF1-SPA using XbaI and BamHI |
| XbaI-SEP-26-fwd | TCTAGATCCGCAATTCAAATCAGAGGAGG | Primer used for construction of puORF1-SPA using XbaI and BamHI |
| uORF1_S3-L10-ch_Fwd | TGGATTCGAATCTGGTGTTTGTGAGGCTGTGCGGCGGAACGGCTATCA | Primer used for construction of pS3-L10-ch by mutation of pDUF'-SPA |
| uORF1_S3-L10-ch_Rev | CGCCGCACAGCCTCACAAACACCAGATTCGAATCCATCTTACGCCTCC | Primer used for construction of pS3-L10-ch by mutation of pDUF'-SPA |
| uORF1-S3-L10-ch_CGC-CGG_Fwd | TGGATTCGAATCTGGTGTTTGTGCGGCTGTGCGGCGGAACGGCTATCA | Primer used for construction of pS3-L10-ch2 by mutation of pDUF'-SPA |
| uORF1-S3-L10-ch_CGC-CGG_Rev | CGCCGCACAGCCGCACAAACACCAGATTCGAATCCATCTTACGCCTCC | Primer used for construction of pS3-L10-ch2 by mutation of pDUF'-SPA |
| uORF1_Del-S3-L10_Fwd | CAGAGGAGGCGTAAGATGGATTGCGGCGGAACGGCTATCACGC | Primer used for construction of pΔS3-L10 by mutagenesis of pDUF'-SPA |
| uORF1_Del-S3-L10_Rev | GCGTGATAGCCGTTCCGCCGCAATCCATCTTACGCCTCCTCTG | Primer used for construction of pΔS3-L10 by mutagenesis of pDUF'-SPA |
| sORF26_scramble-mut_fwd | TCGAGCTCTCGTCCGGCAACCATGCGTTTCAGCCGCTACTGATC | Primer used for construction of pscramble by mutagenesis of pDUF'-SPA |
| sORF26_scramble-mut_rev | CATGGTTGCCGGACGAGAGCTCGAGATAGCCGTTCCGCCGCAG | Primer used for construction of pscramble by mutagenesis of pDUF'-SPA |
| Del-20-35nt_fwd | CTCATCCGCAATTCAAATCAGATTCCAATCTCGTGTTTGTGC | Primer used for construction of pΔ18-33nt by mutagenesis of pDUF'-SPA |
| Del-20-35nt_rev | GCACAAACACGAGATTGGAATCTGATTTGAATTGCGGATGAG | Primer used for construction of pΔ18-33nt by mutagenesis of pDUF'-SPA |
| 2024_IGR_Term-proof-1_fwd | TGACGGGATCATTGTTCGCATTTTTGCGT | Primer used for construction of pCGC 192-194 ATC by mutation of pDUF'-SPA |
| 2024_IGR_Term-proof-1_rev | GAACAATGATCCCGTCATCCGGTCACGTC | Primer used for construction of pCGC 192-194 ATC by mutation of pDUF'-SPA |
| 2024_IGR_AT-proof-1_fwd | CTCACAACGGCGCAATTCCGCCATTTGGC | Primer used for construction of pGCC 135-137 CGG by mutation of pDUF'-SPA |
| 2024_IGR_AT-proof-1_rev | AATTGCGCCGTTGTGAGCCTTGGATCAGT | Primer used for construction of pGCC 135-137 CGG by mutation of pDUF'-SPA |
| NheI_new-sORF_fwd | GCTAGCATGACGGGGCGATTGTTCGCAT | Primer used for construction of puORF2-SPA using SpeI and NheI |
| SpeI_new-sORF_rev | ACTAGTGAGACGTGCGGATGCGGAAC | Primer used for construction of puORF2-SPA using SpeI and NheI |

| | | |
|---|---|---|
| ATG-TAG_new-sORF_fwd | TGACCGGTAGACGGGGCGATTGTTCGCAT | Primer used for construction of pM2/Stop-SPA and pM2/Stop-DUF'-SPA by mutagenesis of puORF2-SPA and pDUF'-SPA, respectively |
| ATG-TAG_new-sORF_rev | CCCCGTCTACCGGTCACGTCAGGTAAAA | Primer used for construction of pM2/Stop-SPA and pM2/Stop-DUF'-SPA by mutagenesis of puORF2-SPA and pDUF'-SPA, respectively |
| NheI-P_PhaP1-fwd | CGGCTAGCCAATGTCGATGAAGGGGTACTGT | Primer used for cloning of pPPha-egfp and pPha-egfp using NheI and BamHI |
| BamHI-P-PhaP1-rev | CGGGATCCATGGCCGTTCTATAGCCGATT | Primer used for cloning of pPPha-egfp using NheI and BamHI |
| BamHI-PhaP1(10CD)-rev | CGGGATCCAAATGCGTCTTCGGTCTTCCT | Primer used for cloning of pPha-egfp using NheI and BamHI |
| NheI_P_RS24515_fwd | GCTAGCGATCCATCGATGAGGGGGA | Primer used for cloning of p*duf1127*$_2$ and pP-*duf1127*$_2$ using NheI and BamHI |
| BamHI_P_RS24515_rev | GGATCCTATAGCCTTTCTATCGGATGCTC | Primer used for cloning of pP-*duf1127*$_2$ using NheI and BamHI |
| BamHI_RS24515-CDS_rev | GGATCCTTGGTCCGTCTTATGTACTGCA | Primer used for cloning of p-*duf1127*$_2$ using NheI and BamHI |
| NheI_P_RS18160_fwd | GCTAGCGGGAAAGCGTGCTCCCGATA | Primer used for construction of pRS18160 using NheI and BamHI |
| BamHI_RS18160-CDS_rev | GGATCCGTACCGGTAATATCCATAGGCAGGC | Primer used for construction of pRS18160 using NheI and BamHI |
| NheI_P_RS36240_fwd | GCTAGCATCTTCCAGCCGTTCGGC | Primer used for construction of pRS36240 using NheI and BamHI |
| BamHI_RS36240-CDS_rev | GGATCCGAGTTTGGCTTGGCAGTATTGC | Primer used for construction of pRS36240 using NheI and BamHI |
| DUF1127_partial-KO_down_fwd | TGCCTCGGATCCGTCGACGGCTGACCTGCAGTGGTCGGCCTGCTG | Primer used for construction of pK18mobsacB-*duf1127*$_1$-part using EcoRI and XbaI |
| DUF1127_partial-KO_up_rev | TGCCTCGGATCCGTCGACGGCTTCGACAACTATAGCTTGTGGTTC | Primer used for construction of pK18mobsacB-*duf1127*$_1$-part using EcoRI and XbaI |
| EcoRI_DUF1127_partial-KO_up_fwd | GAATTCCATCTCGTTTCAGCCGCTAC | Primer used for construction of pK18mobsacB-*duf1127*$_1$-part using EcoRI and XbaI |
| XbaI_DUF1127_partial-KO_down_rev | TCTAGATGACCTGCAGTGGTCGGCC | Primer used for construction of pK18mobsacB-*duf1127*$_1$-part using EcoRI and XbaI |
| NB-SymB8816 | AGCCTTGGATCAGTAGCGGCTG | Northern Blot probe NB1 (nucleotide positions +107 to +129) |
| sORF26_3'_NB | CATCCGGTCACGTCAGGTAAAAAGGG | Northern Blot probe (nucleotide positions +160 to +186) |
| NB-probe_IGR2 | CCCCGTCATCCGGTCACGTCAGGT | Northern Blot probe (nucleotide positions +168 to +192) |
| DUF1127-1-operon_NB_3 | GTGACGCAGCCAGGTCCTTTCGAG | Northern Blot probe NB2 (nucleotide positions +237 to +260) |
| NB-SymB-DUF1127 | CATCCGATTCGACAGATGGGTGATCT | Northern Blot probe (nucleotide positions +412 to +438) |
| NB-FLAG | GTGGTCCTTGTAGTCGCCGTCGTG | Northern Blot probe binding the 3xFLAG part of the SPA tag |
| NB_5S_rRNA | GTTCGGAATGGGAACGGGTGCAG | Northern Blot probe binding in the 5S rRNA of *S. meliloti* |
| 3'-RACE_Fwd_nested-PCR | GCAATTCAAATCAGAGGAGGC | Primer used for nested PCR on RT-qPCR template in 3' RACE |
| 3'-RACE_Rev_nested-PCR | CCGACAGATTGATGGTGC | Primer used for nested PCR on RT-qPCR template in 3' RACE |
| 3'-RACE_Fwd_RT-PCR | ATCCGCAATTCAAATCAGAGGAG | Primer used for RT-qPCR in 3' RACE |

| | | |
|---|---|---|
| 3‘-RACE_Rev _RT-PCR | GACCACCGACAGATTGATGGT GCCTAC | Primer used for RT-qPCR in 3' RACE |
| qRT2-SymB-DUF1127-fwd | GGTCGATGAACTTTACCGGA | Primer used for RT-qPCR of *duf1127*$_1$ (1.94) |
| qRT2-SymB-DUF1127-rev | CCTGAATGAAGGCGCCTATG | Primer used for RT-qPCR of *duf1127*$_1$ (1.94) |
| qRT_RS24515 _fwd | ATCGAGCCAGGGTCTTGC | Primer used for RT-qPCR of *duf1127*$_2$ (1.96) |
| qRT_RS24515 _rev | TGTACTGCATCATCGACGGA | Primer used for RT-qPCR of *duf1127*$_2$ (1.96) |
| qRT-eGFP -Sme fwd | GGACGACGGCAACTACAAGA | Primer used for RT-qPCR of *egfp* (2.04), s. Scheuer et al., 2022) |
| qRT-eGFP -Sme rev | TTGTACTCCAGCTTGTGCCC | Primer used for RT-qPCR of *egfp* (2.04), s. Scheuer et al., 2022) |
| qRT metZ fwd | ACACCAAGGTCTTCTTCCTC | Primer used for RT-qPCR of *metZ* (1.91), s. Scheuer et al., 2022) |
| qRT metZ rev | CGTCTACCCACTGCTTGTC | Primer used for RT-qPCR of *metZ* (1.91), s. Scheuer et al., 2022) |
| qRT_moeA _neu_2_fwd | CTTTCGACAATTCCGCGA | Primer used for RT-qPCR of *moeA* (1.88) |
| qRT_moeA _neu_2_rev | CCGTGTCTTCCTGAATGATG | Primer used for RT-qPCR of *moeA* (1.88) |
| qRT_moeA _fwd | CAGATCATCGCTTCGAACAG | Primer used for RT-qPCR of *moeA* (1.91) |
| qRT_moeA_rev | GCCAGAAATCAAGCGTCATG | Primer used for RT-qPCR of *moeA* (1.91) |
| pdxA-neu_2_ fwd_qRT | CCAGACCGTGCCGATATG | Primer used for RT-qPCR of *pdxA* |
| pdxA-neu_2 _rev_qRT | CTTGGAAATCGGATTGGTGG | Primer used for RT-qPCR of *pdxA* |
| PhaP1-Fw | GCCTACGCCAAGATGAAGAC | Primer used for RT-qPCR of *phaP1* (1.94) |
| PhaP1-Rv | GTCTGCAGTTCGACGAGTTC | Primer used for RT-qPCR of *phaP1* (1.94) |
| qRT_ppiD_fwd | TGACCGAGCAGGATTACATC | Primer used for RT-qPCR of *ppiD* (1.93) |
| qRT_ppiD_rev | CCAGCTTGATGTAGCTGATC | Primer used for RT-qPCR of *ppiD* (1.93) |
| qRT-2-rpob fwd | GAAATGGAGGTCTGGGCTCT | Primer used for RT-qPCR of *rpoB* (1.98) |
| qRT-2-rpob rev | CGTTGAAGCTCTCCGGAATG | Primer used for RT-qPCR of *rpoB* (1.98) |
| Sso41-qPCR-Fw | GCATCCAAGGCACCTATCTC | Primer used for RT-qPCR of *rrp41* mRNA from *Sulfolobus acidocaldarius* (1.96) |
| Sso41-qPCR-Rv | GGAGGCGGCCATTAATGAAA | Primer used for RT-qPCR of *rrp41* mRNA from *Sulfolobus acidocaldarius* (1.96) |
| qRT_RS18160_ fwd | TGAAGCTTTTGACCATCGCA | Primer used for RT-qPCR of RS18160 |
| qRT_RS18160_ rev | CATTTCCGCTCGATCTTGCA | Primer used for RT-qPCR of RS18160 |
| qRT_RS36240_ fwd | CCTCACCATTATCAGCCTGC | Primer used for RT-qPCR of RS36240 |
| qRT_RS36240_ rev | TCAGAGTTTGGCTTGGCAGT | Primer used for RT-qPCR of RS36240 |
| rsmA_qRT-2_fwd | CGTGACAGTGATCGAAGTC | Primer used for RT-qPCR of *rsmA* (1.89) |
| rsmA_qRT-2_rev | TAGGGAAGATTGGCGATGAT | Primer used for RT-qPCR of *rsmA* (1.89) |
| rsmA_qRT_fwd | ATCATCGCCAATCTTCCCTA | Primer used for RT-qPCR of *rsmA* (1.90) |
| rsmA_qRT_rev | CTGCCATAGTGATCGTCATC | Primer used for RT-qPCR of *rsmA* (1.90) |
| qRT_SPA_fwd | AAGAACTTCATCGCGGTCTC | Primer used for RT-qPCR of *spa* mRNA (1.76) |
| qRT_SPA_rev | CTTGTAGTCGATGTCGTGGTC | Primer used for RT-qPCR of *spa* mRNA (1.76) |
| qRT_SEP26+ sRNA_fwd | TCCAATCTCGTGTTTGTGCG | Primer used for RT-qPCR of uORF1 (1.99) |
| qRT_SEP26+ sRNA_rev | GAACAATCGCCCCGTCATC | Primer used for RT-qPCR of uORF1 (1.99) |

| | | |
|---|---|---|
| 16S rRNA-qPCR-f | TCTACGGAATAACGCAGG | Primer used for RT-qCR of 16S rRNA (1.98) |
| 16S rRNA-qPCR-r | GTGTCTCAGTCCCAATGT | Primer used for RT-qCR of 16S rRNA (1.98) |
| check-PCR_DUF1127_part-KO_rev | GCATGGTGACGATGGGAGCTTGCAC | Primer used to check partial deletion of *duf1127*$_1$ |
| check-PCR_DUF1127-part-KO_int_rev | TCCGATTCGACAGATGGGTGATCT | Primer used to check partial deletion of *duf1127*$_1$ |

**Tab. 4:** Length and size markers used in this study.

| **Name** | **Manufacturer** |
|---|---|
| GeneRuler 1 kb Plus | Thermo Fisher Scientific |
| Spectra™ Multicolor protein ladder, Low range | Thermo Fisher Scientific |

### 2.1.3 Kits, enzymes and chemicals

For working with nucleic acids or proteins, different kits or enzymes were used (Tabs. 5-7).

**Tab. 5:** Kits and Reagents used in this study.

| **Name** | **Manufacturer** |
|---|---|
| Brilliant III Ultra-Fast SYBRGreen RT-QPCR Master Mix | Agilent Technologies |
| Deoxyribonucleoside triphosphate (dNTPs) | Thermo Fisher Scientific |
| Lumi-Light Western Blotting Substrate | Merck |
| Luna Universal One-Step RT-qPCR Kit | NEB |
| NucleoSpin Gel and PCR Clean-up, Mini kit for gel extraction or PCR clean up | Macherey-Nagel |
| RNeasy Mini Kit | Qiagen |
| TURBO DNA-free™ Kit | Thermo Fisher Scientific |

**Tab. 6:** Enzymes used in this study.

| **Name** | **Manufacturer** |
|---|---|
| FastDigest restriction enzymes | Thermo Fisher Scientific |
| Lysozyme | Boehringer |
| Phusion DNA polymerase | Thermo Fisher Scientific |
| RNase A | Thermo Fisher Scientific |
| T4 DNA ligase | Thermo Fisher Scientific |
| T4 polynucleotide kinase | Thermo Fisher Scientific |
| Taq DNA polymerase | Thermo Fisher Scientific |
| RNase-free DNase I | Thermo Fisher Scientific |

**Tab. 7:** Chemicals used in this study.

| **Chemical** | **Manufacturer** |
|---|---|
| 2-Propanol/ Isopropanol | Roth |
| Acetic acid | Roth |
| Acrylamide 4K Solution (40 %) | AppliChem |
| Agarose | Biozym Scientific |
| Ammonium peroxydisulphate (APS) | AppliChem |
| Bacto Agar | Roth |
| Blue Slick™ | Serva |

| | |
|---|---|
| Boric acid | Roth |
| Bromophenol blue Sodium salt | Roth |
| Calcium chloride Dihydrate | Roth |
| Chloroform | Roth |
| Coomassie Brilliant Blue G-250 | Serva |
| Deoxyribonucleoside triphosphate | Thermo Scientific |
| Dithiothreitol (DTT) | Sigma Aldrich |
| Ethanol (96 %) | Roth |
| Ethidium bromide | Roth |
| Ethylenediaminetetraacetic acid (EDTA) | Roth |
| Formaldehyde (37%) | Roth |
| Glycerol (96 %) | Roth |
| Hydrochloric acid (HCl) | Roth |
| Isoamyl alcohol | Roth |
| Magnesium chloride | Roth |
| Methanol | Roth |
| Methylene blue | Sigma Aldrich |
| Nuclease-free water | Roth, Thermo Fischer Scientific |
| Phenol water | AppliChem |
| Phenol:Chloroform:Isoamylalcohol (25:24:1) | AppliChem |
| Potassium chloride | Roth |
| RNAprotect Bacteria Reagent | Qiagen |
| Silver nitrate | AppliChem |
| Sodium carbonate | Merck |
| Sodium chloride | Roth |
| Sodium dodecyl sulfate (SDS) | Roth |
| Sodium hydroxide (NaOH) | Roth |
| Sodium thiosulfate | Merck |
| ß-Mercaptoethanol | Roth |
| Tetramethylethylendiamine (TEMED) | Roth |
| Tricine | Roth |
| Tris base | Roth |
| TRIzol reagent | Ambion |
| Tryptone | Roth |
| Tween-20 | Glentham Life Sciences |
| Urea | Roth |
| Xylene cyanole | Serva |
| Yeast extract | Roth |

### 2.1.4 Antibiotics and media

Media and antibiotics used can be found in Tables 8-11. Media were prepared using VE-$H_2O$ and measurements of TY and LB media are for 1 l.

**Tab. 8:** Composition of LB medium used for culturing *E. coli*.

| **Component** | **Amount (g) per liter** |
|---|---|
| NaCl | 10 |
| Tryptone | 10 |
| Yeast extract | 5 |

**Tab. 9:** Composition of Tryptone-Yeast medium used for culturing *S. meliloti*.

| Component | Amount (g) per liter |
|---|---|
| $CaCl_2$ | 0.3 |
| Tryptone | 5 |
| Yeast extract | 3 |

**Tab. 10:** Antibiotics used for selective media (e. g. maintaining plasmids). N.a, not applicable.

| Antibiotic | Stock (mg/ml) | For *E. coli* (µg/ml) | For *S. meliloti* (µg/ml) | Solvent |
|---|---|---|---|---|
| Streptomycin (Sm) | 100 | n.a. | 250 | $H_2O$ |
| Gentamycin (Gm) | 4 | 10 | 10 | $H_2O$ |
| Kanamycin (Km) | 10 | 25 | 200 | $H_2O$ |

**Tab. 11:** Antibiotics used for stress experiments at subinhibitory concentrations. Subinhibitory concentration based on previously described experiments (Melior et al., 2020).

| Antibiotic | Stock (mg/ml) | For *S. meliloti* (µg/ml) | Solvent | Subinhibitory concentration (µg/ml) |
|---|---|---|---|---|
| Tetracycline (Tc) | 10 | n.a. | 70 % EtOH | 1.5 |
| Chloramphenicol (Cm) | 17 | n.a. | 70 % EtOH | 9 |
| Erythromycin (Em) | 20 | n.a. | 70 % EtOH | 27 |
| Kanamycin (Km) | 10 | 200 | $H_2O$ | 45 |

### 2.1.5 Devices

Devices were used as indicated (Tab. 12).

**Tab. 12:** Devices used in this study.

| Device | Manufacturer |
|---|---|
| 96-well microtiter plate (schwarz) | Greiner |
| Cell density meter (40) | Thermo Fischer Scientific |
| Centrifuge, Heraeus Fresco 17 centrifuge | Thermo Fischer Scientific |
| Cooling centrifuge, Heraeus Fresco 17 | Thermo Fischer Scientific |
| Cooling centrifuge, Sorvall RC-5C Plus | Thermo Fischer Scientific |
| Cooling centrifuge, Sorvall RC-6+ | Thermo Fischer Scientific |
| Electro blotter, Perfect Blue ´Semi-dry´ Blotter | VWR PeqLab |
| Electroporation pulser, MicroPulser™ | BioRad |
| Eppendorf reaction tube 1.5 ml | Sarstedt |
| Eppi, reaction tube 2 ml | Sarstedt |
| Heat block | VWR PeqLab |
| Hybridization tube (15 ml; 50 ml) | Sarstedt |
| Imaging Screen | BioRad |
| MicroSpinTM G-25 Columns | Amersham Biosciences |
| NanoDrop 1000 | PeqLab |
| Nylon membrane, Roti-Nylon plus, 0.45 µm | Roth |
| PCR Cycler, T100™ Thermal Cycler | BioRad |
| PCR Tubes 0.2 ml | VWR PeqLab |
| Phosphoimager, Personal Phospho Imager FX | BioRad |
| Pipetboy2 | Integra |
| Pipets; 0.1-10 µl; 2-20 µl; 20-200 µl, 100-1000 µl | HTL |
| Plate Reader Infinite M200 | Tecan |
| Polystyrol cuevette 10 x 4 x 45 mm | Sarstedt |
| Polyvinylidenfluorid (PVDF) membrane | Amersham Bioscience |

| | |
|---|---|
| Rotation oven, PerfectBlot | PeqLab |
| Rotilabo syringe filter, 0.22 µm | Roth |
| RT-qPCR Cycler, CFX Connect | BioRad |
| RT-qPCR Tubes, 0.2 ml Low Profile Thin-walled 8 Tube Strips, white | Thermo Fischer Scientific |
| RT-qPCR Tubes, Optical clear flat 8 Cap Strips | Thermo Fischer Scientific |
| Safelock Eppendorf tube, SafeSeal reaction tube 1.5 ml | Sarstedt |
| Safelock Eppendorf tube, SafeSeal reaction tube 2 ml | Sarstedt |
| Screen Eraser K | BioRad |
| Sonicator, Sonoplus | Bandlin |
| Speedvac, Concentrator plus | Eppendorf |
| ThermoMixer C | Eppendorf |
| Tubes (15 ml, 50 ml) | Sarstedt |
| UV table, UVT-20 M/W | Herolab |
| Vortexer, Vortex Genie 2™ | Scientific Industries |
| Water bath | Albet |
| Whatman paper | GFL |

## 2.2 Methods

### 2.2.1 Cultivation

All media and usables were sterilized by autoclaving for 15 min at 121 °C at 1 bar. Solid usables were dried for 2h at 70 °C prior to use. Media and additives that were heat-sensitive were filtered sterile (0.22 µm; Millipore).

#### 2.2.1.1 Cultivation and growth measurements

*E. coli* was grown aerobically in 10 ml LB at 37 °C and 180 rpm with antibiotics according to plasmid-mediated resistances (see section 2.1.4). To maintain cells for longer time periods, 1 ml of an overnight culture was mixed with 500 µl 80% glycerol. The cultures were snap-frozen in liquid nitrogen and stored at -70 °C.

*S. meliloti* was cultured semi-aerobically (30 ml in a 50 ml Erlenmeyer flask) in TY medium with Sm at 32 °C and 140 rpm unless otherwise stated. Other antibiotics were added based on plasmid-mediated resistances and experimental procedures. To maintain cells for longer time periods, 3 ml of an overnight culture were centrifuged for 10 min at 5 000 rpm. Cells were washed with 1 ml medium and mixed with 500 µl 80 % glycerol. The cultures were snap-frozen in liquid nitrogen and stored at -70 °C.

Prior to inoculation into liquid media, *S. meliloti* was streaked out from -70 °C stocks on solid TY media containing Sm. After a day of growth, cells were inoculated into 30 ml liquid media and cultured semi-aerobically.

For solid media, 1.5 % (w/v) agar was supplied to the media.

To measure cell density, 1 ml culture was transferred into a cuvette and optical density (OD) was measured at 600 nm in a photometer. If the cells had an $OD_{600nm} \geq 0.8$, a 1:10 dilution was prepared and measured to receive an $OD_{600nm}$.

A growth curve was recorded using a plate reader (Tecan). *S. meliloti* 2011 overnight cultures were diluted to OD 0.2 in fresh media and grown to OD 0.5 under standard conditions. At OD 0.5, the culture was diluted into fresh medium to an OD 0.02, and 150 µl each were distributed into wells of a 96-well plate. Measurements were taken at 32 °C, 40 rpm for every hour during 24h. All experiments were performed in triplicates.

#### 2.2.1.2 Transformation

Chemically competent *E. coli* DH5α cells used for cloning and *E. coli* S17-1 used for conjugation were transformed using 100-200 ng plasmid (compare Sambrook et al., 1989). The cells were mixed with the plasmid and kept on ice for 15 min. After a heat shock for 1 min at 42 °C, the cells were incubated on ice for 5 min. After addition of 1 ml LB medium (RT), the cells were allowed to recover and express the respective resistance-mediating gene for 1h at 37 °C and 600 rpm. 100 µl was plated on solid selective media (LB containing 1,8 % agar) with antibiotics.

#### 2.2.1.3 Conjugation

To transfer plasmids to *S. meliloti*, *E. coli* S17-1 cells transformed with the shuttle vector were grown in liquid LB medium overnight, 1.5 ml of *S. meliloti* cells and 1 ml of *E. coli* cells each were harvested and washed 3x with TY. *S. meliloti* cells were resuspended in 500 µl TY and *E. coli* cells were resuspended in 900 µl TY. 500 µl of *S. meliloti* cells were mixed with 200 µl of *E. coli* cells. 600 µl of the mixture were dropped onto solid media without antibiotics in single droplets. The plasmid was then transferred to *S. meliloti* by conjugation at 30 °C overnight. The cells were harvested the next day by scraping off the droplets into an Eppendorf tube. The cells were washed 3x with 1 ml TY and $10^{-2}$ and $10^{-4}$ dilutions were plated onto selective solid media supplemented with Sm (selection against the *E. coli* donor) and an additional antibiotic according to plasmid-mediated resistance. The solid media were incubated at 30 °C for 2-3 days. Only *S. meliloti* cells that received the plasmid were able to grow on the selective media.

#### 2.2.1.4 Stress experiments

All experiments were performed in biological triplicates unless otherwise stated. *S. meliloti* cells were grown over night as described above.

For stress experiments with Tc, the cells were diluted to OD 0.2 in 70 ml pre-warmed, fresh TY medium. 30 ml of the culture was distributed into two 50 ml flasks each and grown to OD 0.5 as described above. At OD 0.5, cells were treated with subinhibitory Tc (see Tab. 11) or the corresponding amount of ethanol (EtOH). Cells were treated for 10 min and then harvested for RNA isolation (see section 2.2.3.1) or Western Blot (see section 2.2.4.2).

For stress experiments with other stressors, cells were diluted as described above and distributed into 5 flasks with 30 ml each. These flasks were grown to OD 0.5 and treated with different stressors (Tab. 13). Each experiment featured a no treatment control and a control with just EtOH added. After 10 min of incubation, cells were harvested as described above for RNA isolation (stressor treatment growth experiments performed by Liana Schank and Simon Beck).

**Tab. 13:** Stressors used for this experiment. Each stressor was applied for 10 min before harvesting the cells. All experiments were performed in biological triplicates (n=3) except for erythromycin, where only 2 biological replicates were used (n=2).

| **Component** | **Stock solution** | **Final concentration** | **Temperature (°C)** |
|---|---|---|---|
| Chloramphenicol (Cm) | 17 mg/ml | 9 µg/ml | 32 |
| Erythromycin (Em) | 10 mg/ml | 27 µg/ml | 32 |
| $H_2O_2$ | 9.33 M | 1 mM | 32 |
| Heat | | | 42 |
| Tetracycline (Tc) | 10 mg/ml | 1.5 µg/ml | 32 |

2.2.1.5 Treatment with Bicyclomycin

Bicyclomycin (BCM) is a drug specific for Rho inhibition in bacteria (Kohn & Widger, 2005). *S. meliloti* cells of three biological replicates were grown overnight and then diluted to OD 0.2. The cells were distributed into 2 flasks with 30 ml each. These bacteria were grown to OD 0.5 and treated with sublethal Tc for 10 min before adding either BCM (10 mg/ml) or its solvent, methanol (MeOH). The final concentration of BCM was 20 µg/ml, and the corresponding volume of MeOH (60 µl) was given to control cultures. Treatment occurred for 30 min before cells were harvested for RNA isolation as described above. RT-qPCR was used for analysis. The *in vitro* transcribed *rrp41* from *S. acidocaldarius* was added at 1 ng/µl to the RNA isolation samples at the step of TRIzol treatment (compare sections 2.2.3.2 and 2.2.3.5). This spike-in offered a possibility of normalization. Another gene, *rpoB*, was used as an internal control to normalize the data.

A minimal inhibitory concentration (MIC) test was performed with a dilution series of 1:2, starting from 150 µg/ml BCM to 4.7 µg/ml. The experiment was performed in a 96-well plate. Results were obtained after 72h of growth.

2.2.1.6 Generation of a partial *duf1127*$_1$ chromosomal deletion mutant

To analyze the function of *duf1127*$_1$, a partial chromosomal deletion mutant was constructed (Fig. 5A). This mutant featured a deletion of *duf1127*$_1$ from codon 11 to codon 83, retaining the 5' region and the stop codon of *duf1127*$_1$. The deleted part was replaced with a synthetic sequence of 22 bp (Fig. 5B).

The construct was cloned into the suicide plasmid pK18mobsacB featuring a kanamycin resistance and introduced into *E. coli* S17-1 cells by transformation. The plasmid was then transferred into *S. meliloti* 2011 by conjugation. The conjugation mixture was plated onto solid TY media containing Sm and Km. At this point, a single crossover should have happened in the cells, and the plasmid integrated into the genome. Single colonies from this step were resuspended in 50 µl 0.9 % NaCl and diluted 1:10 prior to plating on solid media containing Sm and 10 % sucrose. The pK18mobsacB plasmid features a *sacB* gene, which is expressed under sucrose addition, leading to formation of a toxic product. This product will kill all cells that did not have lost the plasmid. Thus, only cells in which a second crossover happened, could grow. The second crossover should lead to either WT or the desired chromosomal deletion. Single colonies from the sucrose selection were resuspended in 0.9 % NaCl, and 2µl were dropped onto two solid media plates: one containing only Sm, and one containing Sm and Km. After incubation, drops that showed growth on Sm but not on plates containing both, Sm and Km, were potential double-crossover progenies and were subjected to PCR to check for the expected deletion (compare Wang et al., 2015).

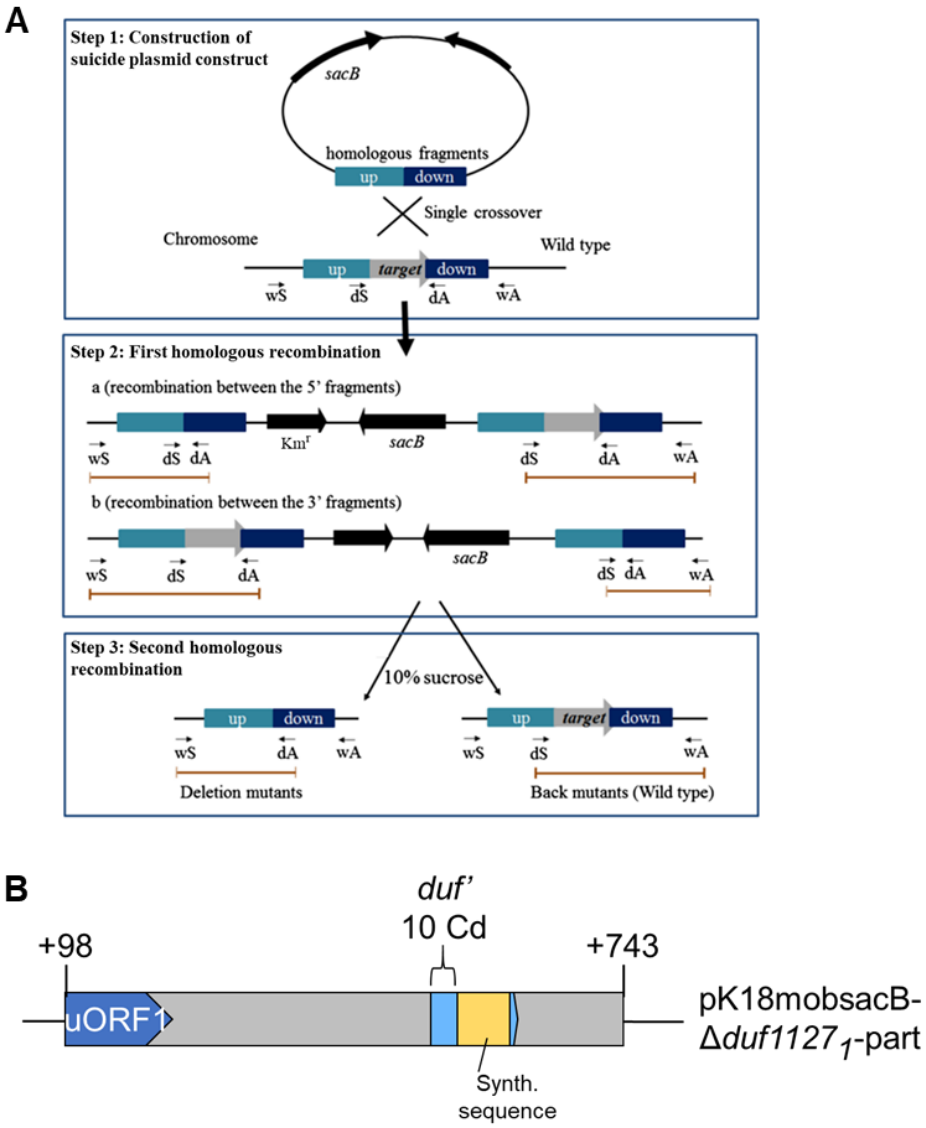


**Fig. 5:** Knockout construct introduced into *S. meliloti*. The construct was introduced via the suicide plasmid pK18mobsacB-Δ*duf1127*$_1$-part. **(A)** Illustrating the process of knockout construction (compare Wang et al., 2015). First, a suicide plasmid was constructed featuring homologous regions for the target DNA region (Step 1). The plasmid integrated via homologous recombination (first crossover, Step 2). Finally, the second crossover happened. Sucrose served as a selection marker, killing all cells that still contain the plasmid and did not undergo the second crossover (Step 3). The deletion was verified by PCR. **(B)** The relevant parts of the plasmid used to create the *duf1127*$_1$-part knockout construct. Homologous regions are marked with the positions relative to the transcription start site. Cd, codons.

### 2.2.2 Working with DNA

#### 2.2.2.1 Polymerase chain reaction (PCR)

Polymerase chain reaction (PCR) was performed to amplify specific DNA fragments either for cloning using Phusion polymerase or Taq polymerase in case of check PCRs. Phusion polymerase has a proofreading function, making it useful for amplifying PCR products used for cloning (Tabs. 14, 15). Thermostable *Taq* polymerase was used for checking PCRs (Tab. 15).

**Tab. 14:** Conditions for Phusion PCR.

| **Composition of a 1 x Phusion PCR mix** | | **PCR protocol for a 50 µl Phusion PCR** | | |
|---|---|---|---|---|
| **Component** | **Amount (µl)** | **Step** | **Temperature (°C)** | **Time** |
| 10 µM dNTP mix | 2 | 1 | 98 | 3 min |
| 10 µM Primer fwd | 1.5 | 2 | 98 | 20 s |
| 10 µM primer rev | 1.5 | 3 | 72 | 20 s |
| 10 x HF buffer | 10 | 4 | 72 | 3 min |
| 2U/µl Phusion Polymerase | 0.1 | To Step 2 | 39x | |
| 50 mM MgCl2 | 2 | 5 | 72 | 5 min |
| DMSO | 1 | | | |
| Nuclease-free water | Ad 50 µl | | | |
| Template plasmid | 50 ng | | | |

**Tab. 15:** Conditions for Taq PCR.

| **Composition of a 1 x Taq PCR mix** | | **PCR protocol for a 25 µl Taq PCR** | | |
|---|---|---|---|---|
| **Component** | **Amount (µl)** | **Step** | **Temperature (°C)** | **Time** |
| 10 µM Primer 1 | 1 | 1 | 95 °C | 3 min |
| 10 µM Primer 2 | 1 | 2 | 95 °C | 30 s |
| 10 mM dNTPs | 1 | 3 | Tm dependent on primers used | 30s |
| 10 x Dream Taq Green Buffer | 2.5 | 4 | 72 °C | 1 min |
| 5 U/µl Taq polymerase | 0.2 | To Step 2 | 39x | |
| Nuclease-free water | Ad 25 µl | | | |
| Template (freeze-thawed cells) | 1 | | | |

#### 2.2.2.2 Plasmid isolation

Plasmid isolation from *E. coli* was performed using an in-house protocol. *E. coli* cells were grown over night and 2x 1.5 ml were harvested into an Eppendorf tube at 6 000 rpm, 10 min. If cultures had not reached full density, this step was repeated. The cells were then subjected to alkalic lysis by first adding 250 µl of solution 1 (EDTA, 10 mM; RNase A, 0.1 mg/ml; Tris-HCl pH 7.5, 50 mM). The cells were well resuspended and 250 µl solution 2 (NaOH, 200 mM; SDS, 1 % w/v) was added. After slowly inverting the tubes 6-8 times, the solution turned clear and very viscous, indicating cell lysis. 250 µl of solution 3 (potassium acetate pH 5, 3M) was added and white flakes formed (SDS precipitation, aggregation of denatures proteins and large chromosomal fragments). Before centrifugation at 13 000 rpm for 15 min, the tubes were slowly inverted and then vigorously shaken for ~ 10s. After centrifugation, 730 µl of the supernatant was transferred into a new tube and centrifuged again for 10 min at 13 000 rpm to separate all white flocks from the plasmid-containing supernatant. 700 µl of the supernatant were then added to a new tube containing 450 µl isopropanol (2-propanol). The tube was inverted 6-8 times and again centrifuged at 13 000 rpm for 15 min. To wash the pellet, 1 ml 70 % EtOH was added. After decanting the supernatant, the tube was centrifuged briefly to collect all remaining liquid at the bottom. The liquid was removed using a pipette and the pellet was dried in a Speedvac for 8 min. It was important to dry the pellet well before it was resuspended in 25 µl of nuclease-free water. At this step, both tubes were reunited to increase plasmid yield. The plasmids were stored at -20 °C or directly transformed into *E. coli*.

#### 2.2.2.3 Quantification of nucleic acids

Nucleic acids were quantified using a Nanodrop reader. Both DNA and RNA concentration were measured at 260 nm. As nucleic acids maximally absorb at 260 nm and proteins at 280 nm, the 260/280 ratio allows to determine protein contamination in DNA or RNA samples. For DNA, this value should be approx. 1.8, while for RNA approx. 2.0 is required. Aromatic and phenolic compounds in a sample are measured at 230 nm, allowing to determine contamination with phenolic compounds using the ratio 260/230 (compare Sambrook et al., 1989).

#### 2.2.2.4 Agarose gel electrophoresis

Agarose gel electrophoresis was performed to analyze PCR products on a gel for their right size and purity. Usually, a 1.2 % agarose solution was prepared in 1 x TBE. For larger fragments > 800 bp, a 0.8 % agarose gel was used instead (compare Sambrook et al., 1989).

Small gels were run at 120 V for at least 30 min, and longer if necessary. Big gels were run at 170 V for at least 45 min. After the run, the gel was incubated in an EtBr (1 µg/ml) solution for 5 min to stain DNA. Excess EtBr was removed by de-staining in VE water for 10 min. UV light visualized the bands for analysis, photodocumentation was performed with a gel documentation system.

#### 2.2.2.5 Sequencing

Samples containing plasmid were sent for sequencing to Microsynth (Göttingen). It was possible to either sequence isolated plasmid, or to send *E. coli* or *S. meliloti* cells to Night Seq, where 5 µl of an overnight culture were sent in a solution provided by Microsynth.

#### 2.2.2.6 Cloning

Cloning was performed by courtesy of Susanne Barth-Weber, while oligonucleotides and the cloning were designed by the author.

For cloning, the desired PCR product was amplified from either *S. meliloti* 2011 lysate or, for mutations, from a pre-existing pJet plasmid. For new clonings, Phusion PCR amplified the desired region from the lysate, as it features a proofreading function and provided blunt ends, which allow cloning of the fragment into the pJET cloning vector. For mutagenesis on a pre-existing plasmid, Phusion PCR amplified the desired region introducing the desired mutation, and the original template was digested using DpnI. In both cases, the pJET plasmid containing the desired region or mutation was transformed into *E. coli* DH5α. The plasmid was isolated from *E. coli* and subjected to an enzymatic digest with restriction enzymes (compare table X Oligonucleotides). The digested fragment was then ligated by a T4 DNA ligase reaction into the desired shuttle vector backbone digested with the same restriction enzymes as the fragment. The ligated plasmid was transformed into *E. coli* DH5α and the final plasmid was then isolated from the *E. coli* strain and sequenced.

As an example, cloning of a mutagenesis PCR is described here. Cloning of pSW1-S3-L10-ch-SPA was started by a Phusion polymerase PCR (2.1.3; compare chapter 2.2.3) on a pre-existent pJET plasmid pJET-$DUF_{10CD}$-SPA (in this work re-named to pDUF'-SPA). PCR was performed as described with mutagenesis primers and addition of $MgCl_2$ and DMSO, since the fragment was over 3500 bp. The PCR was checked on an 0.8% agarose gel and then subjected to DpnI to digest the plasmid template (10 x FastDigest Green buffer, 2 µl; DpnI, 1 µl; PCR product, 17 µl).

The reaction mixture was incubated at 37 °C for 30 min and the enzyme was deactivated afterwards at 81 °C for 8 min. 2 µl of this reaction mixture were used for transformation into chemically competent *E. coli* DH5α cells. After plasmid preparation, the plasmid was subjected

to sequencing. Another digest was prepared using enzymes BamHI and NheI (Tab. 16). This digestion prepared the desired insert for cloning into the shuttle vector backbone. The mixture was incubated at 37 °C for 30 min and afterwards heat inactivated at 75 °C for 5 min.

**Tab. 16:** Reaction mixture for NheI/BamHI digest.

| Component | Amount (µl) |
|---|---|
| 10 x FastDigest Green buffer | 5 |
| BamHI | 1.5 |
| NheI | 1.5 |
| Nuclease-free water | Ad 50 µl |
| Plasmid | 2.5 µg |

Ligation of the fragment and the final vector backbone was performed overnight at 4 °C (digested pSW1 vector backbone, 1 µl; digested insert, 1 µl; 10x ligase buffer, 2 µl; T4 DNA ligase, 0.5 µl; nuclease-free-water, ad 20 µl). The digested vector backbone was received by courtesy of Susanne Barth-Weber. It was then transformed into chemically competent *E. coli* DH5α cells. After plasmid preparation, the final plasmid was subjected to sequencing (Microsynth) before transformation into *E. coli* S17-1 cells to use for conjugation.

### 2.2.3 Working with RNA

#### 2.2.3.1 Cell harvest for RNA isolation

*S. meliloti* was grown in TY medium with Sm and antibiotics corresponding to plasmid-mediated resistance overnight at 32 °C, 140 rpm. The culture was then diluted into fresh, pre-warmed TY medium to $OD_{600nm}$ 0.2 and grown at 32 °C, 140 rpm until $OD_{600nm}$ 0.5. All experiments for growth experiments were performed without antibiotic additives. If required, at $OD_{600nm}$ 0.5, cells were treated with the subinhibitory amount of antibiotic or the corresponding amount of solvent for 10 min (see section 2.2.1.4). The culture was then immediately transferred into a centrifuge tube filled with ice rocks to stop all cellular processes. The tubes were centrifuged at 6 000 rpm for 10 min at 4 °C. The pellet was resuspended in 800 µl pre-cooled TY medium and transferred into Eppendorf tubes for centrifugation at 6 000 rpm for 10 min at 4 °C. The pellet was frozen in liquid nitrogen and kept at -70 °C until further use. All experiments were performed in biological triplicates unless otherwise stated.

#### 2.2.3.2 RNA isolation

RNA isolation was performed from 15 ml cell pellets using a modified protocol of the Hot TRIzol method (assets.thermofisher.com/TFS-Assets/LSG/manuals/trizol_reagent.pdf; last access 16.8.2024, 17:00). It is important to always keep the samples on ice unless otherwise stated.

The *S. meliloti* cell pellet was resuspended in 1 ml TRIzol and incubated at 65 °C, 1 700 rpm for 10 min. After addition of 200 µl chloroform, the tubes were well mixed for 15 sec and centrifuged for 20 min at 10 000 rpm and 4 °C. The upper, aqueous phase was carefully transferred into a fresh Eppendorf tube containing 500 µl 2-propanol, the tubes were inverted and incubated at RT for up to 15 min. The tubes were then centrifuged at 10 000 rpm, 4 °C, for at least 15 min. After centrifugation, the supernatant was removed carefully, the pellet washed with 1 ml 75 % EtOH (v/v) (-20 °C) by centrifuging for 5 min at 10 000 rpm at 4 °C and frozen, if necessary, at -20 °C. If the RNA was kept at -20 °C, re-centrifugation at 10 000 rpm for 10 min at 4 °C was performed before proceeding.

Hot Phenol purification (Jahn et al., 2008) was performed to purify the isolated RNA from DNA and other contaminants. For this, the ethanol was removed and the tubes re-centrifuged briefly to collect and remove all residual ethanol. After briefly drying under the hood, the pellet was then resuspended in 300 µl ice-cold, nuclease-free water and immediately mixed with 300 µl acidic phenol water pre-warmed to 65 °C. The tubes were mixed well by shaking for 15 sec and then incubated at 65 °C for 5 min at 1 100 rpm. After incubation, the tubes were centrifuged at 13 000 rpm for 10 min at RT. With 270 µl of the upper, aqueous phase transferred into a new tube without disturbing the interphase, the RNA was mixed with an equal amount of phenol-chloroform-isoamyl alcohol (PCI, 25:24:1 (v/v)), the tubes were mixed well by shaking for 15 sec, and centrifuged at 13 000 rpm for 10 min at RT. If the interphase was very prominent, this step was repeated. After transfer of 240 µl of the upper, aqueous phase with carefully avoiding transfer any of the interphase to a new tube and mixing with an equal amount of chloroform-isoamyl alcohol (CI, 24:1 (v/v). The tubes were centrifuged at 13 000 rpm for 10 min at RT, and 200 µl of the upper, aqueous phase were transferred into a new tube. After this step, there should be no interphase left and only a phase separation should be visible. The aqueous phase containing the purified RNA was mixed with 1/10 (v/v) 3M sodium acetate (Na-Ac) pH 5.2 and mixed well by pipetting. RNA was never vortexed. After adding Na-Ac, 2.5 volumes of 96 % EtOH (v/v) (-20 °C) was added, and the tubes were inverted multiple times. Usually, RNA was precipitated over night at -20 °C; alternatively, it was frozen in liquid nitrogen for 3 min before proceeding.

After precipitation, the tubes were centrifuged for at least 35 min at 13 000 rpm at 4 °C. The supernatant was discarded, and the pellet washed with 1 ml 75 % EtOH (-20 °C). The tubes were centrifuged again at 13 000 rpm for 5 min at 4 °C and the supernatant was removed and discarded. The tubes were re-centrifuged briefly to collect and remove all residual ethanol. Afterwards, the pellet was dried at RT under the hood for 15 min before resuspending the RNA in 30 µl ice-cold, nuclease-free water. Samples were kept at -20 °C or -80 °C. This RNA was either used for Northern hybridization or subjected to DNase digestion.

#### 2.2.3.3 DNase digest

A DNase digest was performed with a kit (Thermo Fisher) to eliminate remaining amounts of DNA after RNA isolation. The kit supplied all chemicals and reagents necessary for this procedure. The protocol was performed according to the manufacturer's instructions with a slight change in incubation time. Briefly, 10 µg of RNA were treated with 1 µl of DNase (2U/µl) I in a 50 µl reaction at 37 °C for at least 30 min to 1h. The reaction was stopped using 5 µl of the inactivation reagent for 5 min at room temperature, which removes all DNase I. After treatment with inactivation reagent, the sample was centrifuged briefly, and the supernatant was removed. The amount of the reaction was brought up to 200 µl using nuclease-free water. 1/10 (v/v, 20 µl) of 3 M Na-acetate pH 5.2 was added and mixed well with the RNA solution. 2.5 volumes (v/v) 96 % EtOH (-20 °C) were added, and the solution was inverted multiple times to mix. The DNase-treated RNA was precipitated over night at –20 °C and cleanup was performed according to the last part of the RNA isolation described above. Samples were kept at -20 °C or -80 °C.

#### 2.2.3.4 RNA sequencing (RNA seq)

To obtain information on the regulation of changes in gene expression under the influence of sub-lethal Tc treatment, experiments were conducted with/without the antibiotic, and RNA isolation was performed after 10 min of treatment to limit responses to the early effects of the treatment. The preparation of all samples for RNA sequencing was performed by Robina Scheuer and RNA-Sequencing was performed by vertis Biotechnologie AG (Freising). The

bioinformatic evaluation was performed by collaboration partners Till Sauerwein and Konrad Förstner (ZBMed, Cologne).

For this study, the existing RNA Seq data was used. The RNA-seq compared the transcriptomes of *S. meliloti* 2011 without Tc exposure and 10 min exposure to 1.5 µg/ml Tc in three biological experiments. Differentially expressed genes were selected from provided excel files (compare also suppl. Tab. S1). cDNA reads were visualized using integrated genome browser.

2.2.3.5 Reverse transcription followed by real-time quantitative PCR (RT-qPCR)

RT-qPCR was performed to quantitatively determine the amount of RNA at a specific time point or under a specific condition in real time. Two different kits, Brilliant III Ultra Fast SYBR Green RT-QPCR Kit (Agilent) or Luna Universal One-Step RT-qPCR Kit (NEB), were used. Both kits led to similar results when the same RNA samples were used (data not shown).

All reagents were left to thaw on ice, briefly mixed by hand and the master mix was prepared without adding RNA (Tab. 17 and 18 for the two kits used). After a brief centrifugation, 8 µl were distributed into wells, 2 µl of RNA sample (20 ng/µl) were added to each well before running the qPCR program. For mRNA stability analysis, RNA had a concentration of 30 ng/µl.

Foldchanges detected by the RT-qPCR were calculated as previously described (Pfaffl, 2001; Scheuer et al., 2024). Usually, *rpoB* served as an internal control to normalize data (for original values, compare suppl. Tabs. S2-S5). The spike-in *in vitro* transcript *rrp41* was obtained by courtesy of Robina Scheuer and added when cellular transcription was thought to be impaired by rifampicin or bicyclomycin addition. Ratio of *spa* vs *rpoB* mRNA was calculated using the following formulas (Cq, quantitative cycle; PE, primer efficiency):

(1) $\Delta Cq = Cq_{spa} - Cq_{rpoB}$

(2) $Ratio = PE^{-\Delta Cq}$

**Tab. 17:** RT-qPCR Master mix and RT-qPCR protocol used for Brilliant III Ultra Fast SYBR Green RT-QPCR Kit (Agilent).

| **Composition of 1X RT-qPCR mix (10 µl reaction)** | | **PCR protocol for RT-qPCR (Agilent)** | | | |
|---|---|---|---|---|---|
| **Component** | **Amount (µl)** | **Step** | **Temperature (°C)** | **Time** | |
| 10 µM Forward primer | 1 | 1 | 50 | 10 min | |
| 10 µM Reverse primer | 1 | 2 | 95 | 3 min | |
| 2 x SYBR Green QPCR Master mix | 5 | 3 | 94 | 5 s | |
| DTT | 0.1 | 4 | 56 | 5 s | |
| Nuclease-free water | 0.1 | 5 | 60 | 5 s | + plate read |
| Reference Dye (1:50) | 0.3 | 6 | Step 3-5 39 cycles | | |
| RNA (20 µg/µL) | 2 | 7 | 95 | 10 s | |
| RT/RNase block | 0.5 | 8 | Melt curve from 65 to 95 | Increment of 0.5 °C, 5s | + plate read |

**Tab. 18:** RT-qPCR Master mix and RT-qPCR protocol used for Luna Universal One-Step RT-qPCR Kit (NEB).

| **Composition of 1X RT-qPCR mix (10 µl reaction)** | | **PCR protocol for RT-qPCR (NEB)** | | | |
|---|---|---|---|---|---|
| **Component** | **Amount (µl)** | **Step** | **Temperature (°C)** | **Time** | |
| 10 µM Forward primer | 0.4 | 1 | 55 | 10 min | |
| 10 µM Reverse primer | 0.4 | 2 | 95 | 1 min | |
| 20 ng/µl Template RNA | 2 | 3 | 95 | 10 s | |
| 20x Luna WarmStart RT Enzyme Mix | 0.5 | 4 | 56 | 30 s | |
| 2x Luna Universal One-Step Reaction Mix | 5 | 5 | 60 | 5 s | + plate read |
| Nuclease-free water | 1.7 | 6 | Step 3-5 39 cycles | | |
| | | 7 | Melt curve from 65 to 95 | Increment of 0.5 °C, 5s | + plate read |

2.2.3.6 Denaturing polyacrylamide gel electrophoresis

RNA forms many secondary structures, which can alter its apparent length. To assess RNA quality and for subsequent Northern hybridization, a denaturing polyacrylamide gel electrophoresis was performed (polyacrylamide 37. 5:1, 40 %, 11.25 ml; Urea, 18.9 g; 5 x TBE buffer, 10 ml; 10% APS, 200 µl; TEMED. 20 µl; $H_2O$ ad 45 ml for a 10 % polyacrylamide urea gel (1 mm x 20 cm x 20 cm). All ingredients except APS and TEMED were mixed until the urea was dissolved. The gel cast was assembled and, immediately before pouring the gel, APS and TEMED were added, the mixture was mixed and then poured into the gel cast. The gel was left to polymerize for 45 min, or until full polymerization could be seen.

For RNA quality assessment, 1-3 µg of RNA were mixed with 0.7x formamide-urea mix (10x TBE buffer, 10 %; bromo-phenol blue, 0.1 % (w/v); deionized formamide, 80 % (v/v); urea, 6 M; xylene cyanole, 0.1 % (w/v)) and incubated for 10 min at 65 °C prior to gel electrophoresis. This ensured melting of potential RNA secondary structures. For Northern hybridization, 10 µg of RNA was used and treated as above.

After loading, the gel was run at 300V for 3 hours (RNA quality) or until the xylene cyanole running front was in the lower third of the gel. For Northern hybridization, the gel was run for 2 hours, or until the bromo-phenol blue marker had just run out.

2.2.3.7 Northern blot hybridization

For RNA analysis alternatively to RT-qPCR, Northern hybridization using specific probes was performed (compare Sambrook et al., 1989; Alwine et al., 1977; Southern, 1975). The polyacrylamide gel was used to blot the RNA onto a nylon membrane. The blot was assembled as follows (bottom-to-top): 3x Whatman paper, nylon membrane, gel, 3x Whatman Paper. Whatman papers and membrane were dipped into 1X TBE buffer. Blotting occurred at 150 mA for 2h, before the blot was disassembled and the RNA was crosslinked to the membrane by using the auto-crosslink function twice.

After crosslinking, the membrane was pre-hybridized (hybridization buffer, see below, containing additionally 1 ml 50 x Denhardt's reagent) to reduce unspecific binding and prepare the membrane for hybridization. For this, a pre-hybridization mix was prepared using 20x SSC buffer (sodium chloride, 3 M; sodium citrate, 300 mM; VE-$H_2O$ ad 1 l; pre-hybridization buffer: 10 % SDS, 1 ml; 20x SSC, 6 ml; Denhardt's solution, 1 ml; 500 µg/ml salmon sperm DNA, 400 µl; VE- H2O ad 20 ml) and added into a hybridization tube with the membrane. Pre-hybridization was performed at 56 °C for at least 2 h with constant rotation.

After pre-hybridization, hybridization occurred with a probe labelled radioactively with $^{32}P$. This probe was complementary to the RNA that was supposed to be visualized. Probes for Northern hybridization were labelled using γ-[$^{32}P$]-ATP. For this, a master mix of 10 µl (10 pmol/µl oligonucleotide, 1 µl; 10x polynucleotide kinase buffer A, 1 µl; 5 U polynucleotide kinase, 0.5 µl; $H_2O$, 4.5 µl; γ-[$^{32}P$]-ATP, 30 µCi) was prepared and 30 µCi were added per reaction sample. The reaction was incubated at 37 °C for 1 h before performing a cleanup using a G25 column. The cleaned probes were kept at -20 °C and thawed as needed for hybridization.

After mixing 5 µl of the labelled probe with 400 µl of salmon sperm DNA and incubation at 96 °C for 10 min, the denatures probe was added into the hybridization mix (hybridization buffer: 10 % SDS, 1 ml; 20x SSC, 6 ml; 500 µg/ml salmon sperm DNA, 400 µl; VE- $H_2O$ ad 20 ml). The hybridization mix was added to the tube and hybridization occurred at 56 °C overnight with constant rotation.

After hybridization, the membrane was washed with washing solution (10 % SDS, 1 ml; 20x SSC, 250 ml; VE-$H_2O$ ad 1 l) to remove excess and unbound probe. Washing was performed three times by carefully rotating the tube in the hands. The membrane was then dried shortly on paper before being sealed in a clear plastic bag and placed on a phosphor screen for 24h. The screen exposure time was lengthened or shortened depending on the probe and its strength. Signals were visualized using a Phosphor Imager.

#### 2.2.3.8 mRNA stability analysis

Stability of mRNA under Tc treatment and control conditions was analyzed using the half-life of certain mRNAs for comparison (Scheuer et al., 2024). Briefly, 60 ml *S. meliloti* cells grown to OD 0.5 in a 100 ml flask were treated for 10 min with Tc or the same amount of EtOH. Rifampicin (133 mg/ml; added 270 µl) or the corresponding volume of its solvent methanol (MeOH) was added after 10 min and samples were withdrawn. One replicate featured rifampicin exposure times of 0 min, 30 s, 60 s, 90 s, 3 min and 5 min. The two other replicates had samples withdrawn at 0 min, 1 min, 2 min, 4 min, 6 min and 8 min. 500 µl were harvested into 1 ml Bacteria Protect Reagent (Qiagen). Adding 1 ng of *in vitro* transcribed *rrp41* for spike-in to allow normalization, RNA was isolated using RNeasy Mini Kit (Qiagen) according to the manufacturer's instructions. DNase I digest was performed as above, except that DNase I was inactivated using 15 mM EDTA pH 8.0 at 75 °C for 10 min. RT-qPCR was performed as described above using Luna Universal One-Step RT-qPCR Kit, with an RNA concentration of 30 ng/µl.

#### 2.2.3.9 Treatment with Bicyclomycin

Bicyclomycin (BCM) is a drug specific for Rho inhibition in bacteria (Kohn & Widger, 2005). *S. meliloti* cells of three biological replicates were grown overnight and then diluted to OD 0.2. The cells were distributed into 2 flasks with 30 ml each. These bacteria were grown to OD 0.5 and treated with either BCM (10 mg/ml) or its solvent, methanol (MeOH). The final concentration of BCM was 20 µg/ml, and the corresponding volume of MeOH (60 µl) was given to control cultures. Treatment occurred for 30 min before cells were harvested for RNA isolation as described above. RT-qPCR was used for analysis.

A minimal inhibitory concentration (MIC) test was performed with a dilution series of 1:2, starting from 150 µg/ml BCM to 4.7 µg/ml. The experiment was performed in a 96-well plate. Results were obtained after 72h of growth.

#### 2.2.3.10 3'-Rapid Amplification of cDNA ends (3' RACE)

It was of interest to find the 3' ends of the *duf1127₁* operon (compare Rodríguez-Cazorla et al., 2015), as there are multiple uORFs that might be indicative of sRNA existence and a role in regulation in addition to the co-transcriptional control. To test this, *S. meliloti* cells of three biological replicates were grown to OD 0.5 in TY medium without antibiotics. At OD 0.5, Tc or EtOH was added, and cells were harvested as described above. RNA isolation and DNase digestion were performed as described above.

Since in bacteria, up to 95 % of the RNAs in a cell are rRNAs, these rRNA needed to be depleted to be able to find the 3' ends of mRNAs. This was performed using the NEBNext rRNA Depletion Kit (Bacteria; NEB). To deplete rRNAs, the manufacturer's protocol was closely followed. Briefly, the kit includes single-stranded DNA probes that are designed to specifically bind to bacterial rRNA. Afterwards, RNase H degraded the hybridized RNA, thereby removing the rRNA. Finally, a DNase treatment removed the DNA added previously, leaving an rRNA-depleted batch of RNA. 800 ng of RNA were treated, and RNA depletion was tested using RT-qPCR with 16S rRNA primers (compare Tab. 3).

After rRNA depletion, an adapter was added that specifically binds to 3' ends. For this, the Universal miRNA Cloning Linker (NEB) was used. The linker has a 3' amine group blocking it to prevent self-ligation. This reaction was performed according to the kit instructions with a T4 RNA ligase (T4 RNA Ligase 2, truncated, NEB) without ATP.

After adapter ligation, RT-qPCR was performed as described above with primers specific to the adapter and the 5' end of the *duf1127₁* operon. The only difference is that there was no melt curve performed after the PCR amplification. Instead, this RT-qPCR was used as a template for a nested PCR with primers still specific to the adapter and the 5' end of *duf1127₁*, yet a bit shifted. Taq-PCR was performed as described above.

The PCR product was ligated into the pJET cloning vector (CloneJET PCR Cloning Kit, Thermo Scientific) as per the kit manual. Prior to ligation into the vector, a blunting reaction was performed according to the manufacturer's instructions, as Taq-Polymerase created sticky end, yet pJET needs blunt ends for cloning. The vector was transformed into *E. coli* DH5α cells as described above and plated onto LB plates containing ampicillin. 24 clones were picked from each replicate, grown in liquid culture with ampicillin and plasmid was isolated as described above (with friendly acknowledgement of the help of Susanne Barth-Weber). The isolated plasmids were sent for sequencing by Microsynth Seqlab (Göttingen).

### 2.2.4 Working with proteins

#### 2.2.4.1 SDS-Tricine PAGE

SDS-Tricine PAGE was performed to visualize proteins either in a gel or in a Western Blot (based on Schägger, 2006). For this, a 12 % polyacrylamide gel (thickness 1.5 mm; for two mini gels: 40% polyacrylamide 37.5:1, 6.4 ml; 3x gel buffer, 5.4 ml; 60 % glycerol, 2.1 ml; 10 % APS; 65 µl; TEMED, 6.5 µl; VE-$H_2O$, 2 ml; 3 x gel buffer: SDS, 0.3 g; tris base, 36.3 g; VE-$H_2O$ ad 100 ml; pH (adjusted with HCl) 8.45) served as a separation gel where proteins were separated according to size. APS and TEMED were added immediately prior to pouring. The mixture was overlayed with isopropanol (2-propanol) for polymerization for 40 min.

After polymerization, the isopropanol was removed and the upper edge of the gel dried using Whatman Paper. The mixture for the collection gel (4 % polyacrylamide collection gel for two mini gels**:** 40 % polyacrylamide 37.5:1, 600 µl; 3x gel buffer, 1.5 ml; 10 % APS, 50 µl;

TEMED, 5 µl; VE-$H_2O$, 3.9 ml) was prepared and immediately poured into the cast on top of the separation gel. A comb was inserted, and the gel was allowed to polymerize for 30 min.

After polymerization, the gel was kept in between glass plates and placed into a gel running chamber. The inside chamber was filled with 1x cathode buffer (10x cathode buffer**:** SDS, 5 g; tricine, 89.5 g; tris base, 60.5 g; VE-$H_2O$ ad 500 ml; pH (do not adjust!) 8.25). The outside chamber was filled with 1x anode buffer (10x anode buffer**:** tris base, 60.5 g; VE-$H_2O$ ad 500 ml; pH (with HCl), 8.9). The comb was removed, and the gel was now ready for loading.

The pellet of a sample (collection of samples see section 2.2.4.2) was resuspended in 100 µl 2x SDS sample buffer and were thawed on ice and then heated at 96 °C for 10 min. After a brief centrifugation to collect all liquid at the bottom of the tube. Prior to loading the samples onto the gel, they were incubated at 96 °C for 10 min. After a short spin down, 10 µl of sample containing sample buffer (2x SDS sample buffer**:** 0.5 M tris-HCl pH 6.8, 12.5 ml; glycerol, 10 ml; SDS, 2 g; ß-mercaptoethanol, 5 ml; bromophenol blue, 10 mg) were loaded onto the gel, along with 5 µl of marker (Spectra™ Multicolor Low Range Protein Ladder). Any pockets of the gel that were not containing sample were filled with 15 µl 2x SDS buffer to ensure smooth and nice running of the gel.

The gel was run at 60 V initially, until the samples had completely entered the separation gel. Then, the voltage was increased to 100 V and the gel was run until the blue loading dye had run out. The gel chamber and cast were disassembled, and one gel was used for blotting while the other one was used for either Coomassie or silver staining (see below).

2.2.4.2 Western Blot

For Western Blot sampling, *S. meliloti* was grown in TY media with Sm and antibiotics corresponding to plasmid-mediated resistance overnight at 32 °C, 140 rpm. The culture was then diluted into fresh, pre-warmed TY medium to $OD_{600nm}$ 0.2 and grown at 32 °C, 140 rpm until $OD_{600nm}$ 0.5. At $OD_{600nm}$ 0.5, a 1.5 ml sample was taken (= t0) before cells were treated with the subinhibitory amount of antibiotic or the corresponding amount of EtOH for 10 min. Typically, 4.5 µl Tc or EtOH were added to a 30 ml culture. After 10 min, another 1.5 ml sample was taken (= t10). The samples were centrifuged at 10 000 rpm for 3 min. Supernatant was discarded and the pellet resuspended in 100 µl 2x SDS sample buffer. Samples were kept at -20 °C. All experiments were performed in triplicates unless otherwise stated.

For Western Blotting, two SDS PAGE gels and samples were prepared as described above. 10 µl of each sample were loaded onto the gels. In some cases, it was necessary to load 20 µl instead of 10 to observe a signal.

The gels were run as described above. After the run, the gel casts were disassembled and one gel was used for blotting, while the other was used for either Coomassie or silver staining. 6 Whatman paper were cut to the size of the gel. A PVDF membrane was also cut to the size of the gel. Prior to blotting, the membrane was activated in methanol for 30 sec and washed in VE water for 30 sec. This is necessary to allow proteins to transfer onto the membrane as the membrane is hydrophobic and without activation, protein transfer to the membrane would be difficult. Both the membrane and the Whatman papers were incubated in 1 x Western Transfer buffer (1 x Western transfer buffer containing 100 ml methanol per l VE-$H_2O$; 10x Western transfer buffer: glycine, 144.1 g; Tris base, 30.3 g; ad 1 l VE-$H_2O$) for 5 min prior to blot assembly. The blot was assembled as follows (bottom-to-top): 3x Whatman paper, PVDX membrane, gel, 3x Whatman Paper. Blotting occurred over night (for at least 16h) at 0.4 $mA/cm^2$ membrane.

After blotting, the blot was disassembled and the membrane was immediately transferred into a Falcon tube containing 25 ml blocking solution (5 % (w/v) milk powder in 1x PBS-T; 10 x

PBS buffer**:** KCl, 2.01 g; $KH_2PO_4$, 2.45 g; $Na_2HPO_4$, 17.8 g; NaCl, 81.88 g; pH (with HCl) 7.4; 1 x PBS-T buffer; 10x PBS, 100 ml; Tween-20, 1 ml; ad 1 l VE-$H_2O$). The membrane was incubated in blocking solution for 1.5h at RT with constant rotation. Afterwards, the membrane was washed briefly 3 times with 1x PBS-T. The membrane was then transferred to a Falcon tube containing 10 ml antibody solution (anti-FLAG antibody (Thermo Fisher Scientific) diluted 1:1000 in 2 % (w/v) milk powder in 1x PBS-T) and incubated for at least 45 min to 3 hours. The incubation time varied depending on how many times the antibody solution was used. After incubation with the antibody, the membrane was washed 3 times for 10 min with 1x PBS-T and then transferred into a clean see-through plastic bag.

For detection, 750 µl stable peroxidase solution were mixed with 750 µl substrate solution and distributed evenly over the membrane. The antibody is coupled to horseradish peroxidase, therefore not needing incubation with a second antibody. Then, the signals on the membrane were visualized using a chemiluminescence reader.

#### 2.2.4.3 Coomassie staining

Proteins were stained using Coomassie Brilliant Blue dye (compare Laemmli, 1970). The gel was incubated in Coomassie solution over night with light shaking (99 % acetic acid, 50 ml; 99 % MeOH, 200 ml; Coomassie Brilliant Blue G-250, 0.1 %; VE-$H_2O$, 250 ml). After staining, the Coomassie solution was transferred back into its original bottle and the membrane was subjected to de-staining. First, the membrane was washed 3 times for 1 min with VE water and then incubated in de-stain solution (acetic acid, 100 ml; ethanol, 200 ml; VE-$H_2O$ ad 1 l). The de-stain solution was changed every 30 min to an hour until the gel was de-stained and only protein bands remained visible. The gel was transferred into a clear plastic bag and scanned.

#### 2.2.4.4 Silver staining

Silver staining is more sensitive than Coomassie staining and was used to visualize proteins from the 3xFLAG pulldown experiment (Lottspeich & Zorbas, 1998; compare Chevalet et al., 2006). All buffers were always prepared freshly on the same day, and formaldehyde was only added immediately before use. For staining, the gel was incubated in fixing solution + 100 µl 37% formaldehyde (37% formaldehyde, 0.05 % (v/v); 99 % acetic acid, 12 % (v/v); 99% MeOH, 50 % (v/v); VE-$H_2O$ ad 500 ml) over night with light shaking. The solution was discarded, and the gel was washed 3 times with 50 % EtOH for 20 min each. Sometimes, the gel shrunk during over-night incubation in fixing solution but went back to its original size during the EtOH washing and following steps. Afterwards, the gel was incubated for 1 min in Solution 1 ($Na_2S_2O_3$ x 5 $H_2O$, 0.1 g; VE-$H_2O$ ad 500 ml). Solution 1 was discarded; the gel was washed 3 time with VE water for 1 min and then incubated for 20 min in solution 2 (37 % formaldehyde, 187.5 µl; $AgNO_3$, 0.5 g; VE-$H_2O$ ad 250 ml) while shaking. Solution 2 was discarded into a separate container as it contains metal ions, and the gel was washed 3 times with VE water for 1 min. The gel was incubated in solution 3 (37 % formaldehyde, 125 µl; $Na_2CO_3$, 15 g; solution 1, 5 ml; VE-$H_2O$ ad 250 ml) until the desired strength of the band was visible. The reaction was stopped using 99% acetic acid. The gel was then transferred into a clear plastic bag and scanned.

#### 2.2.4.5 3xFLAG pulldown

To identify potential protein interaction partners of $DUF1127_1$, a 3xFLAG pulldown was performed using the existing plasmid with the full-length *duf1127*$_1$ fused to a SPA tag (plasmid *duf1172*$_1$-SPA; protocol compare Zeghouf et al., 2004). All steps were performed at 4 °C. *S. meliloti* cells were diluted to OD 0.2 and cultured in 300 ml TY in a 500 ml flask without antibiotics to OD 0.5 at 32 °C, 140 rpm. At OD 0.5, 1.5 µg/ml Tc or the corresponding amount

of EtOH was added. After 10 min, cells were transferred onto ice rocks in centrifuge tubes and centrifuged at 6 000 rpm for 10 min at 4 °C. Cell pellets were resuspended in 3.6 ml ice-cold sonication buffer (Tab. 19) and split into two tubes with 1.8 ml each. Sonication was performed 4 x 30s at 70% intensity. Cell debris was removed by centrifugation at 13 000 rpm for 20 min at 4 °C.

100 µl of the supernatant from each tube were taken as a lysate sample (L). The remaining supernatant was mixed with 50 µl of washed Anti-FLAG magnetic beads (washed 3x with 500 µl sonication buffer) and the tubes were incubated for 2.5 h with constant rotation. After incubation, the samples were placed on a magnetic stand and another 100 µl sample was taken as flow-through sample (FT). The beads were washed very carefully 4x with 500 µl, saving the wash fractions 1 and 4 (W1 and W4, respectively). Despite washing carefully, it is crucial that the beads are resuspended, as the buffer needs to reach all beads to properly wash unbound material or contaminants. After washing, the beads were resuspended in 100 µl sonication buffer and the two tubes that were previously split were re-merged. A 50 µl sample of beads was taken and mix with 50 µl 2 x SDS buffer as beads sample (B). As the SDS buffer would elute everything from the beads, including the antibody, an acidic elution was performed with the remaining beads. For elution (E), the beads were resuspended in 50 µl 0.1 M glycine-HCl pH 3.0, and incubated for 10 min at RT. After this step, the elution solution was removed into a new tube and was immediately neutralized by adding 30 µl 0.5 M Tris, pH 8.0. The beads were kept and resuspended in sonication buffer. All samples were stored at -20 °C.

**Tab. 19:** Sonication buffer used in this experiment, based on the protocols in Zeghouf et al., 2004 and Grützner et al., 2022.

| **Component** | **Stock solution** | **Final concentration** |
|---|---|---|
| DTT | 1 M | 1 mM |
| EDTA pH 8.0 | 0.5 M | 0.2 mM |
| Glycerol | 80 % | 10 % |
| KCl | 3 M | 150 mM |
| $MgCl_2$ | 1 M | 1 mM, 5 mM |
| PMSF | 0.1 M | 0.5 mM |
| Tris-HCl pH 7.9 | 1 M | 20 M |

### 2.2.4.6 Fluorescence measurements

All fluorescence measurements were performed with cultures harboring plasmids containing an *egfp* reporter construct (Chalfie et al., 1994). Cells of three biological replicates were grown to OD 0.5 and 3 times 150 µl were transferred into 3 separate wells of a black 96-well plate to achieve technical triplicates. Fluorescence was measured with extinction at 488 nm and emission at 522 nm at a plate reader (Tecan).

After subtracting the autofluorescence, the fluorescence was normalized to the OD of the culture at the time of measurement. Reliable measurements with eGFP can only be obtained after 20 min of reporter induction, which made this system impractical for measuring fluorescence with Tc after 10 min, as eGFP would not be fully functional yet.

### 2.2.5 Data evaluation, statistical treatments and RNA structure prediction

All experiments were performed at least in triplicate unless stated otherwise. Statistical treatments including t-Test was performed in R (https://www.r-project.org/; last access 17.8.2024 17:48) with suitable package.

Evaluation of the RNA sequencing was performed by collaboration partners Till Sauerwein and Konrad Förstner (ZB Med, Cologne). Structure predictions were performed using RNAfold available online from the university of Vienna (http://rna.tbi.univie.ac.at/cgi-bin/RNAWebSuite/RNAfold.cgi; last access, 19.8.2024, 11:02). Alignments were performed with ClustalOmega using the EMBL-EBI analysis tool and MView (Madeira et al., 2024; Brown et al., 1998) and visualized in Jalview (Waterhouse et al., 2009). Percentage similarity was calculated in SimIdent (Stothard, 2000) from alignments made in MAFFT (Katoh et al., 2002, 2019).

# 3. Results

## 3.1 RNA Sequencing revealed 373 mRNAs with significantly changed mRNA levels

The global effect of short-term, sublethal tetracycline (Tc) was studied to reveal early regulatory responses in the transcriptome.

To analyze the effect of short-term, sublethal Tc treatment, RNA sequencing of *S. meliloti* 2011 treated with a subinhibitory concentration of 1.5 µg/ml Tc for 10 min was compared to a mock treatment. A volcano plot (Fig. 6) shows that statistically highly significant changes in mRNA levels with a $Log_2$ Foldchange ($Log_2(Fc)$) ≥ 1 and a p-value ≤ 0.05 were abundant. Of the 373 mRNAs with significantly changed abundances, 140 had increased and 233 decreased in response to the treatment. Among those with higher abundance after short-term Tc treatment, the hit with highest $Log_2(Fc)$, visible to the far right, was a gene encoding a protein with a DUF1127 domain.

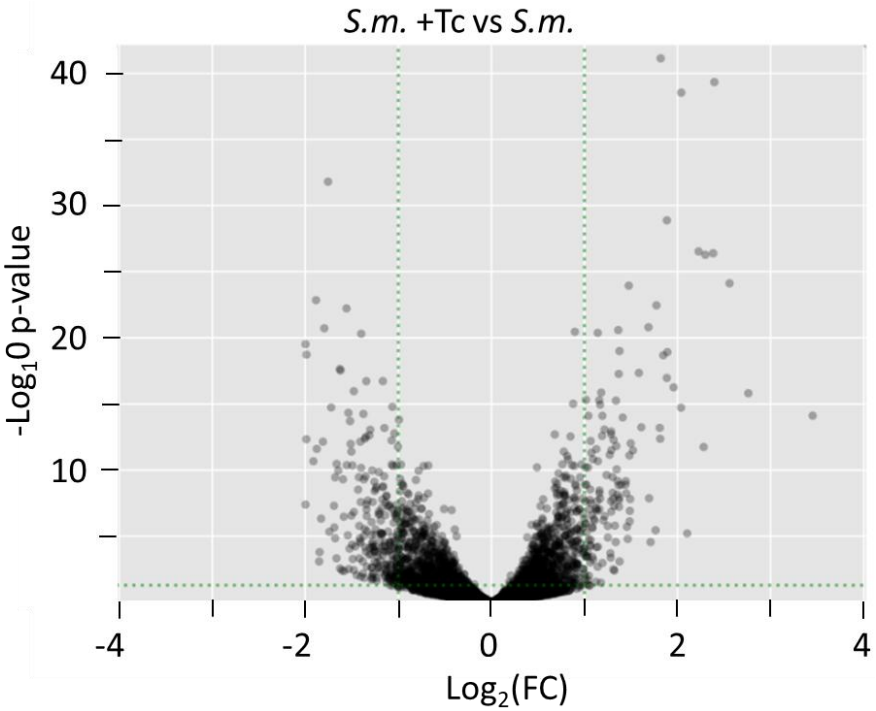


**Fig. 6:** Volcano plot showing significant changes in mRNA levels of cultures treated with Tc (1.5 µg/ml for 10 min) to non-treated controls. The RNA for sequencing was prepared by R. Scheuer and the bioinformatic evaluation was performed by T. Sauerwein and K. Förstner from ZB Med, Cologne. The data originate from three biologically independent experiments.

The genes with a significant and high increase in mRNA level were analyzed in more detail. Interestingly, these genes were found to be mostly at the beginning of operons or in monocistronic transcripts. On the other hand, genes with a decrease in mRNA level were found to be mostly second or further downstream in operons (Theresa Dietz, unpublished).

The RNA seq analysis showed that the top 24 hits with the highest fold-change often coded for small proteins (< 100 amino acids, aa), and genes encoding DUF1127 domain-containing proteins (following: *duf1127* genes) were highly overrepresented with 6 members (Tab. 20).

**Tab. 20:** Top hits with an increased mRNA level found in the RNA seq.

| Locus tag | $Log_2$(FC) | Amino acids | Gene or protein |
|---|---|---|---|
| SM2011_RS13250 | 4,04 | 83 | DUF1127$_1$ |
| SM2011_RS17980 | 3,45 | 148 | *phaP1* |
| SM2011_RS36240 | 2,76 | 57 | HP |
| SM2011_RS18160 | 2,56 | 88 | HP |
| SM2011_RS21095 | 2,40 | 376 | *prfB* |
| SM2011_RS07185 | 2,38 | 91 | TA module |
| SM2011_RS24515 | 2,30 | 66 | DUF1127$_2$ |
| SM2011_RS29675 | 2,28 | 307 | *rocF* |
| SM2011_RS23660 | 2,23 | 617 | ABC transporter |
| SM2011_RS01030 | 2,10 | 95 | XpaX domain |
| SM2011_RS14625 | 2,04 | 224 | L,D transpeptidase |
| SM2011_RS33250 | 2,04 | 45 | DUF1127$_3$ |
| SM2011_RS19100 | 1,96 | 137 | HP |
| SM2011_RS33625 | 1,89 | 66 | DUF1127$_4$ |
| SM2011_RS11895 | 1,89 | 604 | ABC transporter |
| SM2011_RS21220 | 1,88 | 156 | *rpsG* |
| SM2011_RS21215 | 1,85 | 123 | *rpsL* |
| SM2011_RS28640 | 1,82 | 122 | *omp10* |
| SM2011_RS26920 | 1,81 | 179 | peroxiredoxin |
| SM2011_RS36230 | 1,81 | 58 | HP |
| SM2011_RS36180 | 1,77 | 53 | HP |
| SM2011_RS36225 | 1,76 | 51 | HP |
| SM2011_RS18225 | 1,71 | 98 | DUF1127$_5$ |
| SM2011_RS33620 | 1,69 | 47 | DUF1127$_6$ |

13 out of 24 ORF have a length of < 100 amino acids among the genes with the highest $Log_2$(Fc). The top hit was named *duf1127$_1$* according to the protein it encodes. The gene with the second highest induction encodes PhaP1, a phasin, a protein involved in poly-3-hydroxybutyrate (PHB) synthesis (Wang et al., 2007). Hits three and four encode hypothetical proteins, whose gene products and functions remain unknown. Another *duf1127* gene, *duf1127$_2$*, is in the Top10 of the genes with the highest increase in mRNA level at position 7. Overall, 6 *duf1127* genes are present in the Top24 hits. Thus, this family was selected for further investigation.

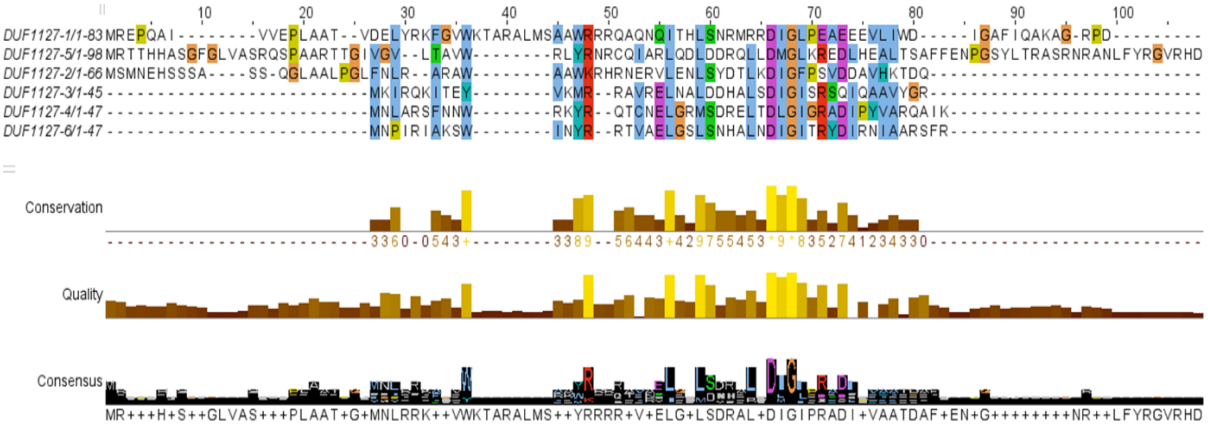


**Fig. 7:** Protein sequence alignment of the six DUF1127 proteins found in this study. Conservation is shown below the sequence alignment in yellow-brownish colors and indicates the conservation of properties in the alignment. Quality scores are shown in the same color scheme and measure the likelihood of observing the mutations. The consensus sequence is given in black.

Using the conceptually translated sequences, a similarity analysis was performed based on the alignment (Fig. 7). The six DUF1127 show some similarity, as there are some residues that are conserved throughout all six DUF1127. On a nucleotide level, this result is reflected (suppl. Fig. S1).

The six DUF1127 can be sorted into three longer (#1, #2, #5) and three shorter (#3, #4, #6) ones. However, the similarity between the DUF1127 is not that high (Fig. 8). There are some conserved residues visible across all six DUF1127. Aspartic acid (D) at position 66 and glycine (G) at position 68 are identical across all six proteins (see Fig. 7). Some residues are not identical but similar, as the amino acids share chemical properties (e. g. positions 48, 59 or 77; see Fig. 7).

The alignment was repeated in MAFFT (Katoh et al., 2002, 2019) and SimIdent (Stothard, 2000) to calculate the percentages of identity and similarity between the six DUF1127 proteins found in this study (Tab. 21). Only $DUF1127_3$ and $DUF1127_6$ as well as $DUF1127_4$ and $DUF1127_6$ exceed 50% similarity. Similarities below 20% were considered as not significant. Sequence identity never exceeded 50 %.

**Tab. 21:** Percentage identity and similarity of the DUF1127 found in this study *versus* each other. Each DUF1127 is labeled with their number according to the annotation established above. #, number.

| DUF1127 # | vs DUF1127 # | % Identity | % Similarity |
|---|---|---|---|
| 1 | 2 | 13.98 | 31.18 |
| | 3 | 8.43 | 24.10 |
| | 4 | 14.46 | 31.33 |
| | 5 | 11.30 | 21.74 |
| | 6 | 10.84 | 20.48 |
| 2 | 3 | 12.33 | 20.55 |
| | 4 | 15.07 | 27.40 |
| | 5 | 14.56 | 24.27 |
| | 6 | 16.44 | 20.55 |
| 3 | 4 | 25.53 | 44.68 |
| | 5 | 10.00 | No similarity |
| | 6 | 34.04 | 51.06 |
| 4 | 5 | 13.00 | 20.00 |
| | 6 | 40.43 | 53.19 |
| 5 | 6 | 12.00 | 22.00 |

These results show that the six DUF1127 proteins share some similarities with each other in terms of amino acids. DUF1127 proteins were also described in other bacteria (suppl. Fig. S2). 14 other DUF1127 proteins from six different bacteria were chosen from literature to assess similarity between organisms.

In the plant-associated bacterium *Agrobacterium tumefaciens*, seven genes encoding DUF1127 proteins were found, three shorter and four longer ones (Kraus et al., 2020). In the zoonotic *Brucella abortus*, three members of the DUF1127 family were analyzed (Budnick et al., 2018; Sheehan et al., 2015). In *S. meliloti* 1021, a single gene was described, as well as in *Rhizobium leguminosarum* symbiovar trifolii (Budnick et al., 2018). Such a gene has also been described in *Rhodobacter sphaeroides* (Grützner et al., 2021). In the human pathogen *Salmonella enterica*, a single small DUF1127 protein is produced, YjiS (Venturini et al., 2020).

**Tab. 22:** Percentage identity and similarity of the six DUF1127 found in this study *versus* DUF1127 proteins described in other bacteria. Blue and green highlight the DUF1127 proteins with highest similarity compared to the DUF1127 proteins from this study. ATU, *A. tumefaciens*; BAB, *B. abortus*; Rleg, *R. leguminosarum*; RSP, *R. sphaeroides*; SM, *S. meliloti* 1021; STMUK, *S. enterica* serovar Typhimurium; #, number.

| DUF # | Gene identifier | % Identity | % Similarity | DUF # | Gene identifier | % Identity | % Similarity |
|---|---|---|---|---|---|---|---|
| 1 | ATU_RS03215 | 11.21 | 25.00 | 2 | ATU_RS03215 | 11.88 | 24.75 |
| | ATU_RS08170 | 9.18 | 25.51 | | ATU_RS08170 | 12.36 | No similarity |
| | ATU_RS08175 | 13.25 | 21.69 | | ATU_RS08175 | 16.44 | 21.92 |
| | ATU_RS08650 | 8.08 | 20.20 | | ATU_RS08650 | 35.90 | 47.44 |
| | ATU_RS09035 | 10.83 | 20.00 | | ATU_RS09035 | 11.32 | No similarity |
| | ATU_RS09125 | 27.06 | 43.53 | | ATU_RS09125 | 16.85 | 28.09 |
| | ATU_RS21905 | 12.05 | 30.12 | | ATU_RS21905 | 15.07 | 26.03 |
| | BAB_RS20300 | 14.46 | 31.33 | | BAB_RS20300 | 17.81 | 30.14 |
| | BAB_RS28790 | 14.46 | 31.33 | | BAB_RS28790 | 16.44 | 26.03 |
| | BAB_RS29075 | 7.23 | 24.10 | | BAB_RS29075 | 12.33 | No similarity |
| | Rleg2_1502 | 13.25 | 28.92 | | Rleg2_1502 | 13.70 | 24.66 |
| | RSP_6037 | 9.78 | 29.35 | | RSP_6037 | 16.00 | 37.33 |
| | SM_RS07875 | 14.46 | 31.33 | | SM_RS07875 | 15.07 | 27.40 |
| | STMUK_4508 | 15.66 | 28.92 | | STMUK_4508 | 22.54 | 29.58 |
| 3 | ATU_RS03215 | 12.24 | 23.47 | 4 | ATU_RS03215 | 11.22 | 23.47 |
| | ATU_RS08170 | 23.08 | 35.38 | | ATU_RS08170 | 52.31 | 56.92 |
| | ATU_RS08175 | 29.79 | 53.19 | | ATU_RS08175 | 44.68 | 57.45 |
| | ATU_RS08650 | 14.29 | 24.68 | | ATU_RS08650 | 10.39 | 20.78 |
| | ATU_RS09035 | 9.90 | No similarity | | ATU_RS09035 | 9.90 | No similarity |
| | ATU_RS09125 | 12.82 | 21.79 | | ATU_RS09125 | 12.82 | 24.36 |
| | ATU_RS21905 | 27.08 | 45.83 | | ATU_RS21905 | 70.83 | 77.08 |
| | BAB_RS20300 | 29.17 | 47.92 | | BAB_RS20300 | 68.75 | 77.08 |
| | BAB_RS28790 | 25.00 | 43.75 | | BAB_RS28790 | 62.50 | 79.17 |
| | BAB_RS29075 | 66.67 | 80.00 | | BAB_RS29075 | 27.66 | 46.81 |
| | Rleg2_1502 | 27.08 | 43.75 | | Rleg2_1502 | 70.83 | 75.00 |
| | RSP_6037 | 21.13 | 32.39 | | RSP_6037 | 25.35 | 35.21 |
| | SM_RS07875 | 25.53 | 44.68 | | SM_RS07875 | 100.00 | 100.00 |
| | STMUK_4508 | 16.67 | 30.00 | | STMUK_4508 | 22.58 | 33.87 |
| 5 | ATU_RS03215 | 33.01 | 46.60 | 6 | ATU_RS03215 | 10.20 | 20.41 |
| | ATU_RS08170 | 17.00 | 29.00 | | ATU_RS08170 | 33.85 | 43.08 |
| | ATU_RS08175 | 13.00 | 21.00 | | ATU_RS08175 | 80.85 | 87.23 |
| | ATU_RS08650 | 15.53 | 22.33 | | ATU_RS08650 | 14.29 | No similarity |
| | ATU_RS09035 | 14.63 | 22.76 | | ATU_RS09035 | 15.84 | 23.76 |
| | ATU_RS09125 | 12.84 | 22.94 | | ATU_RS09125 | 11.54 | 21.79 |
| | ATU_RS21905 | 13.00 | No similarity | | ATU_RS21905 | 37.50 | 47.92 |
| | BAB_RS20300 | 13.00 | 22.00 | | BAB_RS20300 | 43.75 | 52.08 |
| | BAB_RS28790 | 11.00 | 20.00 | | BAB_RS28790 | 41.67 | 52.08 |
| | BAB_RS29075 | 9.00 | 18.00 | | BAB_RS29075 | 29.79 | 53.19 |
| | Rleg2_1502 | 13.00 | 20.00 | | Rleg2_1502 | 43.75 | 52.08 |
| | RSP_6037 | 15.38 | 30.77 | | RSP_6037 | 22.54 | 29.58 |
| | SM_RS07875 | 13.00 | 20.00 | | SM_RS07875 | 40.43 | 53.19 |
| | STMUK_4508 | 14.00 | No similarity | | STMUK_4508 | 19.35 | 30.65 |

Again, similarities below 20 % were considered non-significant. From the DUF1127 proteins analyzed in this study, $DUF1127_1$ had no high similarity with any other protein, except for ATU_RS09125 from *A. tumefaciens* (Tab. 22). Both $DUF1127_1$ and ATU_RS09125 are long DUF1127 proteins. For the other two other long DUF1127 proteins found in this study, $DUF1127_2$ and $DUF1127_5$, #2 had the highest similarity to ATU_RS08650 and #5 had the highest similarity to ATU_RS03215 (see Tab. 22). Both DUF1127 proteins from *A. tumefaciens* are longer DUF1127 (Kraus et al., 2020).

The three shorter DUF1127 proteins from this study showed more similarity towards DUF1127 proteins from other bacteria. $DUF1127_4$ had a similarity of 100 % to the DUF1127 from *S. meliloti* 1021 (Tab. 22). The same $DUF1127_4$ also showed high similarity to Rleg2_1502 from

*R. leguminosarum* and ATU_RS21905 from *A. tumefaciens* (Tab. 22). Both DUF1127$_4$ and ATU_RS21905 are short DUF1127 proteins. High similarity was found as well between DUF1127$_4$ and BAB_RS28790 and BAB_RS20300 from *B. abortus* (Tab. 22). DUF1127$_3$ showed similarity to ATU_RS08175 and a high similarity to BAB_RS29075. DUF1127$_6$ showed high similarity to ATU_RS08175, as well as showing similarities to the three proteins from *Brucella*, and the ones from *R. leguminosarum* and *S. meliloti* 1021 (Tab. 22).

Taken together, the six DUF117 proteins found in this study showed little similarity towards each other, except some conserved residues. Among the six, the three smaller DUF1127 showed more similarity with each other. When compared to DUF1127 proteins from other bacteria, the three longer DUF1127 showed little similarity. The three shorter ones, however, showed more similarities to other DUF1127 proteins, particularly to *B. abortus* and *R. leguminosarum*. All six DUF1127 showed similarities to various DUF1127 proteins from *A. tumefaciens*. The regulation of the gene encoding DUF1127$_1$, which showed little similarity to the other DUF1127 proteins from this study and to proteins from other bacteria, was further investigated.

## 3.2 The top hit *duf1127$_1$* is preceded by an upstream ORF and responds to Tc exposure

The top hit *duf1127$_1$* was analyzed more closely. It was found to be preceded by an upstream ORF, named uORF1. This ORF was recently discovered (SEP26, renamed uORF1; Hadjeras et al., 2023) and in this work was shown that *duf1127$_1$* and uORF1 were co-transcribed and co-regulated (compare section 3.3).

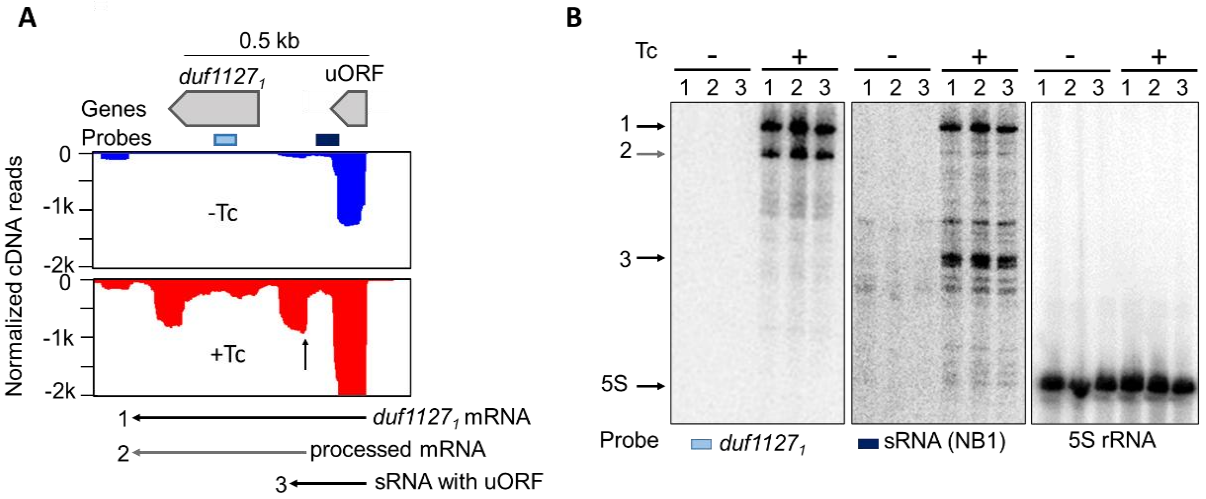


**Fig. 8:** Analysis of the *duf1127$_1$* operon. **(A)** The operon without Tc (blue) and with Tc (red) using the Integrated Genome Browser (IGB, Freese et al., 2016). Induction was clearly visible with Tc, and *duf1127$_1$* is preceded by uORF1 coding for 29 aa in conceptual translation. The black vertical arrow indicates a potential RNA cleavage site; probes for Northern blot hybridization are indicated at the end of uORF1 (dark blue) and in the *duf1127$_1$* (light blue). **(B)** Northern hybridization showed multiple mRNA bands using probes at the end of uORF1 (dark blue) and within *duf1127$_1$* (light blue) in Tc treatments (+). For a loading control, a probe for the 5S rRNA was used.

After 10 min of subinhibitory Tc exposure (red), the induction of uORF1 and *duf1127$_1$* is clearly visible (Fig. 8A). Northern hybridization revealed that a signal only upon Tc exposure for two probes in the operon (Fig. 8B). Dependent on which probe was used, different band sizes could be observed, with two longer and at least one shorter transcript. This suggested that differential

processing occurs. The three transcripts originating from this operon can be interpreted as the full-length mRNA expressed only after Tc exposure visible with either probe and thus covering the entire operon (horizontal arrow marked with 1 in Fig. 8B), a processed version detected only using the probe within *duf1127*$_1$ (horizontal arrow marked with 2), and a shorter sRNA (horizontal arrow marked with 3) with the probe at the 3' end of uORF1. This sRNA might be the result of premature termination of transcription. Additionally, weaker bands were visible with the sRNA probe (NB1).

## 3.3 Increase in mRNA level of selected genes could be validated

The RNA seq identified highly significant changes in mRNA levels upon short-term, sublethal Tc treatment. In order to independently verify the changes, RT-qPCR was applied for the genes with highest change observed during RNA seq using the same RNA batch. The top hits, which include the *duf1127*$_1$-operon with its small upstream open reading frame (uORF1), *phaP1*, and the two hypothetical proteins, as well as *duf1127*$_2$ were analyzed (Fig. 9). For genes with a decrease in mRNA levels, *rsmA* and *pdxA* as well as *mnhG* and RS19365 were analyzed, with the first two and last two genes each being in a polycistronic operon.

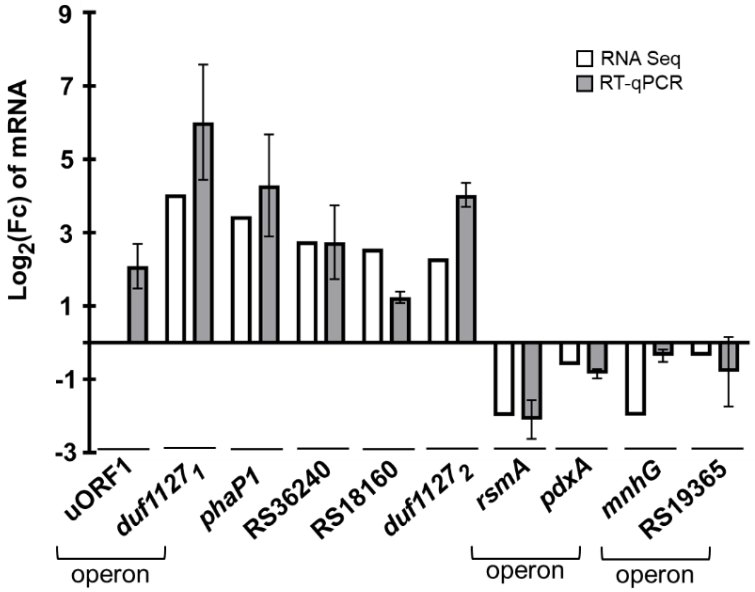


**Fig. 9:** Validation of changes in mRNA abundance discovered in RNA seq by RT-qPCR. Six genes with an increased mRNA level, as well as two with a decreased level (*rsmA* and *mnhG*) and upstream genes in their respective operons, were tested. uORF1 was not tested in the RNA seq due to not being annotated. RT-qPCR of three independent cultures was performed by J. Wähling (*duf1127*$_1$, *phaP1*), J. Kothe (uORF1) and R. Scheuer (all other genes).

All selected genes with an increase in mRNA levels (up-regulated genes) were validated by RT-qPCR (Fig. 9). The highest fold-change, again was visible with *duf1127*$_1$, validating the top hit (compare Tab. 20). Additionally, the operon structure predicted with uORF1 was used and here, this uORF1 was also validated to be up-regulated in the same RNA, despite not being separately detected during the bioinformatic analysis of the RNA-seq data, since it had not previously been annotated as ORF.

For selected genes with a decrease in mRNA level (down-regulated genes), not all changes in mRNA level could be validated. In the *pdxA-rsmA* operon, foldchanges were similar to the RNA seq. For RS19365, first in its operon, RT-qPCR resembled the RNA seq result. Down-regulation of *mnhG,* last in its operon, could not be validated by RT-qPCR.

The increase in mRNA amount after short-term Tc exposure (1.5 µg/ml Tc for 10 min) prompted analysis of whether the Tc concentration and the time of treatment played a role in the increase of mRNA levels. For this, *S. meliloti* 2011 was either treated with 0.5, 1 or 1.5 µg/ml Tc for 10 min (Fig. 10A). A different set of *S. meliloti* cultures was treated with 1.5 µg/ml Tc for 3, 6 or 10 min (Fig. 10B). RNA isolated from the cultures was analyzed by RT-qPCR, which could verify a dose- and time-dependent response.

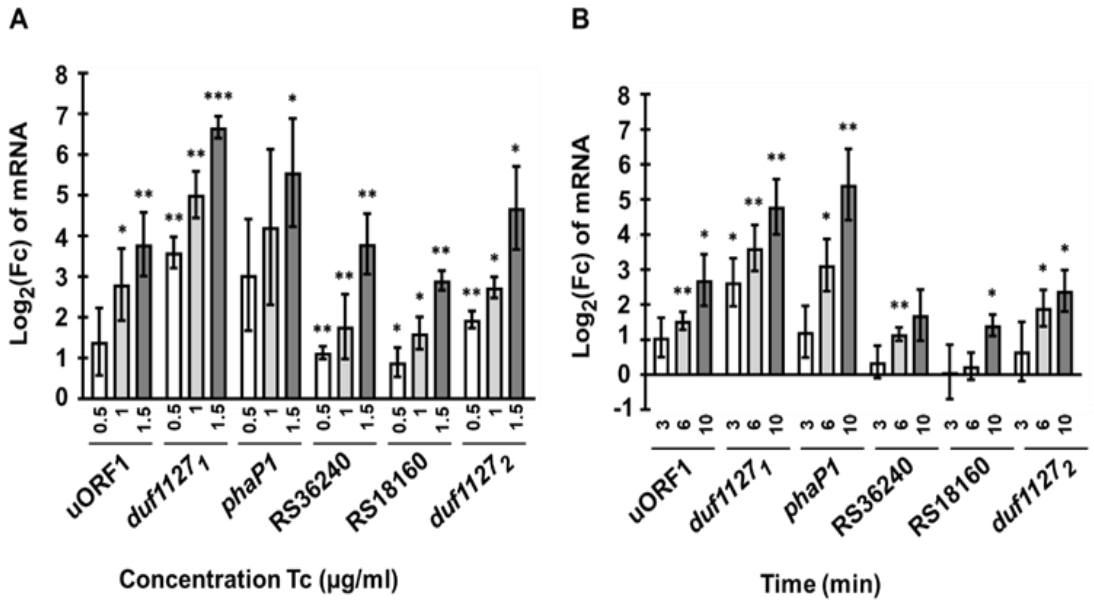


**Fig. 10:** Response of genes found to be up-regulated in the RNA seq to increasing Tc concentrations or to increase in Tc exposure time. **(A)** RT-qPCR of cultures treated with 0.5, 1 or 1.5 µ/ml Tc for 10 min. **(B)** RT-qPCR of cultures treated with 1.5 µg/ml Tc for 3, 6 or 10 min. RT-qPCR was performed by J. Wähling (*duf1127₁, phaP1*), J. Kothe (uORF1) and R. Scheuer (all other genes). Tc-treated cultures were compared to control cultures in three independent biological experiments. Statistical significance: *** $p \leq 0.001$, ** $p \leq 0.01$, * $p \leq 0.05$.

All genes tested showed an increase in mRNA level already at 0.5 µg/ml Tc after 10 min of treatment and this increased with the amount of Tc given (Fig. 10A). All genes also showed an increase in mRNA level over time. After 10 min, all genes showed a significant increase in mRNA level. Only *duf1127₁* showed a significant increase already after 3 min (Fig. 10B).

These results verify that Tc has an influence even early on in the exposure and even at low concentrations. Based on these results, the response to different stressors was tested for uORF1, *duf1127₁*, *duf1127₂* and *phaP1*.

## 3.4 *duf1127₁*, *duf1127₂* and *phaP1* react to different stressors

As uORF1 and *duf1127₁* responded to subinhibitory Tc exposure, the question arose whether other stressors could lead to similar or overlapping responses. For this, uORF1 and *duf1127₁*, as well as *phaP1* and *duf1127₂*, were tested with regards to different translational inhibitors, oxidative stress, and heat stress, all applied for short-term exposure of 10 min (Fig. 11).

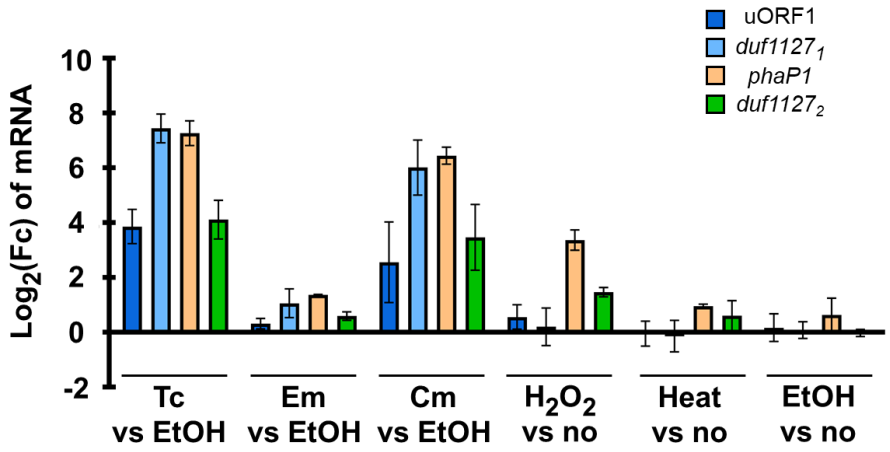


**Fig. 11:** Response of uORF1, *duf1127₁*, *phaP1* and *duf1127₂* to Cm, Em, $H_2O_2$ and heat. RT-qPCR was performed on Tc-treated cultures and compared to control cultures in three independent biological experiments. Tc: tetracycline, 1.5 µg/ml; Cm: chloramphenicol, 9 µg/ml; Em: erythromycin, 27 µg/ml; $H_2O_2$: hydrogen peroxide, 1mM, Heat: heat stress at 42 °C. Controls are indicated with the stressors: EtOH, the highest volume of EtOH was added as with the respective antibiotic treatment; no: no treatment was applied.

Tc exposure had already been shown to influence the *duf1127₁* operon. Tc is a translation inhibitor, inhibiting translation initiation. Chloramphenicol (Cm), like Tc, is a translation inhibitor and inhibits peptide chain elongation by targeting the peptidyl transferase at the ribosome. Therefore, the response of different genes to subinhibitory Cm exposure was tested. The macrolide antibiotic erythromycin (Em) also targets translation, albeit not at ribosome but instead on elongation factor level. All genes tested reacted to Cm and Em exposure. To exclude an unspecific stress reaction, oxidative stress was tested. Hydrogen peroxide ($H_2O_2$) is an agent producing oxygen radicals in the cell, therefore posing oxidative stress. Only *phaP1* and *duf1127₂* showed an increase in mRNA levels when treated with $H_2O_2$ (Fig. 11) This verified that the *duf1127₁* operon was specifically reacting to translational stress. Lastly, when cells were stressed under high temperature conditions (42 °C, 10 min), only *phaP1* showed an increase in mRNA level, indicating a general stress response (Fig. 11). Thus, also the *phaP1* and *duf1127₂* genes could be differentiated in their stress responses as well.

These results suggest that uORF1 and *duf1127₁* react specifically to translation inhibitors, which could give a hint about their regulation or function.

## 3.5 mRNA stability analysis reveals increased mRNA half-life upon Tc exposure

In general, mRNA steady-state levels can be influenced by many factors, such as increased mRNA decay or stabilization, in addition to the polar effect of decoupling between translation and transcription (Blaha & Wade, 2022; Deutscher, 2006; Rochat et al., 2013). To address

changes in mRNA stability upon Tc exposure, mRNA half-lives after 10 min of subinhibitory Tc exposure were measured (Tab. 23). For this, mRNA synthesis was stopped by the addition of rifampicin after 10 min of subinhibitory Tc exposure and samples were collected in defined time intervals. In parallel, the mRNA half-lives in control, non-exposed cultures were determined.

**Tab. 23:** Half-life determined for selected genes with and without Tc exposure by RT-qPCR. The results originate from three independent biological experiments. n.dc, no decay.

| Line | Gene | Half-life -Tc (s) | Half-life +Tc (s) |
|---|---|---|---|
| 1 | *metZ* | 77 ± 6 | 418 ± 106 |
| 2 | uORF1 | 107 ± 10 | 323 ± 150 |
| 3 | *duf1127*$_1$ (1. Pr.) | 179 ± 19 | 547 ± 480 (290, 1100, 250) |
| 4 | *duf1127*$_1$ (2. Pr.) | 142 ± 30 | 461 ± 59 |
| 5 | *phaP1* (1. Pr.) | 224 ± 19 | n.dc., 1760, 480 |
| 6 | *phaP1* (2. Pr.) | 240 ± 60 | n.dc., 725, 1020 |
| 7 | *duf1127*$_2$ | 88 ± 27 | 316 ± 79 |
| 8 | *ppiD* | 43 ± 7 | 255 ± 234 (525, 120, 120) |
| 9 | *moeA* (1. Pr.) | n.dc., 80, 170 | n.dc., n.dc., 218 |
| 10 | *moeA* (2. Pr.) | 165 ± 11 | n.dc., n.dc., 960 |
| 11 | *rsmA* (1. Pr.) | 1220, n.dc., 280 | 1380, n.dc., n.dc. |
| 12 | *rsmA* (2. Pr.) | 258, n.dc., 140 | n.dc., n.dc., 162 |
| 13 | *pdxA* | 214 ± 97 (198, 340, 104) | 360, n.dc., 142 |

In the RNA seq, *metZ*, gene is involved in methionine biosynthesis, remained unaffected by Tc and was thus chosen as a control gene. In a previous study had been determined to be 60 s (Scheuer et al., 2022). This could be verified in this study with a half-life of 77 s for *metZ* without Tc. However, with Tc, half-life increased about 6 times (Tab. 23, line 1).

Genes with an increase in mRNA level included uORF1, *duf1127*$_1$, *phaP1* and *duf1127*$_2$ (Tab. 23, lines 2-4). The half-life of both uORF1 and *duf1127*$_1$ tripled upon Tc exposure. Primers used for uORF1 do measure two transcripts, the 5' end of the full-length mRNA (compare Fig. 9, *duf112*$_1$ mRNA (1)) as well as the sRNA transcript (compare Fig. 9, sRNA (3)). The *phaP1* transcript was strongly stabilized upon Tc exposure, to the point of no decay being measurable for one replicate (compare Tab. 23, lines 5 +6). For *duf1127*$_2$, the half-life was much higher with Tc and within the same range as *duf1127*$_1$ (compare Tab. 23, line 7).

The genes *rsmA* and *pdxA* are in an operon and are the last genes in this operon. Half-live analysis revealed that for both genes, half-lives fluctuated (compare Tab. 23, lines 11 to 13). *rsmA*, last in the operon, was found to be significantly down-regulated (suppl. Fig. S3). Being the second to last gene in the operon, *pdxA* showed a slight but significant down-regulation (suppl. Fig. S3A). It showed a half-life of around 214 s without Tc. With Tc, half-lives seemed to increase.

Further genes tested include *ppiD* and *moeA*, located in an operon. To explore the polar effect of decoupling between transcription and translation as a potential cause for difference in mRNA levels, these genes were analyzed as well. The polar effect shows an increase for the first gene in an operon with a gradual decrease afterwards towards the 3' end (Fig. 12).

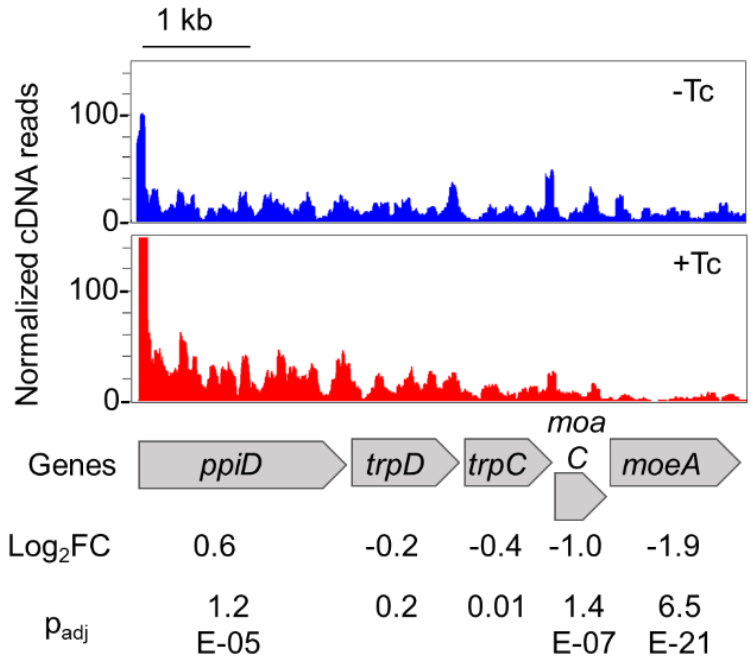


**Fig. 12:** The polar effect observed in the *trpDC* operon of *S. meliloti*. Foldchanges and p-value are given below.

It could be shown that the first gene in the *trpDC* operon, *ppiD*, has a significantly increased $Log_2$(Fc), while the next two genes did not reveal significant increase or decrease. The last two genes in the operon, *moaC and moeA*, were significantly down-regulated (Fig. 12). For *ppiD*, half-life increased with Tc exposure, while for *moeA*, no decay could be detected in two replicates while an increase was measured in the third (Tab. 23, lines 8-10).

In general, half-lives did increase upon Tc exposure, however, at the same time the standard deviation of the measured half-lives strongly increased as well. For some genes, no decay could be detected with Tc in one or more replicates. Thus, subinhibitory Tc exposure seems to generally stabilize mRNA.

## 3.6 Different mechanisms of regulation are observed for *duf1127₁*, *duf1127₂* and *phaP1*

With the results from the RNA seq and the mRNA stability analysis, it was decided to further focus on *duf1127₁*, *duf1127₂* and *phaP1*. While *duf1127₁* and *duf1127₂* both encode for proteins with a DUF1127 domain, their 5'UTRs strongly differ (Fig. 13A). As *duf1127₁* is preceded by at least two uORFs (shown later in this study), the 5'UTR of *duf1127₂* is much shorter and does not exhibit uORFs. The 5' UTR of *phaP1* does not feature any uORFs. In contrast to *duf1127₁*, both *duf1127₂* and *phaP1* are located on monocistronic messengers.

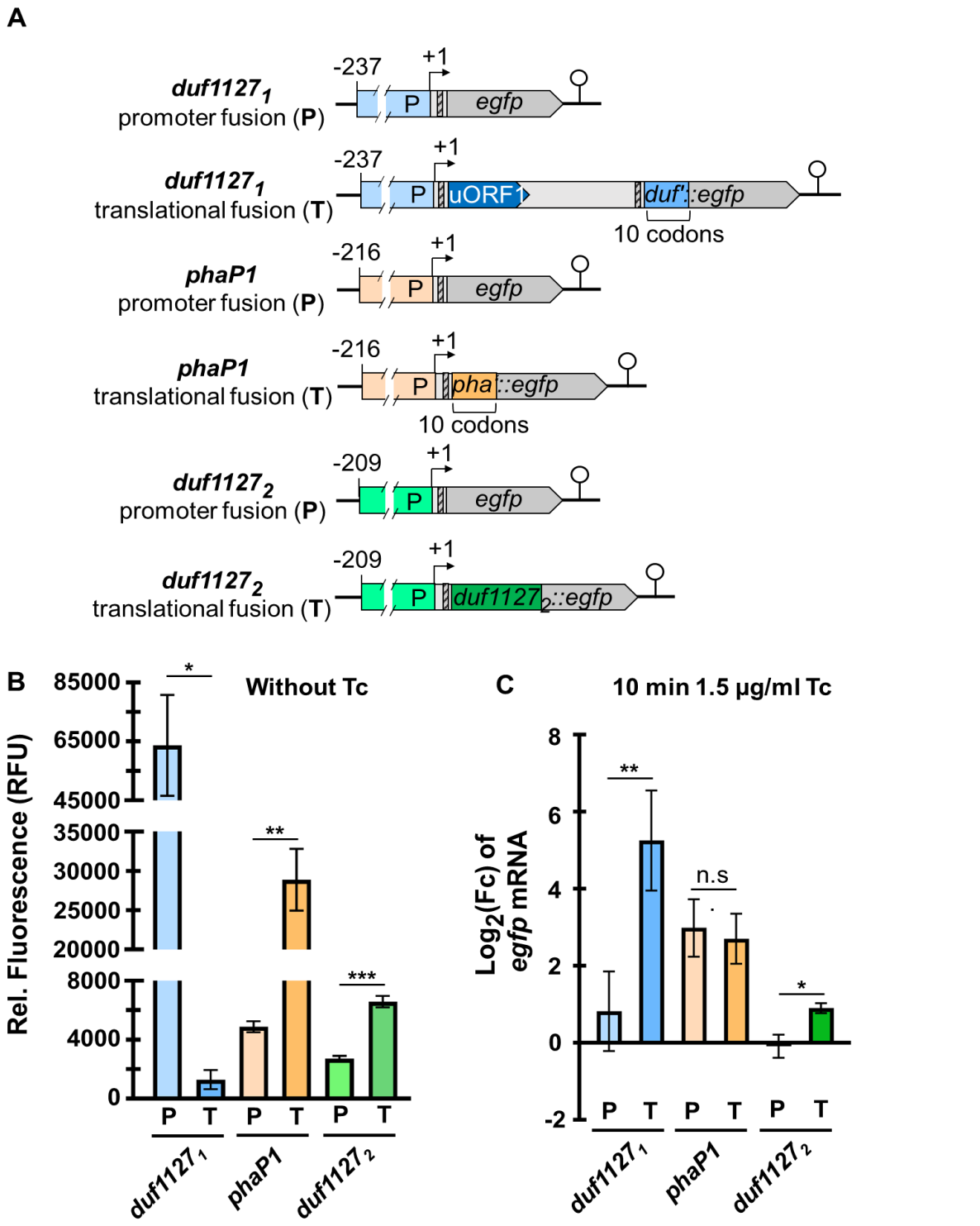


**Fig. 13:** Analysis of *egfp* reporter fusions. Both promoter (P) and translational fusions (T) plasmids were constructed. **(A)** Constructs used for fluorescence measurements and RT-qPCR analysis. Promoter fusions consist of the promoter region until about -200 bp to feature potential regulatory regions. The promoter is fused to a short leader containing a "standard" Shine Dalgarno sequence (sSD) and *egfp*. Translational fusions feature the same promoter region but contain their own 5'UTR with a SD sequence. For *duf1127*$_1$ and *phaP1*, only the first 10 codons were fused to eGFP, while the *duf1127*$_2$ fusion features the entire gene. **(B)** Fluorescence measurement of eGFP without Tc exposure of cultures harboring the indicated constructs. **(C)** RT-qPCR analysis of changes in the level of the reporter *egfp* mRNA upon Tc exposure. The results originate from three independent biological experiments. Statistical significance: **** $p \leq 0.0001$, *** $p \leq 0.001$, ** $p \leq 0.01$, * $p \leq 0.05$

Measuring fluorescence of all reporter constructs, differences between all three genes tested became apparent (Fig. 13B, C). Fluorescence measured without Tc of *duf1127₁* showed a strong fluorescence for the promoter, but little for the translational fusion (Fig. 13B). For *phaP1*, this is inverted, with the translational fusion showing a significantly higher fluorescence without Tc than the promoter fusion (Fig. 13B). For *duf1127₂*, the fusions resemble the result of *phaP1*.

However, eGFP is not suitable for measuring during early time points after Tc addition to cultures, as it needed at least 15-20 min to fold and emit fluorescence. This time was longer than the time that was of interest for Tc exposure in this study, so RT-qPCR was performed on the reporter mRNA instead (Fig. 13C). The results of the RT-qPCR on the reporter mRNA after Tc exposure showed that the promoter fusions of both *duf1127₁* and *duf1127₂* did not show a change in reporter mRNA level after exposure to Tc. The translational fusion did show a strong increase in mRNA level for *duf1127₁*. A lesser but still significant increase in reporter mRNA level was observed for *duf1127₂*. For *phaP1*, there is no difference between the two fusions, suggesting regulation at the promoter.

Taken together, this suggests different regulation mechanisms might be at play for all three genes. For *duf1127₁*, down-regulation in the absence of Tc despite strong promoter activity was suggested. Both fusion constructs feature a strong promoter, while the translational fusion showed less fluorescence, suggesting post-transcriptional regulation mechanisms. With the result of the RT-qPCR showing the strong increase in reporter mRNA level of the translational fusion, it was concluded that the 5' UTR is responsible for this regulation. For *phaP1*, it seemed like the 5'UTR had a positive effect on its expression, and it might be regulated on the promoter level. Finally, *duf11271₂* had a different 5' UTR with no ORFs, but its own ribosome binding site (RBS) seemed to make a difference. Furthermore, the regulation of *duf1127₂* seemed to contain post-transcriptional elements as well.

Since eGFP is not suitable for measuring changes in protein levels during early time points after Tc addition to cultures, as explained above, the reporter eGFP was changed to a SPA tag for following experiments.

For this, two translational fusions were constructed featuring full-length *duf1127₁* (DUF1127₁-SPA) and *duf1127₂ (*DUF1127₂-SPA*)*, each with a SPA tag (Fig. 14A). This tag is often used to visualize small proteins on a Western Blot, as it can be detected by monoclonal anti-FLAG antibodies. It was tested to see whether mRNA increase would also lead to an increased protein level. Fusion mRNA and protein levels were analyzed after Tc exposure by RT-qPCR and Western Blot, respectively. For *duf1127₁*, protein and RNA level were found to be greatly increased, with RNA level being increased 32-fold (Fig. 14B). For *duf1127₂* however, protein level was decreased while the mRNA level was only slightly increased by 1.7-fold, which was less than what was measured in both RNA seq and RT-qPCR (Fig. 14C; compare Tab. 20, Fig. 10).

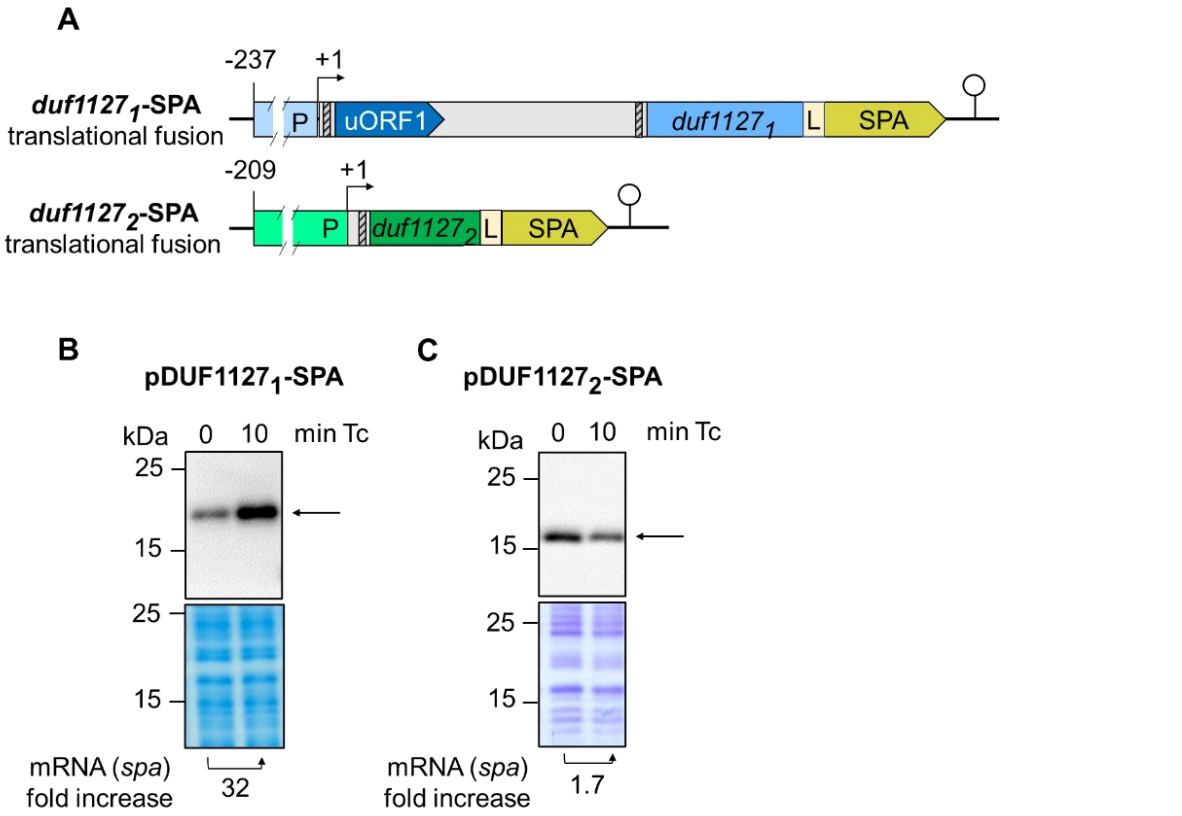


**Fig. 14:** Analysis of response to Tc on mRNA and protein levels for *duf11271* and *duf11272* SPA fusions. **(A)** Fusion constructs where both $duf1127_1$ and $duf1127_2$ with full length were each tagged with a SPA tag ($DUF1127_1$-SPA and $DUF1127_2$-SPA). **(B)** Western Blot with anti-FLAG antibodies for $DUF1127_1$-SPA fusion. The mRNA fold increase is given below the panel. **(C)** Western Blot with anti-FLAG antibodies for $DUF1127_2$-SPA. The RNA fold increase is given below the panels.

In this work, $duf1127_1$ induction has been shown for the native gene located on pSymB on the mRNA level, by fluorescence and mRNA analysis using *egfp* constructs, and by SPA fusions on the mRNA and protein level. These results showed that $duf1127_1$ was indeed induced on both RNA and protein level and suggested an importance of the 5' UTR for this induction.

## 3.7 The regulation of $duf1127_1$ involves translation of uORF1

Fluorescence measurements and RT-qPCR suggested post-transcriptional regulation for $duf1127_1$ (compare chapter 3.6). This was further investigated using again the SPA tag as reporter. Translational fusions were constructed featuring either the uORF1 fused to a linker and the SPA tag encoding sequence (uORF1-SPA), or including the uORF1, the intergenic region, and the first 10 codons of $duf1127_1$ fused to the linker and the SPA tag encoding sequence (DUF'-SPA in pDUF'-SPA; Fig. 15A). To further investigate the role of uORF1, a start-to-stop mutation in uORF1 was introduced into plasmid pDUF'-SPA, destroying the ORF (M1/Stop). The constructs were analyzed by Northern hybridization, RT-qPCR and Western Blot (Fig. 15B-D).

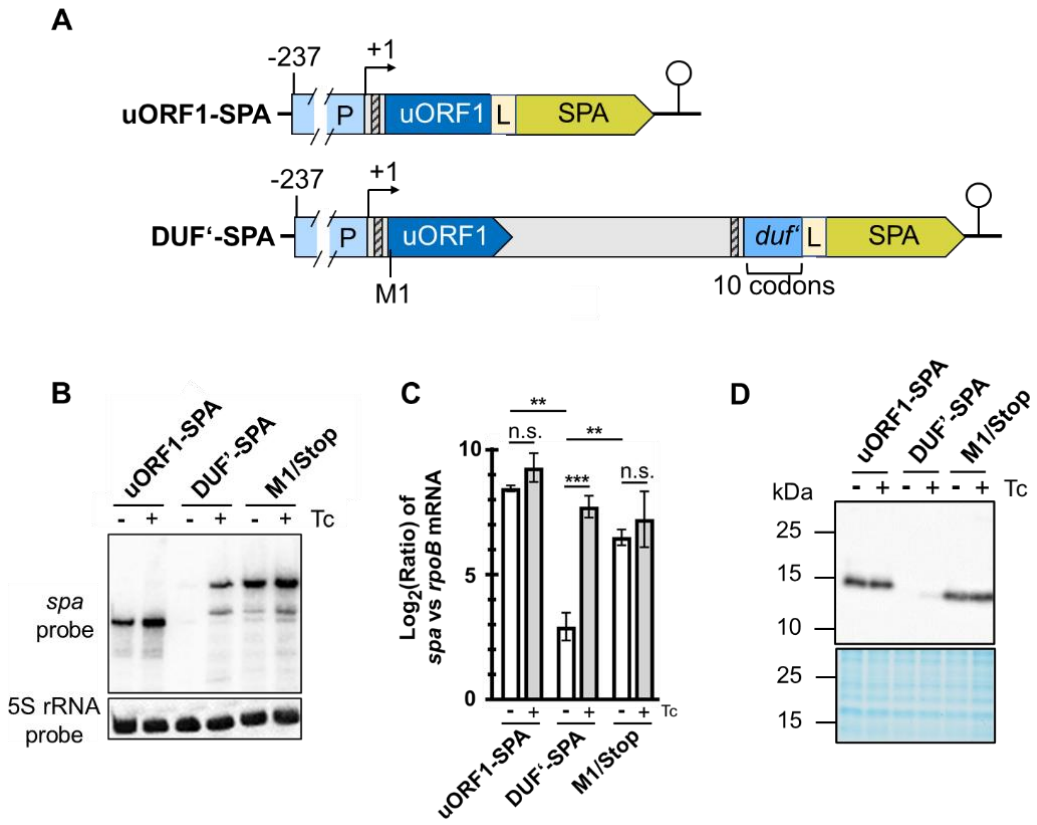


**Fig. 15:** SPA-tagged constructs addressing uORF1 and its importance for post-transcriptional regulation of *duf1127*$_1$. **(A)** Constructs were featuring the tagged uORF1 (uORF1-SPA), the tag fused after the first 10 codons of *duf1127*$_1$ (pDUF'-SPA), or pDUF'-SPA which a start-to-stop mutation destroying uORF1 (M1/Stop); L, linker. **(B)** Northern hybridization after 10 min of Tc (+) or EtOH (-) exposure with a probe specific to the sequence encoding the 3xFLAG part of the SPA tag; 5S rRNA was used as a loading control. **(C)** RT-qPCR targeting the SPA tag encoding sequence; the same RNA samples were used. The level of *spa* vs *rpoB* was determined. *rpoB* served as an internal control as its level was not changed upon Tc exposure according to the RNA seq. The results originate from three independent biological experiments. Statistical significance: **** $p \leq 0.0001$, *** $p \leq 0.001$, ** $p \leq 0.01$, * $p \leq 0.05$. **(D)** Western Blot analysis with a monoclonal anti-FLAG antibody; Coomassie staining served as a loading control.

In these experiments, the Northern hybridization (Fig. 15B) showed that uORF1 is expressed even without Tc and with Tc, a slight induction was detected as a slightly stronger band (Fig. 15B). This was validated using RT-qPCR (Fig. 15C). Protein was present both with and without Tc (Fig. 15D), showing that uORF1 was translated even without Tc, which reflects the mRNA result. There was a slight induction on the RNA level, but not on the protein level.

pDUF'-SPA was constructed, because the full-length DUF1127$_1$-SPA plasmid accumulated mutations. It was tested whether pDUF'-SPA shows similar regulation as the full-length construct (compare Fig. 14) on both RNA and protein level. The Northern hybridization showed no signal without Tc, but signals were detected after 10 min of subinhibitory Tc exposure (Fig. 15B). RT-qPCR on the same RNA allowed a quantitative analysis and this fusion showed repression without Tc and significant induction with Tc (16-fold; Fig. 15C). The induction with Tc was previously shown using *egfp* reporter constructs (16-fold; compare Fig. 13C) and the full-length SPA fusion (32-fold increase; compare Fig. 14B). On Western Blot, the protein induction was barely visible due to the strong signals of the other constructs (Fig. 15D), but induction was reproducibly shown in many experiments in this work. Due to this, in all further

experiments, plasmid pDUF'-SPA was used as a WT control and this regulation was deemed 'WT'-like.

When the start codon of uORF1 was changed to a stop codon (M1/Stop), abolishing its translation, the regulation of the downstream *duf'-spa* was abolished. Northern hybridization showed a signal both with and without Tc, which was validated in RT-qPCR (Fig. 15B, C). No induction by Tc could be observed. On a protein level, the RNA result was reflected with protein being visible even without Tc (Fig. 15D). This showed that the *duf'-spa* became de-repressed even in the absence of Tc.

These results indicated a role for uORF1 translation being crucial for *duf1127₁* regulation. In the absence of Tc, *duf1127₁* (and thus also the *duf'-spa* reporter) is repressed on both RNA and protein level. After 10 min of subinhibitory Tc exposure, *duf'-spa* was induced. However, destroying uORF1 led to constant de-repression independently of Tc exposure. This result was the basis for further investigation of the *duf1127₁* regulation depending on uORF1 translation. It was hypothesized, that a conditional transcriptional termination occurs between uORF1 and *duf1127₁*.

## 3.8 3' RACE revealed 3' ends between uORF1 and *duf1127₁*

In the Northern hybridization (see Fig. 8), different band sizes were visible, which already was the first hint at potential premature termination of transcription. This led to the hypothesis that an sRNA was present, that contains only uORF1. To test this, 3' RACE was performed by depleting rRNA and adding a linker to the 3'ends. These ends were then enriched by RT-qPCR and a nested PCR. The cloned products were sequenced and the results analyzed to detect 3' mRNA ends.

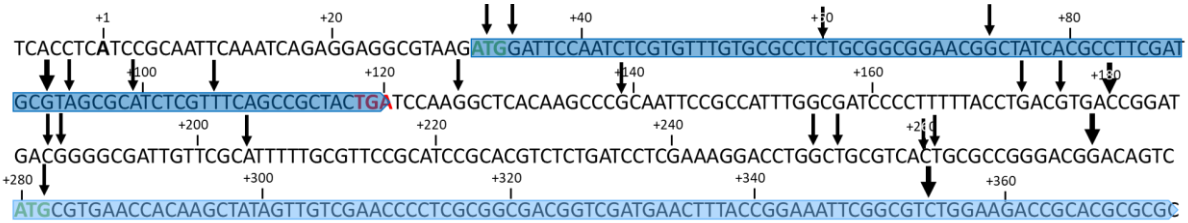


**Fig. 16:** 3' RACE results. **(A)** A part of the sequence of the *duf1127₁* locus on pSymB. The transcriptional start site is marked with +1. 3' ends discovered using 3' RACE. Black arrows indicate 3' ends identified by sequencing; bigger arrows indicate multiple hits. Dark blue shows the location of uORF1, light blue shows the location of *duf1127₁*.

From three biological replicates of the 3'-RACE experiment, 35 clones in total were sequenced. Clones with mutations (bases were exchanged, inserted or deleted; Tab. S6) were excluded and therefore only 18 clones were used for the analysis. In line with the Northern hybridization results (see Fig. 8), using 3'-RACE, 3' ends were detected between uORF1 and *duf1127₁* (Fig. 16) However, these ends could not be mapped to a single nucleotide, but rather to multiple positions in the intergenic region. 15 ends in total mapped in the intergenic region between uORF1 and *duf1127₁* (IGR) and three mapped in *duf1127₁*.

In a previous study, an sRNA was annotated until position +282 of the *duf1127₁* transcript (SM2011_b23415; Sallet et al., 2013). In this study, only one end mapped to this position (Fig. 16). The ends at +180 and +273 each were discovered twice. Within 10 nt of +180, four more 3' ends were detected (positions +188, +189, +176 and +173; Fig. 16). Similarly, around 15 nt of +260, five different ends were discovered. This might suggest premature transcription termination with multiple 3' ends in two IGR regions.

## 3.9 The *duf1127₁*-operon is not regulated by intrinsic termination

Detailed inspection of the IGR between uORF1 and *duf1127₁* revealed two potential stem loop structures, where base-pairing occurred between positions 192-195 and 200-203 (GCGATTGTTCGCATTTTT; dyad symmetry is underlined) as well as positions 126-129 and 134-137 (GGCTCACAAGCCCGCAA, dyad symmetry is underlined). The predicted stems were short, with only 4 nucleotides for base pairing. The stem at position 192-195 was followed by a stretch of U nucleotides, which might indicate a putative intrinsic terminator. The stem at positions 126-129 might form upon Tc exposure, when the pioneering ribosome is stalled at the beginning of uORF1 and does not reach the stop codon. In the absence of Tc, the terminating ribosome, which covers approximately 30 nt, would cover the positions 126-129 and will thus prevent the stem-loop formation.

To test a potential role of these stem-loops, a site-directed mutagenesis of pDUF'-SPA was performed for each of them to destroy the short, base-paired stems. The first stem loop was mutated by changing GCG at positions 192-194 to ATC, while the second one was mutated by changing GCC at positions 35-137 to CGG. Western Blot and RT-qPCR were applied to test the impact of the two predicted stem-loop structures on the expression of the *duf'-spa* reporter and thus to get insight into the post-transcriptional regulation of *duf1127₁* (Fig. 17A).

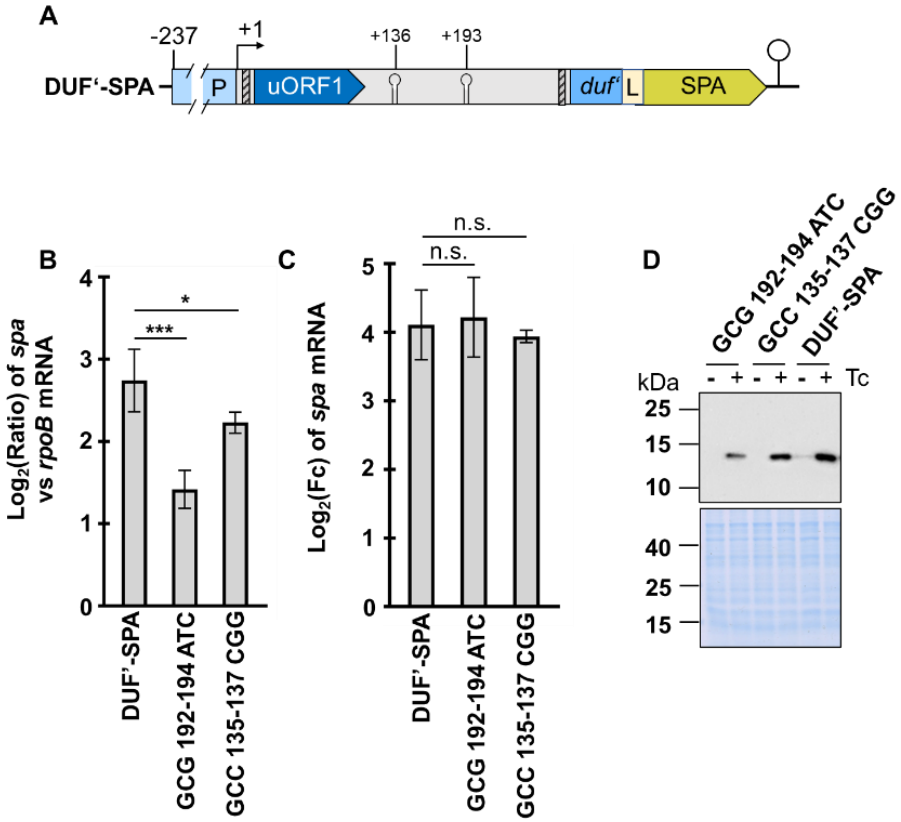


**Fig. 17:** The roles of the two predicted stem-loops were tested using mutagenesis, RT-qPCR and Western Blot. **(A)** Scheme of pDUF'-SPA with the predicted stem-loops in the IGR. **(B)** RT-qPCR of the reporter mRNAs comparing the $Log_2$(Ratio) of *spa* vs *rpoB* mRNA. This ratio shows the basal expression of the reporter fusions without Tc. **(C)** RT-qPCR of the reporter mRNA showing induction by Tc. Tc-exposed cultures were compared to control cultures and $Log_2$(Fc) of the reporter mRNA level was calculated. Statistical significance: **** $p \leq 0.0001$, *** $p \leq 0.001$, ** $p \leq 0.01$, * $p \leq 0.05$. **(D)** Western Blot analysis with a monoclonal anti-FLAG antibody; Coomassie staining served as a loading control. For RT-qPCR of *duf'-spa*, six independent experiments were performed. All other results originate from three independent biological experiments.

Since the putative stem-loop at transcript position 192-203 represents a putative intrinsic terminator, the mutation at positions 192-194 was hypothesized to de-repress *duf'-spa*, since termination would have been impossible. However, RT-qPCR revealed that the reporter mRNA level without Tc exposure was significantly lower than for the WT construct on pDUF'-SPA, which represents WT regulation (Fig. 17B). Induction by Tc exposure, however, was similar for both constructs (Fig. 17C). On a protein level, it was revealed that the regulation of *duf'-spa* was not changed by the mutagenesis because increase in protein level upon Tc exposure was observed. However, the protein band was weaker for the mutated construct than for the WT-like control plasmid (Fig. 17D). This might be due to the lower basal level and similar induction of the *spa* mRNA of this construct, leading to less protein being translated. These results showed that the stem formed between positions 192-195 and 200-203 is not an intrinsic terminator.

The mutation at positions 135-137 was hypothesized to affect *duf'-spa*, since formation was only possible without Tc exposure. However, RT-qPCR revealed that the construct was repressed without Tc exposure like the WT control plasmid (Fig. 17B). Induction by Tc exposure again was similar for both constructs (Fig. 17C). On a protein level, it was revealed that the regulation of *duf'-spa* was not changed by the mutagenesis. These results showed that the stem formed between positions 126-129 and 134-137 had no effect on the $duf1127_1$ regulation.

With both stem-loops not being relevant for $duf1127_1$ regulation, at least one different mechanism must be present. To address this, the intergenic region (IGR) was analyzed in more detail.

## 3.10 The intergenic region between uORF1 and $duf1127_1$ features a regulatory element

The IGR between uORF1 and $duf1127_1$ is long (~160 bp) and thus might feature several regulatory elements. The region was split into three parts, and derivates of plasmid pDUF'-SPA were constructed in which each of the regions was individually deleted (Fig. 18A).

Compared to the WT plasmid (DUF'-SAP), the deletion of region 1 was revealed to cause significant de-repression of the reporter fusion in cultures without Tc exposure (Fig. 18B). Despite this de-repression, induction by Tc still occurred, albeit to a lesser degree than for the WT plasmid (Fig. 18C). On a protein level, it was revealed as well that the deletion of region 1 de-repressed *duf'-spa* (Fig. 18D).

The deletion of regions 2 and 3 caused repression without Tc exposure like the WT plasmid (Fig. 18B), and induction by Tc still occurred on a similar level as the WT plasmid (Fig. 18C). When analyzing regions 2 and 3 on a Western Blot, no signal was visible (Fig. 18D). Only after loading twice the amount of sample onto the gel, using fresh antibody solution and incubating the blot for much longer in the solution, did a weak signal become visible (Fig. 18E). Thus, the regulation of *duf'-spa* on RNA-level was not affected by these deletions, however, translation was severely impaired, with the protein level being much weaker than when the WT plasmid was used.

These results suggested two things: First, there is a regulatory element present in region 1, as de-repression was observed upon deletion. Second, there is an element spanning parts of regions 2 and 3 that seemed to influence translation.

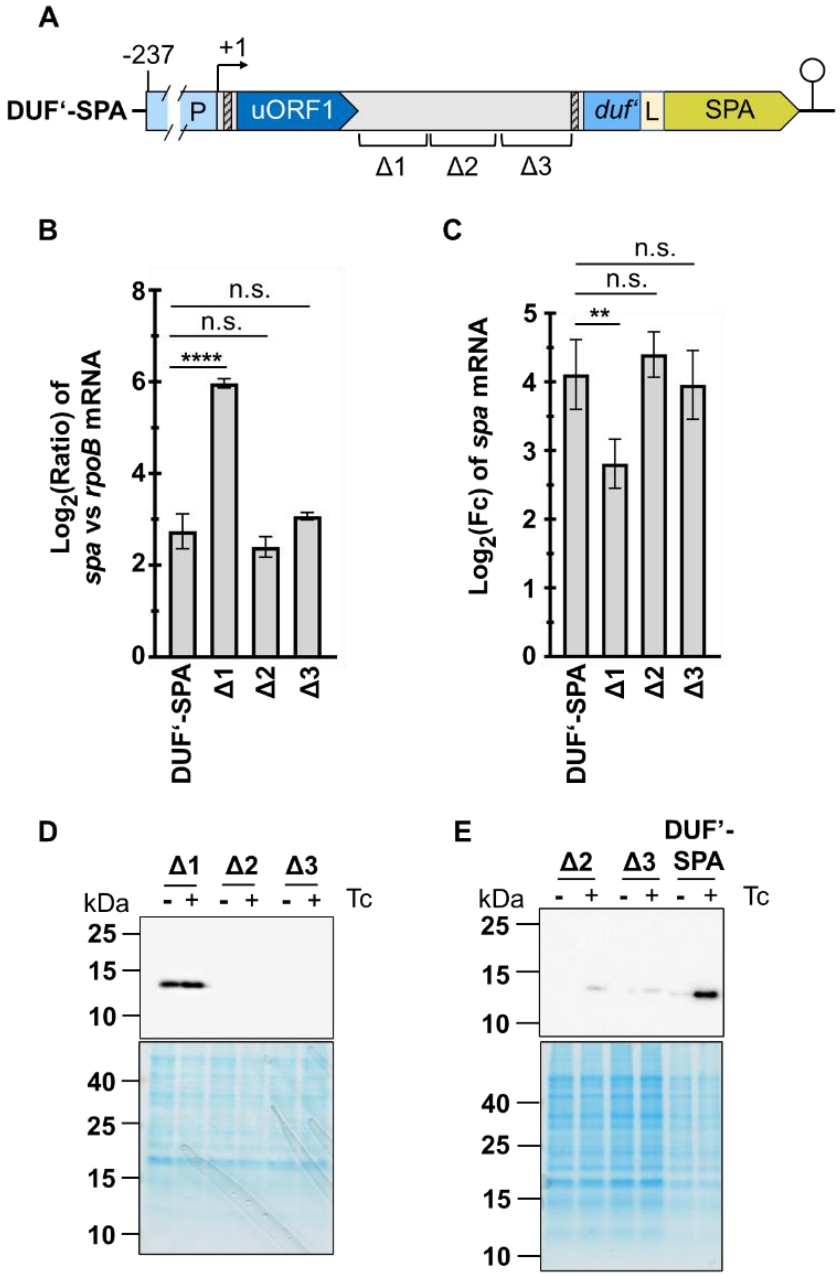


**Fig. 18:** Deletions in the IGR reveal a region crucial for *duf1127*$_1$ regulation. **(A)** Deletion constructs for analysis of the IGR. Three partial deletions covering the IGR were constructed (Δ 1, Δ 2, Δ3). **(B)** RT-qPCR of the reporter mRNAs comparing the $Log_2$(Ratio) of *spa* vs *rpoB* mRNA. This ratio shows the basal expression of the reporter fusions without Tc. **(C)** RT-qPCR of the reporter mRNA showing induction by Tc. Tc-exposed cultures were compared to control cultures and $Log_2$(Fc) of the reporter mRNA level was calculated. Statistical significance: **** $p \leq 0.0001$, *** $p \leq 0.001$, ** $p \leq 0.01$, * $p \leq 0.05$. **(D)** Western Blot analysis with a monoclonal anti-FLAG antibody of all three constructs; Coomassie staining served as a loading control. **(E)** Western Blot analysis with a monoclonal anti-FLAG antibody of all three constructs; Coomassie staining served as a loading control. Deleting regions 2 and 3 still allowed induction, albeit low signal levels necessitated loading twice as many cells as in (D) as well as doubling incubation and extending exposure times. For RT-qPCR of region 3, only two independent experiments were performed. For RT-qPCR of *duf'-spa*, six independent experiments were performed. All other results originate from three independent biological experiments.

## 3.11 A second uORF does not affect *duf1127₁* regulation

Seeing that translation was impaired when deleting either IGR 2 or 3, the genomic sequence was scanned and an additional potential second ORF (uORF2) identified between uORF1 and *duf1127₁* (Fig. 19).

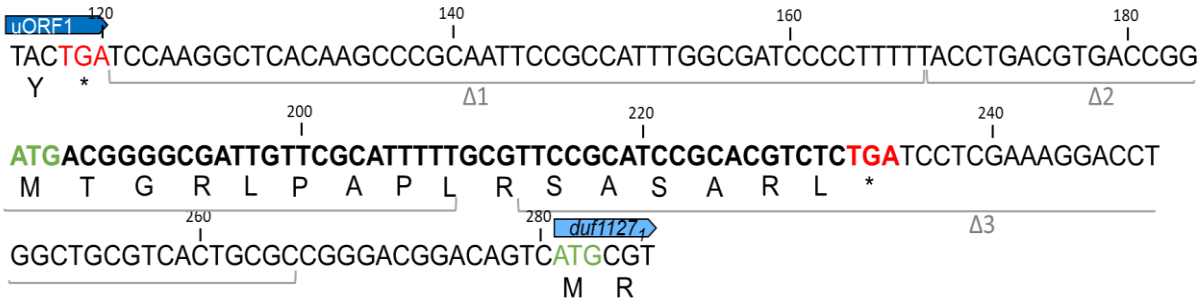


**Fig. 19:** uORF2 was discovered in front of *duf1127₁*. The location of uORF2 is shown in bold. The end of uORF1 and the beginning of *duf1127₁* are marked. Deletions of IGR regions 1, 2 and 3 are marked in grey. For numbering, see Fig. 17 above. +1 is the transcriptional start site of the *duf1127₁* transcript.

This uORF2 starts at position +184 and encodes a peptide with a length of 16 amino acids but lacks an SD sequence. To determine whether this uORF was translated, a SPA fusion was created, as well as a start-to-stop mutation derivate of this fusion (Fig. 20A). Furthermore, uORF2 was analyzed for its influence on *duf1127₁* when mutating the start codon of either uORF2 or both uORF1 and uORF2 in pDUF'-SPA (Fig. 20A).

Mutating the start codon of uORF2 would abolish translation of uORF2, while mutating the start codon of uORF1 and uORF2 was done to reveal a potential dual regulation via both uORFs. As before, RT-qPCR and Western Blot were applied to test the hypothesis.

First, the uORF2-SPA construct showed an increased basal mRNA expression compared to *duf'-spa* when no Tc was added (Fig. 20B). Induction by Tc occurred on a similar level as for *duf'-spa* (Fig. 20C). When the uORF2 start codon was mutated to stop (M2/Stop-SPA), the RNA level without Tc was significantly higher, while Tc induction of the RNA resembled the uORF2-SPA construct (Fig. 20B, C). Western Blot analysis revealed that uORF2 was translated independently of Tc (Fig. 20D), while a start to stop mutation (M2/Stop-SPA) abolished translation (Fig. 20E).

The results showed that uORF2 is in fact an ORF. Importantly, while on mRNA level it was regulated like *duf'-spa*, on the protein level this was not the case, and the protein level did not reflect the mRNA level. On mRNA level, it was repressed without Tc, but protein was present even without Tc. This stood in contrast to uORF1, that was constitutively expressed on both RNA and protein level (see Fig. 15).

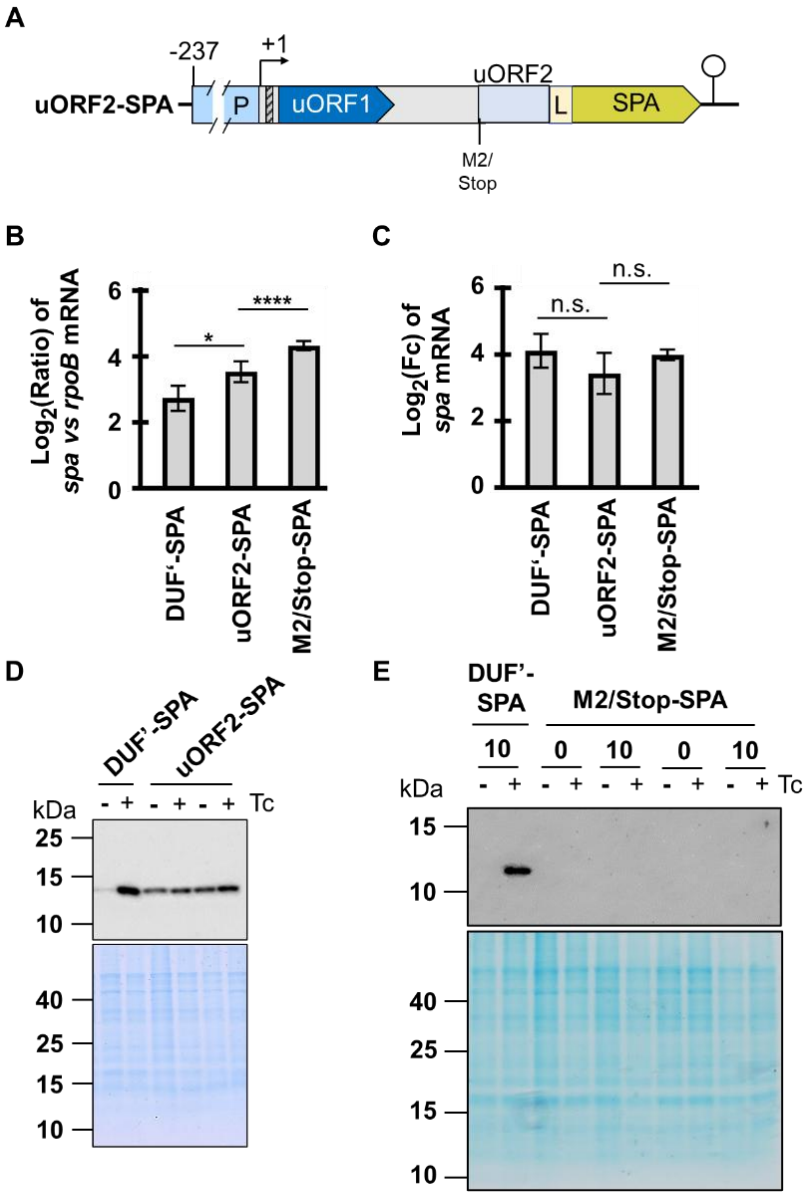


**Fig. 20:** uORF2 is translated. **(A)** To test translation, a construct featuring uORF2 with a SPA tag was designed (uORF2-SPA), and a start-to-stop mutation was introduced (M2/Stop). **(B)** RT-qPCR of the reporter mRNAs comparing the $Log_2$(Ratio) of *spa* vs *rpoB* mRNA. This ratio shows the basal expression of the reporter fusions without Tc. **(C)** RT-qPCR of the reporter mRNA showing induction by Tc. Tc-exposed cultures were compared to control cultures and $Log_2$(Fc) of the reporter mRNA level was calculated. Statistical significance: **** $p \leq 0.0001$, *** $p \leq 0.001$, ** $p \leq 0.01$, * $p \leq 0.05$. **(D)** Western Blot analysis with a monoclonal anti-FLAG antibody; Coomassie staining served as a loading control. **(E)** Western Blot analysis with a monoclonal anti-FLAG antibody; Coomassie staining served as a loading control. For RT-qPCR of *duf'-spa*, six independent experiments were performed. All other results originate from three independent biological experiments.

Initially, it was assumed that the increase of pDUF'-SPA on protein level upon Tc exposure was exclusively because of the increase in mRNA level. The comparison to the uORF2-SPA fusion, however, suggested that *duf'-spa* translation might be induced by Tc. Alternatively, differences and changes in the stabilities of the two fusion proteins might contribute to their different accumulation under -Tc and +Tc conditions.

The results prompted investigation of the impact of uORF2 on *duf1127*$_1$. For this, the uORF2 start codon was mutated in the pDUF'-SPA background (M2/Stop-DUF'-SPA) as well as the M1/Stop background, to see if both uORF work together (M1-M2/Stop-DUF'-SPA; Fig. 21A).

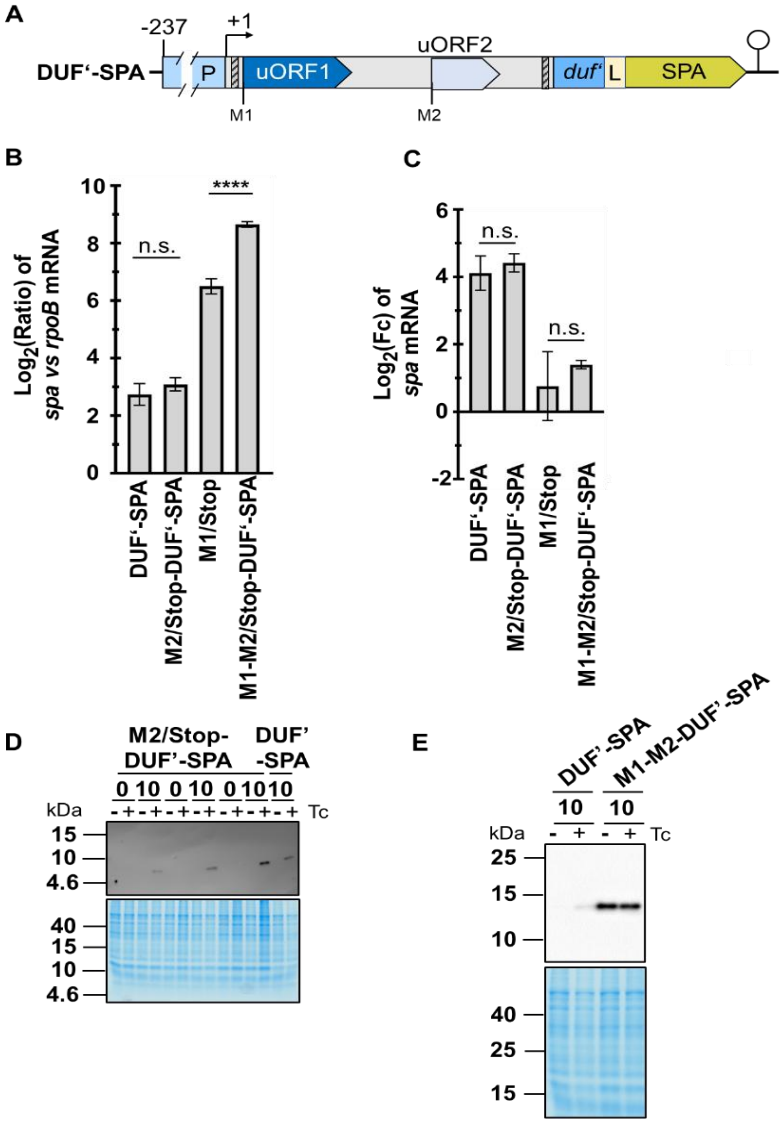


**Fig. 21:** uORF2 does not influence *duf'-spa* regulation. **(A)** The start-to-stop mutation of uORF2 was introduced into *duf'-spa* (M2/Stop-DUF'-SPA) and M1/Stop (M1-M2/Stop-DUF'-SPA). **(B)** RT-qPCR of the reporter mRNAs comparing the $Log_2$(Ratio) of *spa* vs *rpoB* mRNA. This ratio shows the basal expression of the reporter fusions without Tc. **(C)** RT-qPCR of the reporter mRNA showing induction by Tc. Tc-exposed cultures were compared to control cultures and $Log_2$(Fc) of the reporter mRNA level was calculated. Statistical significance: **** $p \leq 0.0001$, *** $p \leq 0.001$, ** $p \leq 0.01$, * $p \leq 0.05$. **(D)** Western Blot analysis with a monoclonal anti-FLAG antibody; Coomassie staining served as a loading control. **(E)** Western Blot analysis with a monoclonal anti-FLAG antibody; Coomassie staining served as a loading control. For RT-qPCR of *duf'-spa*, six independent experiments were performed. All other results originate from three independent biological experiments.

On mRNA level, the construct with the start-to-stop mutation of uORF2 (M2/Stop-DUF'-SPA) showed no significant difference to the WT construct on pDUF'-SPA without Tc (Fig. 21B). Both were repressed without Tc. With Tc, induction was detected for both constructs on a similar level (Fig. 21C). When M2/Stop was introduced in M1/Stop background (M1-M2/Stop-DUF'-SPA), the mRNA level without Tc was significantly higher than for M1/Stop (Fig. 22B). With Tc, weak induction could still be measured for M1-M2/Stop-DUF'-SPA, while this was

not measured for M1/Stop (Fig. 21C), however, there is no significant difference in induction for both constructs. On a protein level, the regulation of M2/Stop-DUF'-SPA was observed to resemble *duf'-spa* (Fig. 21D), where a band was only detected with Tc. When mutating the start codon of uORF2 in M1/Stop background (M1-M2/Stop-DUF'-SPA), the result resembled the result of the M1/Stop mutation (compare Fig. 15), being de-repressed without Tc (Fig. 21E).

Taken together, the results suggest that there is not only a co-transcriptional (transcriptional attenuation) and post-transcriptional (RNA stability) control of *duf1127₁*, but also a potential regulation on the translational level. uORF2 is not involved in this regulation under the conditions tested, and its role remains elusive.

However, the results above (Fig. 21) suggested that premature termination occurred before the end of uORF2, which aligned with the result from the 3' RACE suggesting 3' ends of the sRNA around position +180 (compare Fig. 16). To test whether the detected uORF1-containing sRNA is terminated around position 180 or around position 260, Northern hybridization (Fig. 22) with a probe targeting the sequence between positions 137-260 was performed.

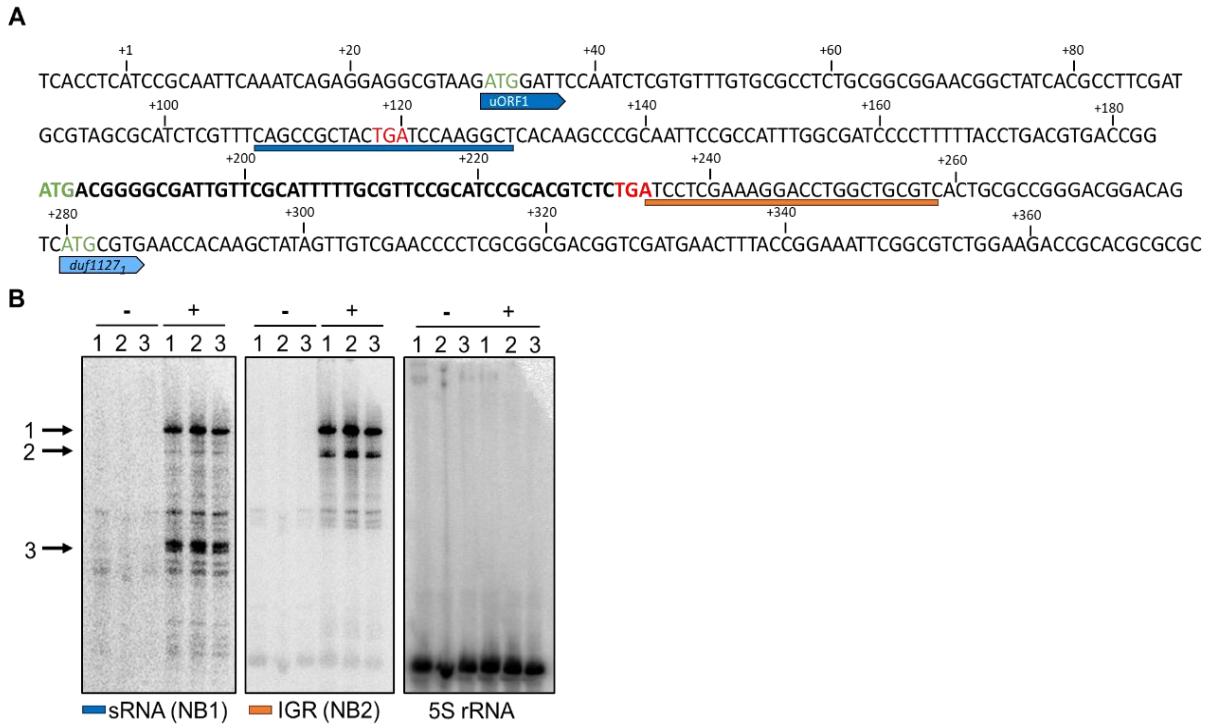


**Fig. 22:** Premature transcription termination occurs before the end of uORF2. **(A)** Location of the Northern probes in the *duf1127₁* operon. The dark blue arrow indicates the location of uORF1, the light blue arrow indicates the location of *duf1127₁*. uORF2 is indicated in bold letters. The blue and orange stripes under the sequence indicate positions of probes used for Northern hybridization of the sRNA (blue, probe NB1) and the downstream part of the intergenic region (IGR) between uORF1 and *duf1127₁* (orange, probe NB2). **(B)** Northern hybridization with the sRNA probe (blue, NB1) and the IGR-directed probe (orange, NB2). The sRNA band (3; black horizontal arrow) is missing in the hybridization with the IGR-directed probe. 5S rRNA served as a loading control.

If premature transcription termination occurred around position +180 as indicated by the 3' RACE (compare Fig. 16) and before the end of uORF2 as indicated by the results above, hybridization with probe NB2 targeting a sequence located after uORF2 should reveal no sRNA signal. Indeed, Northern hybridization with NB2 showed no sRNA band (black vertical arrow marked with 3) was detected with this probe (Fig. 22B). The sRNA probe NB1 used above (compare Fig. 6) was used again as a control, where an sRNA band was detected.

## 3.12 An upstream SD preceding a third uORF impacts *duf1127₁* translation

When the ribosome terminates translation of uORF2, it occupies a reasonable Shine-Dalgarno (SD) sequence located a few nucleotides downstream of the stop codon. If there was an ORF afterwards, the ribosome could initiate translation. Indeed, a CTG codon was found 5 nt downstream of the potential SD, indicating a third uORF which would be overlapping with *duf1127₁*. This uORF, named uORF3, showed ribosome coverage in Ribo-seq data obtained in the absence of Tc (Fig. 23; Hadjeras et al., 2023).

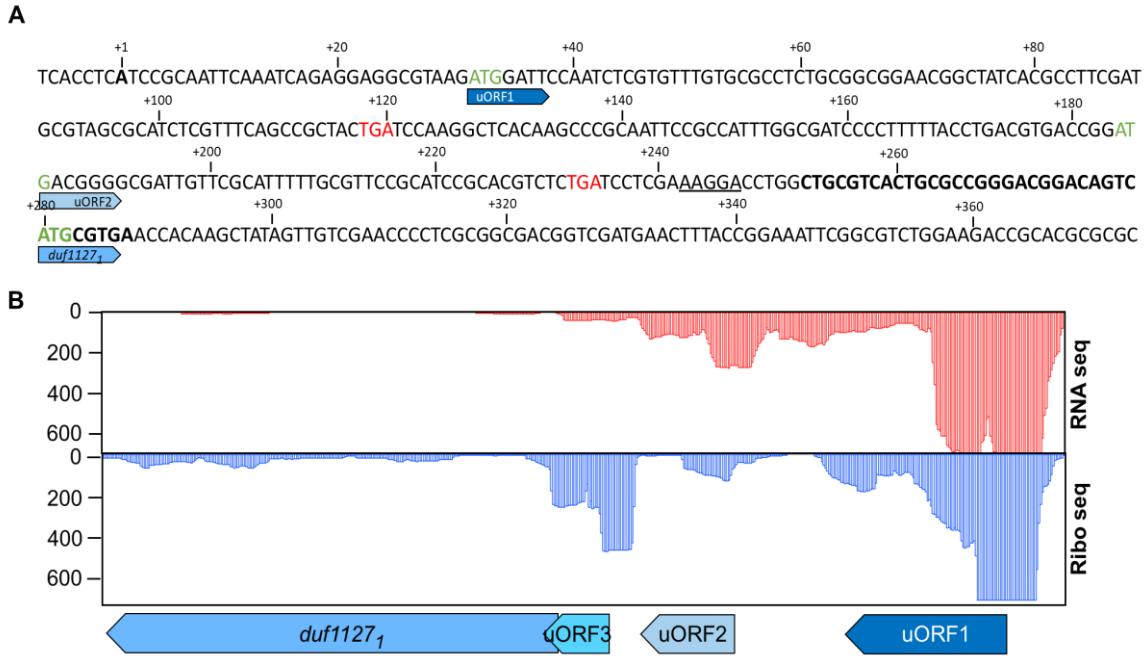


**Fig. 23:** A putative third uORF was discovered in front of *duf1127₁*. **(A)** Location of uORF3 (bold letters) and the SD (underlined) in the *duf1127₁* operon. uORF1, uORF2 and *duf1127₁* are indicated by blue arrows. Start codons are marked in green and stop codons are marked in red. **(B)** Reads from the RNA seq and Ribo seq of the *duf1127₁* operon without Tc. Reads of the Ribo seq were compared to total RNA reads, an enrichment indicates translation.

RNA seq reads indicated RNA is present and correlate with transcript levels. Very few RNA reads for *duf1127₁* were detected, which aligns with the results of this study without Tc, described above. Ribo-seq shows where ribosomes bind to the mRNA. The footprint is left by the 70S ribosome and incorporates around 15 nt before and after the start codon (Hadjeras et al., 2023).

A strong peak can be seen before uORF1 (formerly sORF26; Hadjeras et al., 2023). A very small peak at uORF2 was present without enrichment in the Ribo seq library. Despite this, in this study, translation of uORF2 was shown (compare Fig. 20). Possibly, uORF2 translation is inefficient but the uORF2-SPA fusion protein is quite stable, and therefore accumulates. However, protein stability was not tested. Importantly, a second peak in ribosome coverage (showing enrichment in the Ribo seq compared to the RNA seq) was seen around the CTG start codon of the putative uORF3, including the reasonable SD (Fig. 23B). This peak (and the enrichment in Ribo seq) was even higher than for the start codon of *duf1127₁*.

These results indicate that uORF1 was translated, which was proven in the results above. For uORF2, however, reporter translation was observed, although no ribosome footprint was detected. uORF3 was translated according to the Ribo seq data, however, this could not be verified in this study using a reporter. Reporter translation could not be reproducibly detected

in different experiments (data not shown), which contrasted the Ribo seq data. This placed focus on the SD sequence of uORF3, which might act as an upstream RBS, or an upstream regulatory binding site. To test this hypothesis, the SD was mutated, and RT-qPCR and Western Blot were employed to analyze the consequences of the mutation (Fig. 24).

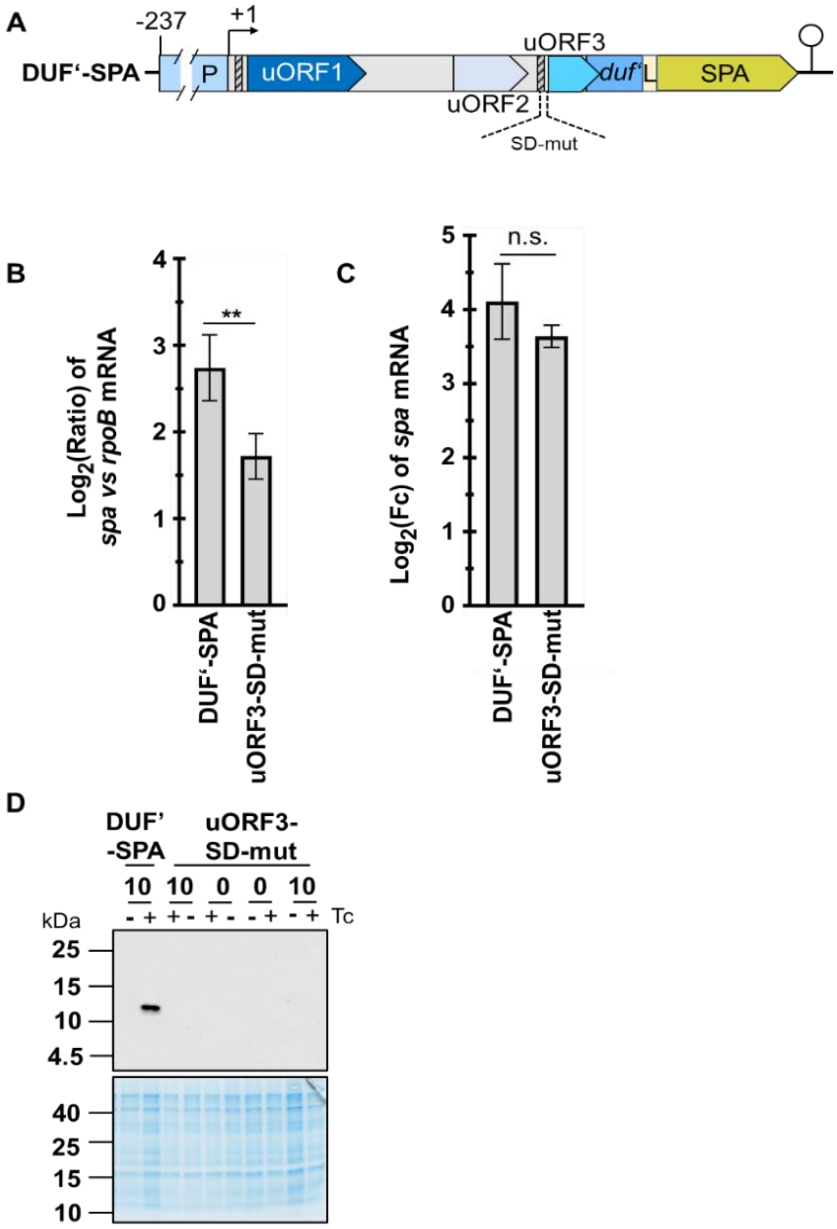


**Fig. 24:** The SD in front of uORF3 is relevant for *duf1127₁* translation. **(A)** Into the pDUF'-SPA plasmid, a mutation abolishing the SD in front of uORF3 was introduced (GAAAGGA to ATACAAT; uORF3-SD-mut). **(B)** RT-qPCR of the reporter mRNAs comparing the $Log_2$(Ratio) of *spa versus rpoB* mRNA. This ratio shows the basal expression of the reporter fusions without Tc. **(C)** RT-qPCR of the reporter mRNA showing induction by Tc. Tc-exposed cultures were compared to control cultures and $Log_2$(Fc) of the reporter mRNA level was calculated. Statistical significance: **** $p \leq 0.0001$, *** $p \leq 0.001$, ** $p \leq 0.01$, * $p \leq 0.05$. **(D)** Western Blot analysis with a monoclonal anti-FLAG antibody. Coomassie staining serving as a loading control. For RT-qPCR of *duf'-spa*, six independent experiments were performed. All other results originate from three independent biological experiments.

RT-qPCR revealed that mutating the SD of uORF3 led to a significantly lower mRNA level without Tc than for the WT construct on pDUF'-SPA (Fig. 24B). Induction by Tc exposure was similar for both constructs (Fig. 24C). When the SD of uORF3 was mutated, no pDUF'-SPA

protein was detected (Fig. 24D). These results showed that the upstream SD in front of the putative uORF3 was relevant for the translation of *duf'-spa*. Whether the accessibility of this upstream SD is regulated in response to Tc exposure remains to be analyzed in the future.

Overall, the results above further indicated that not only the level of *duf1127*$_1$ mRNA is regulated, but also its translation. The regulatory mechanisms might involve all levels of RNA regulation, including post-transcriptional as well as translational control elements. The IGR between uORF1 and *duf1127*$_1$ was substantially contributing to regulation.

## 3.13 A stem-loop structure of uORF1 and the intergenic region is not relevant for *duf1127*$_1$ regulation

After finding that deleting region 1 in the IGR leads to de-repression of *duf1127*$_1$, and uORF2 is not involved in regulation, it was predicted that a part of the IGR 1 (+121-128, region 1-1) could base-pair with a part of uORF1, participating in a stem-loop structure. This stem-loop structure could only form under certain conditions, depending on which part of uORF1 is occupied by the ribosome (Fig. 25).

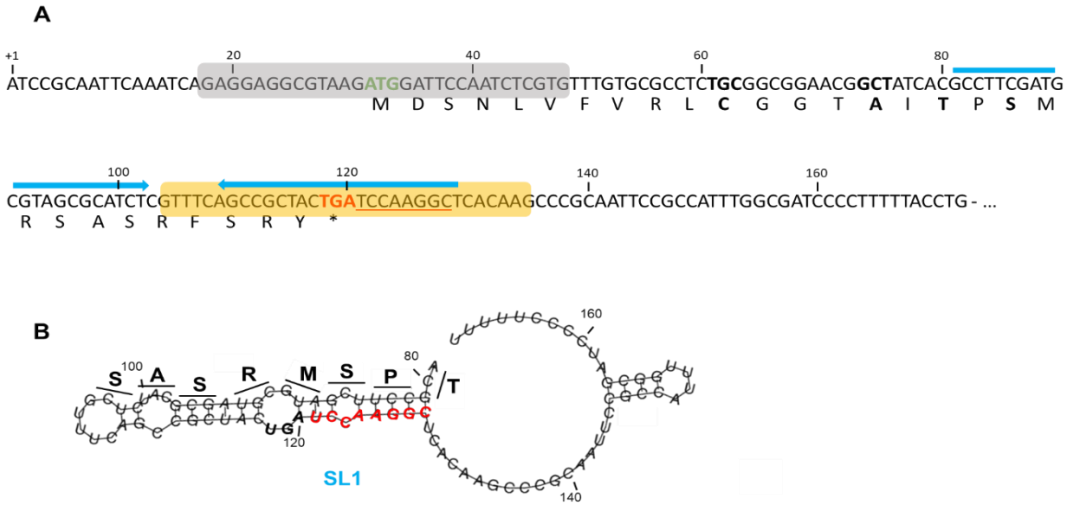


**Fig. 25:** Ribosome occupation determines stem-loop formation. **(A)** Under normal conditions, uORF1 is translated and the ribosome reaches at the stop codon (yellow), occupying a 31 nt region. Upon Tc exposure, the ribosome stalls at the start codon (grey). The blue arrows indicate a region that can form a stem-loop structure. **(B)** Stem-loop structure 1 (SL1) that could be formed starting from T17 of uORF1, if the ribosome is stalled at the start codon in the presence of Tc. Codons T14 to S24 that were changed by the scramble mutation are indicated above the stem loop in bold letters. Nucleotides marked in red correspond to the nucleotides underlined in (A) that were occluded by the ribosome terminating translation in the absence of Tc. Structure prediction was done via RNAfold.

Under standard conditions, without Tc exposure, the ribosome would start translation at the start codon of uORF1 and translate until the stop codon. As initiation and termination of translation are slower than elongation, the ribosome remains longer at the start and stop codons. When pausing at the stop codon, the ribosome masks the 8 nt immediately after the stop codon of uORF1 (Fig. 25A), blocking formation of the proximal part of the stem. Additionally, the full-length *duf1127*$_1$ construct on DUF1127$_1$-SPA as well as the M1/Stop on pDUF'-SPA derivative were found to accumulate mutations in the region reaching from +121 to +128. It was hypothesized that, if no stem-loop formed, *duf'-spa* might be repressed even upon Tc exposure or even in M1/Stop background. To test this hypothesis, the region was changed to reflect the mutations that were accumulated in the aforementioned constructs (TCCAAGGC to GTATTGGT; mutated bases are underlined) and placed into the WT-background (pDUF'-SPA;

Fig. 26) or the M1 background (M1/Stop, see below Fig. 28). Additionally, a deletion of the region +121 to +128 was introduced in plasmid pDUF'-SPA. Furthermore, the codons T17 to S24 forming the upper part of the stem were scrambled to interrupt stem-loop formation, changing RNA (as well as amino acid) structure.

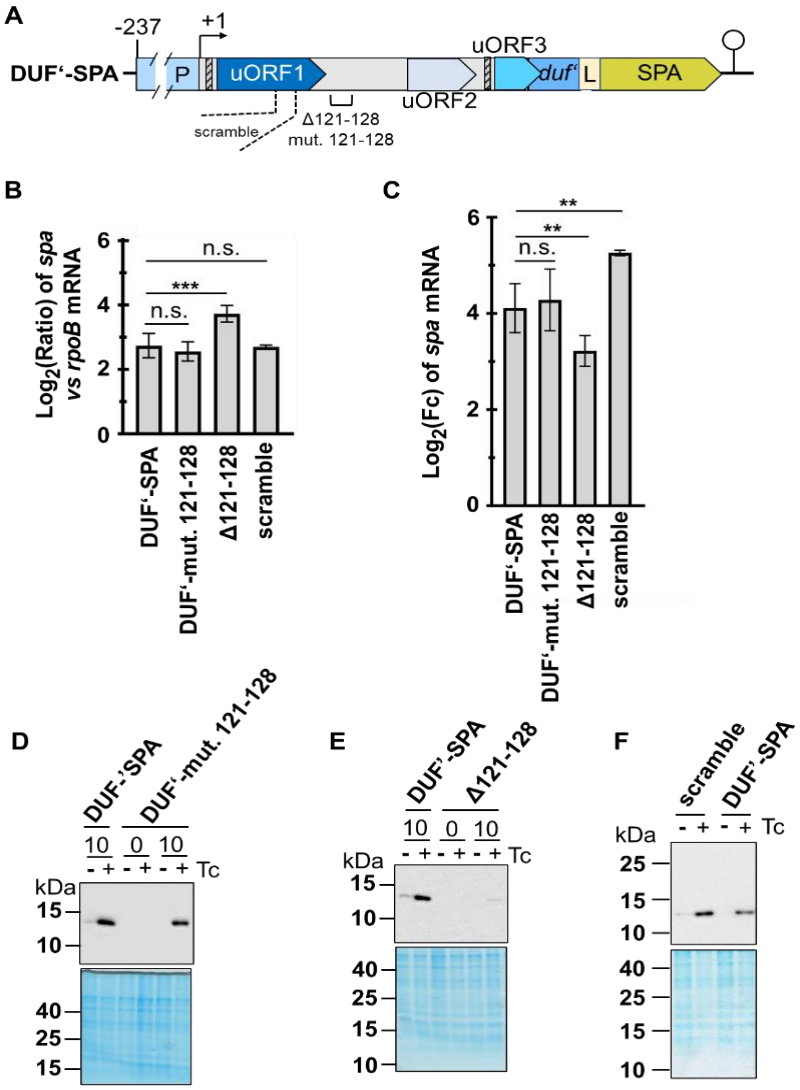


**Fig. 26:** Scrambling the second half of uORF1 and base exchanges in region +121 to +128 do not affect *duf1127₁* regulation. **(A)** Schematic depicting of region +121 to +128 used for construction of a deletion or mutated region (TCCAAGGC to GTATTGGT; mutated bases are underlined) in the pDUF'-SPA background, and codons 17 to 24 scrambled (scramble; from ACGCCTTCGATGCGTAGCGCATCT to TCGAGCTCTCGTCCGGCAACCATG). **(B)** RT-qPCR of the reporter mRNAs comparing the $Log_2$(Ratio) of *spa* vs *rpoB* mRNA. This ratio showed the basal expression of the reporter fusions without Tc. **(C)** RT-qPCR of the reporter mRNA showing induction by Tc. Tc-exposed cultures were compared to control cultures and $Log_2$(Fc) of the reporter mRNA level was calculated. Statistical significance: **** $p \leq 0.0001$, *** $p \leq 0.001$, ** $p \leq 0.01$, * $p \leq 0.05$. **(D-F)** Western Blot analyses using a monoclonal anti-FLAG antibody; Coomassie staining served as a loading control. Used constructs as indicated above the panels. Six biological experiments were performed for both constructs in RT-qPCR. For Western Blots, one representative replicate of three experiments is shown.

If the stem-loop SL1 was relevant for *duf1127₁* regulation, mutating or deleting region +121 to +128 should lead to repression even upon Tc exposure. RT-qPCR showed that mutating +121 to +128 did not change the basal mRNA level, which was similar to that of the WT construct on pDUF'-SPA without Tc (Fig. 26B). Induction with Tc occurred at a level similar to the WT

(Fig. 26C). Western Blot analysis revealed that mutating +121 to +128 had no strong effect on the protein accumulation upon Tc exposure (Fig. 26D).

Unexpectedly, deleting the region changed the regulation. RT-qPCR showed a significantly higher mRNA level compared to the WT construct without Tc (Fig. 26B). Induction with Tc occurred significantly less after deletion of region +121 to +128 (Fig. 26C). These results indicate partial de-repression and are in line with the observations for the Δ1 deletion (compare Fig. 18). However, although induction by Tc at the protein level was still detected for the +121 to +128 deletion construct (Fig. 26E), the signal was much lower than of the WT construct on pDUF'-SPA. This suggested that translation is impaired upon deletion of the +121 to +128 region.

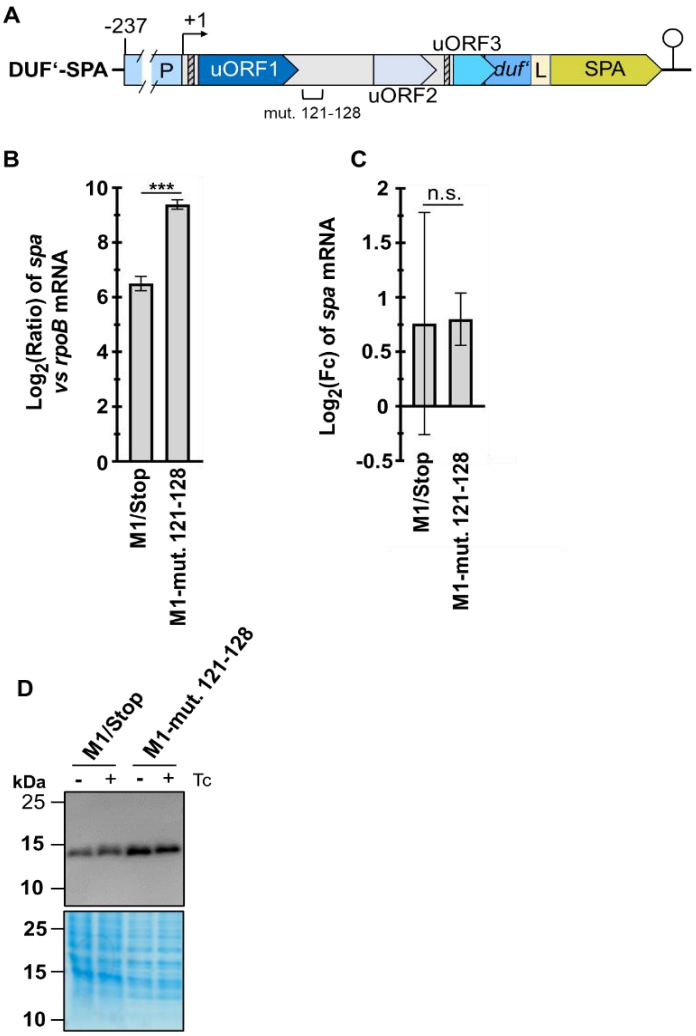


**Fig. 27:** Mutating region +121 to +128 in M1/Stop background does not affect *duf1127₁* regulation. **(A)** Schematic depicting of region +121 to +128 used for construction of a mutated region (TCCAAGGC to GTATTGGT; mutated bases are underlined) in the M1 background. **(B)** RT-qPCR of the reporter mRNAs comparing the Log2(Ratio) of *spa* vs *rpoB* mRNA. This ratio showed the basal expression of the reporter fusions without Tc. **(C)** RT-qPCR of the reporter mRNA showing induction by Tc. Tc-exposed cultures were compared to control cultures and $Log_2$(Fc) of the reporter mRNA level was calculated. Statistical significance: **** $p \leq 0.0001$, *** $p \leq 0.001$, ** $p \leq 0.01$, * $p \leq 0.05$. **(D)** Western Blot analysis using a monoclonal anti-FLAG antibody; Coomassie staining served as a loading control. Used constructs as indicated above the panels. Six biological experiments were performed for both constructs in RT-qPCR. For Western Blots, one representative replicate of three experiments is shown.

The scramble mutation completely changed the bases and amino acid structure of this region from uORF1, thus preventing SL1 formation (compare Fig. 25). RT-qPCR revealed that without Tc, scrambling codons 17 to 24 of uORF1 did not change the mRNA level compared to the WT construct on pDUF'-SPA (Fig. 26B). Induction with Tc occurred but was significantly higher for the scramble mutant (Fig. 26C). Western Blot analysis revealed that after scrambling, induction on protein level was similar to the WT construct (Fig. 26D-F).

Taken together, mutating region +121 to +128, or scrambling codon 17 to 24, did not alter *duf'-spa* regulation. Therefore, the stem-loop structure SL1 is not involved in the regulatory mechanism of induction of *duf1127$_1$* by Tc. However, deleting the region +121 to +128 seemed to slightly weaken the transcriptional attenuation and, strikingly, to negatively influence protein production. However, mutating the region +121 to +128 in the M1/Stop background did not affect *duf1127$_1$* regulation on RNA or protein level (Fig. 27).

With this SL1 hypothesis being falsified, focus was placed on the translation of uORF1 that had already been proven necessary for *duf1127$_1$* regulation.

## 3.14 Translation of the first half of uORF1 is necessary for regulation of *duf1127$_1$*

As shown above, translation of uORF1 is relevant, as abolishing translation leads to de-repression. To test which part of uORF1 is relevant for regulation, stop mutations were introduced at various codons in uORF1: C11, A15, T17 and S19 were targeted to stop translation (Fig. 28).

The stop mutation at codon 11 (C11/Stop) caused significant de-repression without Tc exposure compared to the WT construct on pDUF'-SPA. The mRNA level of the C11/Stop construct was even higher than the level of the de-repressed M1/Stop (Fig. 28B). Despite this de-repression, induction by Tc still occurred, albeit to a lesser degree than for the WT plasmid and without statistical significance of the difference to both WT and M1/Stop (Fig. 28C). On a protein level, it was revealed as well that the C11/Stop mutation led to de-repression of *duf'-spa* expression. (Fig. 29D). The stop mutations at codon 15 (A15/Stop), 17 (T17/Stop) and 19 (S19/Stop) were revealed not to change the *duf'-spa* regulation: At the level of RNA, repression without Tc exposure (Fig. 28B) and induction by Tc occurred on a similar level as for the WT plasmid (Fig. 29C). On a protein level, all three constructs also showed WT-like regulation (repression in the absence of Tc and induction upon Tc exposure), although differences in the signal strength were observed (Fig. 28D).

Taken together, the results showed that uORF1 translation is necessary for *duf1127$_1$* regulation and suggested that C11 and A15 are positions of interest that affect regulation. Together with the above results showing that scrambling uORF1 codons 17 to 24 has no influence *duf1127$_1$* regulation, this led to the hypothesis that there is an attenuation element present in the first half of uORF1. Since no intrinsic terminator was found, it was suggested that this attenuation element is used for Rho-dependent transcriptional termination.

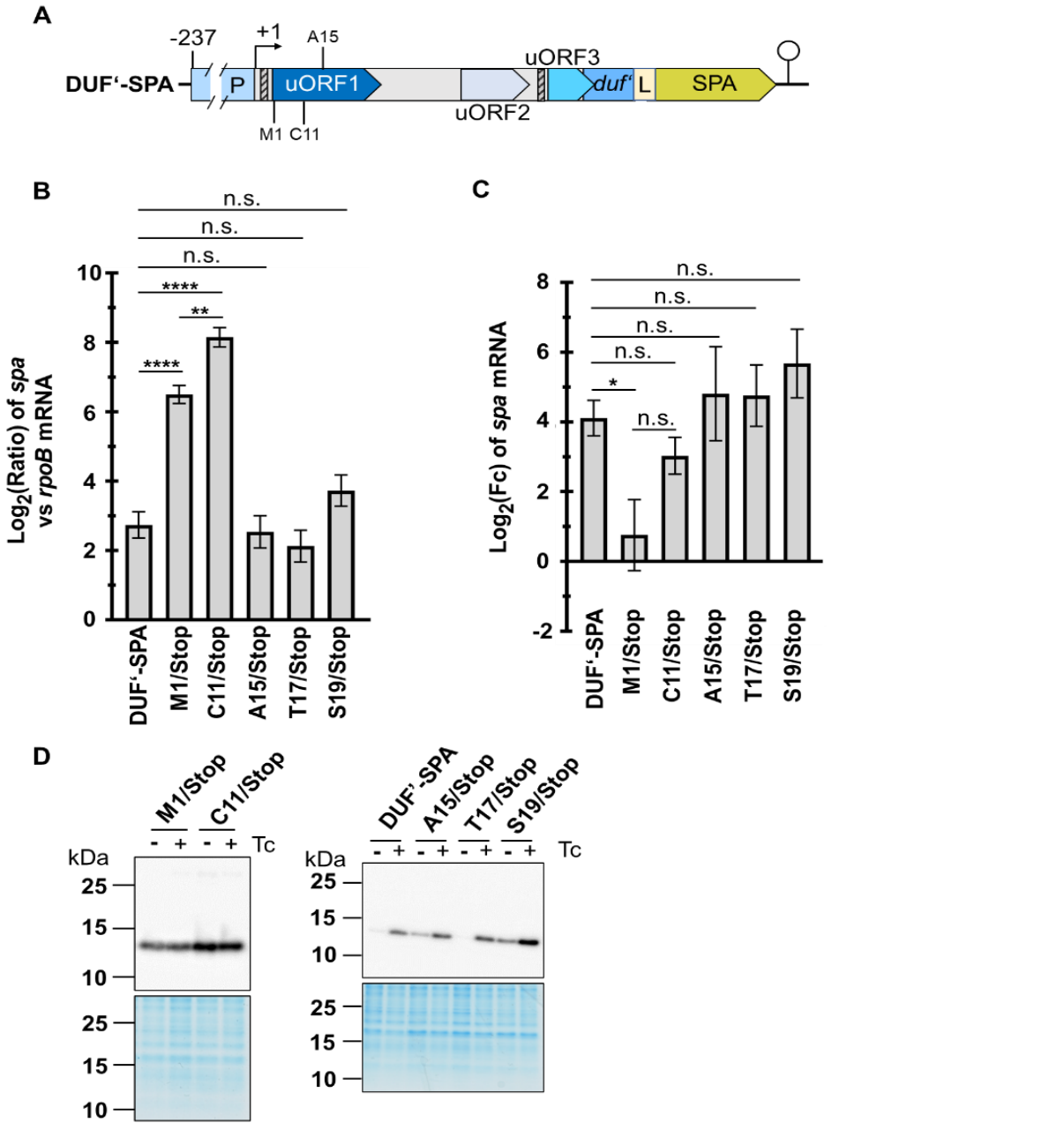


**Fig. 28:** Mutations in uORF1 reveal a second region crucial for regulation. **(A)** Further stop-mutations introduced into uORF1 at codons 11, 15, 17 and 19. **(B)** RT-qPCR of the reporter mRNAs comparing the $Log_2$(Ratio) of *spa* vs *rpoB* mRNA. This ratio shows the basal expression of the reporter fusions without Tc. **(C)** RT-qPCR of the reporter mRNA showing induction by Tc. Tc-exposed cultures were compared to control cultures and $Log_2$(Fc) of the reporter mRNA level was calculated. Statistical significance: **** $p \leq 0.0001$, *** $p \leq 0.001$, ** $p \leq 0.01$, * $p \leq 0.05$. **(D)** Western Blot analysis with a monoclonal anti-FLAG antibody of all constructs; Coomassie staining served as a loading control. For RT-qPCR of *duf'-spa*, six independent experiments were performed. All other results originate from three independent biological experiments.

## 3.15 An attenuation element in codons 3 to 10 of uORF1 is accessible upon translation

To combine the different levels of regulation for *duf1127*$_{1,}$ potential regulatory functions needed to be integrated. First, potential transcriptional contribution was checked with the idea that Rho-dependent transcriptional termination may play a role. The Rho protein identifies a rho utilization site (*rut*) to bind to the nascent mRNA and eventually terminates RNA polymerase transcription. While the characteristics of *rut* sites are not well defined, it has been shown that they contain more C than G bases. The actual termination site is usually much further downstream from the *rut* site.

In the uORF1-*duf1127*$_1$ operon, a potential *rut* site could be identified from positions +37 to +60, shortly after the start codon of uORF1 (codons S3-L10, +37 to +60; Fig. 29). As a first step to validate *duf1127*$_1$ regulation being by Rho-dependent termination, C bases were exchanged to G in this region. As *rut* sites contain more C than G bases, the mutations should abolish Rho-dependent termination. Two mutated constructs with base exchanges were created, both with C to G shifts (mut. S3-L10_1, mut. S3-L10_2; Fig. 29); in the second construct, a rare codon that was present in the first mutated construct was avoided, resembling the original codon usage. Furthermore, a plasmid with a deletion covering this region was constructed (ΔS3-L10).


**Fig. 29:** Mutations created to analyze a potential Rho-dependent termination. Exchange of G for C with change of codon 9 (AGG, a rare codon) and reversion to normal codon usage, as well as a deletion (crossed in red) are shown. The start codon is indicated in green. Amino acids given in bold are the stop mutations used above (compare chapter 3.14, Fig. 29).

The accessibility of the proposed *rut* site would be different in the WT and the above constructs with stop mutations in uORF1 (Fig. 30A). This would explain the observed repression and induction, or de-repression, in the absence or presence of Tc (compare Fig. 28 in chapter 3.14). If the pioneering ribosome terminates translation at codon 11 in the absence of Tc (Fig. 30A, cyan) or is stalled at the start codon (Fig. 30A, grey) due to Tc exposure, the putative *rut* site is inaccessible, leading to induction/derepression. However, when the ribosome terminates translation at codon 15 in the absence of Tc (Fig. 30A, green), the putative *rut* site is not blocked by the ribosome, and this would explain the observed repression under these conditions. To test this hypothesis, RT-qPCR and Western Blot were performed with cultures harboring the constructs with manipulated S3-L10 region.

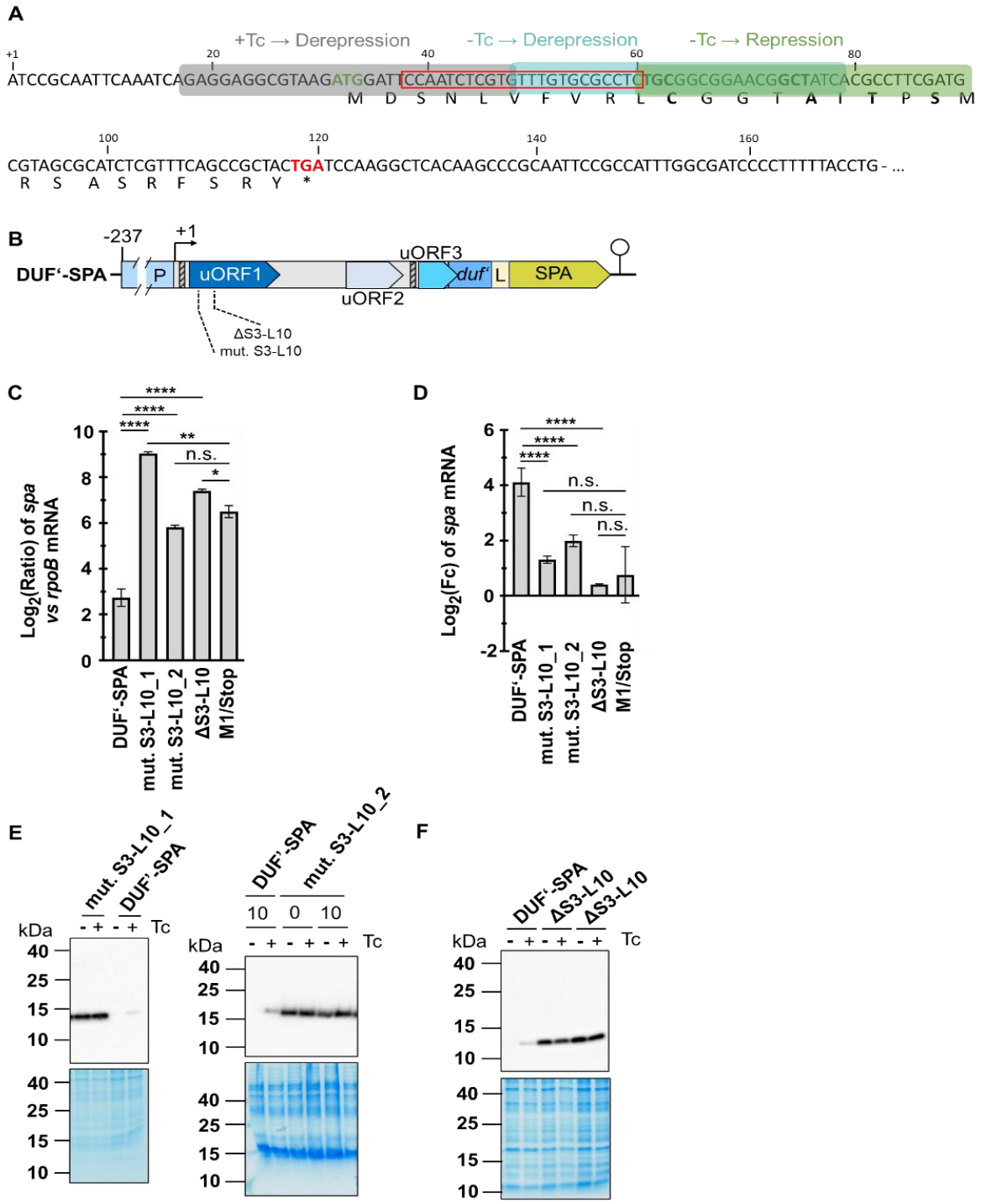


**Fig. 30:** Mutations of a potential *rut* site reveal a potential involvement of Rho in *duf1127₁* regulation. **(A)** Schematic drawing of ribosome coverage of the potential *rut* site (marked in red; S3-L10, positions +36 to +60) depending on whether the ribosome stops at the start codon, codon 11 or codon 15 indicated in colorings grey, cyan and green, respectively. Coverage at the start codon or at codon 11 occludes the *rut* site. **(B)** Constructs used with deletion of the potential *rut* site (ΔS3-L10), and two mutations in the same site (mut. S3-L10). **(C)** RT-qPCR of the reporter mRNAs comparing the $Log_2$(Ratio) of *spa* vs *rpoB* mRNA. This ratio shows the basal expression of the reporter fusions without Tc. **(D)** RT-qPCR of the reporter mRNA showing induction by Tc via $Log_2$(Fc). Tc-exposed cultures were compared to control cultures and log2(Fc) of the reporter mRNA level was calculated. Statistical significance: **** $p \leq 0.0001$, *** $p \leq 0.001$, ** $p \leq 0.01$, * $p \leq 0.05$. **(E, F)** Western Blot analysis with a monoclonal anti-FLAG antibody. Coomassie staining served as a loading control. For RT-qPCR of *duf'-spa*, six independent experiments were performed. For all other results, three independent experiments were performed.

The mutations in region S3 to L10 caused a significantly higher basal mRNA level without Tc compared to the WT construct on pDUF'-SPA (Fig. 30C). Mutation 1, which features the rare codon, caused a much higher mRNA level without Tc than mutation 2 (no rare codon). The basal mRNA level caused by mutation 1was even higher than the level of the M1/Stop construct (Fig. 30C). Induction by Tc was still detected for both mutated constructs, albeit significantly less than for the WT (Fig. 30D). When compared to the de-repressed M1/Stop construct, the induction by Tc was not significantly different for either mutated construct (Fig. 30D). On protein level, both constructs showed de-repression of the *duf'-spa* reporter (Fig. 30E).

Like the mutations above, the deletion of region S3 to L10 (ΔS3-L10) was revealed to cause a significantly higher mRNA level without Tc exposure compared to the WT construct on pDUF'-SPA plasmid as well as to M1/Stop (Fig. 30C). Induction by Tc was hardly measurable (Fig. 30D), and protein levels confirmed de-repression (Fig. 30F). Taken together, the results suggest that the region from codon 3 to 10 of uORF1 harbors an attenuation element, potentially a *rut* site, that allows for Rho-dependent termination (Fig. 30C-F). Deleting or mutating this region caused de-repression on RNA and protein level.

A bicyclomycin (BCM) assay, known to inhibit Rho in Gram-negative bacteria, was performed; however, *S. meliloti* did not react to the drug, indicating lack of uptake or insusceptibility to BCM (suppl. Fig. S4B). This was independently supported by lack of significant changes in transcripts for genes *duf1127*$_1$, *duf1127*$_2$, uORF1 and *phaP1* (suppl. Fig. S4A). Therefore, the function of the putative *rut* site could not be further corroborated in this work.

The results above suggested that Rho-dependent termination could be the mechanism behind *duf1127*$_1$ regulation. They suggested the possible involvement of an attenuation element (a *rut* site) in the first third of uORF1. uORF1 translation was required for the element to be accessible, potentially by Rho. Thus, Rho, or a corresponding unknown factor, has only a very short time window to access the attenuation element, entering in between the translating ribosomes. The results above, however, did not explain the observed de-repression of M1/Stop, that featured no start codon, which obliterates ribosome coverage, leaving the question of uORF1 SD and start codon requirement for regulation.

## 3.16 The uORF1 SD and start codon are relevant for *duf1127*$_1$ regulation in the absence of translation

The discovery of the attenuation element at the beginning of uORF1 and the fact that it does not easily explain the observations made using the M1/Stop construct, prompted investigation of the SD region and the start codon of uORF1, which was found to potentially form a secondary structure if no ribosome binding takes place. To this end, a pDUF'-SPA derivative with a deletion of region +18 to +33 was constructed, deleting the SD of uORF1 as well as the start codon (Δ18-33; Fig. 31A).

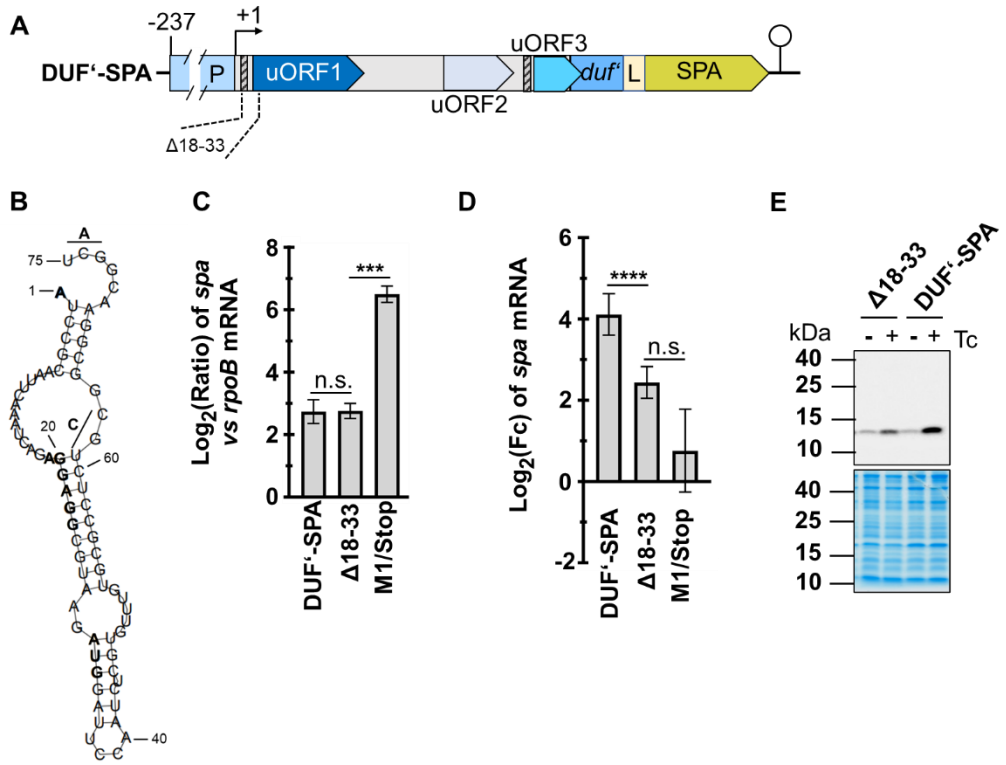


**Fig. 31:** The uORF1 SD and start codon is involved in *duf1127₁* regulation. **(A)** Construct used with deletion of the region +18 to -33 (deletion of the SD and start codon. **(B)** Secondary structure from +1 to +75 (A15), depicting the SD (AGGAGG, bold) and the start codon (AUG, bold) hidden in a secondary structure when no ribosome is translating uORF1. This secondary structure masks the proposed *rut* site (post +38 to +60). The secondary structure for M1/Stop is shown in suppl. Fig. S5. **(C)** RT-qPCR of the reporter mRNAs comparing the $Log_2$(Ratio) of *spa* vs *rpoB* mRNA. This ratio shows the basal expression of the reporter fusions without Tc. **(D)** RT-qPCR of the reporter mRNA showing induction by Tc. Tc-exposed cultures were compared to control cultures and log2(Fc) of the reporter mRNA level was calculated. Statistical significance: **** $p \leq 0.0001$, *** $p \leq 0.001$, ** $p \leq 0.01$, * $p \leq 0.05$. **(E)** Western Blot analysis with a monoclonal anti-FLAG antibody. Coomassie staining served as a loading control. For RT-qPCR of *duf'-spa* and Δ18-33nt, six independent experiments were performed. For all other results, 3 independent experiments were performed.

When no ribosome is translating the uORF1 (and in the case with the M1/Stop mutation), the SD sequence and the start codon can form a secondary structure leading to inaccessibility of the putative *rut* site (+38 to +60, Fig. 31B; suppl. Fig. S5). It was expected that the deletion of that region (+18 to +33) would lead to permanent accessibility of the *rut* site and thus permanent repression. In the absence of Tc, construct Δ18-33 showed reporter mRNA level similar to that of the WT construct on pDUF'-SPA and, accordingly, much lower than the level of M1/Stop (Fig. 31C). This result indicates repression of *duf'-spa* expression in the absence of uORF1 translation and supports the hypothesis of the *rut* site accessibility for this deletion construct even in the absence of Tc. Upon Tc exposure, induction of Δ18-33 was detected. This induction was significantly weaker than the induction of the WT construct but higher than that of M1/Stop, the latter without statistical significance (Fig. 31D). On protein level, a signal was detected after induction with Tc for the Δ18-33 construct, although this induction seemed weaker than for the WT on pDUF'-SPA (Fig. 31E).

This result supported the hypothesis that the potential *rut* site is masked by a secondary structure with the SD and start codon when no translation occurs. This also further corroborates the idea that the first halt of uORF1 must be translated for *duf1127₁* to be repressed.

## 3.17 Reporter mutagenesis results support potential *rut* site in uORF1 only accessible upon translation

On its genomic locus on pSymB, *duf1127₁* is considered repressed in the absence of Tc. It is induced upon Tc exposure, when the mRNA level was significantly increased. In this study, a plasmid pDUF'-SPA was used, as it showed similar behavior to its genomic counterpart, and the reporter mRNA was repressed without Tc and induced upon Tc exposure. Mutation of uORF1 start codon to a stop codon (M1/Stop) showed increased mRNA level without Tc and no induction with Tc. It was considered as de-repressed.

With the results presented in this study, it was shown that translation of the first half of uORF1 is necessary for *duf1127₁* regulation. Furthermore, this regulation might be Rho-dependent, and the SD of uORF1 might also be involved. The following table summarizes the results of mutations introduced into the pDUF'-SPA background and, in some cases, in the M1/Stop derivative (Tab. 24). If, in the absence of Tc, the basal mRNA level was significantly higher than that of pDUF'-SPA or its M1/Stop derivate (> pDUF'-SPA or M1/Stop), the construct was regarded as de-repressed. If there was significantly lower induction of the construct compared to pDUF'-SPA (< pDUF'-SPA) or if there was no statistically significant difference in induction compared to M1/Stop (= M1/Stop) upon Tc exposure, the induction was regarded as impaired.

**Tab. 24:** Summary of the mRNA level obtained in this study for derivates of pDUF'-SPA. De-repression categories for the mutated reporter constructs were defined as "+" when, in the absence of Tc, the basal mRNA level was significantly higher than if pDUF'-SPA was used (> pDUF'-SPA). If compared only to the M1/Stop construct, this was defined as a level higher or equal to M1/Stop (≥ M1/Stop). If, in the absence of Tc, the basal mRNA level is not significantly higher or is even lower than for pDUF'-SPA (≤ pDUF'-SPA), mutated reporter constructs were defined as not de-repressed: "-". For constructs impaired in induction upon Tc exposure, category "-" (meaning induction was not impaired) represents no statistically significant difference in or even higher induction compared to WT on pDUF'-SPA (≥ pDUF'-SPA). No statistically significant difference in induction compared to M1/Stop or statistically lower induction compared to pDUF'-SPA (= M1/Stop or < pDUF'-SPA) is represented by "+", indicating that induction was impaired. For the C11/Stop construct, there was no statistically significant difference in induction compared to both pDUF'-SPA and the M1/Stop derivate and is therefore represented as "-/+".

| | ***duf'-spa* mRNA level** | |
|---|---|---|
| **Construct** | **De-repression (-Tc)**<br>> DUF'-SPA or M1/Stop | **Induction impaired (+Tc vs -Tc)**<br>< DUF'-SPA or = M1/Stop |
| DUF'-SPA | - | - |
| M1/Stop | + | + |
| GCG 192-194 ATC | - | - |
| GCC 135-137 CGG | - | - |
| Δ1 | + | + |
| Δ2 | - | - |
| Δ3 | - | - |
| M2/Stop-DUF'-SPA | - | - |
| uORF3-SD-mut | - | - |
| DUF'-mut. 121-128 | - | - |
| Δ121-128 | + | + |
| scramble | - | - |
| M1-mut. 121-128 | + | + |

| | | |
|---|---|---|
| C11/Stop | + | +/- |
| A15/Stop | - | - |
| T17/Stop | - | - |
| S19/Stop | - | - |
| mut. S3-L10_1 | + | + |
| mut. S3-L10_2 | + | + |
| ΔS3-L10 | + | + |
| **Δ18-33** | - | + |

The only construct that showed similar repression, but lower induction in its RNA level compared to the WT construct on pDUF'-SPA, was Δ18-33 (Tab. 24). That construct seemed to be permanently repressed (or induction-impaired), which further proved an attenuation element in uORF1, which is accessible only upon translation.

## 3.18 First evaluation of the DUF1127$_1$ function

A function of the *duf1127* motif is still awaiting characterization, not only in *S. meliloti*, but also in other proteins of that family. To gain a first insight, a deletion of the genomic *duf1127$_1$* was evaluated.

Deletion proved difficult, as no clone with the full *duf1127$_1$* gene deleted from start to stop codon could be obtained. This was also true for the attempted deletion of uORF1. However, a deletion of a large part of *duf1127$_1$* (covering the amino acid sequence from codon 11 until codon 83, leaving the stop codon intact) was successful and was analyzed (Fig. 32). Again, however, many clones were false positives (Fig. 32B).

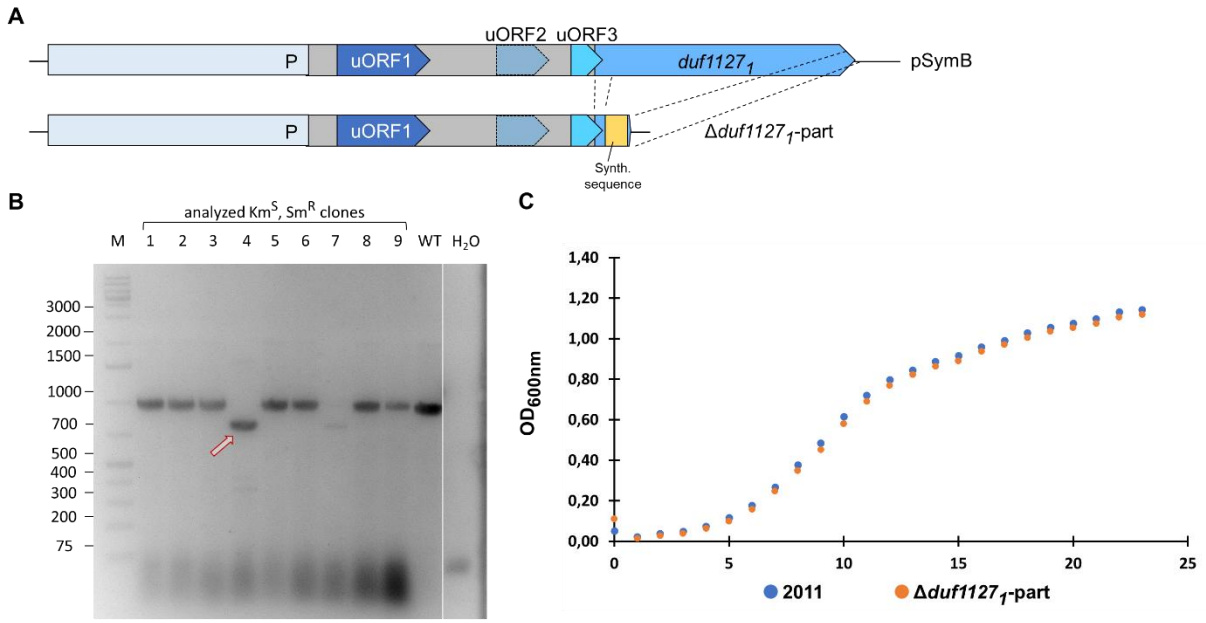


**Fig. 32:** A partial genomic deletion of *duf1127$_1$*. **(A)** Scheme of the genomic deletion, with *duf1127$_1$* deleted from codons 11 to 83, but leaving the stop codon intact. *duf1127$_1$* has a length of 252 bp. The length of the genomic deletion is 219 bp. For technical reasons, the deleted sequence was replaced by a synthetic oligonucleotide (Synth. sequence, yellow) that has a length of 22 bp. Primers located outside of the *duf1127$_1$* operon were used for check PCR. The PCR product was 982 bp long, the PCR product upon deletion/replacement with the synthetic oligo was 763 bp long. **(B)** PCR to check potential clones (correct clone #4 indicated by red arrow). M, Marker; WT, WT control (no deletion); $H_2O$, water control that was on the same gel as the conjugants tested. **(C)** Growth curve of *S. meliloti* 2011 (WT; 2011) and *S. meliloti* Δ*duf1127$_1$*-part without Tc. This result was obtained with the help of Tessa Wenz.

The generation of a partial genomic deletion was successful, as a smaller product of 763 bp was visible compared to the WT-like band of 982 bp in one out of 9 analyzed Km-sensitive, Sm-resistant clones (Fig. 32B), although many more had been tested previously. A growth curve under standard conditions showed no difference in growth (Fig. 32C).

To further address the role of the yet functionally uncharacterized *duf1172₁* in *S. meliloti*, a pulldown of potential interaction partners was attempted. The pulldown was performed using the full-length *duf1127₁* construct tagged with SPA as described above (DUF1127$_1$-SPA).

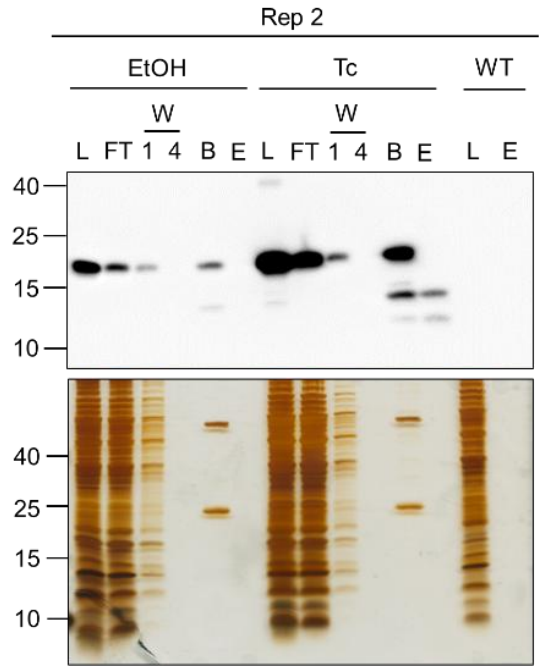


**Fig. 33:** Western Blot and silver-stained gel of 3xFLAG pulldown of full-length *duf1127₁*. L, lysate; FT, flow-through; W, wash (fraction 1 and 4); B, beads before elution; E, eluate; WT, wildtype as a negative control.

The lysate (L) was obtained after sonication and represented the protein amount before the pulldown, while the flow-through (FT) was taken after the incubation of the cell lysate on the beads. The beads sample (B) represents the beads loaded directly onto the gel without prior elution or treatment after the pulldown was completed. The eluate sample (E) was obtained after acidic elution.

The Western Blot showed that the DUF1127$_1$ protein, indeed, was recognized by the antibody against SPA and was bound to the beads (Fig. 33, additional replicates see suppl. Fig. S6). The two strong bands visible in the silver-stained gel of the beads fraction (B) are most likely the heavy and light chain of the antibody. Wash 4 yielded no residual bands, showing that all unspecific binding was removed. In the Western Blot, the eluate of the WT that did not carry the tag remained empty, which was also true for the non-treated (EtOH) cell carrying the SPA-tagged DUF1127$_1$ version. The acidic elution proved to be unsuccessful, as only a small amount was eluted, indicating strong binding of the antibody and protein. Only after Tc treatment, a band in the elution sample of the SPA-tagged protein was visible. The smaller bands might be indictive of protein degradation.

# 4. Discussion

## 4.1 Effects of antibiotic exposure

### 4.1.1. Subinhibitory Tc exposure for short-time read-out

In this work, the early response of *S. meliloti* to sub-inhibitory Tc exposure was analyzed. In particular, focus was placed on *duf1127*$_1$, the gene with the highest increase in mRNA level, and its potential regulation mechanism.

The selection of sub-inhibitory antibiotics concentrations was based on the increasing evidence that antibiotics can serve as communication molecules in interspecies interactions constantly present in microbial communities. This clearly includes a role of sub-inhibitory concentrations of antibiotics being discussed to involve a role of infochemical. Such a role includes development, but also can lead to responses in physiology upon perception of such infochemicals (Jones et al., 2016; Straight & Kolter, 2009; Sengupta et al., 2013). Depending on the antibiotics target, different responses may be expected.

In general, the application of the translational inhibitor drug Tc will induce cellular stress, even with sub-inhibitory Tc exposure. Thus, increasing mRNA levels for genes that are involved in antibiotic resistance or general stress response were expected. This was shown already in early transcriptomic (microarray) and proteomic studies with different antibiotics, including Tc (Wecke & Mascher, 2011). In *Burkholderia cenocepacia*, a bacterium that causes infections with cystic fibrosis, microarrays revealed more genes were up- than down-regulated in response to different antimicrobial compounds when treated during growth until OD 0.5 (Sass et al., 2011). Among these antibiotics was also amikacin, an aminoglycoside targeting protein synthesis. In addition to up-regulation of tRNAs, heat shock protein encoding genes were enriched (Sass et al., 2011). In an RNA-seq study recently conducted using *E. coli*, sub-inhibitory amounts (50 % inhibition) of different classes of antibiotics, including Tc, chloramphenicol and erythromycin, were analyzed for effects on the transcriptome in cells grown to mid-log phase in the antibiotic presence (Bie et al., 2023). In that study, Tc exposure has changed expression levels of more than 2 000 genes, with a down-regulation in glycogen metabolism and an up-regulation in the metabolism of amino sugars being the prominent classes of differentially regulated mRNAs (Bie et al., 2023). Already earlier, a study using microarrays in *Streptococcus pneumoniae* R6 revealed that after 10 min of subinhibitory treatment with translation inhibitors, genes encoding ribosomal proteins and translation factors showed an increased mRNA level, while genes involved in tRNA charging and amino acid biosynthesis were decreased (Ng et al., 2003). A more recent RNA-seq study in *Acinetobacter baumanii* tested the effect of a subinhibitory concentration of minocycline, a member of the tetracycline family of drugs. After exposing the bacteria to the drug for 10 min, 25 genes were differentially expressed, and in addition to coding genes, 48 sRNAs were either up- or down-regulated (Gao et al., 2022).

With our study, RNA sequencing revealed a higher level of up- than down-regulation of genes in accordance with those earlier findings. In addition, the slow-growing *Sinorhizobium* investigated in this study showed an enrichment specifically of members of the *duf1127* encoding transcripts being increased upon short-term Tc exposure, which had not been reported yet.

### 4.1.2 Genes with increased mRNA level upon short-term, subinhibitory Tc exposure

RNA-seq analysis of *S. meliloti* 2011 treated for 10 min with Tc revealed significantly changed mRNA levels of 373 mRNAs ($Log_2(Fc) \geq 1$, p-value $\leq 0.05$). The enriched mRNAs were often short (with a length below 100 amino acids being encoded), among them a high over-representation of genes containing the domain of unknown function DUF1127 was observed. The pfam entry for DUF1127 (PF06568) lists a large group with the domain being located at the protein's C-terminus or spanning the entire ORF (Mistry et al., 2021). In this work, six members of the *duf1127* family showed highly increased mRNA levels, among them the gene with highest up-regulation, *duf1127*$_1$. However, the response to Tc in this study encompassed many more genes which was more consistent with a transcriptome-wide, general response rather than being specific only to a subset of genes while still, DUF1127 genes were highly over-represented. The top hit with the highest increase in mRNA level was a *duf1127* gene.

Among genes that may be expected to increase in abundance upon antibiotic treatment, factors increasing tolerance against the drug might be expected. In Bacteria, and especially soil-dwelling bacteria, antibiotic resistance can be achieved by so called multidrug resistance efflux pumps (Blair et al., 2015; Paulsen, 2003). These pumps have been identified for *S. meliloti* (Eda et al., 2011), and they were expected to be among the genes with increased mRNA levels in response to Tc. In this study, two ATP-Binding Cassette (ABC) transporters were present among genes with the highest increase in mRNA. ABC transporters can be important in virulence and represent both, bacterial uptake and efflux systems (Davidson & Chen, 2004). A study in *A. baumanii* revealed that ABC transporter ATP-binding proteins were up-regulated 11.3-fold (Gao et al., 2022). Along the same lines, transpeptidases, which are peptidoglycan-crosslinking enzymes, have recently been associated with cell wall adaptation to stress including stress by ß-lactam antibiotics, as well as stress to outer membrane stability and toxin delivery (Aliashkevich & Cava, 2021). Such an L,D-transpeptidase was among the top hits, although Tc is not a ß-lactam antibiotic, but instead is targeting translation.

The regulatory circuits by which antibiotic resistance is regulated have been found to include several layers. Dar et al. (2016) found abundant involvement of regulatory RNAs including riboswitches as well as attenuators acting in *cis*. In case of erythromycin resistance genes, ribosome stalling has been found to be required for induction (Vasquez-Laslop et al., 2008). Bacteria are able to sense extremely low amounts of antibiotics in order to up-regulate multidrug efflux pumps as the most rapid and efficient way to clear antibiotics from the cell (Zhang & Chen, 2022; Rahman et al., 2017; Bernier and Surette, 2013). In their natural environment, bacteria usually live in microbial communities where not only nutrients are shared, but also antibiotics as well as or other secondary metabolites are produced that may have signaling functions (Jones et al., 2016; Bernier & Surette, 2013).

The second-most up-regulated gene, *phaP1*, encodes phasin, a polyhydroxy butyrate storage related protein (Wang et al., 2007). PHB granules are formed by *S. meliloti* as the main carbon storage compound, and PhaP1 is among the proteins required for PHB granule accumulation, associated with symbiosis (Wang et al., 2007). These storage compounds were suggested to have a cryoprotective effect (Obrucs et al., 2016). When PHB was heterologously produced in *E. coli*, proteome analysis revealed an increase in heat shock proteins, and PHB accumulation caused stress to the cell, while PhaP1 seemed to relieve that stress (de Almeida et al., 2011). In our study, *phaP1* was found to react to different stressors, including heat, suggesting that it may be induced under stress conditions in general.

Peptide chain release factors, like PrfB up-regulated under the tested conditions, have been shown to be connected to predation of *S. meliloti* by *Myxococcus xanthus*, another soil-dwelling bacterium (Soto et al., 2023). *S. meliloti* encodes three of these factors, *prfA*, *prfB* and *prfC*. Along with *prfB*, *rpsG* and *rpsL* were among the genes with the highest increase in mRNA

level, all of which associated to the ribosome, with *rpsL* and *rpsG* encoding the 30S ribosomal proteins S12 and S7, respectively. This might be explained with Tc being a translation inhibitor known for ribosome stalling (Lin et al., 2018), leading to increase transcription of ribosomal genes by the affected cells to counter that effect.

Another hit putatively connected to antibiotic response includes the toxin-antitoxin system RS07185. The up-regulated antitoxin of a type II of the ParD family is the (less stable) antidote to the toxin (Kamruzzaman et al., 2021) and potentially linked to plasmid maintenance and antibiotic resistance (Yang & Walsh, 2017). Furthermore, *rocF* encoding an arginase hydrolyzing L-arginine to L-ornithine and urea (Hernández et al., 2021) was among the up-regulated genes. In *Staphylococcus aureus*, a recent study has shown that restricting arginine synthesis can induce antibiotic tolerance (Freiberg et al., 2024). Thus, *rocF*-depletion of arginine may well be connected to up-regulation by Tc exposure.

A further up-regulated mRNA belongs to a protein containing an XpaX domain, although it also has been classified as a member of the DUF1427 family (pfam07235). The outer membrane lipoprotein Omp10 (Tibor et al., 1999) was characterized as providing a barrier for antibiotics (Lehman et al., 2022). A peroxiredoxin was found as well among the up-regulated genes and is involved in defending cells against toxic peroxides (Dubbs & Mongkolsuk, 2007; de Oliveira et al., 2021).

Strikingly, many genes coding for proteins with unknown function had increased mRNA levels in the early response to Tc, including the above mentioned DUF1127 members. For the hypothetical proteins encoded by RS36240 an RS18160 nothing is known yet. In our laboratory, translational evidence was found for the gene RS36240, but not for RS18160 under the conditions tested (Bachelor theses: Beck, 2023; Schank, 2023).

In contrast to genes with an increase in mRNA level, down-regulated genes were longer, and no over-representation of specific classes could be found. The respective genes usually were coded as the second gene, or further downstream in operons, while the genes with an increase in mRNA levels mostly were monocistronic or first genes in an operon (Theresa Dietz, unpublished). The down-regulation detected by RNA-seq (compare suppl. Tab. S1) might be attributed to a polar effect, where downstream genes in operons, a polarized unit, are less transcribed (Blaha & Wade, 2022; Jacob & Monod, 1961; Lawrence, 2002; Madigan et al., 2021; Mateus et al., 2021; Rochat et al., 2013). Furthermore, gene regulation in bacteria is adaptive, and genes may be under an indirect control from signals that are not directly related to the function of the gene, such as regulation by growth rate (Morgan et al., 2013). Validation of down-regulation detected by RNA seq was attempted using RT-qPCR for genes in two operons. For the genes *pdxA*/*rsmA*, being the last ORFs in their operon, validation by RT-qPCR was successful. In contrast, for the second operon encoding RS19365 (first) and *mnhG* (last), among others, only RS19365 (first in operon) resembled the result of the RNA seq (compare Fig. 10, Fig. S3).

Validation of increase in mRNA levels for the top 4 hits and hit #7 (compare Fig. 10), as well as uORF1 being annotated later, revealed higher fold-changes using RT-qPCR than observed during mRNA sequencing. The time-dependent response of the genes with an increase in mRNA level could show the specificity of the response, with *duf1127*$_1$ showing a very early response after three minutes already. This is indicative of an RNA-dependent regulation mechanisms, which would be expected to be much faster than transcriptional regulation. Increase in mRNA level was also dose-dependent, where already 0.5 µg/ml Tc were sufficient to elicit the response.

### 4.1.3 Comparative analysis of *duf1127₁*, *phaP1*, and *duf1127₂*

Three genes were further analyzed to address the mechanisms and the specificity of their up-regulation found in the RNA-seq analysis. In addition to addressing the question of a (post)transcriptional regulation under Tc treatment by using eGFP and SPA reporter, other stress conditions were tested to obtain a profile for the regulatory response of each of the three genes, which were among those with the highest up-regulation.

For *duf1127₁*, posttranscriptional regulation was suggested by the eGFP reporter fusions, as the promoter fusion exhibited a much higher fluorescence than the translational fusion without Tc. When Tc was added, RT-qPCR on the reporter mRNA was performed as eGFP takes time to fold into its final structure before it exhibits fluorescence. For *duf1127₁*, which is preceded by uORF1 in the mRNA leader, the results confirmed the hypothesis of a posttranscriptional regulation, as the translational fusion had a much higher mRNA fold-change increase than the promoter fusion (compare Fig. 13). Induction by Tc was also confirmed at the protein level using the *duf1127₁-spa* fusion, which also showed strong increase at the level of the reporter mRNA (see Fig. 13).

In contrast, *duf1127₂* is not preceded by an uORFs in the 5' UTR, which likely explains the difference in regulation without Tc observed using eGFP fusions and fluorescence measurement (compare Fig. 13). For *duf1127₂*, as measured by RT-qPCR, the *egfp* promotor fusion did not show increase after Tc exposure, while the *egfp* translational fusion showed a significantly higher reporter mRNA level, although the increase was less strong compared to *duf1127₁*. The *duf1127₂* encoded on the chromosome might show elements of a posttranscriptional regulation, because its mRNA half-life was increased upon Tc exposure as shown by RNA-seq and RT-qPCR (Figs 6, 8, 9, 10). Half-life analysis revealed that the mRNA was stabilized upon Tc exposure (Table 23), which might explain the fact that *duf1127₂* was found among the top hits in the RNA-seq. However, the protein level of the *duf1127₂-spa* fusion was lower under Tc conditions and the RNA level was not highly induced (compare Fig. 14). Since Tc is a translational inhibitor, a potential explanation might be given with the fusion protein being not stable. However, more sophisticated regulation cannot be ruled out at this level of initial investigation.

To evaluate posttranscriptional effects of the applied Tc, other translational inhibitors were tested. Both erythromycin and chloramphenicol are antibiotics that inhibit translation (Lin et al., 2018). Chloramphenicol binds the peptidyl transferase center, with its aromatic ring preventing the aminoacyl tRNA from binding, although recent evidence suggests that chloramphenicol activity critically depends on the amino acids as well as the identity of the residue entering the ribosome (Lin et al., 2018). Erythromycin, a natural macrolide, was shown to bind at the entrance of the nascent peptide exit tunnel, leading to its partial blocking (Lin et al., 2018). There has been evidence suggesting translation inhibition in a context specific manner and only interfering with certain amino acid sequences (Lin et al., 2018). Even with both mechanisms being different, and different from Tc that prevents binding of the aminoacyl-tRNA (Lin et al., 2018), their function in translation inhibition could lead to a similar response of the cells in reacting to translational stress. In *E. coli*, Cm exposure led to an up-regulation of nucleotide biosynthesis and osmotic stress response, while iron uptake and assimilation were down-regulated (Bie et al., 2023). The same study found that erythromycin up-regulated the osmotic stress response as well as dNTP biosynthesis pathways.

To test, whether a general stress response could explain the effect (increase of mRNA level) seen with Tc, other stressors different from antibiotics were also applied. Both *duf1127₁* and *duf1127₂* were found to respond to chloramphenicol (Cm) and erythromycin (Em) exposure, but not to heat. The response to erythromycin was very low. Furthermore, *duf1127₂* responded

to $H_2O_2$ exposure. The newly identified uORF1 upstream of *duf1127₁*, on the other hand, showed a very slight reaction to $H_2O_2$, while responding with the same behavior towards Em.

A different response was recorded for the *phaP1* gene that was strongly regulated by Tc. It appeared that *phaP1* might be regulated on the promoter level, and its 5' UTR under normal conditions does not inhibit gene regulation. The *phaP1* gene being strongly regulated by Tc is consistent with phasin being implicated in stress response earlier (de Almeida et al., 2011; Wang et al., 2007). In this study, *phaP1* reacted to all stressors tested, which was expected as PHB accumulation is involved in global stress response.

Thus, different patterns of response to the investigated stressors were obtained using a set of antibiotics targeting several cellular pathways. Independent of their target within the cell, antibiotics are prone to be cleared from the cytosol by activity of MDR efflux pumps that therefore can confer resistance to multiple antibiotics (Blair et al., 2014). A study in *Staphylococcus equorum*, which is resistant to Cm and Em, revealed that genes related to efflux were up-regulated, and down-regulated genes related to influx transporters (Heo et al., 2022). In *S. meliloti*, a transmembrane protein *tep1* was found to confer Cm resistance, showing that the cells are able to counter-act the effects by actively expelling Cm from the cytosol (van Dillewijn et al., 2009).

As a different stressor not targeting translation directly, oxidative stress was tested. $H_2O_2$ leads to increase of toxic reactive oxygen species in the cell. *S. meliloti*, as it can either be free-living or symbiotic, encounters oxidative stress in both environments (Lehman & Long, 2018; Sauviac et al., 2007; Tian et al., 2016). Thus, its general stress response could be expected to cover a wide range of genes up-regulated also after recognition of the translational inhibitor Tc. Exposure to 42 °C constituted a heat shock, another abiotic factor of stress. In *A. tumefaciens*, heat stress at 42 °C caused a strong induction in gene expression of the three small DUF1127 as well as two of the longer ones (Kraus et al., 2020), while in *R. sphaeroides*, heat stress caused an extensive and differentiated global transcriptomic response, while a DUF1127 protein was identified to be a heat shock protein (McIntosh et al., 2021). This shows that heat stress has a wide effect on the cells. However, in *S. meliloti duf1127₁* or *duf1127₂* expression were not generally stress-induced, but rather shown to be specifically involved in translational stress response.

### 4.1.4 DUF1127-encoding genes in *S. meliloti* and their homologs in other bacteria

In this study, six genes, each encoding a protein with a domain of unknown function DUF1127, were identified to be among the transcripts with the highest increase in mRNA levels in *S. meliloti* 2011. Sequence alignment did not reveal a large sequence similarity, either nucleotide or on conceptionally translated protein levels (see Figs. S1, S2) between the six *duf1127* genes. They can be sorted into three longer (#1, #2, #5) and three shorter (#3, #4, #6) ones. This warrants to look into other DUF1127 proteins with specific emphasis on whether they contain only the domain for DUF1127 or also additional sequences, and whether or not they contain known pfam domains in addition to the DUF1127 domain. The three shorter *S. meliloti* genes encoded only the domain and showed some similarity towards each other, while the three bigger with additional amino acids showed poor similarity between each other (Tab. 21).

In the plant-associated bacterium *A. tumefaciens*, seven *duf1127* genes have been identified. The three smaller DUF1127 (ATU_RS08170, ATU_RS08175 and ATU_RS21905) were – again - more similar, yet they displayed moderate similarity to the four longer DUF1127s (Kraus et al., 2020). In *A. tumefaciens*, the small DUF1127 protein ATU_RS08175 showed the highest similarity to $DUF1127_6$ from this study (Tab. 22). ATU_RS21905 showed the highest similarity to $DUF1127_4$ and ATU_RS08175 to $DUF1127_3$ (Tab. 22). From the three longer

ones, DUF1127$_1$ showed the highest similarity to ATU_RS09125, DUF1127$_2$ showed the highest similarity to ATU_RS08650 and DUF1127$_5$ to ATU_RS03215 (Tab. 22). In the zoonotic *Brucella abortus*, three members of the DUF1127 family were described, with two of them, RS20300 and RS28790, sharing a high sequence similarity of over 85 %, and share homology with *S. meliloti* 1021 gene RS07875, *A. tumefaciens* ATU_RS08170 and *Rhizobium leguminosarum* symbiovar *trifolii* Rleg2_1502 (Budnick et al., 2018). DUF1127$_4$ showed a 100% similarity to *S. meliloti* 1021 DUF1127 gene RS07875 (Tab. 22). This might be attributed to the fact that *S. meliloti* 2011, the strain used in this study, is genetically almost identical to *S. meliloti* 1021 (Casse et al., 1979; Meade & Signer, 1977).

In *Brucella*, it was found that RS20300 and RS28790 encode small proteins (48 aa) and are expressed under oxidative and acidic stress and were also activated during the stationary growth phase; the bacterium then cannot use fucose as a sole carbon source (Budnick et al., 2018). DUF1127$_4$ was highly similar to the two *Brucella* DUF1127, while DUF1127$_6$ showed moderate similarity towards both *Brucella* DUF1127 (Tab. 22). DUF1127$_3$ was highly similar to BAB_RS29075 (Tab. 22). DUF1127$_2$, despite showing no or very poor similarity to the *Brucella* DUF1127, was shown to be induced by oxidative stress. Thus, it is possible that the two DUF1127$_4$ and DUF1127$_6$ might be involved in a similar mechanism also within *S. meliloti*.

In *R. sphaeroides*, CcaF1 (RSP_6037) showed low sequence similarity to other, well-studied RNA-binding proteins (Grützner et al., 2021). This DUF1127 member is belonging to the longer subclass (71 aa). *S. meliloti* and *R. sphaeroides* are Alphaproteobacteria belonging to different phylogenetic orders, and probably therefore *Rhodobacter* CcaF1 showed only moderate similarity towards all six *S. meliloti* DUF1127 from this study (Tab. 22). While the similarity might be poor, CcaF1 having RNA binding activity might hint at other DUF1127 proteins having a similar function, which has, however, not been addressed with these DUF1127 proteins yet. Aside from DUF1127$_1$, other DUF1127 were not investigated here in detail, but the above-mentioned stress experiments showed that DUF1127$_2$ reacts to oxidative stress, while DUF1127$_1$ does not. This, along with studies in other organisms, shows that DUF1127 proteins might have different or redundant functions in the cell. These results show that the DUF1127 family is rather diverse, and in *A. tumefaciens* it has been suggested that the DUF1127 family consists of at least three subclasses (Kraus et al., 2020).

In this work, a physical characterization of DUF1127 function allows to extract some results. The DUF1127 domain is listed as being found in Alpha- and Gamma-proteobacteria, with substantial protein sequence conservation albeit a yet undefined function. This is well in accordance with a high number of domain of unknown function gene models being identified through genomics (Wan et al., 2023). The DUF1127 domains are members of the superfamily cl23975 that has been described based on similarity. The proteins with this domain are usually between approx. 60-140 amino acids (aa) in size, which is also the case for *duf1127$_1$*, which encodes an 83 aa protein.

First hints on assigning a function for DUF1127 proteins was obtained from *A. tumefaciens*, where the deletion of the three small DUF1127 encoding genes caused a growth phenotype (Kraus et al., 2020). Sucrose and salt were shown to influence the growth of the triple knockout mutant, and cell attachment as well as biofilm formation were increased. The arginine-rich protein was involved in carbon and phosphate metabolism (Kraus et al., 2020). In *R. sphaeroides*, deletion of the *ccaF1-ccsR1-4* locus was impossible, but over-expression resulted in slower growth and, using a 3xFLAG pulldown, the CcaF1 protein was identified as an RNA-binding protein (Grützner et al., 2021). Especially sRNA maturation and RNA turn-over were affected.

For *S. meliloti* DUF1127$_1$, a partial chromosomal deletion with only 10 codons remaining was possible. Thus, the protein was non-essential. Since *S. meliloti* 2011 harbors at least five

additional DUF1127 genes. Hence, compensation from other genes was possible, which is in line with especially Alphaproteobacteria possessing multiple members of this protein domain family which could easily substitute for each other. However, the sophisticated differential regulation of *duf1127$_1$* may indicate a specific role in short-term, sub-inhibitory Tc response, although DUF1127 members showed increased mRNA levels after short-term Tc exposure.

The knock-out construct did not yield a growth phenotype, which may well be attributed to the compensatory activity of other members of the protein family in *S. meliloti*. A functional characterization by identification of interaction partners did not yield substantial evidence for specific protein-protein interactions. This leaves the possibility of essential, yet very short-term protein-protein interactions, which might be expected to lead to changes in the interacting proteins' function. Such a role was, e.g., found for archerases, which can lead to interacting enzymes being activated (Buckel et al., 2012).

Using the recently developed ACIT system (Kretz et al, 2023), which allows control of the gene of interest on a genomic level, the *duf1127$_1$* operon or its parts can be depleted in the case that full chromosomal deletions fail. The existing *duf1127$_1$* partial deletion, however, has not been investigated in the presence of Tc or other stressors or under different growth conditions yet.

## 4.2 Half-life determination revealed global mRNA stabilization upon Tc exposure

In general, bacterial mRNAs have a short half-life, mostly ranging from 40s to 60 min (Richards et al., 2008). mRNA half-life is affected by many factors, such as elements at either the 5' or the 3' end, posttranscriptional modifications, interactions of sRNAs with mRNAs, or the control of intracellular ribonuclease levels (Mohanty and Kushner, 2016). Growth conditions as well as growth rate can influence bacterial half-life, as it allows rapid adaptation to changing environments (Vargas-Blanco & Shell, 2020). The role of stem-loop structures at the mRNA 3' end has been shown to increase mRNA half-life, as 3'-5' exoribonucleases perform at a low rate when encountering such structures (Richards et al., 2008). In operons, segments are protected from decay by such RNA structures (Dar & Sorek, 2018). Polyadenylation in E. coli is a degradation signal, used by both RNase R and the exonuclease PNPase, while sRNAs through imperfect base-pairing around the bacterial ribosome binding site usually also leads to mRNA degradation including exo- and endoribonuclease activity (Mohanty & Kushner, 2016, 2023; Richards et al., 2008).

In this study, mRNA half-life was determined before and after 10 min of sub-inhibitory Tc exposure by stopping transcription using rifampicin (Campbell et al., 2001). RT-qPCR revealed that the half-life of all analyzed mRNAs increased after Tc application, with standard deviations increasing concomitantly, up to no decay being measured for some genes. The control mRNA *metZ* was confirmed to have a half-life of 77 ± 6s without Tc, which corresponds with previously described half-life for this transcript (Scheuer at al., 2022). The *ppiD* mRNA showed a half-life of 43 ± 7s without Tc. Upon Tc exposure, the stability of both mRNAs was increased 3- to 5-fold (Tab. 23). Despite this, for both genes, mRNA levels in the RNA-seq were not significantly increased or decreased. Both *metZ* and *ppiD* are rather long transcripts, which makes the mechanism of premature transcriptional termination by de-coupling of transcription and translation likely. However, although in the RNA-seq mRNA level was measured over the entire gene, the decay was measured only using a primer pair.

### 4.2.1 Simultaneous mechanisms are active during Tc exposure

Selected genes that showed an increase or decrease in mRNA level in the RNA-seq (up-regulated and down-regulated genes, respectively) were also found to be stabilized upon Tc exposure (Tab. 23). On genes down-regulated upon Tc exposure, probably two mechanisms are working simultaneously upon Tc exposure: premature transcriptional termination due to decoupling of translation, and mRNA stabilization This was, e.g., shown by analysis of the *trpDC* operon featuring *ppiD* (first gene) and *moeA* (last gene). A second operon featuring *rsmA* and *pdxA* – both last in their respective operon – were analyzed as well. The results showed that not only the half-life had increased, but downstream genes were strongly affected (like *moeA*, Tab. 23*)*. Especially for genes that are located downstream in their operons, in some experiments no decay was detected. Specifically with Tc, the half-lives of certain mRNAs varied highly in three experiments, leading to high standard deviations (Tab. 23). Such strong differences between the individual experiments suggested the possibility that, with the primers used, a (more stable) degradation product is detected, which accumulates. To obtain more reliable results, for several genes (*duf1127*$_1$, *phaP1*, *moeA* and *rsmA*) a second primer pair was used. The outcome remained the same, as stabilization could be observed with Tc, and sometimes, for example for *phaP1* and *moeA*, no decay was observed (Tab. 23). With these controls, a general increase of half-life could be demonstrated to be the result of Tc application.

In this study, it was observed that, in some cases, after rifampicin addition, mRNA amounts instead of directly decreasing, increased first and then started to decrease (compare suppl. Figs. S7-S15). The reason for that observation remains unclear, but a similar effect had been observed earlier (Basineni et al., 2009). In their study, a high amount of rifampicin had been added. However, it had not been tested whether transcription was blocked entirely. A study in *Synechococcus sp.* PCC 7002 used 200 µg/ml rifampicin dissolved in DMSO (Gordon et al., 2020) in contrast to 600 µg/ml dissolved in MeOH in this study (stock solution: 133 mg/ml).

### 4.2.2 Differential half-lives in a polycistronic messenger

Half-life determination revealed that both the uORF1-sRNA and *duf1127*$_1$ mRNA were stabilized approximately 3-fold upon Tc exposure (Tab. 23). However, upon Tc exposure, the induction of the uORF1-sRNA was lower compared to the *duf1127*$_1$ mRNA induction. Therefore, the small RNA might result from premature transcription termination or attenuation, and/or is influenced by differential RNA stability.

Different half-lives across an operon had been reported previously, and it has been suggested that co-transcriptional degradation could play a role in addition to the polar effect of de-coupling between transcription and translation (Blaha & Wade, 2022; Chen et al., 2018; Lawrence, 2002; Madigan et al., 2021; Mateus et al., 2021; Rochat et al., 2013, and citations therein). In *Synechococcus sp.* PCC 7002 it was reported that polycistronic transcripts showed an increase in mRNA half-life along the transcript (Gordon et al., 2020). The authors suggest that sequence elements, such as a Rho-independent terminator found in that study, might increase transcript stability. In *E. coli*, a transcriptome-wide study analyzing mRNA decay between exponentially growing and stationary phase cells showed that half-life increased in stationary phase (Chen et al. 2015). It has been reported that mRNA is stabilized in response to stress inflicted by conditions that alter growth rate in various organisms (Vargas-Blanco and Shell, 2020 and citations therein). A study of the lactose utilization (*lac*) operon in *E. coli* using chloramphenicol revealed that mRNA decay became slower, without a direct proportionality found between the rates of chemical decay and polypeptide synthesis (Schneider et al., 1978).

## 4.3 Expression of DUF1127$_1$

### 4.3.1 The *duf1127$_1$* operon features a small RNA and uORF

The top hit, *duf1127$_1$*, was of particular interest, as it showed the fast and strong increase in mRNA level using three independent methods. In this work, it was found that it is preceded by at least two upstream ORFs. First uORF1 was detected, which was found to be part of an attenuator sRNA. Thereafter, an uORF2 and uORF3 were found, the latter overlapping *duf1127$_1$*.

Considering the cDNA reads of the RNA-seq, *duf1127$_1$* and the accompanying uORFs were induced by Tc exposure. This was validated by Northern hybridization, and *duf1127$_1$* induction was also validated using reporter fusions (Fig. 13, 14 and 15). The Northern hybridization of RNA from strain 2011 suggested that a processed transcript as well as an uORF1-containing sRNA existed, as probes in *duf1127$_1$* and in uORF2 gave signals different from a probe within uORF1 (Fig. 8; Fig. 22). This suggested that the largest band corresponds to the full-length transcript, while a processed transcript with intermediate length as well as a smaller sRNA were present. This sRNA terminated before uORF2; according to the 3'-RACE results most likely around position +180.

The intergenic region (IGR) between uORF1 and *duf1127$_1$* is rather long and was shown to be involved in regulation of *duf1127$_1$* (Fig. 18). While uORF1 had been detected earlier (sORF26; Hadjeras et al., 2023), a new uORF2 was identified in this study. Both uORF1 and uORF2 are in frame to *duf1127$_1$* and encode proteins of 29 and 16 amino acids, respectively. Using SPA reporter fusions on plasmids, mRNA was analyzed, and protein expression could be validated for uORF1 and uORF2 both with and without Tc exposure (Fig. 17, Fig. 20). On RNA level, uORF1-*spa* mRNA showed a slight increase upon Tc treatment (Fig. 15), while uORF2-*spa* mRNA was strongly induced. The induction was similar to that of *duf'-spa* mRNA (Fig. 20). Despite this difference at the level of mRNA, for both uORF1-SPA and uORF2-SPA, the protein level indicated no change in protein accumulation upon Tc exposure (Fig. 15 and 20).

Using a construct in which the start codon of uORF1 was mutated to stop, a regulation depending on the translation of uORF1 supported posttranscriptional regulation of *duf1127$_1$*. This was seen with the mutation (M1/Stop, Fig. 15) that abolished *duf1127$_1$* regulation, as *duf1127$_1$-spa* was de-repressed even without Tc. Mutating the start codon of uORF2, however, did not affect *duf1127$_1$* regulation, while mutation of both start codons showed the same regulation as the single mutation in uORF1 (Fig. 15). This shows that uORF1 is involved in *duf1127$_1$* regulation, while uORF2 might have a different role or target in the cell.

In addition, a potential third uORF was identified in the genomic sequence in front of *duf1127$_1$*. This ORF overlapped with the first codons of *duf1127$_1$* and was named uORF3. This uORF exhibits a non-canonical start codon (CTG) and its expression could not be validated using Western Blot analysis under the conditions used in this study. However, its functional ribosome binding site seems to be important for translation of *duf1127$_1$* (Abb 25).

### 4.3.2 DUF1127$_1$ expression is independent of translation of uORF2

The second uORF identified, uORF2, seemed to have a different function from uORF1. However, if a part of uORF2 was deleted (construct Δ2, Fig. 18), translation of *duf1127$_1$* was impaired, leading to the hypothesis that uORF2 is also involved in translational control. In *S. enterica* serovar Typhimurium, a newly discovered uORF *mgtQ* in the *mgtCBRU* operon (a virulence operon containing a magnesium transporting ATPase *mgtB*) was found to be translated and affected expression of *mgtB* on a translational level (Choi et al., 2021). However, this uORF had a strong SD sequence, which is not the case for uORF2 investigated in this study.

The constant expression of uORF2 at the protein level (Fig. 20) might indicate an epistatic nature over uORF1, and subsequently *duf1127₁*, or else another target not identified yet might be responding in *trans*.

In the *duf1127₁* operon, uORF1 is separated by 159 bp from *duf1127₁*. This region, although mentioned as an IGR in chapter 3.10, encompasses uORF2 as well as the putative uORF3. Translation of uORF2 was shown even in the absence of Tc, and it had no influence on *duf1127₁* translation. Ribo-seq data did not show enrichment for this uORF2 start codon, which may be related to a low level of translation while at the same time, the uORF2-SPA fusion protein is probably very stable, since it was detected both with and without Tc. The absence of a SD in front of uORF2 is in line with a low translation rate.

In *S. enterica*, formation of alternative stem-loop structures that overlap with the *mgtQ* ORF were found to be controlling translation of *mgtB* (Choi et al., 2021). When translation was inhibited by a start-to-stop mutation, two stem loop structures formed: a stem-loop of *mgtQ* with a downstream region and a translation-inhibitory stem-loop structure formed occluding the RBS of *mgtB*.

The data implied a transcription attenuation mechanism of control for response to sub-lethal, short-term Tc exposition for the *duf1127₁* operon, which was investigated into more detail and a working model was proposed (see Fig. 34 below). To further refine the model proposed, the role of uORF2 remains to be characterized in more detail. While uORF3 was not validated under the conditions tested in this study, it still may have a regulatory function, or is expressed under different conditions.

### 4.3.3 Post-transcriptional control is suggested for *duf1127₁*

In this work, it has been discovered here that the SD of the putative uORF3 impacts *duf1127₁* translation. The SD of *duf1127₁* itself is rather inefficient, making it possible that the uORF3 SD serves as an upstream regulatory binding site for the ribosome (Palmer & Burne, 2015). Ribo-seq suggested uORF3 translation (Hadjeras et al., 2023), which could not be verified here using a SPA translational fusion. Possibly, this fusion protein was rather instable or translated under different conditions than the ones used in this study. In respect to *duf1127₁* regulation, however, neither uORF1 nor uORF2 overlap with *duf1127₁*. Only the out-of-frame, putative uORF3 is overlapping, suggesting translational coupling between uORF3 and *duf1127₁*.

The Ribo-seq data is obtained from the footprint of a 70S (mature) ribosomes. The SD is only recognized by the 30S subunit (Hadjeras et al., 2023; Osada et al., 1999; Rodnina, 2018; Shine & Dalgarno, 1974, and citations therein), which opens also the theoretical possibility of a slow assembly of 70S ribosomes. However, it has been shown that an upstream SD can be used for ribosome binding even though the start codon is much further downstream. This has been shown recently for the SAM-II riboswitch in *S. meliloti* upstream of the gene *metA* (Scheuer at al., 2022). SAM II-riboswitches respond to the level of S-adenosyl methionine, whose binding leads to formation of a pseudoknot. For *metA*, the riboswitch encompasses a SD sequence upstream of a putative start codon AUG (Scheuer et al., 2022). However, a second start codon was discovered 69 nt downstream, also featuring two potential SD sequences. In between both start codons, a Rho-independent terminator was predicted (Corbino et al., 2005; Scheuer, 2023). It was shown that the second AUG was used for translation, but all three SD regions were necessary for efficient translation of *metA* (Scheuer, 2023). This study proposed a mechanism, where the ribosomal 30S subunit binds at a standby region and initiates translation further downstream.

Translational standby sites, usually single-stranded and sequence unspecific, were first described in *E. coli* (Smit und van Duin 2003; Studer und Joseph 2006; Romilly et al. 2019). The authors proposed that the RNA folding kinetics make it impossible for the 30S subunit of the ribosome to access a folded RNA binding site. Thus, the ribosome must have been in contact with the RNA previously, and upon opening of the structure shifts into place (Smit und van Duin 2003; Studer und Joseph 2006; Romilly et al. 2019). This would be true in case of ribosome slipping, where a non-coding region is by-passed to combine separate regions in one protein sequence (Klimova et al., 2019; Senyushkina et al., 2024). In *E. coli*, the *tisB* mRNA has a standby site for the ribosome, which is located upstream of the RBS (~ 100 nt; Darfeuille et al., 2007; Wagner & Unoson, 2012). The RBS is required for efficient translation, but occupied by another sRNA that prevents ribosome binding. This allows cleavage by RNase III, resulting in a truncated *tisB* mRNA that cannot be translated (Darfeuille et al., 2007; Wagner & Unoson, 2012). It is possible that a similar mechanism to one of those mentioned above is possible for *duf1127*$_1$, and it requires the SD in front of uORF3 in addition to the regular start codon of *duf1127*$_1$. To validate this hypothesis a ribosome toeprint assay (Romilly et al., 2019) combined with mutation of the SD sequences and the corresponding start codons would be required.

4.3.3.1 Sequestering RBS as regulatory elements

When the region of the start codon and SD of uORF1 was deleted (Δ18-33), the reporter *duf'-spa* mRNA level was similar compared to the WT construct on pDUF'-SPA, while induction was weaker albeit still occurring. If this constructs' reporter mRNA was stabilized by Tc exposure, this might explain the weak induction, which is suggested to be independent of the attenuation mechanism. The protein level was weaker compared to the WT construct on pDUF'-SPA. Since the mRNA level was lower than for pDUF'-SPA upon induction with Tc, less protein was translated, explaining the weaker protein expression. Furthermore, it is possible that induction of *duf'-spa* translation is dependent on Tc being present, thus giving the increase in protein level detected using Western blot.

It is not uncommon in bacteria that RBS are sequestered in secondary structures, and thus inaccessible to the ribosome, or that translation is otherwise inhibited. Regulation of translation can involve temperature-dependent SD accessibility (Pienkoß et al., 2021, 2022). Alternatively, antisense RNAs can inhibit translation of mRNAs involving sequestering of SD sequences and/or start codons (Malmgren et al., 1996). E.g., in *E. coli*, the RNA binding protein CsrA (regulates translation initiation, among others) binds to two sites in the leader region of the fully processed *pnp* mRNA (encoding PNPase). These binding sites are sequestered in a secondary structure when the mRNA is not fully processed (Park et al, 2015). RNA thermometers have been known to function in a similar way where, at lower temperatures, the RBS is sequestered and thus translation is prevented (Barnawi et al., 2020; Narberhaus et al., 2006; Pienkoß et al., 2021, 2022). This has been described in the case of a type III secretion system assembly in *Yersinia* involved in pathogenesis. In *Campylobacter jejuni*, a bacterium which is the leading bacterial cause of human gastroenteritis worldwide, it has been shown that such an RNA thermometer regulates the *czcD* gene, which encodes for a member of the cation diffusion facilitator family (Barnawi et al., 2020). Sensing an elevated temperature, e. g. upon entering the human body, the RNA thermometer's secondary structure releases, exposing the RBS (Barnawi et al., 2020; Narberhaus et al., 2006).

#### 4.3.3.2 Combined protein binding and stem-loop formation for regulation of expression

An internal complementary sequence (ICS) to the RBS has been identified in *E. coli* within the *gnd* mRNA between codons 71-74 (Chang et al., 1995). This ICS forms a long-range secondary structure that sequesters the RBS (Chang et al., 1995). The *gnd* gene is involved in the pentose phosphate pathway and related to growth rate-dependent regulation. The gene cat-86 in *E. coli*, encoding for a chloramphenicol acetyltransferase, includes a regulatory element consisting of two inverted-repeat sequences. These are predicted to form a stable RNA stem-loop structure, thereby sequestering the ribosome binding site (Ambulos et al., 1985). The authors suggested that chloramphenicol binds to the 50S subunit of the ribosome and leads to uncovering of sequences that are nearly identical to the RBS. These secondary RBS sequences might compete with the formation of the stem-loop (Ambulos et al., 1985).

These different examples of involvement of protein binding as well as stem-loop formation control underline the importance of secondary structures for translation. Putative stem-loop structures also would be important for transcriptional termination discussed below. In addition, a role of binding of a protein, e. g. encoded by uORF1, to the nascent mRNA influencing transcript length, or also transcript stability, cannot be excluded.

### 4.3.4 Attenuation of *duf1127₁* is probably Rho-dependent

In bacteria, 5'UTR regulation by intrinsic termination can produce sRNAs including a regulation involving an uORF in *Escherichia coli* leading to differential 3' ends (Adams et al., 2021; Choe et al., 2022). Here, transcription attenuation between uORF1 and *duf1127₁* was suggested. To identify the 3'-ends of the arising sRNA, 3' RACE was applied and multiple 3' ends were identified in the leader of the *duf1127₁* mRNA. While nine ends mapped in uORF1, 15 ends between uORF1 and *duf1127₁* were found, and three were within the *duf1127₁* gene (Fig. 16). Previously, an sRNA at this locus had been annotated from position +1 until position +282, the third nucleotide of the start codon of *duf1127₁* (Fig. 16; Sallet et al., 2013). In this study, only one end mapped to this specific position (Fig. 16). Many different 3' ends in the gene for uORF1 might be indicative of RNA being partially broken down by 3'-5'RNases intracellularly, or a non-defined transcriptional termination. The results of the 3' RACE as well as Northern hybridization (Fig. 22) revealed an sRNA that ends before nucleotide position +250, most likely around position +180. This would be in accordance with both, RNA degradation or a premature termination.

The similar increase in stability for uORF1- and *duf1127₁*-containing transcripts, although according to RT-qPCR, the *duf1127₁* mRNA level increases stronger than the level of the uORF1- containing is suggestive for a transcriptional attenuation mechanism regulating the expression of *duf1127₁*. According to the presented data, the *duf1127₁* expression is increased upon Tc exposure by at least two mechanisms: mRNA stabilization and relief of transcription attenuation. Additional upregulation of *duf1127₁*, and upon Tc exposure by induction of protein production seems also possible. Therefore, attenuation might be involved in the multi-layered regulation system governing *duf1127₁* expression. Since transcriptional termination, including premature termination, can be achieved in Rho-dependent and intrinsic termination, it was attempted to identify terminator sequences. Attenuation is a common way of premature transcription termination in bacteria, using alternative secondary structures that are mutually exclusive (Naville & Gautheret, 2009). A terminator/anti-terminator region downstream of uORF1 might be responsible for the above discussed transcription attenuation. In *Streptomyces coelicolor*, the *whiB7*/*wblC* leader RNA features a Rho-independent terminator that serves as an attenuator, and contains an anti-terminator (Lee et al., 2022). The conserved terminator

structure of the *wblC* leader sequence was found to be responsible for transcriptional attenuation, while the anti-terminator was critical for antibiotic-responsive *wblC* induction as well as antibiotic resistance mediated by WblC. Inhibition of translation of an uORF in their mRNA leader facilitated folding of the anti-terminator (Lee et al., 2022).

In *E. coli*, the RNAP pauses at the terminator site and adopts a conformation that accommodates an RNA-DNA hybrid in its active site (You et al., 2023). The initial folding of the terminator structure then enlarges the RNA exit channel and weakens the upstream RNA-DNA interaction. The RNAP then clears the energetic barrier, allowing RNA hairpin completion, and the completed terminator hairpin then extracts the RNA from the exit channel. This can occur by hybrid shearing, hyper-translocation or following an allosteric activation (Mandell et al., 2022).

Intrinsic terminators usually are identified using energy models for structural motifs, although the mechanism of folding for transcriptional terminators is yet to be fully understood (Brandenburg et al., 2022). There, the short RNA observed indicated a potential role of the terminator/anti-terminator structure. However, this was not supported by the search for potential terminator sequences in *S. meliloti duf1127*$_1$. As the putative terminator/anti-terminator structures were not involved in *duf1127*$_1$ regulation (since mutating the stem-loops did not change *duf1127*$_1$ regulation on either RNA or protein level, Fig. 17), the hypothesis for Rho-independent transcriptional control was falsified. Further investigation for identification of putative intrinsic termination sites was not yielding further motifs, leading to the alternative hypothesis of Rho-dependent termination.

After intrinsic termination could be excluded as a termination mechanism, Rho-dependent termination shifted into focus. The hexameric Rho protein recognizes C-rich regions (*rut* sites) to bind and then catch up with the transcription elongation complex (Said et al., 2023). The region +37 to +60 (with codons S3 to L10 of uORF1) was identified as a putative Rho binding site. Mutating and deleting this region, indeed, showed a higher mRNA level without Tc, and weak induction with Tc as well as de-repression on protein level. Although bicyclomycin treatment did not achieve inhibition of *S. meliloti* growth and therefore could not be applied to test for Rho-dependent termination, this mechanism cannot be ruled out. *S. meliloti* seemed to be insusceptible to BCM, and therefore Rho depletion should be attempted in future to validate a Rho-dependent mechanism.

In *Bordetella pertussis*, an operon sensing copper with a gene encoding a protein of the DUF2946 (named CruR) family was found to be terminated by Rho-dependent termination, enhanced by Rho facilitating factors NusA and NusG (Roy et al., 2022). There, premature translation termination abolished the expression of the downstream gene. The authors argue that the lead ribosome limits access for Rho to the *rut* site or the RNA polymerase (Roy et al., 2022) and propose a model where the downstream gene *bfrG* is regulated by the uORF CruR. The RNA polymerase paused in between *cruR* and *bfrG*, and the lead ribosome stalled at a specific motif in the uORF, masking a *rut* site. In the absence of a ligand, in this case copper, Rho was prevented from binding to the *rut* site, allowing transcription to continue. In presence of copper, the stalled ribosome is relieved and completes translation of *cruR*. This allows Rho to access the *rut* site and terminate transcription (Roy et al., 2022).

It has been shown in *Salmonella* that translation of a small ORF interferes with the ability of Rho-dependent termination of transcription in response to the arginine level (Ben-Zvi et al., 2019). The translation helps in unfolding an RNA structure that sequesters the RBS of the downstream gene.

## 4.4 Proposed mechanism

### 4.4.1 Evidence for multi-level expression control

In this work, it was shown that the *duf1127₁* operon has a leader region with three uORFs, and also featuring an sRNA. While the uORFs and their corresponding proteins as well as the sRNA might have their own functions, the leader region controls *duf1127₁* expression. The presented data show that transcriptional regulation of *duf1127₁* required translation of uORF1, probably until at least till the 15$^{th}$ codon (A15). If translation was terminated before, at codon 11 (C11), regulation was abolished (Fig. 28). This allows to conclude that at least partial translation of uORF1is essential for the correct transcriptional response upon Tc exposure.

However, not only is translation of the first half of uORF1 relevant, but successful initiation of uORF1 translation in time is also important for the regulation. This was explained by a potential RNA structure masking a putative *rut* site (attenuation element in codons 3 to 10 of the uORF). This RNA structure can fold if a ribosome does not bind to the RBS of uORF1 in time. In the absence of ribosome binding, the SD of uORF1 and the start codon base pair to the potential *rut* site, rendering it inaccessible. This interpretation is supported by Fig. 15, showing the de-repressed M1/Stop construct and Fig 30 showing the de-repression upon mutations in codons 3 to 10 or a deletion of these codons. It is also supported by Fig 31 showing that deletion of nt 18-33, which harbor the uORF1 RBS, leads to transcriptional attenuation even in the absence of uORF1 translation, and to impaired induction by Tc (see also Table 24 summarizing the SPA results with SPA reporter constructs). Thus, ribosome binding to the SD and the start codon of uORF1 as well as efficient initiation and elongation of translation are necessary to keep the attenuation element accessible. This would allow a factor such as Rho to access the attenuation element located in region S3-L10.

In case of ribosome binding to the RBS of uORF1 in the presence of Tc in subinhibitory amount, translation initiation is impeded. Since the ribosome covers approximately 30 nt, a part of the putative rut site between codons 3 and 10 is blocked, which leads to attenuation relieve (*duf1127₁* induction). This interpretation is supported by Fig. 30 above. Similarly, if in the absence of Tc, the ribosome terminates at codon 11, a process that is slower than elongation, a part of the *rut* site is blocked. This explains the de-repression of the reporter construct harboring the C11/Stop mutation (Fig. 28). This should then also apply for other translation inhibitors, which was partly the case.

As has been shown here (Fig 18), a part of the intergenic region between uORF1 and *duf1127₁* is crucial for regulation of *duf1127₁*. This region, uncovered by the Δ1 construct, led to de-repression on both RNA and protein levels. The RNA analysis suggests that this region also contains a *rut* site necessary for the transcription attenuation. This is plausible, because a *rut* site has the length of approximately 70 to 90 nt, and the attenuation element at codons 3 to 10 of uORF1 is too short to act alone in Rho binding.

Deleting downstream parts of the IGR, as shown with Δ2 and Δ3 constructs, did not affect *duf1127₁* regulation at the level of RNA, but still had an effect on translation (Fig. 18), most likely due to uORF2 encoded within this region. However, since destroying uORF2 by a start to stop mutation did not change the regulation of the reporter construct (Figs. 20, 21), the role of uORF2 remains unclear. Interestingly, the proximal sequence of the Δ1 region (nt +121 to +128, immediately after uORF1) was found also to be important for translation of *duf1127₁*. However, mutations of the region from +121 to +128 did not alter *duf1127₁* regulation at the level of RNA, showing that these nucleotides are not a part of a *rut* site. Interestingly, deleting this region slightly de-repressed *duf1127₁* expression at the level of RNA, but gave a weaker signal on the protein level (Fig. 26). Concerning the observed de-repression at the level of RNA, it is possible that a *rut* site located after +128 was “shifted” upward upon deletion of the region

+121 to +128. This probably leads to its partial coverage by the terminating ribosome. This would explaining the de-repression without Tc of the Δ121-128 construct. This would also explain the weaker induction when comparing the mRNA level upon Tc exposure to Tc absence, which was shown for construct Δ121-128 (compare Fig. 26). However, it remains unresolved how this affects translation.

### 4.4.2 A model for Tc regulation of the *duf1127₁*

With all evidence combined, this study attempted to propose a mechanism of *duf1127₁* regulation. It is proposed that *duf1127₁* is being co-transcriptionally (transcriptional attenuation) and post-transcriptionally (mRNA stabilization upon Tc exposure) regulated. Most probably, translation is also regulated. The results discussed above of no intrinsic terminator present, scattered 3' ends, and putative *rut* sites suggest Rho as a factor involved in the transcription attenuation (compare chapter 4.3.3). The presented data allow to propose the following model for the attenuation regulation of *duf1127₁* (Fig. 34).

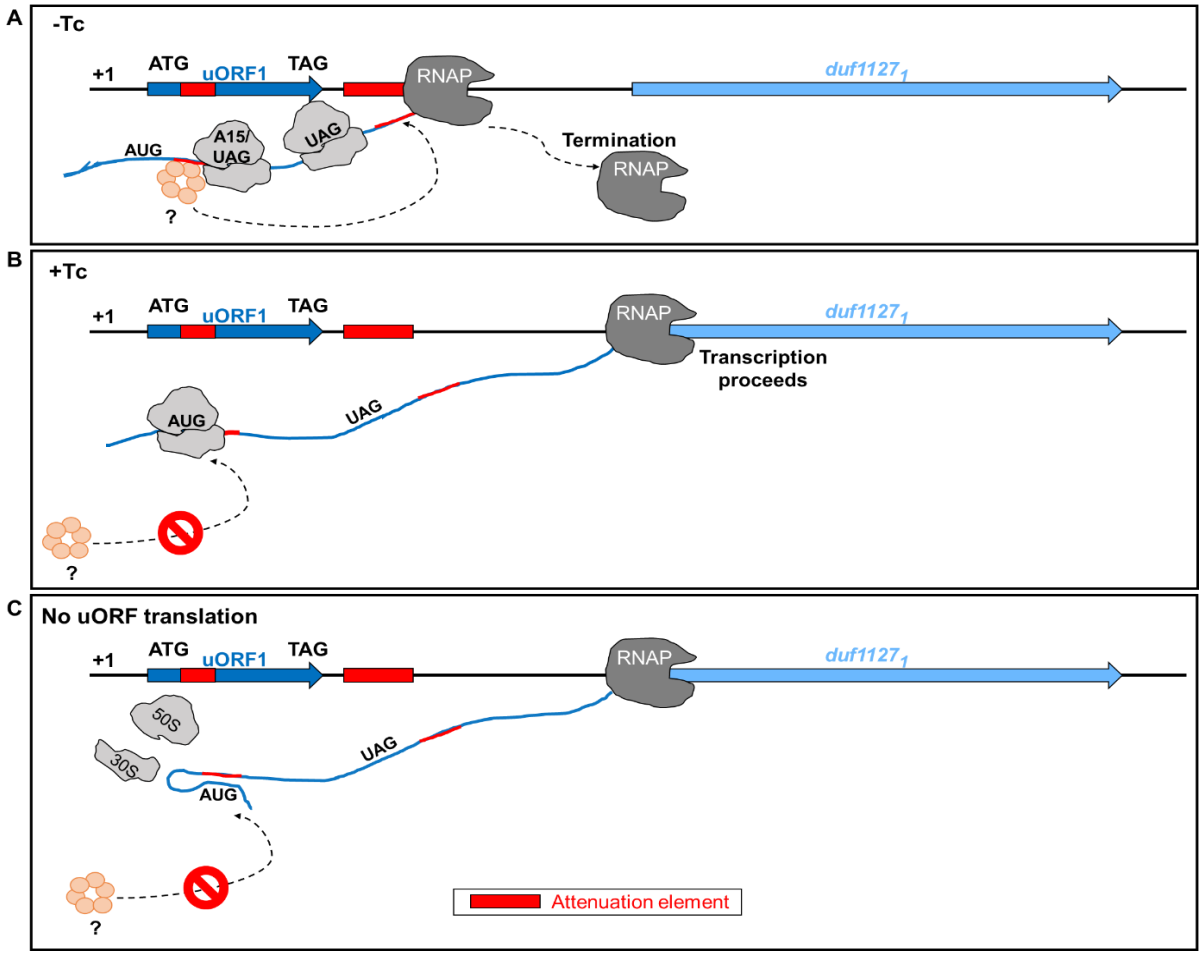


**Fig. 34:** Proposed model for the transcriptional attenuation regulating *duf1127₁* including the elements important for induction upon Tc exposure. The attenuation mechanism involves two elements (red) needed for premature transcriptional termination in the absence of Tc. The first element is located at codons 3 to 10 of uORF1 while the second element is located downstream. Element 1 is accessible under conditions of normal translation. **(A)** In the absence of Tc, attenuation is successful when the lead ribosome translates the first 14 codons and, before the second ribosome occupies the SD of uORF1, a factor can access the binding site. **(B)** Presence of Tc leads to stalling of the lead ribosome at the start codon, as translation initiation is impaired. This blocks accessibility of attenuation element 1, relieving attenuation. **(C)** No translation of uORF1 leads to attenuation relief, as a secondary structure blocks the accessibility of the first element.

In this model, we propose that for attenuation to be successful in the absence of Tc, the lead ribosome needs to translate the first 14 codons of uORF1. Termination at codon 15 still allows for attenuation.

Before the second ribosome occupies the RBS of uORF1, a factor, potentially Rho, can access the attenuation element located in uORF1 at codons 3 o 10. The factor then also binds the second element downstream of the uORF1 and leads to premature transcription termination around position +180, in the vicinity of the start codon of uORF2 (Fig. 34A). In the presence of Tc, the lead ribosome is impaired at translation initiation, remaining at the start codon of uORF1. This blocks accessibility of the first attenuation element, leading to attenuation relief and thus allows for transcription of *duf1127*$_1$ (Fig. 34B). Alternatively, under conditions of low ribosome concentration in the cell, when no lead ribosome does bind to the RBS of uORF1 in time, attenuation is also relieved. And similar to Tc exposure, *duf1127*$_1$ is expressed, as the nascent RNA is able to form a secondary structure that blocks the first attenuation element (Fig. 34C).

To validate the role of Rho in the transcriptional attenuation of *duf1127*$_1$, conditional Rho mutants may be constructed and investigated. Another means to study this mechanism is by depleting Rho using the recently developed ACIT system (Kretz et al., 2023). However, the proposed mechanism of attenuation is rather unusual, making it possible for other factors to be involved, either instead of, or in combination with, Rho.

With this model, all data available can be combined to explain how short-term Tc exposure leads to regulation of *duf1127*$_1$. With this investigation, therefore, a new mechanism of multi-level control of expression was identified that might also be transferable to other genes responding early to environmental cues like antibiotics. The regulatory circuits identified are suggesting a monitoring of translational efficacy which goes beyond the effect expected for a translational inhibition, and thus might reflect an unusual, more general mechanism in expression control in *Sinorhizobium*. This indication of a more general role might help to further uncover the function of DUF1127 proteins. Furthermore, this suggests *duf1127*$_1$ not being involved in antibiotic adaptation, but rather securing cellular homeostasis in the translation machinery.

# 5. References


Acosta-Jurado S, Alías-Villegas C, Almozara A, Espuny MR, Vinardell JM, Pérez-Montaño F (2020). Deciphering the symbiotic significance of quorum sensing systems of *Sinorhizobium fredii* HH103. Microorganisms 8, 68.

Adams PP, Baniulyte G, Esnault C, Chegireddy K, Singh N, Monge M, Dale RK, Storz G, Wade JT (2021). Regulatory roles of *Escherichia coli* 5' UTR and ORF-internal RNAs detected by 3' end mapping. Elife 10, e62438. Erratum in: Elife 10, e69260.

Adhya S, Gottesman M (1978). Control of transcription termination. Annu Rev Biochem 47, 967-996.

Aliashkevich A, Cava F (2022). LD-transpeptidases: the great unknown among the peptidoglycan cross-linkers. FEBS J 289, 4718-4730.

Alifano P, Rivellini F, Limauro D, Bruni CB, Carlomagno MS (1991). A consensus motif common to all Rho-dependent prokaryotic transcription terminators. Cell 64, 553-563.

Alvarez AF, Georgellis D (2023). Environmental adaptation and diversification of bacterial two-component systems. Curr Opin Microbiol 76, 102399.

Alwine JC, Kemp DJ, Stark GR (1977). Method for detection of specific RNAs in agarose gels by transfer to diazobenzyloxymethyl-paper and hybridization with DNA probes. Proc Natl Acad Sci USA 74, 5350-5354.

Ambulos NP Jr, Mongkolsuk S, Kaufman JD, Lovett PS (1985). Chloramphenicol-induced translation of *cat-86* mRNA requires two cis-acting regulatory regions. J Bacteriol 164, 696-703.

Balleza E, López-Bojorquez LN, Martínez-Antonio A, Resendis-Antonio O, Lozada-Chávez I, Balderas-Martínez YI, Encarnación S, Collado-Vides J (2009). Regulation by transcription factors in bacteria: beyond description. FEMS Microbiol Rev 33, 133-151.

Baniulyte G, Wade JT (2024). A bacterial regulatory uORF senses multiple classes of ribosome-targeting antibiotics. eLife 13, RP101217.

Barnawi H, Masri N, Hussain N, Al-Lawati B, Mayasari E, Gulbicka A, Jervis AJ, Huang MH, Cavet JS, Linton D (2020). RNA-based thermoregulation of a *Campylobacter jejuni* zinc resistance determinant. PLoS Pathog 16, e1009008.

Basineni SR, Madhugiri R, Kolmsee T, Hengge R, Klug G (2009). The influence of Hfq and ribonucleases on the stability of the small non-coding RNA OxyS and its target *rpoS* in *E. coli* is growth phase dependent. RNA Biol 6, 584-594.

Baumgardt K, Melior H, Madhugiri R, Thalmann S, Schikora A, McIntosh M, Becker A, Evguenieva-Hackenberg E (2017). RNase E and RNase J are needed for S-adenosylmethionine homeostasis in *Sinorhizobium meliloti*. Microbiology, 163, 570-583.

Beck S (2023). Die RNA-Antwort auf Tetracyclin-Exposition bei *Sinorhizobium meliloti*: Vergleich mit Temperaturstress. Bachelor-Arbeit, Justus-Liebig-Universität, Gießen.

Ben-Zvi T, Pushkarev A, Seri H, Elgrably-Weiss M, Papenfort K, Altuvia S (2019). mRNA dynamics and alternative conformations adopted under low and high arginine concentrations control polyamine biosynthesis in *Salmonella*. PLoS Genet 15, e1007646.

Bernier SP, Surette MG (2013). Concentration-dependent activity of antibiotics in natural environments. Front Microbiol 4, 20.

Bernstein JA, Khodursky AB, Lin PH, Lin-Chao S, Cohen SN (2002). Global analysis of mRNA decay and abundance in *Escherichia coli* at single-gene resolution using two-color fluorescent DNA microarrays. Proc Natl Acad Sci USA 99, 9697-9702.

Bie L, Zhang M, Wang J, Fang M, Li L, Xu H, Wang M (2023). Comparative analysis of transcriptomic response of *Escherichia coli* K-12 MG1655 to nine representative classes of antibiotics. Microbiol Spectr 11, e0031723.

Blaha GM, Wade JT (2022). Transcription-translation coupling in bacteria. Annu Rev Genet 56, 187-205.

Blair JMA, Webber MA, Baylay AJ, Ogbolu DO, Piddock LJV (2015). Molecular mechanisms of antibiotic resistance. Nat Rev Microbiol 13, 42-51.

Borgmann J, Schäkermann S, Bandow JE, Narberhaus F (2018). A small regulatory RNA controls cell wall biosynthesis and antibiotic resistance. mBio 9, e02100.

Brandenburg VB, Narberhaus F, Mosig A (2022). Inverse folding based pre-training for the reliable identification of intrinsic transcription terminators. PLoS Comput Biol 18, e1010240.

Brantl S (2007). Regulatory mechanisms employed by cis-encoded antisense RNAs. Curr Opin Microbiol 10, 102-109.

Brown NL, Stoyanov JV, Kidd SP, Hobman JL (2003). The MerR family of transcriptional regulators. FEMS Microbiol Rev 27, 145-163.

Brown NP, Leroy C, Sander C (1998). MView: A Web compatible database search or multiple alignment viewer. Bioinformatics 14, 380-381.

Browning DF, Busby SJW (2004). The regulation of bacterial transcription initiation. Nat Rev Microbiol 2, 57-65.

Buckel W, Zhang J, Friedrich P, Parthasarathy A, Li H, Djurdjevic I, Dobbek H, Martins BM (2012). Enzyme catalyzed radical dehydrations of hydroxy acids. Biochim Biophys Acta 1824, 1278-1290.

Budnick JA, Sheehan LM, Kang L, Michalak P, Caswell CC (2018). Characterization of three small proteins in *Brucella abortus* linked to fucose utilization. J Bacteriol 200, e00127.

Campbell EA, Korzheva N, Mustaev A, Murakami K, Nair S, Goldfarb A, Darst SA (2001). Structural mechanism for rifampicin inhibition of bacterial rna polymerase. Cell 104, 901-912.

Carpousis AJ (2007). The RNA degradosome of *Escherichia coli*: an mRNA-degrading machine assembled on RNase E. Annu Rev Microbiol 61, 71-87.

Carpousis AJ, Van Houwe G, Ehretsmann C, Krisch HM (1994). Copurification of *E. coli* RNAase E and PNPase: evidence for a specific association between two enzymes important in RNA processing and degradation. Cell 76, 889-900.

Casse F, Boucher C, Julliot JS, Michel M, DÉNari J (1979). Identification and Characterization of Large Plasmids in Rhizobium meliloti using Agarose Gel Electrophoresis. Gen Microbiol 113, 229–242.

Chalfie M, Tu Y, Euskirchen G, Ward WW, Prasher DC (1994). Green fluorescent protein as a marker for gene expression. Science 263, 802-805.

Chan WT, Verma CS, Lane DP, Gan SK (2013). A comparison and optimization of methods and factors affecting the transformation of *Escherichia coli*. Biosci Rep 33, e00086.

Chang JT, Green CB, Wolf RE Jr (1995). Inhibition of translation initiation on *Escherichia coli* gnd mRNA by formation of a long-range secondary structure involving the ribosome binding site and the internal complementary sequence. J Bacteriol 177, 6560-6567.

Chao Y, Papenfort K, Reinhardt R, Sharma CM, Vogel J (2012). An atlas of Hfq-bound transcripts reveals 3' UTRs as a genomic reservoir of regulatory small RNAs. EMBO J 31, 4005-4019.

Chen H, Shiroguchi K, Ge H, Xie XS (2015). Genome-wide study of mRNA degradation and transcript elongation in *Escherichia coli*. Mol Syst Biol 11, 781. Erratum in: Mol Syst Biol 11, 808.

Chen M, Fredrick K (2018). Measures of single- versus multiple-round translation argue against a mechanism to ensure coupling of transcription and translation. PNAS 115, 10774–10779.

Chen S, Lesnik EA, Hall TA, Sampath R, Griffey RH, Ecker DJ, Blyn LB (2002). A bioinformatics based approach to discover small RNA genes in the *Escherichia coli* genome. Biosyst 65, 157-177.

Chen X, Chowdhury MN, Jin H (2024). An intrinsically disordered RNA binding protein modulates mRNA translation and storage. J Mol Biol 2024, 168884 (epup ahead pf print).

Chevallet M, Luche S, Rabilloud T (2006). Silver staining of proteins in polyacrylamide gels. Nat Protoc 1, 1852-1858.

Cho KH (2017). The structure and function of the Gram-positive bacterial RNA Degradosome. Front Microbiol 8, 154.

Choe D, Kim K, Kang M, Lee SG, Cho S, Palsson B, Cho BK (2022). Synthetic 3'-UTR valves for optimal metabolic flux control in *Escherichia coli*. Nucleic Acids Res. 50, 4171-4186.

Choi E, Han Y, Park S, Koo H, Lee JS, Lee EJ (2021). A translation-aborting small open reading frame in the intergenic region promotes translation of a $Mg^{2+}$ transporter in *Salmonella typhimurium*. mBio 12, e03376-20.

Clardy J, Fischbach MA, Currie CR (2009). The natural history of antibiotics. Curr Biol 19, R437-R441.

Compton KK, Hildreth SB, Helm RF, Scharf BE (2020). An updated perspective on *Sinorhizobium meliloti* chemotaxis to alfalfa flavonoids. Front Microbiol 11, 581482.

Corbino KA, Barrick JE, Lim J, Welz R, Tucker BJ, Puskarz I, Mandal M, Rudnick ND, Breaker RR (2005). Evidence for a second class of S-adenosylmethionine riboswitches and other regulatory RNA motifs in alpha-proteobacteria. Genome Biol 6, R70.

Cycoń M, Mrozik A, Piotrowska-Seget Z (2019). Antibiotics in the soil environment – degradation and their impact on microbial activity and diversity. Front Microbiol 10, 338.

Dai X, Shen Z, Wang Y, Zhu M (2018). *Sinorhizobium meliloti*, a slow-growing bacterium, exhibits growth rate dependence of cell size under nutrient limitation. mSphere 3, e00567-18.

Dar D, Shamir M, Mellin JR, Koutero M, Stern-Ginossar N, Cossart P, Sorek R (2016). Term-seq reveals abundant ribo-regulation of antibiotics resistance in bacteria. Science 352, aad9822.

Dar D, Sorek R (2018). Extensive reshaping of bacterial operons by programmed mRNA decay. PLoS Genet 14, e1007354.

Darfeuille F, Unoson C, Vogel J, Wagner EG (2007). An antisense RNA inhibits translation by competing with standby ribosomes. Mol Cell 26, 381-392.

Davidson AL, Chen J (2004). ATP-binding cassette transporters in Bacteria. Annu Rev Biochem 73, 241-268.

de Almeida A, Catone MV, Rhodius VA, Gross CA, Pettinari MJ (2011). Unexpected stress-reducing effect of PhaP, a poly(3-hydroxybutyrate) granule-associated protein, in *Escherichia coli*. Appl Environ Microbiol 77, 6622-6629.

de Oliveira MA, Tairum CA, Netto LES, de Oliveira ALP, Aleixo-Silva RL, Cabrera VIM, Breyer CA, Dos Santos MC (2021). Relevance of peroxiredoxins in pathogenic microorganisms. Appl Microbiol Biotechnol 105, 5701-5717.

de Smit MH, van Duin J (2003). Translational standby sites: How ribosomes may deal with the rapid folding kinetics of mRNA. J Mol Biol 331, 737-743.

Deana A, Celesnik H, Belasco JG (2008). The bacterial enzyme RppH triggers messenger RNA degradation by 5' pyrophosphate removal. Nature 451, 355-358.

Demeester W, De Paepe B, De Mey M (2024). Fundamentals and exceptions of the LysR-type transcriptional regulators. ACS Synth Biol 13, 3069-3092.

Dersch P, Khan MA, Mühlen S, Görke B (2017). Roles of regulatory RNAs for antibiotic resistance in bacteria and their potential value as novel drug targets. Front Microbiol 8, 803.

Deutscher MP (2006). Degradation of RNA in bacteria: comparison of mRNA and stable RNA. Nucleic Acids Res 34, 659-666.

Dever TE, Ivanov IP, Sachs MS (2021). Conserved upstream open reading frame nascent peptides that control translation. Annu Rev Genet 54, 237-264.

Djordjevic MA (2004). *Sinorhizobium meliloti* metabolism in the root nodule: a proteomic perspective. Proteomics 4, 1859-1872.

Donald L, Pipite A, Subramani R, Owen J, Keyzers RA, Taufa T (2022). *Streptomyces*: still the biggest producer of new natural secondary metabolites, a current perspective. Microbiol Res (Pavia) 13, 418-465.

Dressaire C, Picard F, Redon E, Loubière P, Queinnec I, Girbal L, Cocaign-Bousquet M (2013). Role of mRNA stability during bacterial adaptation. PLoS One 8, e59059.

Dubbs JM, Mongkolsuk S (2007). Peroxiredoxins in bacterial antioxidant defense. Subcell Biochem 44, 143-193.

Duggar BM (1948). Aureomycin: a product of the continuing search for new antibiotics. Ann N Y Acad Sci 51, 177-181.

Eda S, Mitsui H, Minamisawa K (2011). Involvement of the SmeAB multidrug efflux pump in resistance to plant antimicrobials and contribution to nodulation competitiveness in *Sinorhizobium meliloti*. Appl Environ Microbiol 77, 2855-2862.

Egorov AA, Atkinson GC (2023). uORF4u: A tool for annotation of conserved upstream open reading frames. Bioinformatics 39, btad323.

El-Gebali S, Mistry J, Bateman A, Eddy SR, Luciani A, Potter SC, Qureshi M, Richardson LJ, Salazar GA, Smart A, Sonnhammer ELL, Hirsh L, Paladin L, Piovesan D, Tosatto SCE, Finn RD (2019). The Pfam protein families database in 2019. Nucleic Acids Res 8, D427-D432.

Evguenieva-Hackenberg E, Klug G (2011). New aspects of RNA processing in prokaryotes. Curr Opin Microbiol 14, 587-592.

Förstner KU, Reuscher CM, Haberzettl K, Weber L, Klug G (2018). RNase E cleavage shapes the transcriptome of *Rhodobacter sphaeroides* and strongly impacts phototrophic growth. Life Sci Alliance 1, e201800080.

Freese NH, Norris DC, Loraine AE (2016). Integrated Genome Browser: Visual analytics platform for genomics. J Bioinform 32, 2089-2095.

Freiberg JA, Reyes Ruiz VM, Gimza BD, Murdoch CC, Green ER, Curry JM, Cassat JE, Skaar EP (2024). Restriction of arginine induces antibiotic tolerance in *Staphylococcus aureus*. Nat Commun 15, 6734.

Gao L, Ma X (2022). Transcriptome analysis of *Acinetobacter baumannii* in rapid response to subinhibitory concentration of minocycline. Int J Environ Res Public Health 19, 16095.

Gordon GC, Cameron JC, Gupta STP, Engstrom MD, Reed JL, Pfleger BF (2020). Genome-wide analysis of RNA decay in the cyanobacterium *Synechococcus sp.* Strain PCC 7002. mSystems 5, e00224-20.

Gottesman S (2003). Proteolysis in bacterial regulatory circuits. Annu Rev Cell Dev Biol 19, 565.

Gottesman S (2005). Micros for microbes: non-coding regulatory RNAs in bacteria. Trends Genet 21, 399-404.

Gottesman S, Storz G (2011). Bacterial small RNA regulators: Versatile roles and rapidly evolving variations. Cold Spring Harb Perspect Biol 3, a003798.

Goudreau PN, Stock AM (1998). Signal transduction in bacteria: Molecular mechanisms of stimulus-response coupling. Curr Opin Microbiol 1, 160-169.

Grützner J, Billenkamp F, Spanka DT, Rick T, Monzon V, Förstner KU, Klug G (2021). The small DUF1127 protein CcaF1 from *Rhodobacter sphaeroides* is an RNA-binding protein involved in sRNA maturation and RNA turnover. Nucleic Acids Res 6, 3003-3019.

Gutiérrez-Preciado A, Henkin TM, Grundy FJ, Yanofsky C, Merino E (2009). Biochemical features and functional implications of the RNA-based T-box regulatory mechanism. Microbiol Mol Biol Rev 73, 36-61.

Hadjeras L, Heiniger B, Maaß S, Scheuer R, Gelhausen R, Azarderakhsh S, Barth-Weber S, Backofen R, Becher D, Ahrens CH, Sharma CM, Evguenieva-Hackenberg, E (2023). Small proteome of the nitrogen-fixing plant symbiont *Sinorhizobium meliloti*. Microlife 4, uqad012.

Hafeezunnisa M, Sen R (2020). The Rho-dependent transcription termination is involved in broad-spectrum antibiotic susceptibility in *Escherichia coli*. Front Microbiol 11, 605305.

Harrison PM, Kumar A, Lang N, Snyder M, Gerstein M (2002). A question of size: The eukaryotic proteome and the problems in defining it. Nucleic Acids Res 30, 1083-1090.

Hecht A, Glasgow J, Jaschke PR, Bawazer LA, Munson MS, Cochran JR, Endy D, Salit M (2017). Measurements of translation initiation from all 64 codons in *E. coli*. Nucleic Acids Res 45, 3615-3626.

Heo S, Kim T, Na HE, Lee G, Lee JH, Jeong DW (2022). Transcriptomic analysis of *Staphylococcus equorum* KM1031 from the high-salt fermented seafood jeotgal under chloramphenicol, erythromycin and lincomycin stresses. Sci Rep 12, 15541.

Hernández VM, Arteaga A, Dunn MF (2021). Diversity, properties and functions of bacterial arginases. FEMS Microbiol Rev 45, 1-26.

Hover BM, Kim SH, Katz M, Charlop-Powers Z, Owen JG, Ternei MA, Maniko J, Estrela AB, Molina H, Park S, Perlin DS, Brady SF (2018). Culture-independent discovery of the malacidins as calcium-dependent antibiotics with activity against multidrug-resistant Gram-positive pathogens. Nat Microbiol 3, 415-422.

Howden BP, Beaume M, Harrison PF, Hernandez D, Schrenzel J, Seemann T, Francois P, Stinear TP (2013). Analysis of the small RNA transcriptional response in multidrug-resistant *Staphylococcus aureus* after antimicrobial exposure. Antimicrob Agents Chemother 57, 3864-3874.

Hoyos M, Huber M, Förstner KU, Papenfort K (2020). Gene autoregulation by 3' UTR-derived bacterial small RNAs. Elife 9, e58836.

Ito K, Chiba S (2013). Arrest peptides: *cis*-acting modulators of translation. Annu Rev Biochem 82, 171-202.

Jacob F, Monod J (1961). On the regulation of gene activity. Cold Spring Harb Symp Quant Biol 26, 193-211.

Jahn CE, Charkowski AO, Willis, DK (2008). Evaluation of isolation methods and RNA integrity for bacterial RNA quantitation. J. Microbiol Methods 75, 318-324.

Jones C, Allsopp L, Horlick J, Kulasekara H, Filloux A (2013). Subinhibitory concentration of kanamycin induces the *Pseudomonas aeruginosa* type VI secretion system. PLoS One 8, e81132.

Jørgensen MG, Pettersen JS, Kallipolitis BH (2020). sRNA-mediated control in bacteria: An increasing diversity of regulatory mechanisms. Biochim Biophys Acta Gene Regul Mech 1863, 194504.

Kamruzzaman M, Wu AY, Iredell JR (2021). Biological functions of type II toxin-antitoxin systems in bacteria. Microorganisms 9, 1276.

Katoh K, Misawa K, Kuma K, Miyata T (2002). MAFFT: a novel method for rapid multiple sequence alignment based on fast Fourier transform. Nucleic Acids Res 30, 3059-3066.

Katoh K, Rozewicki J, Yamada KD (2019). MAFFT online service: multiple sequence alignment, interactive sequence choice and visualization. Brief Bioinform 20, 1160-1166.

Khan MA, Göpel Y, Milewski S, Görke B (2016). Two small RNAs conserved in Enterobacteriaceae provide intrinsic resistance to antibiotics targeting the cell wall biosynthesis enzyme glucosamine-6-phosphate synthase. Front Microbiol 7, 908.

Klimova M, Senyushkina T, Samatova E, Peng BZ, Pearson M, Peske F, Rodnina MV (2019). EF-G-induced ribosome sliding along the noncoding mRNA. Sci Adv 5, eaaw9049.

Kohn H, Widger W (2005). The molecular basis for the mode of action of bicyclomycin. Curr Drug Targets Infect Disord 5, 273-295.

Kormanec J (2022). Bacterial regulatory proteins. Int J Mol Sci 23, 6854.

Kraus A, Weskamp M, Zierles J, Balzer M, Busch R, Eisfeld J, Lambertz J, Nowaczyk MM, Narberhaus F (2020). Arginine-rich small proteins with a domain of unknown function, DUF1127, play a role in phosphate and carbon metabolism of *Agrobacterium tumefaciens*. J Bacteriol 22, e00309-20.

Kretz J, Israel V, McIntosh M (2023). Design–build–test of synthetic promoters for inducible gene regulation in Alphaproteobacteria. ACS Synth Biol 12, 2663-2675.

Kwak JH, Choi EC, Weisblum B (1991). Transcriptional attenuation control of *ermK*, a macrolide-lincosamide-streptogramin B resistance determinant from *Bacillus licheniformis*. J Bacteriol 173, 4725-4735.

Laemmli UK (1970). Cleavage of structural proteins during the assembly of the head of bacteriophage T4. Nature 227, 680-685.

Lawrence JG (2002). Shared strategies in gene organization among prokaryotes and eukaryotes. Cell 110, 407-413.

Lee DJ, Minchin SD, Busby SJW (2012). Activating transcription in bacteria. Annu Rev Microbiol 66, 125-152.

Lee JH, Lee EJ, Roe JH (2022). uORF-mediated riboregulation controls transcription of *whiB7/wblC* antibiotic resistance gene. Mol Microbiol 117, 179-192.

Lee CL, Ng HF, Ngeow YF, Thaw Z (2021). A stop-gain mutation in sigma factor SigH (MAB_3543c) may be associated with tigecycline resistance in *Mycobacteroides abscessus*. J Med Microbiol 70, 10.1099/jmm.0.001378.

Lehman AP, Long SR (2018). OxyR-dependent transcription response of *Sinorhizobium meliloti* to oxidative stress. J Bacteriol 200, e00622-17.

Lehman KM, Smith HC, Grabowicz M (2022). A biological signature for the inhibition of outer membrane lipoprotein biogenesis. mBio 13, e0075722.

Li Y, Altman S (2004). Polarity effects in the lactose operon of *Escherichia coli*. J Mol Biol 339, 31-39.

Lin J, Zhou D, Steitz TA, Polikanov YS, Gagnon MG (2018). Ribosome-targeting antibiotics: Modes of action, mechanisms of resistance, and implications for drug design. Annu Rev Biochem 87, 451-478.

Liou GG, Chang HY, Lin CS, Lin-Chao S (2002). DEAD box RhlB RNA helicase physically associates with exoribonuclease PNPase to degrade double-stranded RNA independent of the degradosome-assembling region of RNase E. J Biol Chem 277, 41157-41162.

Lottspeich F, Zorbas H (1998). Bioanalytik. Spektrum Akademischer Verlag: Heidelberg.

Lovett PS, Rogers EJ (1996). Ribosome regulation by the nascent peptide. Microbiol Rev 60, 366-385.

Lv P, Wan J, Zhang C, Hina A, Al Amin GM, Begum N, Zhao T (2023). Unraveling the diverse roles of neglected genes containing domains of unknown function (DUFs): Progress and perspective. Int J Mol Sci 24, 4187.

Madan Babu M, Teichmann SA (2003). Evolution of transcription factors and the gene regulatory network in *Escherichia coli*. Nucleic Acids Res 31, 1234-1244.

Madeira F, Madhusoodanan N, Lee J, Eusebi A, Niewielska A, Tivey ARN, Lopez R, Butcher S (2024). The EMBL-EBI Job Dispatcher sequence analysis tools framework in 2024. Nucleic Acids Res 52, 521-525.

Madhugiri R, Evguenieva-Hackenberg E (2009). RNase J is involved in the 5'-end maturation of 16S rRNA and 23S rRNA in *Sinorhizobium meliloti*. FEBS Lett 583, 2339-2342.

Madigan MT, Sattley WM, Aiyer J, Stahl DA, Buckley DH (2021). Brock Biology of Microorganisms. Pearson, London

Malmgren C, Engdahl HM, Romby P, Wagner EG (1996). An antisense/target RNA duplex or a strong intramolecular RNA structure 5' of a translation initiation signal blocks ribosome binding: the case of plasmid R1. RNA 2, 1022-1032.

Mandell ZF, Zemba D, Babitzke P (2022). Factor-stimulated intrinsic termination: getting by with a little help from some friends. Transcription 13, 96-108.

Margolin P (1967). Genetic polarity in bacteria. Am Nat 101, 301-312.

Martínez LC, Vadyvaloo V (2014). Mechanisms of post-transcriptional gene regulation in bacterial biofilms. Front Cell Infect Microbiol 4, 38.

Mateus A, Shah M, Hevler J, Kurzawa N, Bobonis J, Typas A, Savitski MM (2021). Transcriptional and post-transcriptional polar effects in bacterial gene deletion libraries. mSystems 6, 10.1128/msystems.00813-21.

McDowall KJ, Lin-Chao S, Cohen SN (1994). A+U content rather than a particular nucleotide order determines the specificity of RNase E cleavage. J Biol Chem 269, 10790-10796.

McIntosh M, Köchling T, Latz A, Kretz J, Heinen S, Konzer A, Klug G (2021). A major checkpoint for protein expression in *Rhodobacter sphaeroides* during heat stress response occurs at the level of translation. Environ Microbiol 23, 6483-6502.

Meade HM, Signer ER (1977). Genetic mapping of *Rhizobium meliloti*. Proc Natl Acad Sci USA 74, 2076-2078.

Melior H, Maaß S, Li S, Förstner KU, Azarderakhsh S, Varadarajan AR, Stötzel M, Elhossary M, Barth-Weber S, Ahrens CH, Becher D, Evguenieva-Hackenberg E (2020). The leader peptide peTrpL forms antibiotic-containing ribonucleoprotein complexes for posttranscriptional regulation of multiresistance genes. mBio 11, e01027-20.

Mistry J, Chuguransky S, Williams L, Qureshi M, Salazar GA, Sonnhammer ELL, Tosatto SCE, Paladin L, Raj S, Richardson LJ, Finn RD, Bateman A (2021). Pfam: The protein families database in 2021. Nucleic Acids Res 49, D412-D419.

Mitra P, Ghosh G, Hafeezunnisa M, Sen R (2017). Rho protein: Roles and mechanisms. Annu Rev Microbiol 71, 687-709.

Mitsui H, Minamisawa K (2017). Expression of two RpoH sigma factors in *Sinorhizobium meliloti* upon heat shock. Microbes Environ 32, 394-397.

Miyamura S, Ogasawara N, Otsuka H, Niwayama S, Tanaka H, Take T, Uchiyama T, Ochiai H, Abe K (1972). Antibiotic no. 5879, a new water-soluble antibiotic against gram-negative bacteria. J. Antibiot 25, 610-612.

Miyoshi T, Miyairi N, Aoki H, Kohsaka M, Sakai H, Imanaka HJ (1972). Bicyclomycin, a new antibiotic. I. Taxonomy, isolation and characterization. Antibiot 25, 569-575.

Mizuno T, Chou MY, Inouye M (1984). A unique mechanism regulating gene expression: translational inhibition by a complementary RNA transcript (micRNA). Proc Natl Acad Sci USA 81, 1966-1970.

Mohanty BK, Kushner SR (2016). Regulation of mRNA decay in bacteria. Annu Rev Microbiol 70, 25-44.

Mohanty BK, Kushner SR (2023). Regulation of mRNA decay in *E. coli*. Crit Rev Biochem Mol Biol 57, 48-72.

Moon K, Gottesman S (2009). A PhoQ/P-regulated small RNA regulates sensitivity of *Escherichia coli* to antimicrobial peptides. Mol Microbiol 74, 1314-1330.

Morfeldt E, Taylor D, von Gabain A, Arvidson S (1995). Activation of alpha-toxin translation in *Staphylococcus aureus* by the trans-encoded antisense RNA, RNAIII. EMBO J 14, 4569-4577.

Murayama Y, Ehara H, Aoki M, Goto M, Yokoyama T, Sekine S-I (2023). Structural basis of the transcription termination factor Rho engagement with transcribing RNA polymerase from *Thermus thermophilus*. Sci Adv 9, eade7093.

Narberhaus F, Waldminghaus T, Chowdhury S (2006). RNA thermometers. FEMS Microbiol Rev 30, 3-16.

Naville M, Gautheret D (2009). Transcription attenuation in bacteria: theme and variations. Brief Funct Genomic Proteomic 8, 482-492.

Newton WA, Beckwith JR, Zipser D, Brenner S (1965). Nonsense mutants and polarity in the lac operon of *Escherichia coli*. J Mol Biol 14, 290-296.

Ng WL, Kazmierczak KM, Robertson GT, Gilmour R, Winkler ME (2003). Transcriptional regulation and signature patterns revealed by microarray analyses of *Streptococcus pneumoniae* R6 challenged with sublethal concentrations of translation inhibitors. J Bacteriol 185, 359-370.

Nitzan M, Rehani R, Margalit H (2017). Integration of bacterial small RNAs in regulatory networks. Annu Rev Biophys 46, 131-148.

Obruca S, Sedlacek P, Krzyzanek V, Mravec F, Hrubanova K, Samek O, Kucera D, Benesova P, Marova I (2016). Accumulation of poly(3-hydroxybutyrate) helps bacterial cells to survive freezing. PLoS One 11, e0157778.

Opdyke JA, Kang JG, Storz G (2004). GadY, a small-RNA regulator of acid response genes in *Escherichia coli*. J. Bacteriol 186, 6698-6705.

Orr MW, Mao Y, Storz G, Qian SB (2020) Alternative ORFs and small ORFs: shedding light on the dark proteome. Nucleic Acids Res 48, 1029-1042.

Osada Y, Saito R, Tomita M (1999). Analysis of base-pairing potentials between 16S rRNA and 5' UTR for translation initiation in various prokaryotes. Bioinformatics 15, 578-581.

Paget MS, Helmann JD (2003). The sigma70 family of sigma factors. Genome Biol 4, 203.

Paget MS (2015). Bacterial sigma factors and anti-sigma factors: Structure, function and distribution. Biomolecules 5, 1245-1265.

Palmer SR, Burne RA (2015). Post-transcriptional regulation by distal Shine-Dalgarno sequences in the *grpE-dnaK* intergenic region of *Streptococcus mutans*. Mol Microbiol 98, 302-317.

Panter F, Bader CD, Müller R (2021). Synergizing the potential of bacterial genomics and metabolomics to find novel antibiotics. Chem Sci 12, 5994-6010.

Papenfort K, Melamed S (2023). Small RNAs, large networks: Posttranscriptional regulons in gram-negative bacteria. Annu Rev Microbiol 77, 23-43.

Park H, Yakhnin H, Connolly M, Romeo T, Babitzke P (2015). CsrA Participates in a PNPase autoregulatory mechanism by selectively repressing translation of *pnp* transcripts that have been previously processed by RNase III and PNPase. J Bacteriol 197, 3751-3759.

Paulsen IT (2003). Multidrug efflux pumps and resistance: regulation and evolution. Curr Opin Microbiol 6, 446-451.

Pfaffl MW (2001). A new mathematical model for relative quantification in real-time RT-PCR. Nucleic Acids Res 29, e45.

Pienkoß S, Javadi S, Chaoprasid P, Holler M, Roßmanith J, Dersch P, Narberhaus F (2022). RNA Thermometer-coordinated assembly of the yersinia injectisome. J Mol Biol 434, 167667.

Pienkoß S, Javadi S, Chaoprasid P, Nolte T, Twittenhoff C, Dersch P, Narberhaus F (2021). The gatekeeper of *Yersinia* type III secretion is under RNA thermometer control. PLoS Pathog 17, e1009650.

Ponath F, Hör J, Vogel J (2022). An overview of gene regulation in bacteria by small RNAs derived from mRNA 3' ends. FEMS Microbiol Rev 46, fuac017.

Py B, Causton H, Mudd EA, Higgins CF (1994). A protein complex mediating mRNA degradation in *Escherichia coli*. Mol Microbiol 14, 717-729.

Rahman T, Yarnall B, Doyle DA (2017). Efflux drug transporters at the forefront of antimicrobial resistance. Eur Biophys J 46, 647-653.

Rauhut R, Klug G (1999). mRNA degradation in bacteria. FEMS Microbiol Rev 23, 353-370.

Ray-Soni A, Bellecourt MJ, Landick R (2016). Mechanisms of bacterial transcription termination: All good things must end. Ann Rev Biochem 85, 319-347.

Reen FJ, Barret M, Fargier E, O'Muinneacháin M, O'Gara F (2013). Molecular evolution of LysR-type transcriptional regulation in *Pseudomonas aeruginosa*. Mol Phylogenet Evol 66, 1041– -1049.

Regmi R, Penton CR, Anderson J, Gupta VVSR (2022). Do small RNAs unlock the below ground microbiome-plant interaction mystery? Front Mol Biosci 9, 1017392.

Richards J, Sundermeier T, Svetlanov A, Karzai AW (2008). Quality control of bacterial mRNA decoding and decay. Biochim Biophys Acta 1779, 574-582.

Richardson LV, Richardson JP (1996). Rho-dependent termination of transcription is governed primarily by the upstream Rho utilization (*rut*) sequences of a terminator. J Biol Chem 271, 21597-21603.

Robledo M, García-Tomsig NI, Jiménez-Zurdo JI (2020). Riboregulation in nitrogen-fixing endosymbiotic bacteria. Microorganisms 8, 384.

Rochat T, Bouloc P, Repoila F (2013). Gene expression control by selective RNA processing and stabilization in bacteria. FEMS Microbiol Lett 344, 104-113.

Rodnina MV (2018). Translation in prokaryotes. Cold Spring Harb Perspect Biol 10, a032664.

Rodríguez-Cazorla E, Andújar A, Ripoll JJ, Bailey LJ, Martínez-Laborda A, Yanofsky MF, Vera A (2015). 3' Rapid Amplification of cDNA Ends (3' RACE) using *Arabidopsis* samples. Bio Protoc 5, e1604.

Romilly C, Deindl S, Wagner EGH (2019). The ribosomal protein S1-dependent standby site in *tisB* mRNA consists of a single-stranded region and a 5′ structure element. Proc Natl Acad Sci USA 116, 15901-15906.

Roy G, Antoine R, Schwartz A, Slupek S, Rivera-Millot A, Boudvillain M, Jacob-Dubuisson F (2022). Posttranscriptional regulation by copper with a new upstream open reading frame. mBio 13, e0091222.

Said N, Finazzo M, Hilal T, Wang B, Selinger TL, Gjorgjevikj D, Artsimovitch I, Wahl MC (2024). Sm-like protein Rof inhibits transcription termination factor ρ by binding site obstruction and conformational insulation. Nat Commun 15, 3186.

Sallet E, Roux B, Sauviac L, Jardinaud M-F, Carrère S, Faraut T, de Carvalho-Niebel F, Gouzy J, Gamas P, Capela D, Bruand C, Schiex T (2013). Next-generation annotation of prokaryotic genomes with EuGene-P: Application to *Sinorhizobium meliloti* 2011. DNA Res 20, 339-354.

Sambrook J, Fritsch E, Maniatis T (1989). Molecular Cloning: A Laboratory Manual (2nd ed.). Cold Spring Harbor, NY: Cold Spring Harbor Laboratory Press.

Saramago M, Robledo M, Matos RG, Jiménez-Zurdo JI, Arraiano CM (2018). *Sinorhizobium meliloti* RNase III: Catalytic features and impact on symbiosis. Front Genet 9, 350.

Sass A, Marchbank A, Tullis E, Lipuma JJ, Mahenthiralingam E (2011). Spontaneous and evolutionary changes in the antibiotic resistance of *Burkholderia cenocepacia* observed by global gene expression analysis. BMC Genomics 12, 373.

Sauviac L, Philippe H, Phok K, Bruand C (2007). An extracytoplasmic function sigma factor acts as a general stress response regulator in *Sinorhizobium meliloti*. J Bacteriol 189, 4204-4216.

Schägger H (2006). Tricine-SDS-PAGE. Nat Protoc 1, 16-22.

Schank L (2023). Die RNA-Antwort auf Tetracyclin-Exposition bei *Sinorhizobium meliloti*: Vergleich mit oxidativem Stress. Bachelor-Arbeit, Justus-Liebig-Universität, Gießen.

Scheuer R, Dietz T, Kretz J, Hadjeras L, McIntosh M, Evguenieva-Hackenberg E (2022). Incoherent dual regulation by a SAM-II riboswitch controlling translation at a distance. RNA Biol 19, 980-995.

Scheuer R, Kothe J, Wähling J, Evguenieva-Hackenberg E. (2024). Analysis of sRNAs and their mRNA targets in *Sinorhizobium meliloti*: Focus on half-life determination. Methods Mol Biol 2741, 239-254.

Scheuer R (2023). Multiple Funktionen des SAM-II Riboswitches in *Sinorhizobium meliloti*. Dissertation, Justus-Liebig-Universität, Gießen.

Schilder A, Görke B (2023). Role of the 5' end phosphorylation state for small RNA stability and target RNA regulation in bacteria. Nucleic Acids Res 51, 5125-5143.

Schlüter JP, Reinkensmeier J, Daschkey S, Evguenieva-Hackenberg E, Janssen S, Jänicke S, Becker JD, Giegerich R, Becker A (2010). A genome-wide survey of sRNAs in the symbiotic nitrogen-fixing alpha-proteobacterium *Sinorhizobium meliloti*. BMC Genomics 11, 245.

Schneider E, Blundell M, Kennell D (1978). Translation and mRNA decay. Molec Gen Genet 160, 121-129.

Sedlyarova N, Shamovsky I, Bharati BK, Epshtein V, Chen J, Gottesman S, Schroeder R, Nudler E (2016). sRNA-mediated control of transcription termination in *E. coli*. Cell 167, 111-121.

Sengupta S, Chattopadhyay MK, Grossart HP (2013). The multifaceted roles of antibiotics and antibiotic resistance in nature. Front Microbiol 4, 47.

Senyushkina T, Samatova E, Klimova M, Rodnina MV (2024). Kinetics of programmed and spontaneous ribosome sliding along the mRNA. Nucleic Acids Res 52, 6507-6517.

Sevostyanova A, Groisman EA (2015). An RNA motif advances transcription by preventing Rho-dependent termination. Proc Natl Acad Sci USA 112, E6835-6843.

Sharma CM, Darfeuille F, Plantinga TH, Vogel J (2007). A small RNA regulates multiple ABC transporter mRNAs by targeting C/A-rich elements inside and upstream of ribosome-binding sites. Genes Dev 21, 2804-2817.

Sheehan LM, Budnick JA, Blanchard C, Dunman PM, Caswell CC (2015). A LysR-family transcriptional regulator required for virulence in *Brucella abortus* is highly conserved among the α-proteobacteria. Mol Microbiol 98, 318-328.

Shine J, Dalgarno L (1974). The 3'-terminal sequence of *Escherichia coli* 16S ribosomal RNA: Complementarity to nonsense triplets and ribosome binding sites. Proc Nat Acad Sci USA 71, 1342-1346.

Smirnov A, Wang C, Drewry LL, Vogel J (2017). Molecular mechanism of mRNA repression in trans by a ProQ-dependent small RNA. EMBO J 36, 1029-1045.

Soto MJ, Pérez J, Muñoz-Dorado J, Contreras-Moreno FJ, Moraleda-Muñoz A (2023). Transcriptomic response of *Sinorhizobium meliloti* to the predatory attack of *Myxococcus xanthus*. Front Microbiol 14, 1213659.

Southern EM (1975). Detection of specific sequences among DNA fragments separated by gel electrophoresis. Journal Mol Biol 98, 503–517.

Storz G, Wolf YI, Ramamurthi KS (2014). Small proteins can no longer be ignored. Annu Rev Biochem 83, 753-777.

Stothard P (2000). The Sequence Manipulation Suite: JavaScript programs for analyzing and formatting protein and DNA sequences. Biotechniques 28, 1102-1104.

Straight PD, Kolter R (2009). Interspecies chemical communication in bacterial development. Annu Rev Microbiol 63, 99-118.

Studer SM, Joseph S (2006). Unfolding of mRNA secondary structure by the bacterial translation initiation complex. Mol Cell 22, 105-115.

Tian S, Wang X, Li P, Wang H, Ji H, Xie J, Qiu Q, Shen D, Dong H (2016). Plant aquaporin AtPIP1;4 links apoplastic $H_2O_2$ induction to disease immunity pathways. Plant Physiol 171, 1635-1650.

Tibor A, Decelle B, Letesson JJ (1999). Outer membrane proteins Omp10, Omp16, and Omp19 of *Brucella* spp. are lipoproteins. Infect Immun 67, 4960-4962.

Tollerson R 2nd, Ibba M (2020). Translational regulation of environmental adaptation in bacteria. J Biol Chem 295, 10434-10445.

Torres-Quesada O, Millán V, Nisa-Martínez R, Bardou F, Crespi M, Toro N, Jiménez-Zurdo JI (2013). Independent activity of the homologous small regulatory RNAs AbcR1 and AbcR2 in the legume symbiont *Sinorhizobium meliloti*. PLoS One 8, e68147.

Tramonti A, De Canio M, De Biase D (2008). GadX/GadW-dependent regulation of the *Escherichia coli* acid fitness island: transcriptional control at the *gadY-gadW* divergent promoters and identification of four novel 42 bp GadX/GadW-specific binding sites. Mol Microbiol 70, 965-982.

Urbanowski ML, Stauffer LT, Stauffer GV (2000). The *gcvB* gene encodes a small untranslated RNA involved in expression of the dipeptide and oligopeptide transport systems in *Escherichia coli*. Mol Microbiol 37, 856-868.

Valabhoju V, Agrawal S, Sen R (2016). Molecular basis of NusG-mediated regulation of Rho-dependent transcription termination in bacteria. J Biol Chem 291, 22386-22403.

Valverde C, Livny J, Schlüter JP, Reinkensmeier J, Becker A, Parisi G (2008). Prediction of *Sinorhizobium meliloti* sRNA genes and experimental detection in strain 2011. BMC Genomics 9, 416.

van Dillewijn P, Sanjuán J, Olivares J, Soto MJ (200). The *tep1* gene of *Sinorhizobium meliloti* coding for a putative transmembrane efflux protein and N-acetyl glucosamine affect *nod* gene expression and nodulation of alfalfa plants. BMC Microbiol 9, 17.

Vargas-Blanco DA, Shell SS (2020). Regulation of mRNA stability during bacterial stress responses. Front Microbiol 11, 2111.

Vasilchenko AS, Rogozhin EA (2019). Sub-inhibitory effects of antimicrobial peptides. Front Microbiol 10, 1160.

Vazquez-Laslop N, Sharma CM, Mankin A, Buskirk AR (2022). Identifying small open reading frames in prokaryotes with ribosome profiling. J Bacteriol 204, e0029421.

Vazquez-Laslop N, Thum C, Mankin AS (2008). Molecular mechanism of drug-dependent ribosome stalling. Mol Cell 30, 190-202.

Venturini E, Svensson SL, Maaß S, Gelhausen R, Eggenhofer F, Li L, Cain AK, Parkhill J, Becher D, Backofen R, Barquist L, Sharma CM, Westermann AJ, Vogel J (2020). A global data-driven census of *Salmonella* small proteins and their potential functions in bacterial virulence. Microlife 1, uqaa002.

Vind AC, Zhong FL, Bekker-Jensen S (2024). Death by ribosome. Trends Cell Biol S0962-8924(24)00230-7.

Vitreschak AG, Lyubetskaya EV, Shirshin MA, Gelfand MS, Lyubetsky VA (2004). Attenuation regulation of amino acid biosynthetic operons in proteobacteria: comparative genomics analysis. FEMS Microbiol Lett 234, 357-70.

Vogel J, Wagner EG (2007). Target identification of small noncoding RNAs in bacteria. Curr Opin Microbiol 10, 262-270.

Wagner EG, Unoson C (2012). The toxin-antitoxin system *tisB-istR1*: Expression, regulation, and biological role in persister phenotypes. RNA Biol 9, 1513-1519.

Wagner EGH, Simos RW (1994). Antisense RNA control in bacteria, phages, and plasmids. Annu Rev Microbiol 48, 713-742.

Walsh F, Duffy B (2013). The culturable soil antibiotic resistome: a community of multi-drug resistant bacteria. PLoS One 8, e65567.

Wang C, Sheng X, Equi RC, Trainer MA, Charles TC, Sobral BW (2007). Influence of the poly-3-hydroxybutyrate (PHB) granule-associated proteins (PhaP1 and PhaP2) on PHB accumulation and symbiotic nitrogen fixation in *Sinorhizobium meliloti* Rm1021. J Bacteriol 189, 9050-9056.

Wang S, Blahut M, Wu Y, Philipkosky KE, Outten FW (2014). Communication between binding sites is required for YqjI regulation of target promoters within the *yqjH-yqjI* intergenic region. J Bacteriol 196, 3199-3207.

Wang W, Zhu X, Luo H, Wang Z, Hong A, Zeng J, Li L, Wang D, Deng X, Zhao X (2023). Bicyclomycin activity against multidrug-resistant gram-negative pathogens. Microbiol Spectr 11, e0379022.

Wassarman KM, Zhang A, Storz G (1999). Small RNAs in *Escherichia coli*. Trends Microbiol 7, 37-45.

Waterhouse AM, Procter JB, Martin DMA, Clamp M, Barton GJ (2009). Jalview Version 2 – a multiple sequence alignment editor and analysis workbench. Bioinformatics 25, 1189-1191.

Waters LS, Storz G (2009). Regulatory RNAs in bacteria. Cell 136, 615-628.

Wecke T, Mascher T (2011). Antibiotic research in the age of omics: from expression profiles to interspecies communication. J Antimicrob Chemother 66, 2689-2704.

Wells DH, Long SR (2002). The *Sinorhizobium meliloti* stringent response affects multiple aspects of symbiosis. Mol Microbiol 43, 1115-1127.

Yakhnin H, Babitzke P (2022). Toeprint assays for detecting RNA structure and protein-RNA interactions. Methods Mol Bio 2516, 305-316.

Yang QE, Walsh TR (2017). Toxin-antitoxin systems and their role in disseminating and maintaining antimicrobial resistance. FEMS Microbiol Rev 41, 343-353.

Yanofsky C (1981). Attenuation in the control of expression of bacterial operons. Nature 289, 751-758.

Yanofsky C, Platt T, Crawford IP, Nichols BP, Christie GE, Horowitz H, VanCleemput M, Wu AM (1981). The complete nucleotide sequence of the tryptophan operon of *Escherichia coli*. Nucleic Acids Res 9, 6647-6668.

You L, Omollo EO, Yu C, Mooney RA, Shi J, Shen L, Wu X, Wen A, He D, Zeng Y, Feng Y, Landick R, Zhang Y (2023). Structural basis for intrinsic transcription termination. Nature 613, 783-789.

Yu J, Schneiders T (2012). Tigecycline challenge triggers sRNA production in *Salmonella enterica* serovar Typhimurium. BMC Microbiol 12, 195.

Yuan L, Fan L, Dai H, He G, Zheng X, Rao S, Yang Z, Jiao XA (2023). Multi-omics reveals the increased biofilm formation of *Salmonella typhimurium* M3 by the induction of tetracycline at sub-inhibitory concentrations. Sci Total Environ 899, 165695.

Zeghouf M, Li J, Butland G, Borkowska A, Canadien V, Richards D, Beattie B, Emili A, Greenblatt JF (2004). Sequential Peptide Affinity (SPA) system for the identification of mammalian and bacterial protein complexes. J Proteome Res 3, 463-468.

Zhang F, Cheng W (2022). The mechanism of bacterial resistance and potential bacteriostatic strategies. Antibiotics (Basel) 11, 1215.

Zhang S, Liu S, Wu N, Yuan Y, Zhang W, Zhang Y (2018). Small non-coding RNA *ryhB* mediates persistence to multiple antibiotics and stresses in uropathogenic *Escherichia coli* by reducing cellular metabolism. Front Microbiol 9, 136.

Zhu M, Mori M, Hwa T, Dai X (2019). Disruption of transcription-translation coordination in *Escherichia coli* leads to premature transcriptional termination. Nat Microbiol 4, 2347-2356.

# Acknowledgements

I would like to thank Apl. Prof. Dr. Elena Evguenieva-Hackenberg, who not only gave me the opportunity to do my doctoral research in her lab but also supported and guided me through every high and low that came with it.

I would furthermore like to thank my second supervisor, Dr. Cornelia Kilchert, for all the help and advice I received, not only for this thesis but also in finding my way through, dealing with the emotional toll that this thesis took on me.

I would like to thank the remaining members of my thesis committee, Prof. Dr. Kai Thormann and Prof. Dr. Michael Niepmann, who helped advance my research with their helpful advice and opinions. I would also like to thank our RTG research coordinator Dr. Vera Bettenworth for not only organizing all RTG events, but also giving advice for both life and research.

I would like to give special and big thanks to Susanne Barth-Weber, who did all my cloning work for me, as well as helped me with everyday lab work. Without you, I would not have been able to finish this thesis, and I mean that. I really enjoyed having someone to talk to in the lab, no matter what the topic was.

Furthermore, I would like to thank my colleagues Robi and Theresa for all their help and for always lending an ear to all my troubles, be it personal life, research or just everyday things that were on my mind. Thank you for making me laugh and for letting me cry when things got rough and for all the time we shared just chatting away. Furthermore, I would like to thank our Hiwi Jan and my master student Tessa as well as my bachelor students for their help provided with this project.

I would like to thank our all our institute members, both present and former. In particular, I would like to thank Meike, Timon, Jonas, Nicole, Vanessa and Sophie for all the fun times we shared and all the lunch breaks that made every day a little more bearable. A special thank you as well to our other technicians Andreas, Andrea, Nicole, Florian and Ulrike.

I would also like to thank my friends Jannik, Undine and Sandra for all the support, help and love I received, and for all the fun evenings we shared throughout the last 6 years, with many stories that I will keep telling for the rest of my life as some of my best memories. I promise I will be careful around fire. Thank you for not letting go of me, even when things got very rough, and sticking with me until the end. Thank you for making me laugh, for letting me cry, for giving me advice and just about anything you did for me and that would be too much to list here. Thank you, Undine, for all the help with the alignments and tree generation. Let's keep our fun evenings and get together every once in a while, even if we are split across many places. I would like to thank my best friend Lena, and I just want to say, I am glad you are still alive and still with me. It has been 10 years since we met and you have been with me for everything ever since, even if we are far apart now. I enjoy talking to you on the phone, about everything and nothing, and it really helped me through the toughest times I have experienced. Furthermore, I would also like to thank my RTG members and friends Kai, Daniel and Fabienne for the fun times we shared and hopefully will continue to share over dinner, climbing or other activities. A special shoutout and thank you to my former master's supervisors from the Randau Lab, Vicente and Ruth, for all the support and for still thinking of me, even years after I left the lab. I hope to keep all these friendships for the years yet to come.

Finally, I saved the best for last. I would like to thank my parents for their love and support, for their pep talks and for everything they did for me. I am sorry for all the pain I put you through these past 4 years, but thank you for not giving up on me. Thank you for picking and building me up every time I fell or struggled. Thank you for all the advice I received, even when I did not want to hear it or take it to heart. Without your help and support, I would not have been able

to complete this thesis and this chapter of my life. I will be forever grateful. If there is a next life, I promise I will meet you again and I will make everything up to you that I cannot do in this one. I love you with all my heart.

# Supplemental Material

**Supplemental Tab. S1:** Top25 genes with the highest decrease in mRNA level. In contrast to the genes with an increase, genes with a decrease are longer and usually second or further downstream in an operon.

| Locus tag | $Log_2$(Fc) | Amino acids | Gene or protein |
|---|---|---|---|
| SM2011_RS20165 | -2,00 | 274 | *rsmA* |
| SM2011_RS25940 | -2,00 | 377 | ABC transporter substrate-binding protein |
| SM2011_RS19395 | -1,99 | 116 | *mnhG* |
| SM2011_RS17655 | -1,99 | 183 | HP |
| SM2011_RS20575 | -1,91 | 414 | glycosyltransferase family 4 protein |
| SM2011_RS22835 | -1,88 | 406 | *moeA* |
| SM2011_RS20925 | -1,88 | 394 | MFS transporter |
| SM2011_RS17145 | -1,85 | 334 | *cydB* |
| SM2011_RS14245 | -1,85 | 94 | *paaB* |
| SM2011_RS21410 | -1,83 | 125 | *crcB* |
| SM2011_RS19455 | -1,81 | 181 | membrane protein |
| SM2011_RS17345 | -1,80 | 1065 | type I restriction endonuclease subunit R |
| SM2011_RS19055 | -1,75 | 1153 | chromosome segregation SMC family protein |
| SM2011_RS13845 | -1,74 | 333 | branched-chain amino acid ABC transporter permease |
| SM2011_RS29195 | -1,72 | 547 | monovalent cation/H+ antiporter subunit D |
| SM2011_RS19930 | -1,69 | 334 | NAD regulator |
| SM2011_RS23315 | -1,69 | 420 | VWA domain-containing protein |
| SM2011_RS30520 | -1,68 | 160 | *rlmH* |
| SM2011_RS17805 | -1,68 | 137 | HP |
| SM2011_RS00280 | -1,66 | 311 | ABC transporter permease |
| SM2011_RS24490 | -1,66 | 220 | chloramphenicol phosphotransferase CPT family protein |
| SM2011_RS23290 | -1,64 | 135 | NUDIX domain-containing protein |
| SM2011_RS28855 | -1,63 | 721 | *glgB* |
| SM2011_RS13075 | -1,63 | 263 | SURF1 family protein |
| SM2011_RS30810 | -1,62 | 863 | ABC transporter permease |

**Supplemental Tab. S2:** Cq values of reporter mRNA *spa* obtained by RT-qPCR of all constructs used in this study. Cond, condition; Rep, replicate; Diff, difference, MW, mean value.

| Plasmid | Cond. | Rep. | Cq | Diff | MW per Rep | MW Condition | Cq | Diff | MW per Rep | MW Condition |
|---|---|---|---|---|---|---|---|---|---|---|
| DUF'-SPA | -Tc | I | 15,29 | 0,19 | 15,20 | 14,71 | 15,45 | -0,05 | 15,48 | 15,59 |
| | | | 15,10 | | | | 15,50 | | | |
| | | II | 14,86 | -0,18 | 14,95 | | 15,47 | -0,12 | 15,53 | |
| | | | 15,04 | | | | 15,59 | | | |
| | | III | 13,82 | -0,31 | 13,98 | | 15,70 | -0,11 | 15,76 | |
| | | | 14,13 | | | | 15,81 | | | |
| | +Tc | I | 10,01 | 0,19 | 9,92 | 9,64 | 10,29 | -0,37 | 10,48 | 10,84 |
| | | | 9,82 | | | | 10,66 | | | |
| | | II | 9,44 | 0,26 | 9,31 | | 11,17 | -0,18 | 11,26 | |
| | | | 9,18 | | | | 11,35 | | | |
| | | III | 9,84 | 0,28 | 9,70 | | 10,75 | -0,05 | 10,78 | |
| | | | 9,56 | | | | 10,80 | | | |
| M1-SPA | -Tc | I | 10,44 | 0,20 | 10,34 | 10,41 | | 0,00 | | |
| | | | 10,24 | | | | | | | |
| | | II | 10,75 | 0,16 | 10,67 | | | 0,00 | | |
| | | | 10,59 | | | | | | | |
| | | III | 10,18 | | 10,23 | | | 0,00 | | |

| | | | | | | | | | | |
|---|---|---|---|---|---|---|---|---|---|---|
| | | | 10,28 | -0,10 | | | | | | |
| | +Tc | I | 9,92 | 0,17 | 9,84 | 10,20 | | 0,00 | | |
| | | | 9,75 | | | | | | | |
| | | II | 11,56 | 0,10 | 11,51 | | | 0,00 | | |
| | | | 11,46 | | | | | | | |
| | | III | 9,21 | -0,07 | 9,25 | | | 0,00 | | |
| | | | 9,28 | | | | | | | |
| uORF1-SPA | -Tc | I | 9,74 | 0,27 | 9,61 | 10,03 | 9,68 | -0,22 | 9,79 | 10,03 |
| | | | 9,47 | | | | 9,90 | | | |
| | | II | 10,27 | 0,08 | 10,23 | | 10,20 | 0,19 | 10,11 | |
| | | | 10,19 | | | | 10,01 | | | |
| | | III | 10,36 | 0,21 | 10,26 | | 10,25 | 0,14 | 10,18 | |
| | | | 10,15 | | | | 10,11 | | | |
| | +Tc | I | 8,57 | 0,19 | 8,48 | 9,06 | 8,34 | -0,04 | 8,36 | 8,44 |
| | | | 8,38 | | | | 8,38 | | | |
| | | II | 9,26 | -0,34 | 9,43 | | 8,53 | 0,15 | 8,46 | |
| | | | 9,60 | | | | 8,38 | | | |
| | | III | 9,32 | 0,09 | 9,28 | | 8,46 | -0,09 | 8,51 | |
| | | | 9,23 | | | | 8,55 | | | |
| DUF1127$_1$-SPA | -Tc | I | 15,49 | 0,30 | 15,34 | 15,16 | | 0,00 | | |
| | | | 15,19 | | | | | | | |
| | | II | 15,03 | -0,45 | 15,26 | | | 0,00 | | |
| | | | 15,48 | | | | | | | |
| | | III | 14,93 | 0,09 | 14,89 | | | 0,00 | | |
| | | | 14,84 | | | | | | | |
| | +Tc | I | 9,82 | -0,37 | 10,01 | 9,78 | | 0,00 | | |
| | | | 10,19 | | | | | | | |
| | | II | 9,54 | 0,05 | 9,52 | | | 0,00 | | |
| | | | 9,49 | | | | | | | |
| | | III | 9,98 | 0,33 | 9,82 | | | 0,00 | | |
| | | | 9,65 | | | | | | | |
| CGC 192-194 ATC | -Tc | I | 16,47 | -0,21 | 16,58 | 16,50 | | 0,00 | | |
| | | | 16,68 | | | | | | | |
| | | II | 16,65 | -0,02 | 16,66 | | | 0,00 | | |
| | | | 16,67 | | | | | | | |
| | | III | 16,23 | -0,06 | 16,26 | | | 0,00 | | |
| | | | 16,29 | | | | | | | |
| | +Tc | I | 10,55 | 0,10 | 10,50 | 11,25 | | 0,00 | | |
| | | | 10,45 | | | | | | | |
| | | II | 11,64 | -0,16 | 11,72 | | | 0,00 | | |
| | | | 11,80 | | | | | | | |
| | | III | 11,50 | -0,06 | 11,53 | | | 0,00 | | |
| | | | 11,56 | | | | | | | |
| GCC 135-137 CGG | -Tc | I | 15,61 | 0,10 | 15,56 | 15,72 | | 0,00 | | |
| | | | 15,51 | | | | | | | |
| | | II | 15,55 | 0,18 | 15,46 | | | 0,00 | | |
| | | | 15,37 | | | | | | | |
| | | III | 16,12 | -0,03 | 16,14 | | | 0,00 | | |
| | | | 16,15 | | | | | | | |
| | +Tc | I | 10,62 | -0,12 | 10,68 | 10,59 | | 0,00 | | |
| | | | 10,74 | | | | | | | |
| | | II | 10,58 | -0,27 | 10,72 | | | 0,00 | | |
| | | | 10,85 | | | | | | | |
| | | III | 10,38 | -0,01 | 10,39 | | | 0,00 | | |
| | | | 10,39 | | | | | | | |
| uORF2-SPA | -Tc | I | 14,47 | 0,13 | 14,41 | 14,53 | | 0,00 | | |
| | | | 14,34 | | | | | | | |
| | | II | 14,46 | 0,07 | 14,43 | | | 0,00 | | |

| | | | | | | | | | | |
|---|---|---|---|---|---|---|---|---|---|---|
| | | | 14,39 | | | | | | | |
| | | III | 14,66 | - | 14,77 | | | 0,00 | | |
| | | | 14,88 | 0,22 | | | | | | |
| | +Tc | I | 10,31 | 0,25 | 10,19 | 10,10 | | 0,00 | | |
| | | | 10,06 | | | | | | | |
| | | II | 10,13 | 0,22 | 10,02 | | | 0,00 | | |
| | | | 9,91 | | | | | | | |
| | | III | 10,03 | - | 10,10 | | | 0,00 | | |
| | | | 10,16 | 0,13 | | | | | | |
| M2/Stop-SPA | -Tc | I | 14,08 | 0,17 | 14,00 | 13,77 | | 0,00 | | |
| | | | 13,91 | | | | | | | |
| | | II | 13,72 | 0,05 | 13,70 | | | 0,00 | | |
| | | | 13,67 | | | | | | | |
| | | III | 13,63 | 0,03 | 13,62 | | | 0,00 | | |
| | | | 13,60 | | | | | | | |
| | +Tc | I | 9,43 | 0,05 | 9,41 | 9,43 | | 0,00 | | |
| | | | 9,38 | | | | | | | |
| | | II | 9,39 | 0,25 | 9,27 | | | 0,00 | | |
| | | | 9,14 | | | | | | | |
| | | III | 9,62 | - | 9,63 | | | 0,00 | | |
| | | | 9,64 | 0,02 | | | | | | |
| M2/Stop-DUF'-SPA | -Tc | I | 15,61 | 0,16 | 15,53 | 14,83 | | 0,00 | | |
| | | | 15,45 | | | | | | | |
| | | II | 15,32 | - | 15,35 | | | 0,00 | | |
| | | | 15,37 | 0,05 | | | | | | |
| | | III | 13,64 | 0,06 | 13,61 | | | 0,00 | | |
| | | | 13,58 | | | | | | | |
| | +Tc | I | 10,38 | 0,22 | 10,27 | 10,12 | | 0,00 | | |
| | | | 10,16 | | | | | | | |
| | | II | 9,89 | 0,04 | 9,87 | | | 0,00 | | |
| | | | 9,85 | | | | | | | |
| | | III | 10,20 | - | 10,22 | | | 0,00 | | |
| | | | 10,24 | 0,04 | | | | | | |
| M1-M2-DUF'-SPA | -Tc | I | 9,19 | - | 9,20 | 9,13 | | 0,00 | | |
| | | | 9,21 | 0,02 | | | | | | |
| | | II | 9,15 | - | 9,19 | | | 0,00 | | |
| | | | 9,22 | 0,07 | | | | | | |
| | | III | 9,12 | 0,23 | 9,01 | | | 0,00 | | |
| | | | 8,89 | | | | | | | |
| | +Tc | I | 8,08 | 0,05 | 8,06 | 8,09 | | 0,00 | | |
| | | | 8,03 | | | | | | | |
| | | II | 8,10 | 0,17 | 8,02 | | | 0,00 | | |
| | | | 7,93 | | | | | | | |
| | | III | 7,89 | - | 8,21 | | | 0,00 | | |
| | | | 8,52 | 0,63 | | | | | | |
| Δ121-128 | -Tc | I | 13,78 | 0,21 | 13,68 | 14,04 | 12,87 | -0,21 | 12,98 | 13,27 |
| | | | 13,57 | | | | 13,08 | | | |
| | | II | 14,61 | 0,75 | 14,24 | | 13,29 | 0,17 | 13,21 | |
| | | | 13,86 | | | | 13,12 | | | |
| | | III | 14,22 | 0,02 | 14,21 | | 13,68 | 0,13 | 13,62 | |
| | | | 14,20 | | | | 13,55 | | | |
| | +Tc | I | 10,56 | - | 10,60 | 10,55 | 9,98 | -0,16 | 10,06 | 10,03 |
| | | | 10,63 | 0,07 | | | 10,14 | | | |
| | | II | 10,72 | 0,32 | 10,56 | | 10,14 | 0,09 | 10,10 | |
| | | | 10,40 | | | | 10,05 | | | |
| | | III | 10,49 | 0,02 | 10,48 | | 10,07 | 0,28 | 9,93 | |
| | | | 10,47 | | | | 9,79 | | | |
| | -Tc | I | 15,01 | | 15,07 | 15,15 | 14,87 | 0,07 | 14,84 | 15,21 |

| | | | | | | | | | | |
|---|---|---|---|---|---|---|---|---|---|---|
| DUF'-mut. 121-128 | | | 15,12 | -0,11 | | | 14,80 | | | |
| | | II | 15,40 | 0,31 | 15,25 | | 14,77 | 0,21 | 14,67 | |
| | | | 15,09 | | | | 14,56 | | | |
| | | III | 15,23 | 0,16 | 15,15 | | 14,85 | -2,55 | 16,13 | |
| | | | 15,07 | | | | 17,40 | | | |
| | +Tc | I | 10,43 | 0,22 | 10,32 | 10,42 | 10,18 | 0,17 | 10,10 | 9,87 |
| | | | 10,21 | | | | 10,01 | | | |
| | | II | 10,70 | 0,00 | 10,70 | | 10,29 | 0,03 | 10,28 | |
| | | | 10,70 | | | | 10,26 | | | |
| | | III | 10,21 | -0,06 | 10,24 | | 9,35 | 0,25 | 9,23 | |
| | | | 10,27 | | | | 9,10 | | | |
| M1-mut. 121-128 | -Tc | I | 8,26 | 0,27 | 8,13 | 8,17 | 7,81 | 0,32 | 7,65 | 7,71 |
| | | | 7,99 | | | | 7,49 | | | |
| | | II | 8,39 | 0,20 | 8,29 | | 8,01 | 0,21 | 7,91 | |
| | | | 8,19 | | | | 7,80 | | | |
| | | III | 8,08 | -0,04 | 8,10 | | 7,48 | -0,19 | 7,58 | |
| | | | 8,12 | | | | 7,67 | | | |
| | +Tc | I | 7,34 | -0,01 | 7,35 | 7,53 | 6,80 | -1,30 | 7,45 | 7,25 |
| | | | 7,35 | | | | 8,10 | | | |
| | | II | 7,61 | 0,21 | 7,51 | | 7,16 | 0,31 | 7,01 | |
| | | | 7,40 | | | | 6,85 | | | |
| | | III | 7,90 | 0,30 | 7,75 | | 7,33 | 0,05 | 7,31 | |
| | | | 7,60 | | | | 7,28 | | | |
| C11/Stop | -Tc | I | 9,45 | -0,28 | 9,59 | 9,16 | | 0,00 | | |
| | | | 9,73 | | | | | | | |
| | | II | 9,10 | 0,09 | 9,06 | | | 0,00 | | |
| | | | 9,01 | | | | | | | |
| | | III | 9,17 | 0,69 | 8,83 | | | 0,00 | | |
| | | | 8,48 | | | | | | | |
| | +Tc | I | 7,20 | -0,79 | 7,60 | 7,22 | | 0,00 | | |
| | | | 7,99 | | | | | | | |
| | | II | 7,43 | -0,35 | 7,61 | | | 0,00 | | |
| | | | 7,78 | | | | | | | |
| | | III | 6,32 | -0,30 | 6,47 | | | 0,00 | | |
| | | | 6,62 | | | | | | | |
| S19/Stop | -Tc | I | 13,83 | -0,21 | 13,94 | 14,27 | | 0,00 | | |
| | | | 14,04 | | | | | | | |
| | | II | 14,66 | -0,11 | 14,72 | | | 0,00 | | |
| | | | 14,77 | | | | | | | |
| | | III | 14,30 | 0,29 | 14,16 | | | 0,00 | | |
| | | | 14,01 | | | | | | | |
| | +Tc | I | 6,99 | -0,05 | 7,02 | 7,89 | | 0,00 | | |
| | | | 7,04 | | | | | | | |
| | | II | 7,83 | -0,18 | 7,92 | | | 0,00 | | |
| | | | 8,01 | | | | | | | |
| | | III | 9,21 | 0,98 | 8,72 | | | 0,00 | | |
| | | | 8,23 | | | | | | | |
| A15/Stop | -Tc | I | 14,49 | -0,13 | 14,56 | 14,77 | | 0,00 | | |
| | | | 14,62 | | | | | | | |
| | | II | 14,33 | 0,02 | 14,32 | | | 0,00 | | |
| | | | 14,31 | | | | | | | |
| | | III | 15,47 | 0,06 | 15,44 | | | 0,00 | | |
| | | | 15,41 | | | | | | | |
| | +Tc | I | 9,80 | 0,00 | 9,80 | 9,61 | | 0,00 | | |
| | | | 9,80 | | | | | | | |
| | | II | 10,35 | -0,21 | 10,46 | | | 0,00 | | |
| | | | 10,56 | | | | | | | |
| | | III | 8,65 | 0,15 | 8,58 | | | 0,00 | | |

| | | | | | | | | | | |
|---|---|---|---|---|---|---|---|---|---|---|
| | | | 8,50 | | | | | | | |
| T17/Stop | -Tc | I | 17,04 | -0,07 | 17,08 | 15,91 | | 0,00 | | |
| | | | 17,11 | | | | | | | |
| | | II | 16,13 | 0,08 | 16,09 | | | 0,00 | | |
| | | | 16,05 | | | | | | | |
| | | III | 14,68 | 0,26 | 14,55 | | | 0,00 | | |
| | | | 14,42 | | | | | | | |
| | +Tc | I | 11,14 | 0,75 | 10,77 | 9,99 | | 0,00 | | |
| | | | 10,39 | | | | | | | |
| | | II | 10,62 | -0,11 | 10,68 | | | 0,00 | | |
| | | | 10,73 | | | | | | | |
| | | III | 8,44 | -0,19 | 8,54 | | | 0,00 | | |
| | | | 8,63 | | | | | | | |
| Δ1 | -Tc | I | 11,49 | 0,07 | 11,46 | 11,27 | | 0,00 | | |
| | | | 11,42 | | | | | | | |
| | | II | 11,23 | 0,06 | 11,20 | | | 0,00 | | |
| | | | 11,17 | | | | | | | |
| | | III | 11,05 | -0,23 | 11,17 | | | 0,00 | | |
| | | | 11,28 | | | | | | | |
| | +Tc | I | 8,10 | -0,11 | 8,16 | 8,30 | | 0,00 | | |
| | | | 8,21 | | | | | | | |
| | | II | 8,53 | -0,10 | 8,58 | | | 0,00 | | |
| | | | 8,63 | | | | | | | |
| | | III | 8,06 | -0,21 | 8,17 | | | 0,00 | | |
| | | | 8,27 | | | | | | | |
| Δ2 | -Tc | I | 15,35 | 0,21 | 15,25 | 15,35 | | 0,00 | | |
| | | | 15,14 | | | | | | | |
| | | II | 15,51 | -0,14 | 15,58 | | | 0,00 | | |
| | | | 15,65 | | | | | | | |
| | | III | 15,21 | -0,03 | 15,23 | | | 0,00 | | |
| | | | 15,24 | | | | | | | |
| | +Tc | I | 10,14 | 0,29 | 10,00 | 10,18 | | 0,00 | | |
| | | | 9,85 | | | | | | | |
| | | II | 10,05 | -0,03 | 10,07 | | | 0,00 | | |
| | | | 10,08 | | | | | | | |
| | | III | 10,45 | -0,05 | 10,48 | | | 0,00 | | |
| | | | 10,50 | | | | | | | |
| Δ3 | -Tc | I | 13,69 | -0,52 | 13,95 | 14,16 | | 0,00 | | |
| | | | 14,21 | | | | | | | |
| | | II | 14,19 | -0,13 | 14,26 | | | 0,00 | | |
| | | | 14,32 | | | | | | | |
| | | III | 14,34 | 0,13 | 14,28 | | | 0,00 | | |
| | | | 14,21 | | | | | | | |
| | +Tc | I | 14,11 | -0,09 | 14,16 | 11,41 | | 0,00 | | |
| | | | 14,20 | | | | | | | |
| | | II | 10,61 | 0,10 | 10,56 | | | 0,00 | | |
| | | | 10,51 | | | | | | | |
| | | III | 9,51 | 0,01 | 9,51 | | | 0,00 | | |
| | | | 9,50 | | | | | | | |
| scramble | -Tc | I | 15,03 | -0,15 | 15,11 | 15,03 | | 0,00 | | |
| | | | 15,18 | | | | | | | |
| | | II | 15,01 | -0,03 | 15,03 | | | 0,00 | | |
| | | | 15,04 | | | | | | | |
| | | III | 14,98 | 0,02 | 14,97 | | | 0,00 | | |
| | | | 14,96 | | | | | | | |
| | +Tc | I | 7,92 | 0,08 | 7,88 | 8,68 | | 0,00 | | |
| | | | 7,84 | | | | | | | |
| | | II | 8,76 | | 8,99 | | | 0,00 | | |

| | | | | | | | | | | |
|---|---|---|---|---|---|---|---|---|---|---|
| | | | 9,21 | -0,45 | | | | | | |
| | | III | 9,26 | 0,18 | 9,17 | | | 0,00 | | |
| | | | 9,08 | | | | | | | |
| ΔS3-L10 | -Tc | I | 9,22 | -0,09 | 9,27 | 9,39 | | 0,00 | | |
| | | | 9,31 | | | | | | | |
| | | II | 9,36 | -0,04 | 9,38 | | | 0,00 | | |
| | | | 9,40 | | | | | | | |
| | | III | 9,54 | 0,03 | 9,53 | | | 0,00 | | |
| | | | 9,51 | | | | | | | |
| | +Tc | I | 9,38 | 0,06 | 9,35 | 9,53 | | 0,00 | | |
| | | | 9,32 | | | | | | | |
| | | II | 9,52 | -0,10 | 9,57 | | | 0,00 | | |
| | | | 9,62 | | | | | | | |
| | | III | 9,72 | 0,11 | 9,67 | | | 0,00 | | |
| | | | 9,61 | | | | | | | |
| mut. S3-L20_1 | -Tc | I | 8,79 | 0,18 | 8,70 | 8,53 | | 0,00 | | |
| | | | 8,61 | | | | | | | |
| | | II | 8,61 | 0,13 | 8,55 | | | 0,00 | | |
| | | | 8,48 | | | | | | | |
| | | III | 8,40 | 0,14 | 8,33 | | | 0,00 | | |
| | | | 8,26 | | | | | | | |
| | +Tc | I | 7,52 | 0,05 | 7,50 | 7,41 | | 0,00 | | |
| | | | 7,47 | | | | | | | |
| | | II | 7,56 | 0,21 | 7,46 | | | 0,00 | | |
| | | | 7,35 | | | | | | | |
| | | III | 7,37 | 0,17 | 7,29 | | | 0,00 | | |
| | | | 7,20 | | | | | | | |
| Δ18-33 | -Tc | I | 14,70 | 0,05 | 14,68 | 14,59 | 14,95 | 0,21 | 14,85 | 15,00 |
| | | | 14,65 | | | | 14,74 | | | |
| | | II | 14,44 | -0,10 | 14,49 | | 14,80 | -0,44 | 15,02 | |
| | | | 14,54 | | | | 15,24 | | | |
| | | III | 14,68 | 0,16 | 14,60 | | 15,17 | 0,09 | 15,13 | |
| | | | 14,52 | | | | 15,08 | | | |
| | +Tc | I | 12,50 | 0,27 | 12,37 | 12,13 | 13,06 | 0,22 | 12,95 | 12,66 |
| | | | 12,23 | | | | 12,84 | | | |
| | | II | 12,19 | 0,02 | 12,18 | | 12,63 | -0,15 | 12,71 | |
| | | | 12,17 | | | | 12,78 | | | |
| | | III | 11,75 | -0,18 | 11,84 | | 12,19 | -0,25 | 12,32 | |
| | | | 11,93 | | | | 12,44 | | | |
| mut. S3-L20_2 | -Tc | I | 11,26 | -0,17 | 11,35 | 11,42 | | 0,00 | | |
| | | | 11,43 | | | | | | | |
| | | II | 11,28 | -0,21 | 11,39 | | | 0,00 | | |
| | | | 11,49 | | | | | | | |
| | | III | 11,38 | -0,28 | 11,52 | | | 0,00 | | |
| | | | 11,66 | | | | | | | |
| | +Tc | I | 9,24 | -0,01 | 9,25 | 9,29 | | 0,00 | | |
| | | | 9,25 | | | | | | | |
| | | II | 9,08 | -0,05 | 9,11 | | | 0,00 | | |
| | | | 9,13 | | | | | | | |
| | | III | 9,53 | 0,00 | 9,53 | | | 0,00 | | |
| | | | 9,53 | | | | | | | |
| uORF3-SD-mut | -Tc | I | 16,16 | -0,17 | 16,25 | 16,15 | | 0,00 | | |
| | | | 16,33 | | | | | | | |
| | | II | 15,94 | -0,01 | 15,95 | | | 0,00 | | |
| | | | 15,95 | | | | | | | |
| | | III | 16,25 | -0,03 | 16,27 | | | 0,00 | | |
| | | | 16,28 | | | | | | | |
| | +Tc | I | 10,81 | | 10,83 | 11,59 | | 0,00 | | |

| | | | | | | | | | | |
|---|---|---|---|---|---|---|---|---|---|---|
| | | | 10,85 | -0,04 | | | | | | |
| | | II | 11,96 | 0,04 | 11,94 | | | 0,00 | | |
| | | | 11,92 | | | | | | | |
| | | III | 11,92 | - | 12,01 | | | 0,00 | | |
| | | | 12,10 | 0,18 | | | | | | |

**Supplemental Tab. S3:** Cq values of housekeeping mRNA *rpoB* obtained by RT-qPCR of all constructs used in this study. Cond, condition; Rep, replicate; Diff, difference, MW, mean value.

| **Strain** | **Condition** | **Replicate** | **Cq** | **Diff** | **MW per Rep** | **MW Condition** | **Cq** | **Diff** | **MW per Rep** | **MW Condition** |
|---|---|---|---|---|---|---|---|---|---|---|
| DUF'-SPA | -Tc | I | 18,02 | 0,10 | 17,97 | 18,01 | 18,36 | -0,32 | 18,52 | 18,48 |
| | | | 17,92 | | | | 18,68 | | | |
| | | II | 18,26 | 0,38 | 18,07 | | 18,43 | -0,02 | 18,44 | |
| | | | 17,88 | | | | 18,45 | | | |
| | | III | 17,75 | -0,45 | 17,98 | | 18,48 | 0,00 | 18,48 | |
| | | | 18,20 | | | | 18,48 | | | |
| | +Tc | I | 18,26 | -0,22 | 18,37 | 18,37 | 18,30 | -0,06 | 18,33 | 18,83 |
| | | | 18,48 | | | | 18,36 | | | |
| | | II | 18,53 | -0,17 | 18,62 | | 19,02 | -0,02 | 19,03 | |
| | | | 18,70 | | | | 19,04 | | | |
| | | III | 17,91 | -0,42 | 18,12 | | 19,20 | 0,17 | 19,12 | |
| | | | 18,33 | | | | 19,03 | | | |
| M1-SPA | -Tc | I | 18,18 | 0,38 | 17,99 | 17,76 | | 0,00 | | |
| | | | 17,80 | | | | | | | |
| | | II | 17,87 | -0,46 | 18,10 | | | 0,00 | | |
| | | | 18,33 | | | | | | | |
| | | III | 17,36 | 0,37 | 17,18 | | | 0,00 | | |
| | | | 16,99 | | | | | | | |
| | +Tc | I | 18,51 | 0,35 | 18,34 | 18,36 | | 0,00 | | |
| | | | 18,16 | | | | | | | |
| | | II | 18,23 | -0,09 | 18,28 | | | 0,00 | | |
| | | | 18,32 | | | | | | | |
| | | III | 18,58 | 0,24 | 18,46 | | | 0,00 | | |
| | | | 18,34 | | | | | | | |
| uORF1-SPA | -Tc | I | 18,86 | -0,31 | 19,02 | 19,59 | 19,35 | -0,15 | 19,43 | 20,09 |
| | | | 19,17 | | | | 19,50 | | | |
| | | II | 19,60 | -0,52 | 19,86 | | 20,04 | -0,13 | 20,11 | |
| | | | 20,12 | | | | 20,17 | | | |
| | | III | 20,15 | 0,52 | 19,89 | | 21,28 | 1,07 | 20,75 | |
| | | | 19,63 | | | | 20,21 | | | |
| | +Tc | I | 19,19 | -0,94 | 19,66 | 19,55 | 19,55 | 0,13 | 19,49 | 19,44 |
| | | | 20,13 | | | | 19,42 | | | |
| | | II | 19,19 | -1,27 | 19,83 | | 19,39 | 0,17 | 19,31 | |
| | | | 20,46 | | | | 19,22 | | | |
| | | III | 19,01 | -0,31 | 19,17 | | 19,58 | 0,12 | 19,52 | |
| | | | 19,32 | | | | 19,46 | | | |
| DUF1127$_1$-SPA | -Tc | I | 17,37 | -0,09 | 17,42 | 17,66 | | 0,00 | | |
| | | | 17,46 | | | | | | | |
| | | II | 18,02 | 0,48 | 17,78 | | | 0,00 | | |
| | | | 17,54 | | | | | | | |
| | | III | 17,59 | -0,40 | 17,79 | | | 0,00 | | |
| | | | 17,99 | | | | | | | |
| | +Tc | I | 18,55 | 0,67 | 18,22 | 18,30 | | 0,00 | | |
| | | | 17,88 | | | | | | | |
| | | II | 18,14 | -0,65 | 18,47 | | | 0,00 | | |

| | | | | | | | | | | |
|---|---|---|---|---|---|---|---|---|---|---|
| | | | 18,79 | | | | | | | |
| | | III | 18,28 | 0,14 | 18,21 | | | 0,00 | | |
| | | | 18,14 | | | | | | | |
| CGC 192-194 ATC | -Tc | I | 17,91 | -0,10 | 17,96 | 18,11 | | 0,00 | | |
| | | | 18,01 | | | | | | | |
| | | II | 18,06 | -0,14 | 18,13 | | | 0,00 | | |
| | | | 18,20 | | | | | | | |
| | | III | 18,17 | -0,11 | 18,23 | | | 0,00 | | |
| | | | 18,28 | | | | | | | |
| | +Tc | I | 18,41 | 0,14 | 18,34 | 18,31 | | 0,00 | | |
| | | | 18,27 | | | | | | | |
| | | II | 18,12 | -0,25 | 18,25 | | | 0,00 | | |
| | | | 18,37 | | | | | | | |
| | | III | 18,27 | -0,13 | 18,34 | | | 0,00 | | |
| | | | 18,40 | | | | | | | |
| GCC 135-137 CGG | -Tc | I | 17,85 | -0,12 | 17,91 | 18,23 | | 0,00 | | |
| | | | 17,97 | | | | | | | |
| | | II | 18,07 | 0,26 | 17,94 | | | 0,00 | | |
| | | | 17,81 | | | | | | | |
| | | III | 18,86 | 0,02 | 18,85 | | | 0,00 | | |
| | | | 18,84 | | | | | | | |
| | +Tc | I | 18,04 | -0,05 | 18,07 | 18,26 | | 0,00 | | |
| | | | 18,09 | | | | | | | |
| | | II | 18,25 | 0,14 | 18,18 | | | 0,00 | | |
| | | | 18,11 | | | | | | | |
| | | III | 18,32 | -0,40 | 18,52 | | | 0,00 | | |
| | | | 18,72 | | | | | | | |
| uORF 2-SPA | -Tc | I | 18,74 | -0,27 | 18,88 | 18,53 | | 0,00 | | |
| | | | 19,01 | | | | | | | |
| | | II | 18,31 | 0,01 | 18,31 | | | 0,00 | | |
| | | | 18,30 | | | | | | | |
| | | III | 18,41 | -0,01 | 18,42 | | | 0,00 | | |
| | | | 18,42 | | | | | | | |
| | +Tc | I | 18,15 | -0,13 | 18,22 | 18,57 | | 0,00 | | |
| | | | 18,28 | | | | | | | |
| | | II | 18,69 | 0,09 | 18,65 | | | 0,00 | | |
| | | | 18,60 | | | | | | | |
| | | III | 18,76 | -0,18 | 18,85 | | | 0,00 | | |
| | | | 18,94 | | | | | | | |
| M2/Stop-SPA | -Tc | I | 18,72 | -0,04 | 18,74 | 18,66 | | 0,00 | | |
| | | | 18,76 | | | | | | | |
| | | II | 18,44 | -0,16 | 18,52 | | | 0,00 | | |
| | | | 18,60 | | | | | | | |
| | | III | 18,44 | -0,56 | 18,72 | | | 0,00 | | |
| | | | 19,00 | | | | | | | |
| | +Tc | I | 19,04 | -0,29 | 19,19 | 19,33 | | 0,00 | | |
| | | | 19,33 | | | | | | | |
| | | II | 19,25 | -0,16 | 19,33 | | | 0,00 | | |
| | | | 19,41 | | | | | | | |
| | | III | 19,45 | -0,07 | 19,49 | | | 0,00 | | |
| | | | 19,52 | | | | | | | |
| M2/Stop-DUF'-SPA | -Tc | I | 18,71 | 0,07 | 18,68 | 18,32 | | 0,00 | | |
| | | | 18,64 | | | | | | | |
| | | II | 19,10 | -0,05 | 19,13 | | | 0,00 | | |
| | | | 19,15 | | | | | | | |
| | | III | 17,16 | 0,01 | 17,16 | | | 0,00 | | |
| | | | 17,15 | | | | | | | |
| | +Tc | I | 18,61 | -0,21 | 18,72 | 19,14 | | 0,00 | | |

| | | | | | | | | | | |
|---|---|---|---|---|---|---|---|---|---|---|
| | | | 18,82 | | | | | | | |
| | | II | 19,80 | 0,31 | 19,65 | | | 0,00 | | |
| | | | 19,49 | | | | | | | |
| | | III | 18,78 | -0,53 | 19,05 | | | 0,00 | | |
| | | | 19,31 | | | | | | | |
| M1-M2-DUF'-SPA | -Tc | I | 18,82 | 0,03 | 18,81 | 18,90 | | 0,00 | | |
| | | | 18,79 | | | | | | | |
| | | II | 18,90 | -0,23 | 19,02 | | | 0,00 | | |
| | | | 19,13 | | | | | | | |
| | | III | 18,92 | 0,11 | 18,87 | | | 0,00 | | |
| | | | 18,81 | | | | | | | |
| | +Tc | I | 19,25 | -0,02 | 19,26 | 19,50 | | 0,00 | | |
| | | | 19,27 | | | | | | | |
| | | II | 19,77 | 0,16 | 19,69 | | | 0,00 | | |
| | | | 19,61 | | | | | | | |
| | | III | 19,59 | 0,08 | 19,55 | | | 0,00 | | |
| | | | 19,51 | | | | | | | |
| Δ121-128 | -Tc | I | 17,60 | -0,21 | 17,71 | 18,03 | 17,33 | -0,29 | 17,48 | 17,71 |
| | | | 17,81 | | | | 17,62 | | | |
| | | II | 18,64 | 0,54 | 18,37 | | 17,99 | 0,21 | 17,89 | |
| | | | 18,10 | | | | 17,78 | | | |
| | | III | 18,10 | 0,15 | 18,03 | | 17,75 | -0,02 | 17,76 | |
| | | | 17,95 | | | | 17,77 | | | |
| | +Tc | I | 18,31 | -0,38 | 18,50 | 18,56 | 18,07 | -0,29 | 18,22 | 18,47 |
| | | | 18,69 | | | | 18,36 | | | |
| | | II | 18,49 | -0,05 | 18,52 | | 18,40 | -0,13 | 18,47 | |
| | | | 18,54 | | | | 18,53 | | | |
| | | III | 18,74 | 0,17 | 18,66 | | 18,62 | -0,23 | 18,74 | |
| | | | 18,57 | | | | 18,85 | | | |
| DUF'-mut. 121-128 | -Tc | I | 18,04 | -0,08 | 18,08 | 18,23 | 17,69 | -0,11 | 17,75 | 17,92 |
| | | | 18,12 | | | | 17,80 | | | |
| | | II | 18,36 | 0,00 | 18,36 | | 17,85 | 0,22 | 17,74 | |
| | | | 18,36 | | | | 17,63 | | | |
| | | III | 18,32 | 0,14 | 18,25 | | 18,32 | 0,11 | 18,27 | |
| | | | 18,18 | | | | 18,21 | | | |
| | +Tc | I | 18,26 | -0,11 | 18,32 | 18,51 | 18,22 | -0,31 | 18,38 | 18,48 |
| | | | 18,37 | | | | 18,53 | | | |
| | | II | 18,92 | -0,03 | 18,94 | | 18,35 | -0,10 | 18,40 | |
| | | | 18,95 | | | | 18,45 | | | |
| | | III | 18,31 | 0,05 | 18,29 | | 18,21 | -0,89 | 18,66 | |
| | | | 18,26 | | | | 19,10 | | | |
| M1-mut. 121-128 | -Tc | I | 18,93 | -0,06 | 18,96 | 18,82 | 18,55 | 0,04 | 18,53 | 18,28 |
| | | | 18,99 | | | | 18,51 | | | |
| | | II | 19,01 | 0,33 | 18,85 | | 18,25 | 0,01 | 18,25 | |
| | | | 18,68 | | | | 18,24 | | | |
| | | III | 18,58 | -0,15 | 18,66 | | 18,07 | 0,04 | 18,05 | |
| | | | 18,73 | | | | 18,03 | | | |
| | +Tc | I | 19,43 | -0,14 | 19,50 | 19,18 | 19,02 | 0,05 | 19,00 | 18,68 |
| | | | 19,57 | | | | 18,97 | | | |
| | | II | 18,69 | -0,32 | 18,85 | | 18,77 | 0,21 | 18,67 | |
| | | | 19,01 | | | | 18,56 | | | |
| | | III | 19,18 | 0,01 | 19,18 | | 18,43 | 0,11 | 18,38 | |
| | | | 19,17 | | | | 18,32 | | | |
| C11/Stop | -Tc | I | 18,07 | -0,55 | 18,35 | 18,36 | | 0,00 | | |
| | | | 18,62 | | | | | | | |
| | | II | 18,39 | -0,20 | 18,49 | | | 0,00 | | |
| | | | 18,59 | | | | | | | |
| | | III | 18,24 | -0,03 | 18,26 | | | 0,00 | | |

| | | | | | | | | | | |
|---|---|---|---|---|---|---|---|---|---|---|
| | | | 18,27 | | | | | | | |
| | +Tc | I | 19,59 | 0,16 | 19,51 | 19,92 | | 0,00 | | |
| | | | 19,43 | | | | | | | |
| | | II | 19,74 | -0,54 | 20,01 | | | 0,00 | | |
| | | | 20,28 | | | | | | | |
| | | III | 19,84 | -0,79 | 20,24 | | | 0,00 | | |
| | | | 20,63 | | | | | | | |
| S19/Stop | -Tc | I | 17,63 | -1,50 | 18,38 | 18,48 | | 0,00 | | |
| | | | 19,13 | | | | | | | |
| | | II | 18,24 | 0,06 | 18,21 | | | 0,00 | | |
| | | | 18,18 | | | | | | | |
| | | III | 18,22 | -1,23 | 18,84 | | | 0,00 | | |
| | | | 19,45 | | | | | | | |
| | +Tc | I | 20,22 | 0,95 | 19,75 | 19,27 | | 0,00 | | |
| | | | 19,27 | | | | | | | |
| | | II | 19,08 | 0,05 | 19,06 | | | 0,00 | | |
| | | | 19,03 | | | | | | | |
| | | III | 19,11 | 0,18 | 19,02 | | | 0,00 | | |
| | | | 18,93 | | | | | | | |
| A15/Stop | -Tc | I | 17,45 | 0,00 | 17,45 | 17,64 | | 0,00 | | |
| | | | 17,45 | | | | | | | |
| | | II | 17,76 | -0,11 | 17,82 | | | 0,00 | | |
| | | | 17,87 | | | | | | | |
| | | III | 17,65 | 0,00 | 17,65 | | | 0,00 | | |
| | | | 17,65 | | | | | | | |
| | +Tc | I | 18,17 | -0,60 | 18,47 | 18,50 | | 0,00 | | |
| | | | 18,77 | | | | | | | |
| | | II | 18,10 | 0,00 | 18,10 | | | 0,00 | | |
| | | | 18,10 | | | | | | | |
| | | III | 18,98 | 0,09 | 18,94 | | | 0,00 | | |
| | | | 18,89 | | | | | | | |
| T17/Stop | -Tc | I | 19,22 | -0,06 | 19,25 | 18,31 | | 0,00 | | |
| | | | 19,28 | | | | | | | |
| | | II | 18,10 | 0,20 | 18,00 | | | 0,00 | | |
| | | | 17,90 | | | | | | | |
| | | III | 17,86 | 0,38 | 17,67 | | | 0,00 | | |
| | | | 17,48 | | | | | | | |
| | +Tc | I | 18,26 | 0,18 | 18,17 | 18,54 | | 0,00 | | |
| | | | 18,08 | | | | | | | |
| | | II | 18,60 | 0,27 | 18,47 | | | 0,00 | | |
| | | | 18,33 | | | | | | | |
| | | III | 18,79 | -0,38 | 18,98 | | | 0,00 | | |
| | | | 19,17 | | | | | | | |
| Δ1 | -Tc | I | 18,21 | -0,01 | 18,22 | 18,02 | | 0,00 | | |
| | | | 18,22 | | | | | | | |
| | | II | 18,29 | 0,43 | 18,08 | | | 0,00 | | |
| | | | 17,86 | | | | | | | |
| | | III | 17,81 | 0,10 | 17,76 | | | 0,00 | | |
| | | | 17,71 | | | | | | | |
| | +Tc | I | 18,99 | 0,39 | 18,80 | 18,56 | | 0,00 | | |
| | | | 18,60 | | | | | | | |
| | | II | 18,39 | 0,03 | 18,38 | | | 0,00 | | |
| | | | 18,36 | | | | | | | |
| | | III | 18,49 | -0,01 | 18,50 | | | 0,00 | | |
| | | | 18,50 | | | | | | | |
| Δ2 | -Tc | I | 17,75 | 0,08 | 17,71 | 18,06 | | 0,00 | | |
| | | | 17,67 | | | | | | | |
| | | II | 18,12 | -0,14 | 18,19 | | | 0,00 | | |

| | | | | | | | | | | |
|---|---|---|---|---|---|---|---|---|---|---|
| | | | 18,26 | | | | | | | |
| | | III | 18,37 | 0,19 | 18,28 | | | 0,00 | | |
| | | | 18,18 | | | | | | | |
| | +Tc | I | 18,27 | -0,21 | 18,38 | 18,50 | | 0,00 | | |
| | | | 18,48 | | | | | | | |
| | | II | 18,59 | 0,08 | 18,55 | | | 0,00 | | |
| | | | 18,51 | | | | | | | |
| | | III | 18,45 | -0,25 | 18,58 | | | 0,00 | | |
| | | | 18,70 | | | | | | | |
| Δ3 | -Tc | I | 17,63 | -0,16 | 17,71 | 17,72 | | 0,00 | | |
| | | | 17,79 | | | | | | | |
| | | II | 17,91 | 0,21 | 17,81 | | | 0,00 | | |
| | | | 17,70 | | | | | | | |
| | | III | 17,67 | 0,03 | 17,66 | | | 0,00 | | |
| | | | 17,64 | | | | | | | |
| | +Tc | I | 18,15 | 0,12 | 18,09 | 18,33 | | 0,00 | | |
| | | | 18,03 | | | | | | | |
| | | II | 18,43 | -0,01 | 18,44 | | | 0,00 | | |
| | | | 18,44 | | | | | | | |
| | | III | 18,43 | -0,08 | 18,47 | | | 0,00 | | |
| | | | 18,51 | | | | | | | |
| scram ble | -Tc | I | 18,03 | -0,11 | 18,09 | 18,08 | | 0,00 | | |
| | | | 18,14 | | | | | | | |
| | | II | 17,87 | -0,39 | 18,07 | | | 0,00 | | |
| | | | 18,26 | | | | | | | |
| | | III | 18,03 | -0,14 | 18,10 | | | 0,00 | | |
| | | | 18,17 | | | | | | | |
| | +Tc | I | 17,56 | -0,44 | 17,78 | 18,48 | | 0,00 | | |
| | | | 18,00 | | | | | | | |
| | | II | 18,55 | -0,20 | 18,65 | | | 0,00 | | |
| | | | 18,75 | | | | | | | |
| | | III | 19,01 | 0,01 | 19,01 | | | 0,00 | | |
| | | | 19,00 | | | | | | | |
| ΔS3-L10 | -Tc | I | 17,49 | -0,03 | 17,51 | 17,75 | | 0,00 | | |
| | | | 17,52 | | | | | | | |
| | | II | 17,76 | -0,01 | 17,77 | | | 0,00 | | |
| | | | 17,77 | | | | | | | |
| | | III | 17,98 | 0,01 | 17,98 | | | 0,00 | | |
| | | | 17,97 | | | | | | | |
| | +Tc | I | 17,91 | -0,23 | 18,03 | 18,27 | | 0,00 | | |
| | | | 18,14 | | | | | | | |
| | | II | 18,40 | 0,17 | 18,32 | | | 0,00 | | |
| | | | 18,23 | | | | | | | |
| | | III | 18,40 | -0,11 | 18,46 | | | 0,00 | | |
| | | | 18,51 | | | | | | | |
| mut. S3-L20_1 | -Tc | I | 18,97 | 0,14 | 18,90 | 18,73 | | 0,00 | | |
| | | | 18,83 | | | | | | | |
| | | II | 18,57 | -0,16 | 18,65 | | | 0,00 | | |
| | | | 18,73 | | | | | | | |
| | | III | 18,49 | -0,29 | 18,64 | | | 0,00 | | |
| | | | 18,78 | | | | | | | |
| | +Tc | I | 19,20 | 0,04 | 19,18 | 19,19 | | 0,00 | | |
| | | | 19,16 | | | | | | | |
| | | II | 19,03 | -0,03 | 19,05 | | | 0,00 | | |
| | | | 19,06 | | | | | | | |
| | | III | 19,37 | 0,07 | 19,34 | | | 0,00 | | |
| | | | 19,30 | | | | | | | |
| | -Tc | I | 17,63 | 0,00 | 17,63 | 17,48 | 18,38 | 0,04 | 18,36 | 18,34 |

| | | | | | | | | | | |
|---|---|---|---|---|---|---|---|---|---|---|
| Δ18-33 | | | 17,63 | | | | 18,34 | | | |
| | | II | 17,26 | -0,36 | 17,44 | | 18,38 | -0,14 | 18,45 | |
| | | | 17,62 | | | | 18,52 | | | |
| | | III | 17,43 | 0,13 | 17,37 | | 18,17 | -0,09 | 18,22 | |
| | | | 17,30 | | | | 18,26 | | | |
| | +Tc | I | 17,82 | -0,07 | 17,86 | 18,06 | 19,15 | 0,32 | 18,99 | 18,97 |
| | | | 17,89 | | | | 18,83 | | | |
| | | II | 18,01 | 0,05 | 17,99 | | 18,74 | -0,53 | 19,01 | |
| | | | 17,96 | | | | 19,27 | | | |
| | | III | 18,29 | -0,11 | 18,35 | | 18,77 | -0,26 | 18,90 | |
| | | | 18,40 | | | | 19,03 | | | |
| mut. S3-L20_2 | -Tc | I | 18,07 | 0,12 | 18,01 | 17,99 | | 0,00 | | |
| | | | 17,95 | | | | | | | |
| | | II | 17,78 | -0,11 | 17,84 | | | 0,00 | | |
| | | | 17,89 | | | | | | | |
| | | III | 18,06 | -0,13 | 18,13 | | | 0,00 | | |
| | | | 18,19 | | | | | | | |
| | +Tc | I | 18,17 | 0,07 | 18,14 | 18,36 | | 0,00 | | |
| | | | 18,10 | | | | | | | |
| | | II | 18,38 | 0,08 | 18,34 | | | 0,00 | | |
| | | | 18,30 | | | | | | | |
| | | III | 18,59 | -0,04 | 18,61 | | | 0,00 | | |
| | | | 18,63 | | | | | | | |
| uORF 3-SD-mut | -Tc | I | 19,21 | 1,22 | 18,60 | 18,09 | | 0,00 | | |
| | | | 17,99 | | | | | | | |
| | | II | 17,68 | -0,09 | 17,73 | | | 0,00 | | |
| | | | 17,77 | | | | | | | |
| | | III | 18,03 | 0,18 | 17,94 | | | 0,00 | | |
| | | | 17,85 | | | | | | | |
| | +Tc | I | 18,30 | 0,01 | 18,30 | 18,24 | | 0,00 | | |
| | | | 18,29 | | | | | | | |
| | | II | 18,15 | -0,14 | 18,22 | | | 0,00 | | |
| | | | 18,29 | | | | | | | |
| | | III | 18,23 | 0,07 | 18,20 | | | 0,00 | | |
| | | | 18,16 | | | | | | | |

**Supplemental Tab. S4:** $Log_2$(Fc) calculated from Cq values obtained by RT-qPCR, comparing cells treated with 1.5 µg/ml Tc to control samples. SD, standard deviation.

| | **I** | **II** | **III** | **IV** | **V** | **VI** | **Mean** | **SD** |
|---|---|---|---|---|---|---|---|---|
| DUF'-SPA | 4,44 | 4,86 | 3,42 | 3,64 | 3,86 | 4,44 | 4,11 | 0,51 |
| M1/Stop-SPA | 0,73 | -0,47 | 2,03 | | | | 0,76 | 1,02 |
| uORF1-SPA | 1,51 | 0,58 | 0,03 | | | | 0,70 | 0,61 |
| $DUF1127_1$-SPA | 4,88 | 5,08 | 4,30 | | | | 4,75 | 0,33 |
| CGC 192-194 ATC | 5,03 | 3,90 | 3,73 | | | | 4,22 | 0,58 |
| GCC 135-137 CGG | 3,89 | 3,87 | 4,07 | | | | 3,94 | 0,09 |
| uORF2-SPA | 2,57 | 3,71 | 4,01 | | | | 3,43 | 0,62 |
| M2/Stop-SPA | 3,96 | 4,20 | 3,81 | | | | 3,99 | 0,16 |
| M2/Stop-DUF'-SPA | 4,07 | 4,71 | 4,47 | | | | 4,42 | 0,27 |
| M1-M2-DUF'-SPA | 1,33 | 1,57 | 1,29 | | | | 1,40 | 0,12 |
| Δ121-128 | 3,15 | 2,96 | 3,48 | 2,97 | 2,96 | 3,79 | 3,22 | 0,32 |
| DUF'-mut. 121-128 | 3,87 | 4,05 | 3,79 | 4,25 | 4,02 | 5,67 | 4,28 | 0,64 |
| M1/Stop-mut. 121-128 | 1,13 | 0,61 | 0,78 | 0,62 | 1,11 | 0,53 | 0,80 | 0,24 |
| C11/Stop | 2,69 | 2,62 | 3,77 | | | | 3,03 | 0,53 |
| S19/Stop | 6,65 | 6,04 | 4,34 | | | | 5,68 | 0,98 |
| A15/Stop | 4,65 | 3,24 | 6,53 | | | | 4,81 | 1,35 |
| T17/Stop | 3,76 | 4,61 | 5,91 | | | | 4,76 | 0,88 |
| Δ1 | 3,10 | 2,30 | 3,03 | | | | 2,81 | 0,36 |

| | | | | | | | | |
|---|---|---|---|---|---|---|---|---|
| Δ2 | 4,68 | 4,58 | 3,93 | | | | 4,40 | 0,33 |
| Δ3 | 0,22 | 3,46 | 4,46 | | | | 2,71 | 1,81 |
| scramble | 5,23 | 5,21 | 5,34 | | | | 5,26 | 0,06 |
| ΔS3-L10 | 0,45 | 0,40 | 0,37 | | | | 0,41 | 0,03 |
| Mut. S3-L10_1 | 1,20 | 1,23 | 1,50 | | | | 1,31 | 0,13 |
| Δ18-33 | 1,99 | 2,31 | 3,09 | 2,08 | 2,32 | 2,83 | 2,44 | 0,39 |
| uORF3-SD-mut | 3,84 | 3,55 | 3,51 | | | | 3,64 | 0,15 |
| Mut. S3-L10_2 | 1,73 | 2,24 | 2,00 | | | | 1,99 | 0,21 |

**Supplemental Tab. S5:** Values obtained by RT-qPCR of the reporter mRNAs comparing the $Log_2$(Ratio) of *spa* vs *rpoB* mRNA. This ratio shows the basal expression of the reporter fusions without Tc. SD, standard deviation.

| | **I** | **II** | **III** | **IV** | **V** | **VI** | **Mean** | **SD** |
|---|---|---|---|---|---|---|---|---|
| DUF'-SPA | 2,46 | 2,76 | 3,54 | 2,70 | 2,58 | 2,41 | 2,74 | 0,38 |
| M1/Stop-SPA | 6,77 | 6,58 | 6,15 | | | | 6,50 | 0,26 |
| uORF1-SPA | 8,33 | 8,53 | 8,53 | 8,53 | 8,86 | 9,36 | 8,69 | 0,34 |
| $DUF1127_1$-SPA | 1,84 | 2,24 | 2,57 | | | | 2,22 | 0,30 |
| CGC 192-194 ATC | 1,23 | 1,30 | 1,74 | | | | 1,42 | 0,23 |
| GCC 135-137 CGG | 2,08 | 2,20 | 2,40 | | | | 2,23 | 0,13 |
| uORF2-SPA | 3,96 | 3,44 | 3,23 | | | | 3,54 | 0,31 |
| M2/Stop-SPA | 4,20 | 4,27 | 4,52 | | | | 4,33 | 0,14 |
| M2/Stop-DUF'-SPA | 2,79 | 3,35 | 3,14 | | | | 3,09 | 0,23 |
| M1-M2-DUF'-SPA | 8,51 | 8,71 | 8,73 | | | | 8,65 | 0,10 |
| Δ121-128 | 3,57 | 3,66 | 3,38 | 3,99 | 4,14 | 3,67 | 3,73 | 0,26 |
| DUF'-mut. 121-128 | 2,67 | 2,76 | 2,75 | 2,58 | 2,72 | 1,90 | 2,56 | 0,30 |
| M1/Stop-mut. 121-128 | 9,60 | 9,35 | 9,35 | 9,64 | 9,16 | 9,28 | 9,39 | 0,17 |
| C11/Stop | 7,75 | 8,36 | 8,35 | | | | 8,15 | 0,28 |
| S19/Stop | 3,94 | 3,10 | 4,14 | | | | 3,73 | 0,45 |
| A15/Stop | 2,56 | 3,10 | 1,96 | | | | 2,54 | 0,46 |
| T17/Stop | 1,93 | 1,69 | 2,76 | | | | 2,13 | 0,46 |
| Δ1 | 5,99 | 6,09 | 5,84 | | | | 5,97 | 0,10 |
| Δ2 | 2,18 | 2,31 | 2,70 | | | | 2,40 | 0,22 |
| Δ3 | 3,33 | 3,14 | 2,99 | | | | 3,16 | 0,14 |
| scramble | 2,64 | 2,69 | 2,77 | | | | 2,70 | 0,05 |
| ΔS3-L10 | 7,30 | 7,43 | 7,48 | | | | 7,40 | 0,08 |
| Mut. S3-L10_1 | 9,03 | 8,95 | 9,13 | | | | 9,04 | 0,07 |
| Δ18-33 | 2,62 | 2,61 | 2,45 | 3,11 | 3,04 | 2,74 | 2,76 | 0,24 |
| Mut. S3-L10_2 | | | | | | | | |
| uORF3-SD-mut | 2,09 | 1,58 | 1,48 | | | | 1,72 | 0,26 |

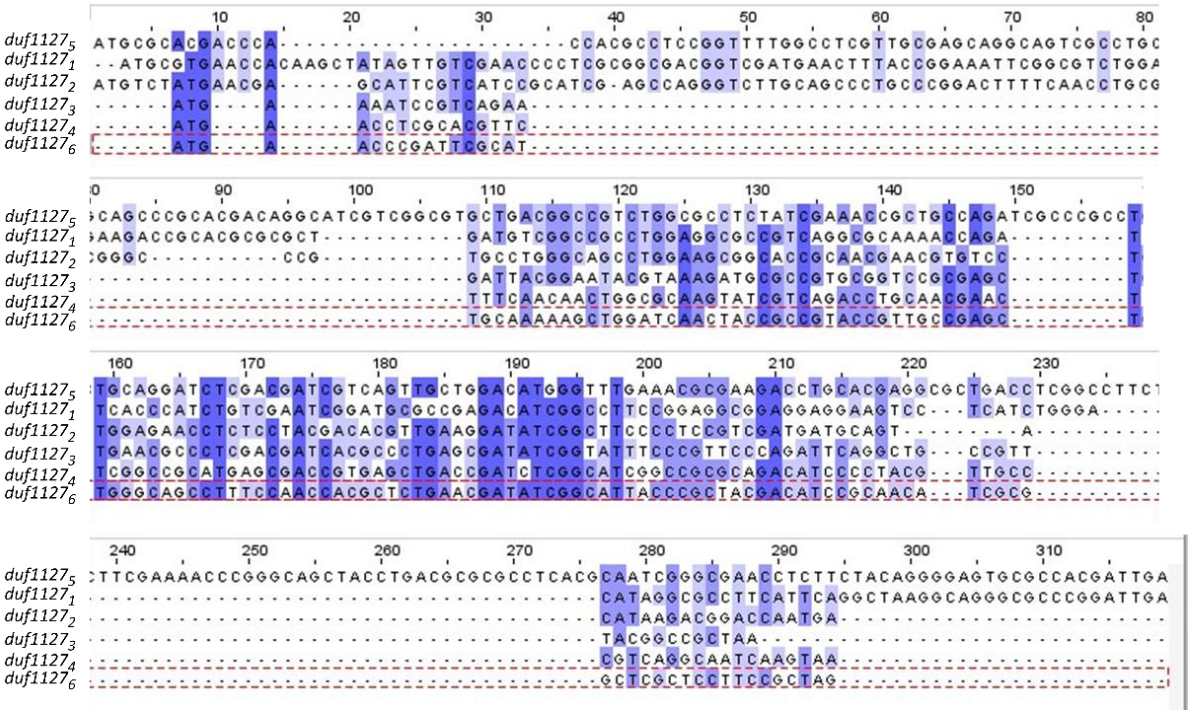


**Supplemental Fig. S1:** DNA sequence alignment of the six *duf1127* genes discovered in this study. Conserved nucleotides are shown in blue, with dark blue for the highest level of conservation. The gene sequence alignment for the six *duf1127* encoding genes shows conserved regions among all six genes between 120 nt to 220 nt into the alignment. In addition, a 10 bp insertions at position 150 and a triplet insertion at position 222 was found solely in gene *duf1127*$_5$, while both N- and C-terminal addition of the largest gene *duf1127*$_5$ were also partly visible with *duf1127*$_1$ and – with even shorter extensions – for *duf1127*$_2$. The highest degree of similarity was found between all six *duf1127* ranging from +120 to +150, and from +160 to +210. In particular, the of 8 nucleotides from +188 to +195 revealed a very high similarity. Overall, the three longer *duf1127* genes showed higher similarity with each other as compared to the shorter ones, with *duf1127*$_4$ being intermediate.

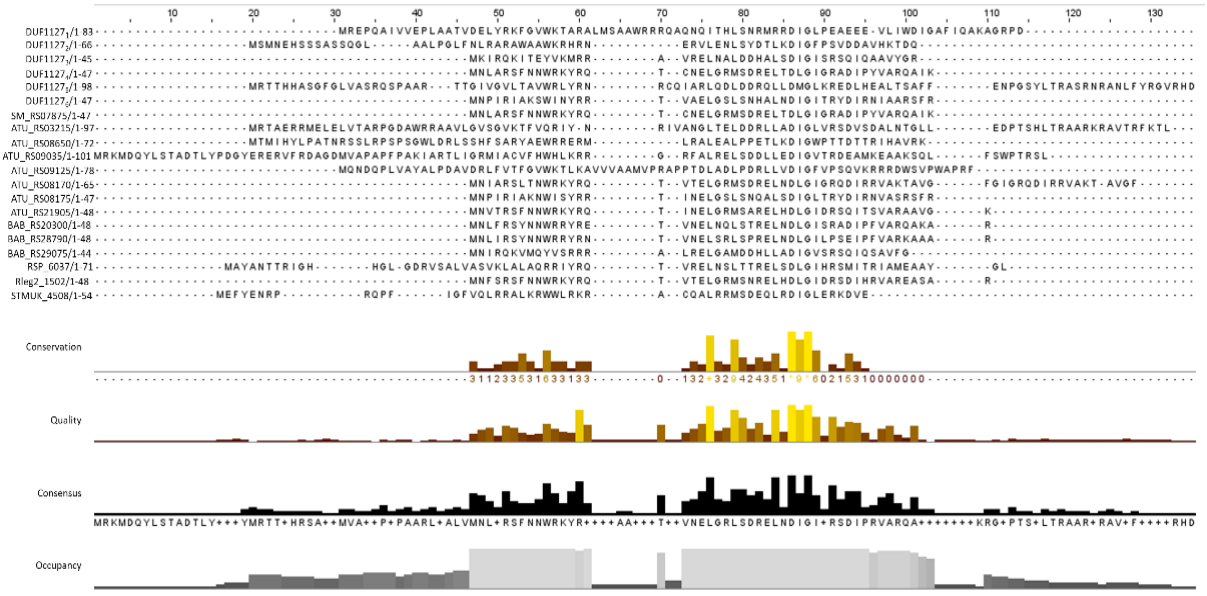


**Supplemental Fig. S2:** Sequence alignments for the six DUF1127 discovered in this study versus other DUF1127 from different organisms. SM, *S. meliloti* 1021; ATU, *A. tumefaciens*; RSP, *R. sphaeroides*; BAB, *Brucella abortus* 2308; Rleg, Rhizobium *leguminosarum*; STMUK, *Salmonella enterica* serovar Typhimurium, str. UK-1.

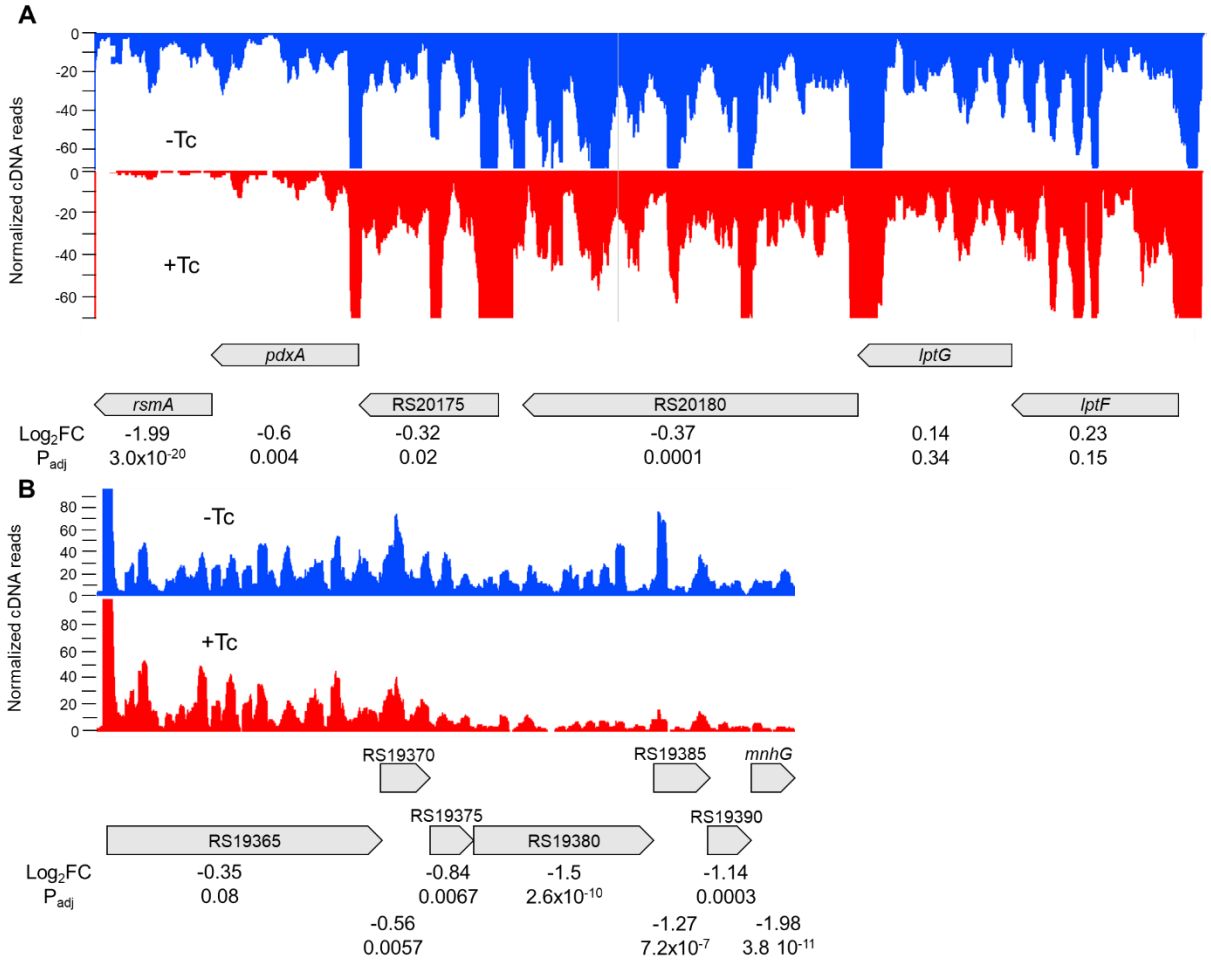


**Supplemental Fig. S3:** Operon structures for down-regulated genes in the RNA seq. **(A)** Structure of the *rsmA*/*pdxA* operon. Both *rsmA* and *pdxA* are last and second to last in the operon. **(B)** Structure of the RS19365/*mnhG* operon. RS19365 is first in the operon, *mnhG* is last. Log 2-fold changes and statistical significance are given below the genes.

**Supplemental Tab. S6:** RNA ends that were found in the 3'RACE. 35 clones from 3 replicates were analyzed, of which 19 had ends after uORF1. 16 ends were discovered in uORF1, while 7 ends were discovered after uORF1. 2 ends were discovered in uORF2 and 2 after uORF2. 5 ends were discovered in a putative uORF3 and 3 ends were discovered in *duf1127*$_1$. The ends in *duf1127*$_1$ are most likely because the maximum sequence read length was reached. Many constructs had acquired mutations. #, number; Cd, codons.

| | | | | **Integrated regulatory features** | | | | |
|---|---|---|---|---|---|---|---|---|
| **Replicate** | **Clone #** | **Start** | **End** | **uORF1** | **uORF2** | **uORF3** | ***duf1127*$_1$** | **Comments** |
| 1 | 3 | 5 | 354 | yes | yes | yes | part (25 Cd) | Mutation at Pos 253 (A -> G) destroying uORF3 |
| | 8 | 5 | 188 | yes | no | no | no | |
| | 1 | 5 | 253 | yes | yes | no | no | |
| | 25 | 5 | 261 | yes | yes | part (3 Cd) | no | |
| | 10 | 5 | 354 | yes | yes | yes | part (25 Cd) | Mutation at Pos 253 (A -> G) destroying uORF3 |

| | | | | | | | | |
|---|---|---|---|---|---|---|---|---|
| | 16 | 5 | 282 | yes | yes | part (10 Cd) | part (1 cd) | Mutation at Pos 142 (A -> G) |
| | 13 | 5 | 273 | yes | yes | part (7 Cd) | no | Mutation at Pos +231 (G -> A) |
| | 20 | | | | | | | uORF1 integrated until A15 (+74) |
| | 27 | | | | | | | Mutation at +4; has part before +1 integrated; part of uORF1 integrated |
| | 5 | | | | | | | Starts at +1; only part of uORF1 integrated |
| | 12 | | | | | | | Mutation at +66; only part of uORF1 integrated |
| | 4 | | | | | | | Only part of uORF1 integrated |
| 2 | 16 | 5 | 251 | yes | yes | no | no | |
| | 15 | 5 | 189 | yes | part (2 Cd) | no | no | |
| | 12 | -2 | 204 | yes | part (7 Cd) | no | no | Has part from before +1 integrated; mutations at Pos +4 (G -> A) and +29 (T -> C) |
| | 4 | 5 | 260 | yes | yes | part (3 Cd) | no | Mutation at Pos +51 (T -> C) |
| | 21 | 5 | 180 | yes | no | no | no | Has part from before +1 integrated; mutation at Pos +4 (G -> A) |
| | 2 | 5 | 34 | part (1.5 Cd) | no | no | no | Only has the 5' UTR |
| | 1 | 5 | 32 | no | no | no | no | Only has the 5' UTR |
| | 25 | 5 | 99 | part (23 Cd) | no | no | no | Partial integration of uORF1 until Ala23; Insertion mutations at positions +89 and +91 (A inserted); Deletion mutation at position +97 (G deleted) |
| | 20 | 5 | 60 | part (11 Cd) | no | no | no | Partial integration of uORF1 until Cys11 |
| | 27 | 5 | 273 | yes | yes | part (7 Cd) | no | |
| | 11 | 5 | 92 | part (21 Cd) | no | no | no | Mutation at Pos +4 (C -> T); uORF1 integrated until Arg 21 |
| | 6 | | | | | | | Double integration of uORF1: 1x until +187, 1x until +181 |
| | 9 | | | | | | | Only part of uORF1 integrated |
| 3 | 22 | 5 | 176 | yes | no | no | no | |
| | 19 | 5 | 92 | part (21 Cd) | no | no | no | uORF1 integrated until Arg 21 |
| | 26 | 5 | 73 | part (14 Cd) | no | no | no | uORF1 integrated until Thr14 |
| | 4 | 5 | 180 | yes | no | no | no | Insertion mutation at +111 and +248 (A inserted); Mutation at +112 (C -> A) |
| | 10 | 1 | 139 | yes | no | no | no | Deletion mutation at +16 (C deleted); insertion mutation at +13 (A inserted); |

| | | | | | | | | |
|---|---|---|---|---|---|---|---|---|
| | | | | | | | | mutation at +4 and +60 (C -> T), has +1 integrated |
| | 21 | 5 | 173 | yes | no | no | no | |
| | 8 | 1 | 106 | part (25 Cd) | no | no | no | Partial integration of uORF1 |
| | 6 | 5 | 94 | part (21 Cd) | no | no | no | |
| | 11 | 1 | 126 | yes | no | no | no | |
| | 27 | | | | | | | Mutation at +4; has part before +1 integrated; part of uORF1 integrated |

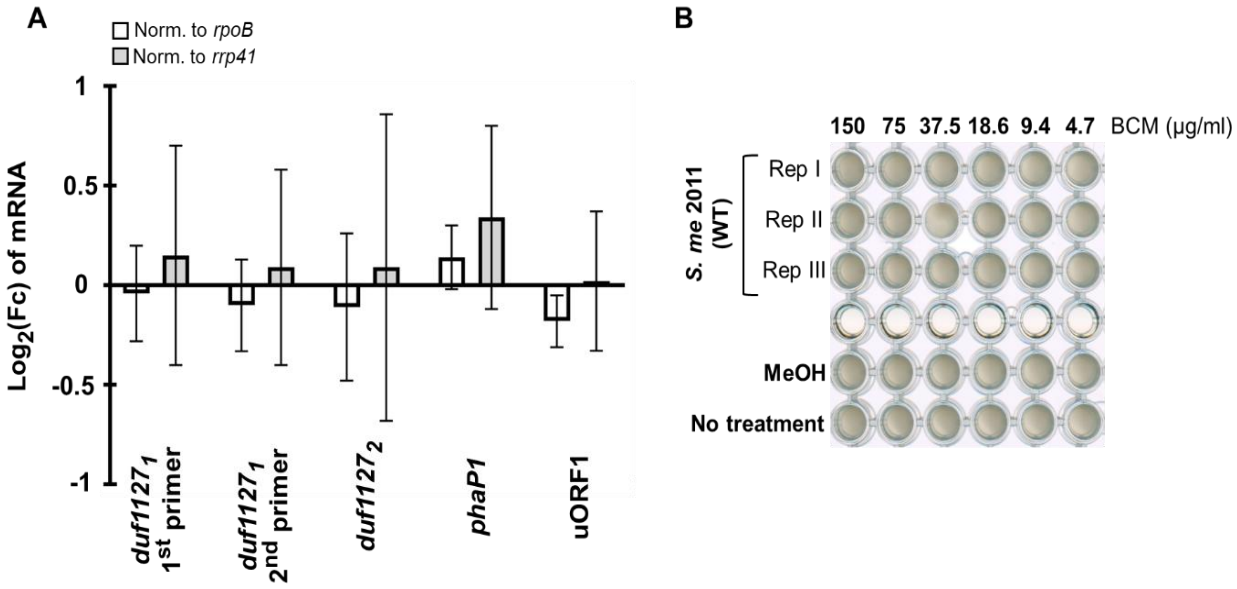


**Supplemental Fig. S4:** Bicyclomycin treatment effect on *duf1127₁* regulation. **(A)** RT-qPCR to show effects of 30 min exposition to bicyclomycin (BCM) on *duf1127₁* with two different primer pairs as well as *duf1127₂*, *phaP1* and uORF1. *rrp41* and *rpoB* were used as internal controls to normalize raw data. **(B)** Bicyclomycin treatment effect using a MIC test, to determine whether BCM affected *S. meliloti* growth with methanol (MeOH) and no treatment controls.

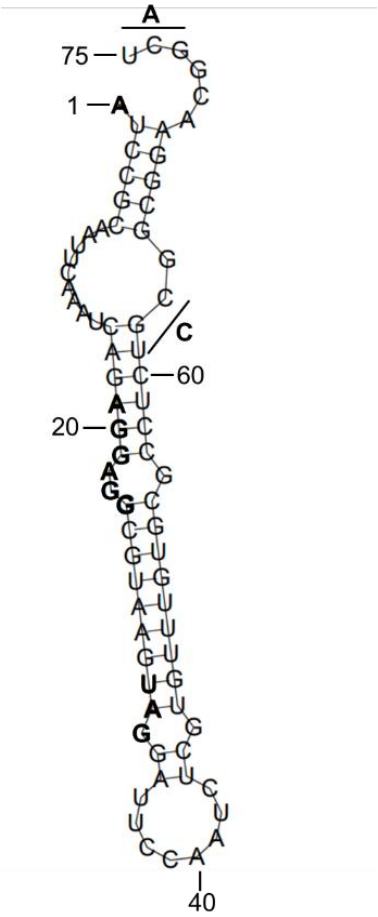


**Supplemental Fig. S5:** Secondary structure from +1 to +75 (A15) of uORF1, depicting the SD (AGGAGG, bold) and the mutated start to stop codon (UAG, bold).

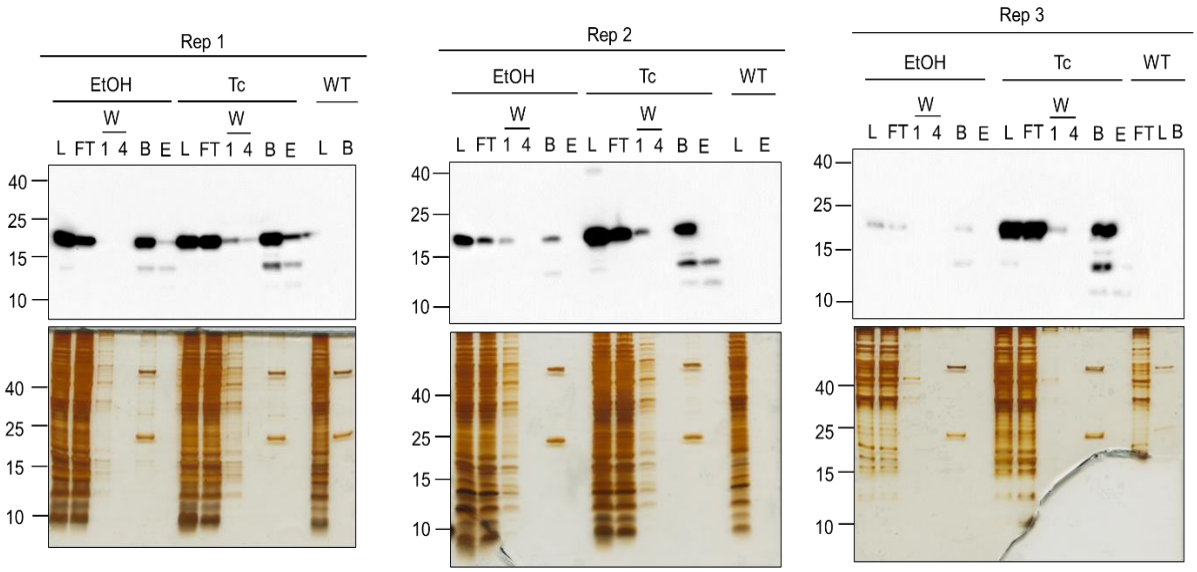


**Supplemental Fig. S6:** Western Blot and silver-stained gels of 3xFLAG pulldown of full-length *duf1127*$_1$. Western Blot analysis showed that with DUF1127$_1$, two additional proteins were pulled down (L, lysate; FT, flow-through; W, wash (fraction 1 and 4); B, beads before elution; E, eluate; WT, wildtype as a negative control).

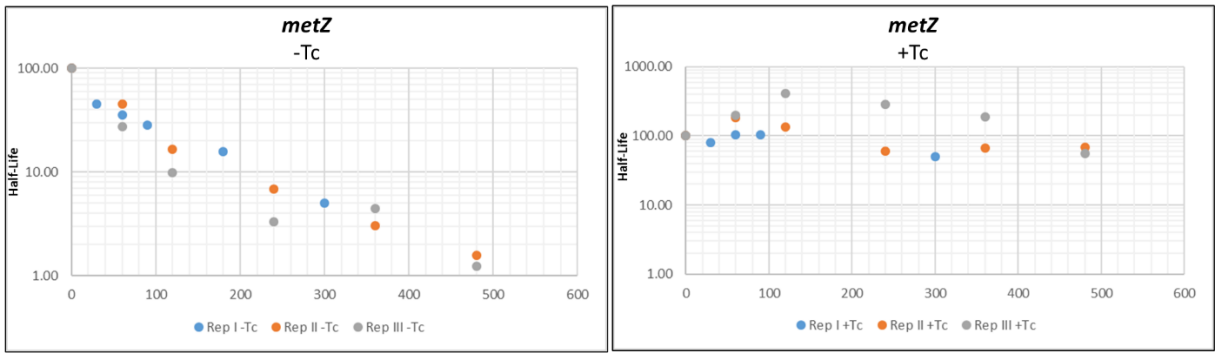


**Supplemental Fig. S7:** Measured half-lives for *metZ* mRNA in 3 biological replicates after rifampicin addition.

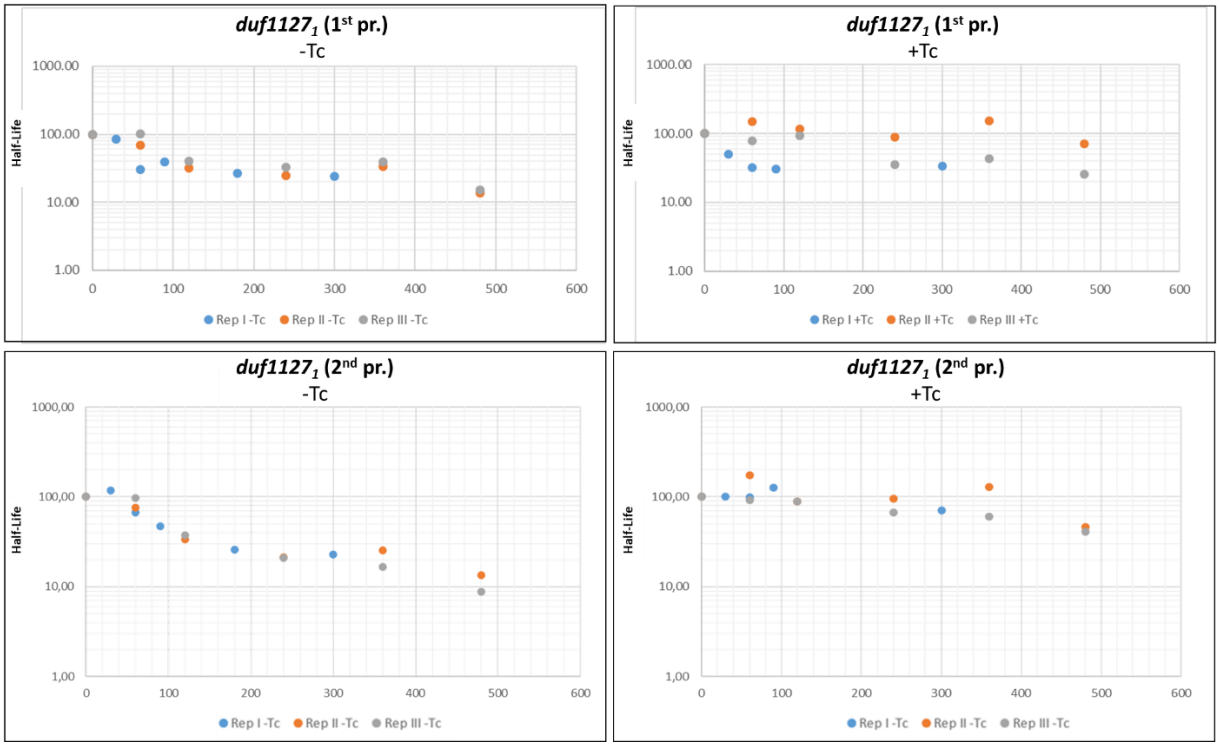


**Supplemental Fig. S8:** Measured half-lives for *duf1127₁* mRNA in 3 biological replicates after rifampicin addition with both primer pairs.

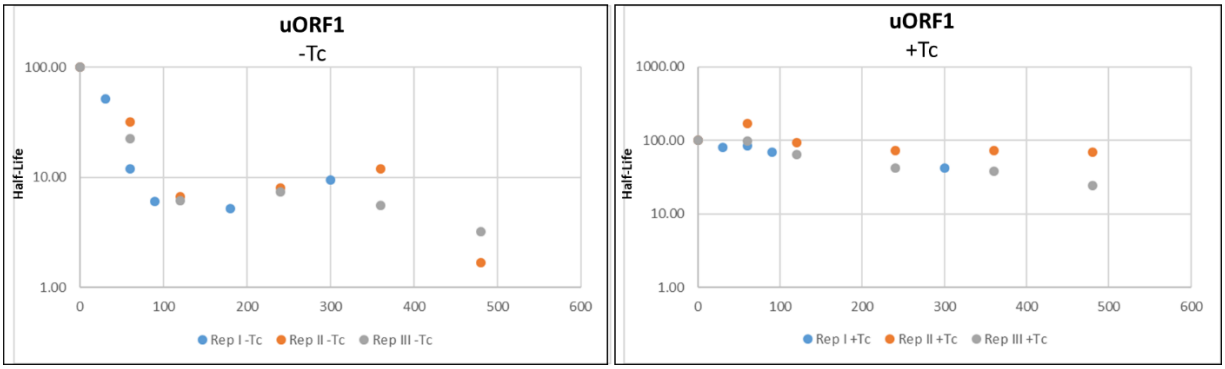


**Supplemental Fig. S9:** Measured half-lives for uORF1 RNA in 3 biological replicates after rifampicin addition.

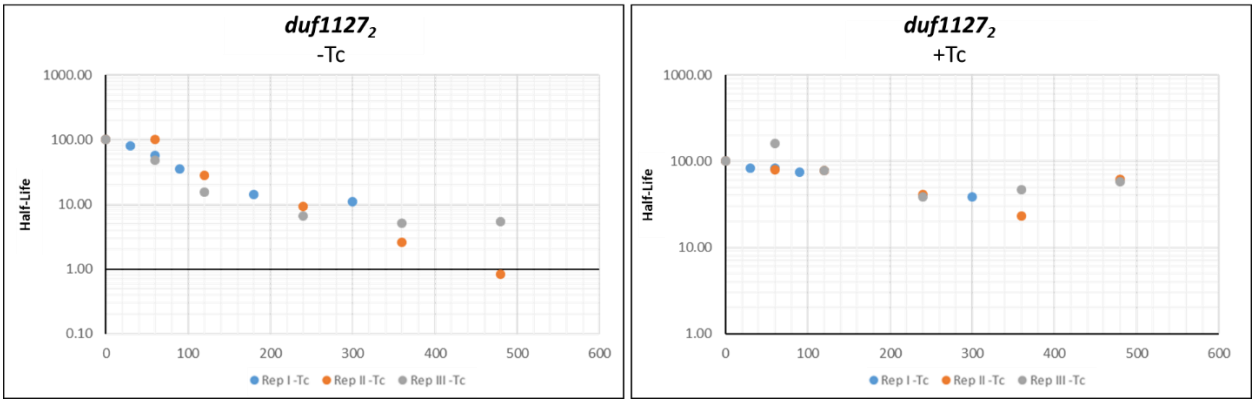


**Supplemental Fig. S10:** Measured half-lives for *duf1127₂* mRNA in 3 biological replicates after rifampicin addition.

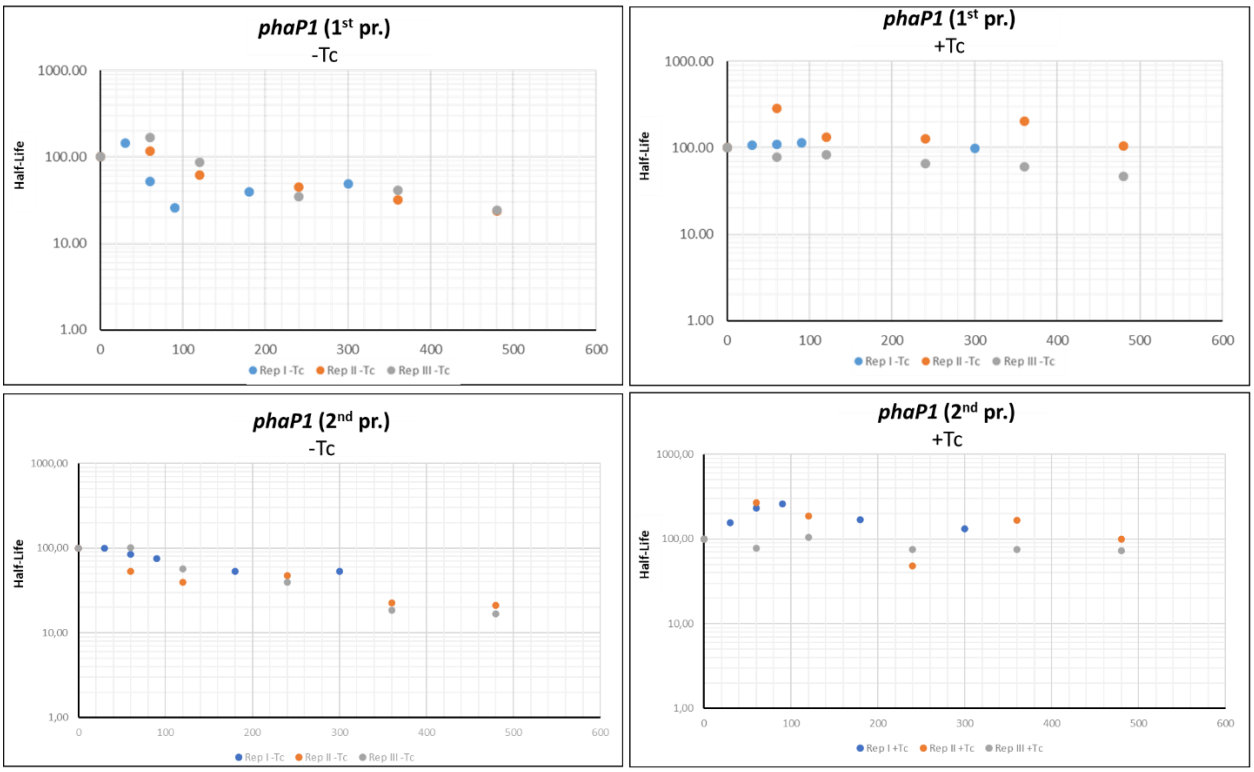


**Supplemental Fig. S11:** Measured half-lives for *phaP1* mRNA in 3 biological replicates after rifampicin addition with both primer pairs.

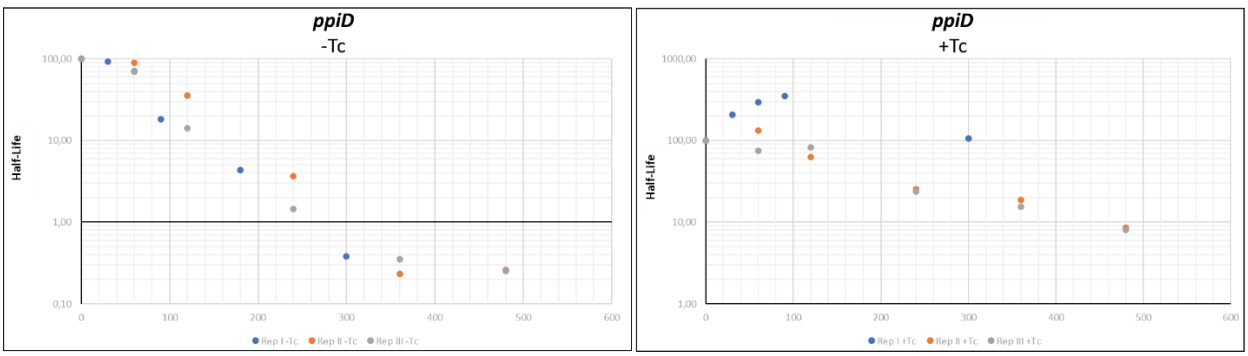


**Supplemental Fig. S12:** Measured half-lives for *ppiD* mRNA in 3 biological replicates after rifampicin addition.

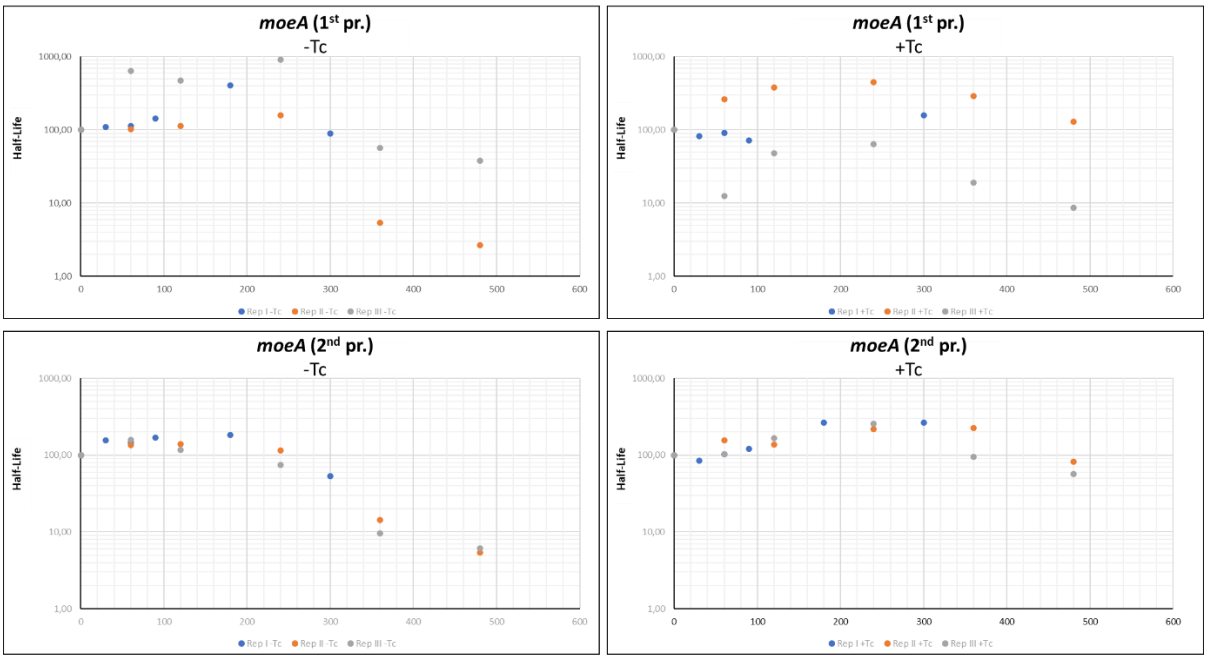


**Supplemental Fig. S13:** Measured half-lives for *moeA* mRNA in 3 biological replicates after rifampicin addition with both primer pairs.

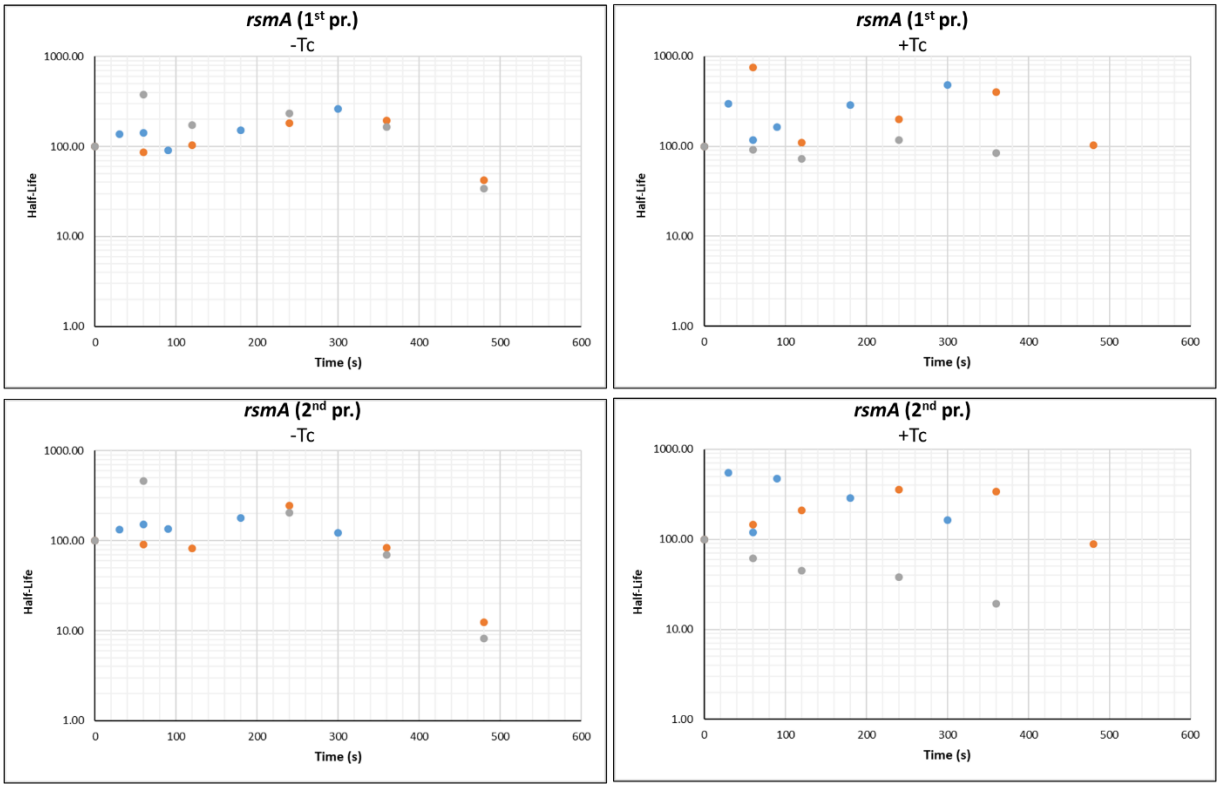


**Supplemental Fig. S14:** Measured half-lives for *rsmA* mRNA in 3 biological replicates after rifampicin addition with both primer pairs.

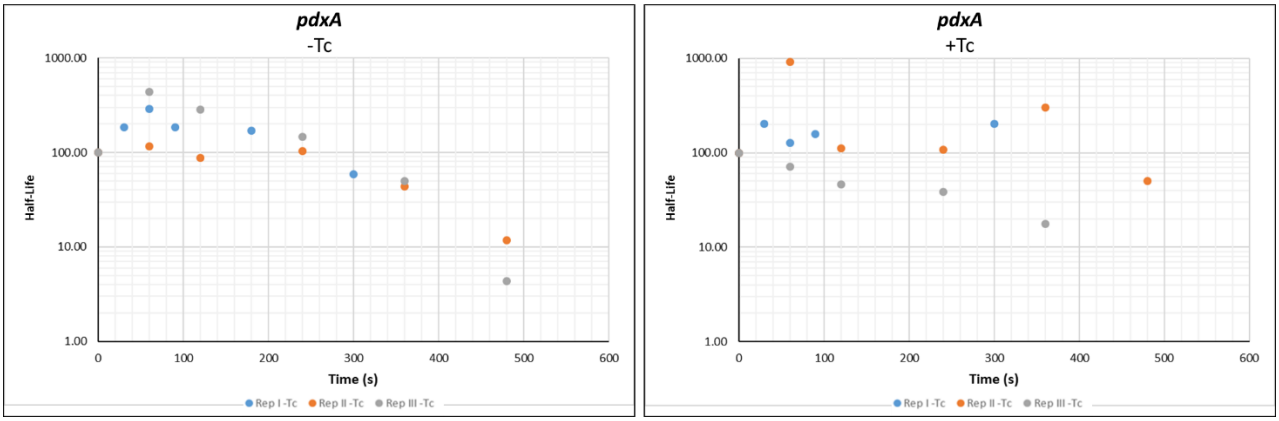


**Supplemental Fig. S15:** Measured half-lives for *pdxA* mRNA in 3 biological replicates after rifampicin addition.

# Statutory declaration

I declare that I have completed this dissertation single-handedly without the unauthorized help of a second party and only with the assistance acknowledged therein. I have appropriately acknowledged and cited all text passages that are derived verbatim from or are based on the content of published work of others, and all information relating to verbal communications. I consent to the use of an anti-plagiarism software to check my thesis. I have abided by the principles of good scientific conduct laid down in the charter of the Justus Liebig University Giessen „Satzung der Justus-Liebig-Universität Gießen zur Sicherung guter wissenschaftlicher Praxis“ in carrying out the investigations described in the dissertation.

_____

Jennifer Kothe Date Place